DEVELOPING AND VALIDATING NEW BOLTED END-PLATE MOMENT CONNECTION CONFIGURATIONS

Nonish Jain

Thesis submitted to the Faculty of the
Virginia Polytechnic Institute and State University
in partial fulfillment of the requirements for the degree of

MASTER OF SCIENCE

in

CIVIL ENGINEERING

Matthew R. Eatherton, Chair
Thomas M. Murray
Roberto T. Leon

June 24, 2015
Blacksburg, Virginia

Keywords: End-Plate Moment Connections, Monotonic Full-Scale Testing and Metal Buildings

DEVELOPING AND VALIDATING NEW BOLTED END-PLATE MOMENT CONNECTION CONFIGURATIONS

Nonish Jain

ABSTRACT

This research has been aimed to introduce larger moment carrying connections for any type of buildings, in particular the metal building industry. A total of four connection configurations, namely eight-bolt extended four wide, eight-bolt extended stiffened, six bolt flush unstiffened and twelve bolt extended unstiffened, have been investigated. The last two configurations are proposed whereas the first two configurations have been tested before, but the design procedures need to be validated against the test results.

Design procedures, namely yield line analysis and bolt force models, were proposed to calculate moment capacity for end-plate yielding, moment capacity at bolt rupture with prying action and moment capacity at bolt rupture without prying action. The calculated values from these procedures were compared with the values obtained from the experimental test data available (whether from the literature or from this testing program).

The experimental data from already tested configurations, eight-bolt extended four wide and eight-bolt extended stiffened, was analyzed. It was concluded that for the eight-bolt extended four wide configuration, the experimental values matched with the calculated values. For the eight-bolt extended stiffened configuration reasonable match was found between the experimentally obtained data and theoretically calculated values only for shallower depths. Hence, it was concluded that two deeper tests need to be performed for this configuration.

A full-scale testing program was conducted for ten specimens covering three configurations. The two new configurations (six bolt flush unstiffened and twelve bolt multiple row extended

unstiffened) were designed for a shallow and deep beam depth and the behavior of each depth observed for a thin end-plate and a thick end-plate respectively (four tests for each configuration). Also, two deep beam tests, one each for thick and thin plate behavior, were done for the eight-bolt extended stiffened configuration. Based on the comparison, it was determined whether the predicted values were in reasonable agreement with the experimental values or not.

The design procedures for both the new configurations appear to be validated for a range of design parameters. The calculated moment capacities for bolt rupture, based on the nominal material properties, were found to be safe when compared with the experimentally obtained moments. The calculations for end-plate yield moments was within ±10% of the experimental yield moment. Also, for the deep tests for eight-bolt extended stiffened the yield line analysis seems to be a valid model and the bolt force model appears to be safe in comparison to the experimental values.

ACKNOWLEDGEMENTS

First of all, I would like to thank my parents who agreed to send me all the way from India to the US for my master's. I was supposed to graduate with coursework only, but then sometime in the summer of 2014, I got an email from Dr. Eatherton, asking me if I wanted to do research. After thinking about it over a few days, I said yes and here I am writing my thesis after all the hard work in the lab.

I would like to extend my deepest sense of gratitude to Dr. Eatherton who is a great advisor and researcher. He has been always very reachable, answering all my questions very patiently. Working with him, has been a continual learning experience both personally and professionally. Also, Dr. Murray's regular review and participation in the project is highly appreciated. Dr. Leon has also been kind enough to serve on my advisory committee.

Thanks to Phillip Bellis for working on the project initially and doing most of the design and validation of the connection configurations. All this work which involves extensive labor wouldn't have been possible without the generous help of David Mokarem, Dennis Huffman and Brett Farmer. Also, I highly appreciate the help of Michael Wood, William McNally, Ebrahim Jumaan, Abhilasha Maurya, Patrick O'Brien, Eric Bianchi, Steve Florig, Osama Bukhamseen and all my friends in the lab, without whom the testing in the lab would have been almost unthinkable.

I am indebted to my parents who have been my inspiritment all through my life. I would like to thank my brother and sister-in-law for their constant support. Their little daughter, Netanya, has been my perpetual source of encouragement. I am also indebted to all my friends and relatives who have always stood by on my side.

This project was funded by the Metal Building Manufacturers Association (MBMA). The advice and suggestions by the MBMA connection steering committee throughout the project is appreciated. Also, thanks to American Buildings and Bluescope Buildings for donating the test specimens.

All photos by author, 2015.

TABLE OF CONTENTS

LIST OF FIGURES ..... **ix**

LIST OF TABLES ..... **xviii**

1 INTRODUCTION **1**

1.1 MOTIVATION FOR THESIS 1

1.2 SCOPE OF RESEARCH 2

1.2.1 Select Design Configurations *2*

1.2.2 Design Procedure and Limit States *3*

1.2.3 Validating Design Procedures Based on Existing Test Data *4*

1.2.4 Full-Scale Tests *4*

1.3 THESIS ORGANIZATION 4

2 LITERATURE REVIEW **6**

2.1 DESIGN GUIDE 16 BACKGROUND 6

2.2 DESIGN METHODOLOGY 8

2.2.1 Design Steps for Thick End-Plate Behavior *8*

2.2.2 Design Steps for Thin End-Plate Behavior *9*

2.3 TYPICAL EXPERIMENTAL VALIDATION 12

3 PROPOSED DESIGN PROCEDURES **14**

3.1 EIGHT BOLT EXTENDED FOUR WIDE UNSTIFFENED (8E-4W) 15

3.1.1 Yield Line Analysis *15*

3.1.2 Bolt Force Model *19*

3.2 EIGHT BOLT EXTENDED STIFFENED (8ES) 22

3.2.1 Yield Line Analysis *22*

3.2.2 Bolt Force Model *27*

3.3 SIX BOLT FLUSH FOUR WIDE/TWO WIDE UNSTIFFENED (6B-4W/2W) 30

3.3.1 Yield Line Analysis *30*

3.3.2 Bolt Force Model *34*

3.4 TWELVE BOLT MULTIPLE ROW EXTENDED FOUR WIDE/TWO WIDE UNSTIFFENED (12B-MRE 1/3-4W/2W) 37

3.4.1 Yield Line Analysis *37*

3.4.2 Bolt Force Model *41*

4 VALIDATION OF CONNECTION CONFIGURATION BASED ON LITERATURE 45

4.1 PREVIOUS TESTING ON THE EIGHT-BOLT EXTENDED FOUR WIDE UNSTIFFENED CONFIGURATION 45

4.1.1 Shallow Section - Thin Plate Behavior 48

4.1.2 Shallow Section - Thick Plate Behavior 53

4.1.3 Deep Section - Thin Plate Behavior 58

4.1.4 Deep Section - Thick Plate Behavior 63

4.1.5 Overall Summary of Eight Bolt Extended Four Wide Configuration and Recommendations 69

4.2 PREVIOUS TESTING ON THE EIGHT-BOLT EXTENDED STIFFENED CONFIGURATION 70

4.2.1 Shallow Section - Thin Plate Behavior 72

4.2.2 Shallow Section - Thick Plate Behavior 81

4.2.3 Overall Summary of the Eight Bolt Extended Stiffened Configuration and Recommendations 91

5 EXPERIMENTAL TESTING 94

5.1 TEST SPECIMENS 94

5.2 TEST SETUP 101

5.3 INSTRUMENTATION 102

5.4 TESTING PROCEDURE 103

5.5 TENSILE COUPON TESTS 112

5.6 BOLT RUPTURE REPORTS 113

6 EXPERIMENTAL RESULTS 118

6.1 TESTING ON THE SIX BOLT, FOUR-WIDE/TWO-WIDE, FLUSH, UNSTIFFENED (6B-4W/2W) CONFIGURATION 119

6.1.1 Shallow Section - Thin Plate Behavior 119

6.1.2 Shallow Section - Thick Plate Behavior 126

6.1.3 Deep Section - Thin Plate Behavior 132

6.1.4 Deep Section - Thick Plate Behavior 138

6.1.5 Overall Summary of the Six Bolt Flush Configuration and Recommendations 144

6.2 TESTING ON THE TWELVE BOLT, MULTIPLE ROW EXTENDED, FOUR-WIDE/TWO-WIDE (12B-MRE 1/3-4W/2W), UNSTIFFENED CONFIGURATION 146

6.2.1 Shallow Section - Thin Plate Behavior 146

6.2.2 Shallow Section - Thick Plate Behavior 152

6.2.3 Deep Section - Thin Plate Behavior *158*
6.2.4 Deep Section - Thick Plate Behavior *166*
6.2.5 Overall Summary of the Twelve Bolt Extended Unstiffened Configuration and Recommendations *172*
6.3 TESTING ON THE EIGHT BOLT EXTENDED STIFFENED (8ES) CONFIGURATION 174
6.3.1 Deep Section - Thin Plate Behavior *174*
6.3.2 Deep Section - Thick Plate Behavior *181*
6.3.3 Overall Summary of the Eight Bolt Extended Configuration and Recommendations *187*
7 SUMMARY AND CONCLUSIONS 189
7.1 SUMMARY 189
7.1.1 8E-4W Configuration *189*
7.1.2 8ES Configuration *189*
7.1.3 6B-4W/2W Configuration *190*
7.1.4 12B-MRE 1/3-4W/2W Configuration *191*
7.2 CONCLUSIONS 192
7.2.1 8E-4W Configuration *192*
7.2.2 8ES Configuration *192*
7.2.3 6B-4W/2W Configuration *192*
7.2.4 12B-MRE 1/3-4W/2W Configuration *193*
REFERENCES 194
APPENDIX A MILL TEST REPORT FOR BEAM MATERIAL 196
APPENDIX B MILL TEST REPORT FOR BOLTS 210
APPENDIX C TEST SUMMARIES 215
APPENDIX D FABRICATION DRAWINGS 226
APPENDIX E SPECIMEN DESIGN CALCULATIONS 233
APPENDIX F LATERAL BRACING DESIGN CALCULATIONS 300
APPENDIX G UNREPORTED DATA FROM STRING POTENTIOMETERS 302
APPENDIX H CITATIONS OF COPYRIGHTED WORKS 313

LIST OF FIGURES

Figure 1-1 Selected Design Configurations 3
Figure 2-1 Flush End-Plate Connections (Murray, T. M., & Shoemaker, W. L. (2002). Flush and Extended Multiple-Row Moment End-Plate Connections. AISC, Used under fair use)..... 7
Figure 2-2 Extended End-Plate Connections (Murray, T. M., & Shoemaker, W. L. (2002). Flush and Extended Multiple-Row Moment End-Plate Connections. AISC, Used under fair use). 8
Figure 3-1 Yield Line Mechanism for 8E-4W configuration 16
Figure 3-2 Bolt force model and contribution of each bolt for 8E-4W configuration..... 20
Figure 3-3 Yield Line Mechanism for 8ES Configuration 23
Figure 3-4 Bolt force model for 8ES configuration..... 28
Figure 3-5 Yield Line Mechanism for 6B-4W/2W Configuration 31
Figure 3-6 Bolt force model and contribution of each bolt for 6B-4W/2W configuration..... 35
Figure 3-7 Yield Line Mechanism for 12B-MRE 1/3-4W/2W Configuration 38
Figure 3-8 Bolt force model and contribution of each bolt for 12B-MRE 1/3-4W/2Wconfiguration 43
Figure 4-1 8E-4W-1.25-1-30 Specimen Dimensions [Sumner, E. A., Mays, T. W., & Murray, T. M. (2000). *Cyclic Testing of Bolted Moment End-Plate Connections. B*lacksburg, VA: Virginia Polytechnic Institute and State University, Used with Permission of T.M. Murray, 2015] 48
Figure 4-2 End Plate Layout for Specimen 8E-4W-1.25-1-30 [Sumner, E. A., Mays, T. W., & Murray, T. M. (2000). *Cyclic Testing of Bolted Moment End-Plate Connections.* Blacksburg, VA: Virginia Polytechnic Institute and State University, Used with Permission of T.M. Murray, 2015] 49
Figure 4-3 Load-deformation behavior for Specimen 8E-4W-1.25-1-30 [Sumner, E. A., Mays, T. W., & Murray, T. M. (2000). *Cyclic Testing of Bolted Moment End-Plate Connections.* Blacksburg, VA: Virginia Polytechnic Institute and State University, Used with Permission of T.M. Murray, 2015] 50
Figure 4-4 End-plate separation for Specimen 8E-4W-1.25-1-30 [Sumner, E. A., Mays, T. W., & Murray, T. M. (2000). *Cyclic Testing of Bolted Moment End-Plate Connections. B*lacksburg,

VA: Virginia Polytechnic Institute and State University, Used with Permission of T.M. Murray, 2015] 52
Figure 4-5 Bolt 2 strains for Specimen 8E-4W-1.25-1-30 [Sumner, E. A., Mays, T. W., & Murray, T. M. (2000). Cyclic Testing of Bolted Moment End-Plate Connections. Blacksburg, VA: Virginia Polytechnic Institute and State University, Used with Permission of T.M. Murray, 2015] 52
Figure 4-6 8E-4W-1.25-1.375-36 Specimen Dimensions [Sumner, E. A., Mays, T. W., & Murray, T. M. (2000). Cyclic Testing of Bolted Moment End-Plate Connections. Blacksburg, VA: Virginia Polytechnic Institute and State University, Used with Permission of T.M. Murray, 2015] 53
Figure 4-7 End Plate Layout for Specimen 8E-4W-1.25-1.375-36 [Sumner, E. A., Mays, T. W., & Murray, T. M. (2000). Cyclic Testing of Bolted Moment End-Plate Connections. Blacksburg, VA: Virginia Polytechnic Institute and State University, Used with Permission of T.M. Murray, 2015] 54
Figure 4-8 Load-deformation behavior for Specimen 8E-4W-1.25-1.375-36 [Sumner, E. A., Mays, T. W., & Murray, T. M. (2000). Cyclic Testing of Bolted Moment End-Plate Connections. Blacksburg, VA: Virginia Polytechnic Institute and State University, Used with Permission of T.M. Murray, 2015] 55
Figure 4-9 End-plate separation for Specimen 8E-4W-1.25-1.375-36 [Sumner, E. A., Mays, T. W., & Murray, T. M. (2000). Cyclic Testing of Bolted Moment End-Plate Connections. Blacksburg, VA: Virginia Polytechnic Institute and State University, Used with Permission of T.M. Murray, 2015] 57
Figure 4-10 Bolt 2 strains for Specimen 8E-4W-1.25-1.375-36 [Sumner, E. A., Mays, T. W., & Murray, T. M. (2000). Cyclic Testing of Bolted Moment End-Plate Connections. Blacksburg, VA: Virginia Polytechnic Institute and State University, Used with Permission of T.M. Murray, 2015] 57
Figure 4-11 8E-4W-1-1/2-62 Specimen Dimensions [Sumner, E. A., & Murray, T. M. (2001). *Experimental Investigation of Four Bolt Wide Extended End-Plate Moment Connections.* Blacksburg, VA: Department of Civil Engineering, Virginia Polytechnic Institute and State University, Used with Permission of T.M. Murray, 2015] 59

Figure 4-12 End Plate Layout for Specimen 8E-4W-1-1/2-62 [Sumner, E. A., & Murray, T. M. (2001). *Experimental Investigation of Four Bolt Wide Extended End-Plate Moment Connections.* Blacksburg, VA: Department of Civil Engineering, Virginia Polytechnic Institute and State University, Used with Permission of T.M. Murray, 2015] 60
Figure 4-13 Load-deformation behavior for Specimen 8E-4W-1-1/2-62 [Sumner, E. A., & Murray, T. M. (2001). *Experimental Investigation of Four Bolt Wide Extended End-Plate Moment Connections.* Blacksburg, VA: Department of Civil Engineering, Virginia Polytechnic Institute and State University, Used with Permission of T.M. Murray, 2015] 61
Figure 4-14 End-Plate Separation for Specimen 8E-4W-1-1/2-62 [Sumner, E. A., & Murray, T. M. (2001). *Experimental Investigation of Four Bolt Wide Extended End-Plate Moment Connections.* Blacksburg, VA: Department of Civil Engineering, Virginia Polytechnic Institute and State University, Used with Permission of T.M. Murray, 2015] 62
Figure 4-15 Bolt forces for Specimen 8E-4W-1-1/2-62 [Sumner, E. A., & Murray, T. M. (2001). *Experimental Investigation of Four Bolt Wide Extended End-Plate Moment Connections.* Blacksburg, VA: Department of Civil Engineering, Virginia Polytechnic Institute and State University, Used with Permission of T.M. Murray, 2015] 63
Figure 4-16 8E-4W-3/4-3/4-62 Specimen Dimensions [Sumner, E. A., & Murray, T. M. (2001). *Experimental Investigation of Four Bolt Wide Extended End-Plate Moment Connections.* Blacksburg, VA: Department of Civil Engineering, Virginia Polytechnic Institute and State University, Used with Permission of T.M. Murray, 2015] 64
Figure 4-17 End Plate Layout for Specimen 8E-4W-3/4-3/4-62 [Sumner, E. A., & Murray, T. M. (2001). *Experimental Investigation of Four Bolt Wide Extended End-Plate Moment Connections.* Blacksburg, VA: Department of Civil Engineering, Virginia Polytechnic Institute and State University, Used with Permission of T.M. Murray, 2015] 65
Figure 4-18 Load-deformation behavior for Specimen 8E-4W-3/4-3/4-62 [Sumner, E. A., & Murray, T. M. (2001). *Experimental Investigation of Four Bolt Wide Extended End-Plate Moment Connections.* Blacksburg, VA: Department of Civil Engineering, Virginia Polytechnic Institute and State University, Used with Permission of T.M. Murray, 2015] 66
Figure 4-19 End-Plate Separation for Specimen 8E-4W-3/4-3/4-62 [Sumner, E. A., & Murray, T. M. (2001). *Experimental Investigation of Four Bolt Wide Extended End-Plate Moment*

Connections. Blacksburg, VA: Department of Civil Engineering, Virginia Polytechnic Institute and State University, Used with Permission of T.M. Murray, 2015] 67
Figure 4-20 Bolt forces for Specimen 8E-4W-3/4-3/4-62 [Sumner, E. A., & Murray, T. M. (2001). *Experimental Investigation of Four Bolt Wide Extended End-Plate Moment Connections.* Blacksburg, VA: Department of Civil Engineering, Virginia Polytechnic Institute and State University, Used with Permission of T.M. Murray, 2015] 68
Figure 4-21 8ES-1.25-1-30 Specimen Dimensions [Sumner, E. A., Mays, T. W., & Murray, T. M. (2000). *Cyclic Testing of Bolted Moment End-Plate Connections.* Blacksburg, VA: Virginia Polytechnic Institute and State University, Used with Permission of T.M. Murray, 2015] 73
Figure 4-22 End-Plate Layout for Specimen 8ES-1.25-1-30 [Sumner, E. A., Mays, T. W., & Murray, T. M. (2000). *Cyclic Testing of Bolted Moment End-Plate Connections.* Blacksburg, VA: Virginia Polytechnic Institute and State University, Used with Permission of T.M. Murray, 2015] 74
Figure 4-23 Load-deformation behavior for Specimen 8ES-1.25-1-30 [Sumner, E. A., Mays, T. W., & Murray, T. M. (2000). *Cyclic Testing of Bolted Moment End-Plate Connections.* Blacksburg, VA: Virginia Polytechnic Institute and State University, Used with Permission of T.M. Murray, 2015] 75
Figure 4-24 End-plate separation for Specimen 8ES-1.25-1-30 [Sumner, E. A., Mays, T. W., & Murray, T. M. (2000). *Cyclic Testing of Bolted Moment End-Plate Connections.* Blacksburg, VA: Virginia Polytechnic Institute and State University, Used with Permission of T.M. Murray, 2015] 76
Figure 4-25 Bolt 11 strains for Specimen 8ES-1.25-1-30 [Sumner, E. A., Mays, T. W., & Murray, T. M. (2000). *Cyclic Testing of Bolted Moment End-Plate Connections.* Blacksburg, VA: Virginia Polytechnic Institute and State University, Used with Permission of T.M. Murray, 2015] 77
Figure 4-26 8ES-0.875-0.75-24 Specimen Dimensions [Ghassemieh, M., Kukreti, A., and Murray, T.M. (1983) *Inelastic Finite Element Analysis of Stiffened End-Plate Moment Connections*, Report No. FSEL/AISC 8302, School of Civil Engineering and Environmental Science, University of Oklahoma, Norman, OK, Used with Permission of T.M. Murray, 2015] 78
Figure 4-27 End-Plate Layout for Specimen 8ES-0.875-0.75-24 [redrawn from Ghassemieh, M., Kukreti, A., and Murray, T.M. (1983) *Inelastic Finite Element Analysis of Stiffened End-*

Plate Moment Connections, Report No. FSEL/AISC 8302, School of Civil Engineering and Environmental Science, University of Oklahoma, Norman, OK, Used with Permission of T.M. Murray, 2015] 78
Figure 4-28 Moment-Deflection behavior for Specimen 8ES-0.875-0.75-24 [Ghassemieh, M., Kukreti, A., and Murray, T.M. (1983) *Inelastic Finite Element Analysis of Stiffened End-Plate Moment Connections*, Report No. FSEL/AISC 8302, School of Civil Engineering and Environmental Science, University of Oklahoma, Norman, OK, Used with Permission of T.M. Murray, 2015] 79
Figure 4-29 End-plate separation for Specimen 8ES-0.875-0.75-24 [Ghassemieh, M., Kukreti, A., and Murray, T.M. (1983) *Inelastic Finite Element Analysis of Stiffened End-Plate Moment Connections*, Report No. FSEL/AISC 8302, School of Civil Engineering and Environmental Science, University of Oklahoma, Norman, OK, Used with Permission of T.M. Murray, 2015] 80
Figure 4-30 Bolt forces for 8ES-0.875-0.75-24 [Ghassemieh, M., Kukreti, A., and Murray, T.M. (1983) *Inelastic Finite Element Analysis of Stiffened End-Plate Moment Connections*, Report No. FSEL/AISC 8302, School of Civil Engineering and Environmental Science, University of Oklahoma, Norman, OK, Used with Permission of T.M. Murray, 2015] 81
Figure 4-31 8ES-1.25-1.25-36 Specimen Dimensions [Sumner, E. A., Mays, T. W., & Murray, T. M. (2000). *Cyclic Testing of Bolted Moment End-Plate Connections.* Blacksburg, VA: Virginia Polytechnic Institute and State University, Used with Permission of T.M. Murray, 2015] 83
Figure 4-32 End-plate Layout for Specimen 8ES-1.25-1.25-36 [Sumner, E. A., Mays, T. W., & Murray, T. M. (2000). *Cyclic Testing of Bolted Moment End-Plate Connections.* Blacksburg, VA: Virginia Polytechnic Institute and State University, Used with Permission of T.M. Murray, 2015] 84
Figure 4-33 Load-deformation behavior for Specimen 8ES-1.25-1.25-36 [Sumner, E. A., Mays, T. W., & Murray, T. M. (2000). *Cyclic Testing of Bolted Moment End-Plate Connections.* Blacksburg, VA: Virginia Polytechnic Institute and State University, Used with Permission of T.M. Murray, 2015] 85
Figure 4-34 End-plate separation for Specimen 8ES-1.25-1.25-36 [Sumner, E. A., Mays, T. W., & Murray, T. M. (2000). *Cyclic Testing of Bolted Moment End-Plate Connections.* Blacksburg,

VA: Virginia Polytechnic Institute and State University, Used with Permission of T.M. Murray, 2015] 86
Figure 4-35 Bolt 3 strains for Specimen 8ES-1.25-1.25-36 [Sumner, E. A., Mays, T. W., & Murray, T. M. (2000). *Cyclic Testing of Bolted Moment End-Plate Connections.* Blacksburg, VA: Virginia Polytechnic Institute and State University, Used with Permission of T.M. Murray, 2015] 86
Figure 4-36 8ES-0.875-1-24 Specimen Dimensions [Ghassemieh, M., Kukreti, A., and Murray, T.M. (1983) *Inelastic Finite Element Analysis of Stiffened End-Plate Moment Connections*, Report No. FSEL/AISC 8302, School of Civil Engineering and Environmental Science, University of Oklahoma, Norman, OK, Used with Permission of T.M. Murray, 2015] 87
Figure 4-37 End-Plate Layout for Specimen 8ES-0.875-1-24 [redrawn from Ghassemieh, M., Kukreti, A., and Murray, T.M. (1983) *Inelastic Finite Element Analysis of Stiffened End-Plate Moment Connections*, Report No. FSEL/AISC 8302, School of Civil Engineering and Environmental Science, University of Oklahoma, Norman, OK, Used with Permission of T.M. Murray, 2015] 88
Figure 4-38 Load-deformation behavior for Specimen 8ES-0.875-1-24 [Ghassemieh, M., Kukreti, A., and Murray, T.M. (1983) *Inelastic Finite Element Analysis of Stiffened End-Plate Moment Connections*, Report No. FSEL/AISC 8302, School of Civil Engineering and Environmental Science, University of Oklahoma, Norman, OK, Used with Permission of T.M. Murray, 2015] 89
Figure 4-39 End-plate separation for Specimen 8ES-0.875-1-24 [Ghassemieh, M., Kukreti, A., and Murray, T.M. (1983) *Inelastic Finite Element Analysis of Stiffened End-Plate Moment Connections*, Report No. FSEL/AISC 8302, School of Civil Engineering and Environmental Science, University of Oklahoma, Norman, OK, Used with Permission of T.M. Murray, 2015] 90
Figure 4-40 Bolt forces for Specimen 8ES-0.875-1-24 [Ghassemieh, M., Kukreti, A., and Murray, T.M. (1983) *Inelastic Finite Element Analysis of Stiffened End-Plate Moment Connections*, Report No. FSEL/AISC 8302, School of Civil Engineering and Environmental Science, University of Oklahoma, Norman, OK, Used with Permission of T.M. Murray, 2015] 91
Figure 5-1 Sections of Beams Used for Testing 94

Figure 5-2 End-Plate for three configurations showing typical bolt to bolt pitch and gage distances 96
Figure 5-3 End-Plate Parameters for 6B-4W/2W Configuration 97
Figure 5-4 End-Plate Parameters for 12B-MRE 1/3-4W/2W Configuration 98
Figure 5-5 End-Plate Dimensions for 8ES Configuration 99
Figure 5-6 Picture of a Typical Deep Beam Test Setup 104
Figure 5-7 Half Diagram of Deep Beam Test Setup..... 105
Figure 5-8 Picture of a Typical Shallow Beam Test Setup..... 106
Figure 5-9 Half Diagram of Shallow Beam Test Setup..... 107
Figure 5-10 Typical Picture of Lateral Bracing..... 108
Figure 5-11 Picture Showing Calipers and String Potentiometer (Wirepot). 108
Figure 5-12 (a) Deep Beam Instrumentation Setup (b) Shallow Beam Instrumentation Setup.. 109
Figure 5-13 Location of Strain Gaged Bolts..... 110
Figure 5-14 Location of Calipers..... 111
Figure 5-15 Typical Time-lapse Camera Views..... 112
Figure 5-16 Results of Tensile Coupon Testing for 1 in. thick end-plate..... 115
Figure 5-17 Results of Tensile Coupon Testing for 0.75 in. thick end-plate..... 115
Figure 5-18 Results of Tensile Coupon Testing for 0.75 in. thick end-plate..... 116
Figure 5-19 Results of Tensile Coupon Testing for 1.00 in. thick end-plate..... 116
Figure 6-1 Applied Moment vs Midspan deflection for Specimen 6B-4W/2W-1.125-0.75-36. 121
Figure 6-2 End-plate separation for Specimen 6B-4W/2W-1.125-0.75-36..... 122
Figure 6-3 Bolt Forces for Specimen 6B-4W/2W-1.125-0.75-36 122
Figure 6-4 Three views of the Specimen 6B-4W/2W-1.125-0.75-36 at the start of the test..... 124
Figure 6-5 Three views of the specimen 6B-4W/2W-1.125-0.75-36 at the end of the test..... 125
Figure 6-6 Applied Moment vs Midspan deflection for Specimen 6B-4W/2W-0.875-1.00-36. 127
Figure 6-7 End-plate separation for Specimen 6B-4W/2W-0.875-1.00-36..... 128
Figure 6-8 Bolt Forces for specimen 6B-4W/2W-0.875-1.00-36..... 129
Figure 6-9 Three views of the Specimen 6B-4W/2W-0.875-1.00-36 at the start of the test..... 130
Figure 6-10 Three views of the specimen 6B-4W/2W-0.875-1.00-36 at the end of the test..... 131
Figure 6-11 Applied Moment vs Midspan deflection for Specimen 6B-4W/2W-1.125-0.75-60133
Figure 6-12 End-plate separation for Specimen 6B-4W/2W-1.125-0.75-60..... 134

Figure 6-13 Bolt Forces for specimen 6B-4W/2W-1.125-0.75-60 135
Figure 6-14 Three views of the Specimen 6B-4W/2W-1.125-0.75-60 at the start of the test 136
Figure 6-15 Three views of the specimen 6B-4W/2W-1.125-0.75-60 at the end of the test 137
Figure 6-16 Applied Moment vs Midspan deflection for Specimen 6B-4W/2W-0.875-1.00-60139
Figure 6-17 End-plate separation for Specimen 6B-4W/2W-0.875-1.00-60 140
Figure 6-18 Bolt Forces for specimen 6B-4W/2W-0.875-1.00-60 141
Figure 6-19 Three views of the Specimen 6B-4W/2W-0.875-1.00-60 at the start of the test 142
Figure 6-20 Three views of the specimen 6B-4W/2W-0.875-1.00-60 at the end of the test 143
Figure 6-21 Applied Moment vs Midspan deflection for Specimen 12B-MRE 1/3-4W/2W-1.00-0.75-36 147
Figure 6-22 End-plate separation for Specimen 12B-MRE 1/3-4W/2W-1.00-0.75-36 148
Figure 6-23 Bolt Forces for specimen 12B-MRE 1/3-4W/2W-1.00-0.75-36 149
Figure 6-24 Three views of the Specimen 12B-MRE 1/3-4W/2W-1.00-0.75-36 at the start of the test 150
Figure 6-25 Three views of the specimen 12B-MRE 1/3-4W/2W-1.00-0.75-36 and the yield lines seen, at the end of the test 151
Figure 6-26 Applied Moment vs Midspan deflection for Specimen 12B-MRE 1/3-4W/2W-0.75-1.00-36 153
Figure 6-27 End-plate separation for Specimen 12B-MRE 1/3-4W/2W-0.75-1.00-36 154
Figure 6-28 Bolt Forces for specimen 12B-MRE 1/3-4W/2W-0.75-1.00-36 155
Figure 6-29 Three views of the Specimen 12B-MRE 1/3-4W/2W-0.75-1.00-36 at the start of the test 156
Figure 6-30 Three views of the specimen 12B-MRE 1/3-4W/2W-0.75-1.00-36 at the end of the test 157
Figure 6-31 Twisting of the Specimen Viewed from the two ends of the specimen 159
Figure 6-32 Applied Moment vs Midspan deflection for Specimen 12B-MRE 1/3-4W/2W-1.00-0.75-60 160
Figure 6-33 End-plate separation for Specimen 12B-MRE 1/3-4W/2W-1.00-0.75-60 (Caliper 1 and 2) 162
Figure 6-34 End-plate separation for Specimen 12B-MRE 1/3-4W/2W-1.00-0.75-60 (Caliper 3 and 4) 162

Figure 6-35 Bolt Forces for specimen 12B-MRE 1/3-4W/2W-1.00-0.75-60 (Bolt 1, 2 and 3) . 163
Figure 6-36 Bolt Forces for specimen 12B-MRE 1/3-4W/2W-1.00-0.75-60 (Bolt 4, 5 and 6) 163
Figure 6-37 Three views of the Specimen 12B-MRE 1/3-4W/2W-1.00-0.75-60 at the start of the test 164
Figure 6-38 Three views of the specimen 12B-MRE 1/3-4W/2W-1.00-0.75-60 and zoomed in views of the connection to show any yield lines, at the end of the test 165
Figure 6-39 Applied Moment vs Midspan deflection for Specimen 12B-MRE 1/3-4W/2W-0.75-1.00-60 167
Figure 6-40 End-plate separation for Specimen 12B-MRE 1/3-4W/2W-0.75-1.00-60..... 168
Figure 6-41 Bolt Forces for specimen 12B-MRE 1/3-4W/2W-0.75-1.00-60..... 169
Figure 6-42 Three views of the Specimen 12B-MRE 1/3-4W/2W-0.75-1.00-60 at the start of the test 170
Figure 6-43 Three views of the specimen 12B-MRE 1/3-4W/2W-0.75-1.00-60 at the end of the test 171
Figure 6-44 Twisting of the Specimen Viewed from one end of the specimen 175
Figure 6-45 Applied Moment vs Midspan deflection for Specimen 8ES-1.25-0.75-56..... 176
Figure 6-46 End-plate separation for Specimen 8ES-1.25-0.75-56..... 177
Figure 6-47 Bolt Forces for specimen 8ES-1.25-0.75-56..... 178
Figure 6-48 Three views of the Specimen 8ES-1.25-0.75-56 at the start of the test 179
Figure 6-49 Three views of the specimen 8ES-1.25-0.75-56 and zoomed in views of the connection to show any yield lines, at the end of the test 180
Figure 6-50 Applied Moment vs Midspan deflection for Specimen 8ES-1.00-1.00-56..... 182
Figure 6-51 End-plate separation for Specimen 8ES-1.00-1.00-56..... 183
Figure 6-52 Bolt Forces for specimen 8ES-1.00-1.00-56..... 184
Figure 6-53 Three views of the Specimen 8ES-1.00-1.00-56 at the start of the test 185
Figure 6-54 Three views of the specimen 8ES-1.00-1.00-56 and zoomed in views to show local yielding around the bolts, at the end of the test 186

LIST OF TABLES

Table 3-1 Rotation of the Yield Line for 8E-4W configuration 17
Table 3-2 Energy Stored in Each Yield Line for 8E-4W Configuration 18
Table 3-3 Summary of Design Procedures for Eight Bolt Extended Four Wide Unstiffened..... 21
Table 3-4 Rotation of the Yield Line for 8ES Configuration 24
Table 3-5 Energy Stored in Each Yield Line for 8ES Configuration 25
Table 3-6 Summary of Design Procedures for Eight Bolt Extended Stiffened 29
Table 3-7 Rotation of the Yield Line for 6B-4W/2W Configuration 32
Table 3-8 Energy Stored in Each Yield Line for 6B-4W/2W Configuration 33
Table 3-9 Summary of Design Procedures for Six Bolt Flush Four Wide/Two Wide Unstiffened 36
Table 3-10 Rotation of the Yield Line for 12B-MRE 1/3-4W/2W Configuration 39
Table 3-11 Energy Stored in Each Yield Line for 12B-MRE 1/3-4W/2W Configuration..... 40
Table 3-12 Summary of Design Procedures for Twelve Bolt Multiple Row Extended Four Wide/Two Wide Unstiffened..... 44
Table 4-1 Summary of Experimental Work..... 46
Table 4-2 Predicted and Experimentally Obtained Moment Capacities for Specimen 8E-4W-1.25-1-30 51
Table 4-3 Predicted and Experimentally Obtained Moment Capacities for Specimen 8E-4W-1.25-1.375-36 56
Table 4-4 Predicted and Experimentally Obtained Moment Capacities for Specimen 8E-4W-1-1/2-62..... 61
Table 4-5 Predicted and Experimentally Obtained Moment Capacities for Specimen 8E-4W-3/4-3/4-62 66
Table 4-6 Summary of the Four Test Specimens (from literature) of the Eight Bolt Extended Four Wide Configuration 69
Table 4-7 Summary of Experiments on the Eight Bolt Extended Stiffened Configuration 71
Table 4-8 Predicted and Experimentally Obtained Moment Capacities 8ES-1.25-1-30 75
Table 4-9 Predicted and Experimentally Obtained Moment Capacities 8ES-0.875-0.75-24 80

Table 4-10 Predicted and Experimentally Obtained Moment Capacities for Specimen 8ES-1.25-1.25-36 84
Table 4-11 Predicted and Experimentally Obtained Moment Capacities for Specimen 8ES-0.875-1-24 89
Table 4-12 Summary of Four Test Specimens (from literature) of Eight Bolt Extended Stiffened Configuration 92
Table 5-1 Test Matrix 100
Table 5-2 Summary of Tensile Coupon Tests 114
Table 5-3 Summary of A325 Bolt Material Testing Reports 117
Table 6-1 Predicted and Experimentally Obtained Moment Capacities for Specimen 6B-4W/2W-1.125-0.75-36 120
Table 6-2 Predicted and Experimentally Obtained Moment Capacities for Specimen 6B-4W/2W-0.875-1.00-36 127
Table 6-3 Predicted and Experimentally Obtained Moment Capacities for Specimen 6B-4W/2W-1.125-0.75-60 133
Table 6-4 Predicted and Experimentally Obtained Moment Capacities for Specimen 6B-4W/2W-0.875-1.00-60 139
Table 6-5 Summary of the Four Test Specimens of the Six Bolt Flush Unstiffened Configuration 144
Table 6-6 Predicted and Experimentally Obtained Moment Capacities for Specimen 12B-MRE 1/3-4W/2W-1.00-0.75-36 148
Table 6-7 Predicted and Experimentally Obtained Moment Capacities for Specimen 12B-MRE 1/3-4W/2W-0.75-1.00-36 154
Table 6-8 Predicted and Experimentally Obtained Moment Capacities for Specimen 12B-MRE 1/3-4W/2W-1.00-0.75-60 161
Table 6-9 Predicted and Experimentally Obtained Moment Capacities for Specimen 12B-MRE 1/3-4W/2W-0.75-1.00-60 167
Table 6-10 Summary of the Four Test Specimens of the Twelve Bolt Extended Unstiffened Configuration 172
Table 6-11 Predicted and Experimentally Obtained Moment Capacities for Specimen 8ES-1.25-0.75-56 176

Table 6-12 Predicted and Experimentally Obtained Moment Capacities for Specimen 8ES-1.00-1.00-56 182
Table 6-13 Summary of the Two Test Specimens of the Eight Bolt Extended Unstiffened Configuration 187

1 INTRODUCTION

1.1 Motivation for Thesis

In the United States, end-plate moment connections are commonly used in the low rise metal building industry. An end-plate connection is generally a rigid connection between a rafter and column or between two segments of a rafter (sometimes referred to as a splice plate connection). End-plate connections can be further subdivided into extended and flush end plates depending on whether the end plate extends beyond the beam flanges or not. Further, these could be stiffened or unstiffened connections where the possible location of stiffeners could be in the web for a flush configuration or outside the flange for an extended configuration. This categorization is shown in AISC Design Guide 16 (Murray and Shoemaker, 2002).

Over the past three decades, there have been numerous analytical and experimental studies validating the design procedures and performance of these connections. A partial summary of testing and development of design procedures is presented in (Murray and Shoemaker, 2002) and (Murray, 1988). Based on previous testing and development, AISC Design Guide 16 included a total of nine end plate configurations. For flush end-plate connections, these include the two-bolt unstiffened, four-bolt unstiffened, four-bolt stiffened with web gusset plate between the tension bolt rows, and four-bolt stiffened with web gusset plate outside the tension bolt rows configuration. The extended end-plate configurations include the four-bolt unstiffened, four-bolt stiffened, multiple row 1/2 unstiffened, multiple row 1/3 unstiffened, and the multiple row 1/3 stiffened connection.

Additionally, there was interest by metal building manufacturers in having end-plate connection configurations made available with larger moment capacity. This will allow more flexibility for the pre-engineered metal building industry in the design, detailing, and construction of end-plate connections. It was this motivation that this research project was undertaken in conjunction with the Metal Building Manufacturers Association (MBMA).

1.2 Scope of Research

The goal of the proposed research is to:

- Propose design procedures for two new configurations, conduct an experimental program and validate the design procedures with the experimental results obtained.
- Propose and validate design procedures for two previously tested configurations.

The scope of work is organized into four phases as follows:

1.2.1 **Select Design Configurations**

Four configurations (shown in Figure 1-1) were selected based on the input of the steering committee organized by MBMA and the literature review of the tests done till date for the extended end plate moment connections. These four configurations were:

1. Eight Bolt Extended Four Wide Unstiffened (8E-4W)
2. Eight Bolt Extended Stiffened (8ES)
3. Six Bolt Flush Four Wide/Two Wide Unstiffened (6B-4W/2W)
4. Twelve Bolt Multiple Row Extended Four Wide/Two Wide Unstiffened (12B-MRE 1/3-4W/2W)

Out of these four configurations, it was determined that the experimental results from previous tests for 8E-4W supported the design procedures. Also, the test data for another connection configuration, 8ES, supported the design procedures for shallow beam depths but a need was felt to investigate connections for a deep beam. The validation of both these configuration is discussed in Chapter 4. Further, two more configurations were examined for which there were no previous tests found in the literature. These were 6B-4W/2W and MRE 1/3 4W/2W configurations.

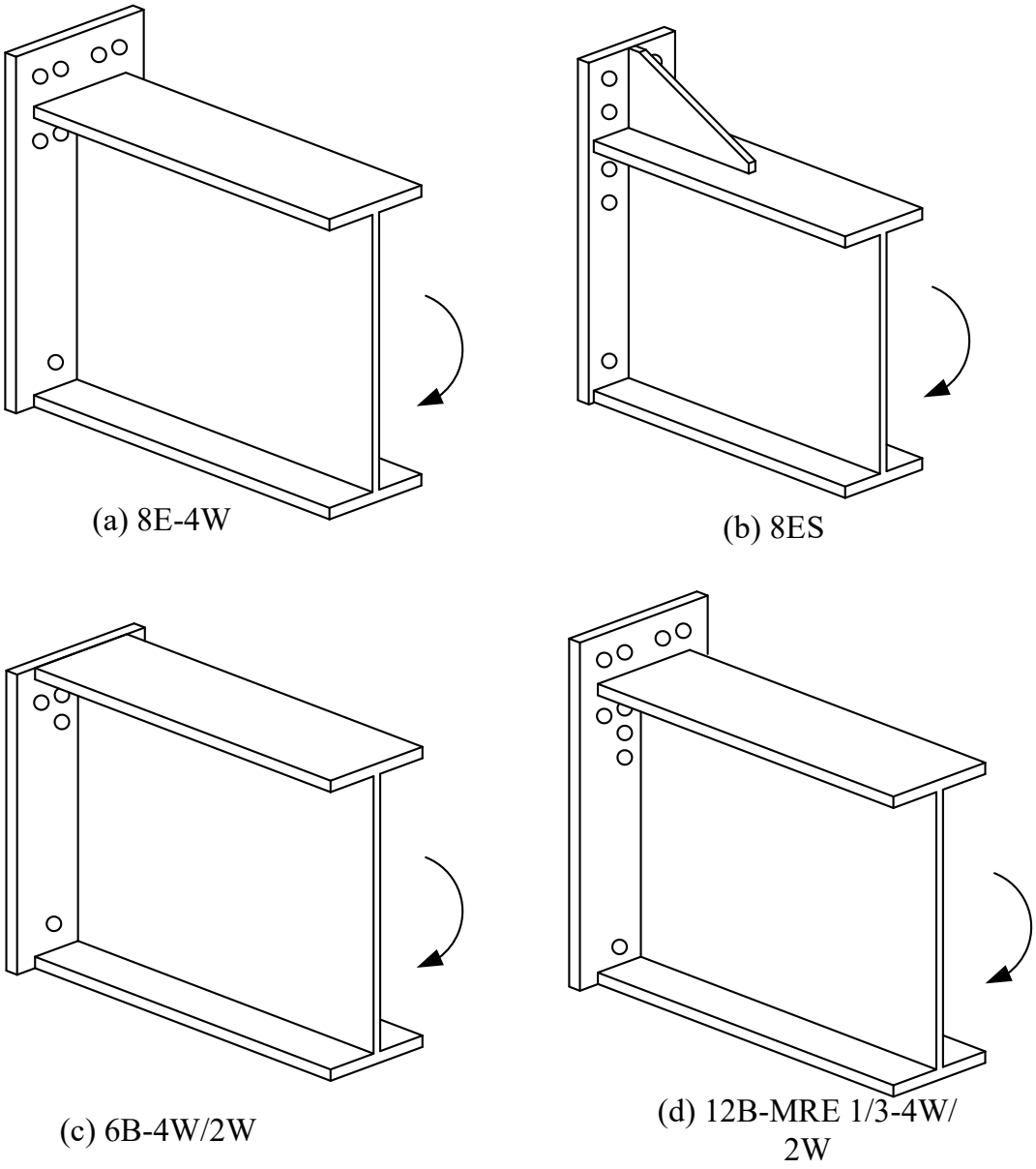

(a) 8E-4W

(b) 8ES

(c) 6B-4W/2W

(d) 12B-MRE 1/3-4W/ 2W

Note: Two Bolts shown near the compression flange are just representative. The actual number of bolts will depend on the loading and calculations.

Figure 1-1 Selected Design Configurations

1.2.2 **Design Procedure and Limit States**

The limit states investigated were bolt rupture with prying (M_q), bolt rupture without prying (M_{np}), and end-plate yielding (M_{pl}). The design procedure for thick end-plate behavior assumes that bolts rupture without any prying action or end-plate yielding, whereas, the

design procedure for thin end-plate behavior assumes that end-plates yield first, followed by bolt rupture with prying action. The limit state associated with thick plate behavior is M_{np} and the limit state associated with thin plate behavior is M_{pl} followed by M_q.

A likely yield line mechanism for the end-plate was identified and related moment capacity associated with end-plate yielding (M_{pl}) was derived. Also, bolt force models were developed to predict the limit states associated with bolt rupture, namely, bolt rupture with prying (M_q) and bolt rupture without prying (M_{np}). Therefore, equations were derived for end plate yielding (M_{pl}) assuming a particular yield line mechanism. Also, M_q and M_{np} were calculated based on the tensile strength of the bolts.

1.2.3 Validating Design Procedures Based on Existing Test Data

For configurations with previous test results (8E-4W and 8ES), the predicted limit states for thin plate and thick plate were compared to the experimental results available.

1.2.4 Full-Scale Tests

Ten full-scale tests were done for three configurations, four tests each for 6B-4W/2W and 12B-MRE 1/3-4W/2W, and two for 8ES configuration. Each test specimen consisted of two built-up beam sections spliced together at midspan using A325 bolts. Each built-up beam had a thick end-plate and a thin end-plate at each end, so that it could be used for two tests.

The shallow built-up beam sections were 3 ft. deep with 3/4 in. by 12 in. flanges and a 1/4 in. thick web. The deep built-up beams were of two types. Firstly, for the 6B-4W/2W and 12B-MRE 1/3-4W/2W configuration, beam section was 5 ft. deep with 3/4 in. by 12 in. flanges and a 3/8 in. thick web. Secondly, for the 8ES connection, beam section was 56 in. deep with 1 in. by 10 in. flanges and a 1/2 in. thick web.

1.3 Thesis Organization

This research is organized into the following chapters:

- Chapter 1 discusses the motivation for research, the scope of the project and thesis organization.
- Chapter 2 consists of a literature review of end-plate moment connections with particular emphasis on the design procedures for configurations included in Design Guide 16.
- Chapter 3 puts light on the yield line solutions and the bolt force models derived for the four configurations. It also tries to correct the yield line solutions already presented in other literature related to these configurations.
- Chapter 4 is on the validation of connection configurations based on previous test results available from the literature. Two configurations (8E-4W and 8ES) are discussed in this chapter.
- Chapter 5 describes the experimental setup for two new configurations (6B-4W/2W and 12B-MRE 1/3-4W/2W) and for the 8ES configuration. It delves into the instrumentation, the drawings of the setup and tensile coupon test results for the end-plate material.
- Chapter 6 presents the results from the ten tests and these are compared to the predicted limit states.
- Chapter 7 presents a summary and conclusions of the four test configurations investigated.

2 LITERATURE REVIEW

This chapter presents a review of the existing end-plate moment connections, their design and testing. It emphasizes on the configurations, design approach and supporting tests that are included in the Design Guide 16.

2.1 Design Guide 16 Background

There are nine configurations already included in the Design Guide 16 (Murray and Shoemaker, 2002). The scope of the design guide is to provide design procedures for the connection configurations included. These configurations are either flush end-plate connections or extended end-plate configurations. The division into extended and flush end-plates depends on whether the end-plate extends beyond the beam flanges or not. The flush configurations are either two-bolt or four-bolt connections on the tension side of the flange. Further, these could be stiffened or unstiffened. These are shown below in Figure 2-1.

Also, there are five extended end-plate configurations that are included. Again, the end-plate could be stiffened or unstiffened thereby giving a different configuration set. They are shown below in Figure 2-2:

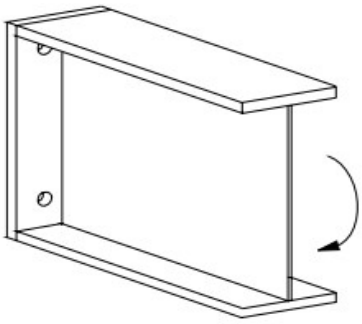

(a) Two Bolt Unstiffened

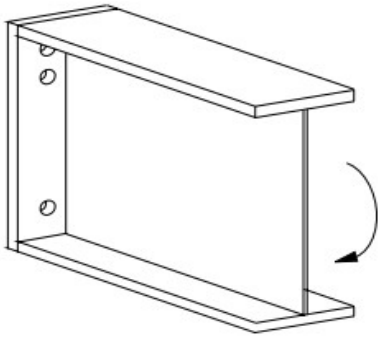

(b) Four Bolt Unstiffened

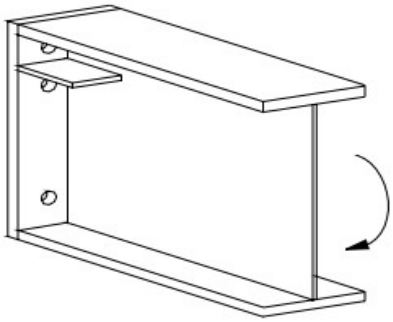

(c) Four Bolt Stiffened with web Gusset Plate Between the Tension Bolts

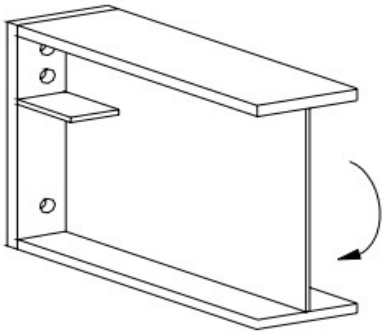

(d) Four Bolt Stiffened with Web Gusset Plate Outside the Tension Bolts

Figure 2-1 Flush End-Plate Connections (Murray, T. M., & Shoemaker, W. L. (2002). Flush and Extended Multiple-Row Moment End-Plate Connections. AISC, Used under fair use)

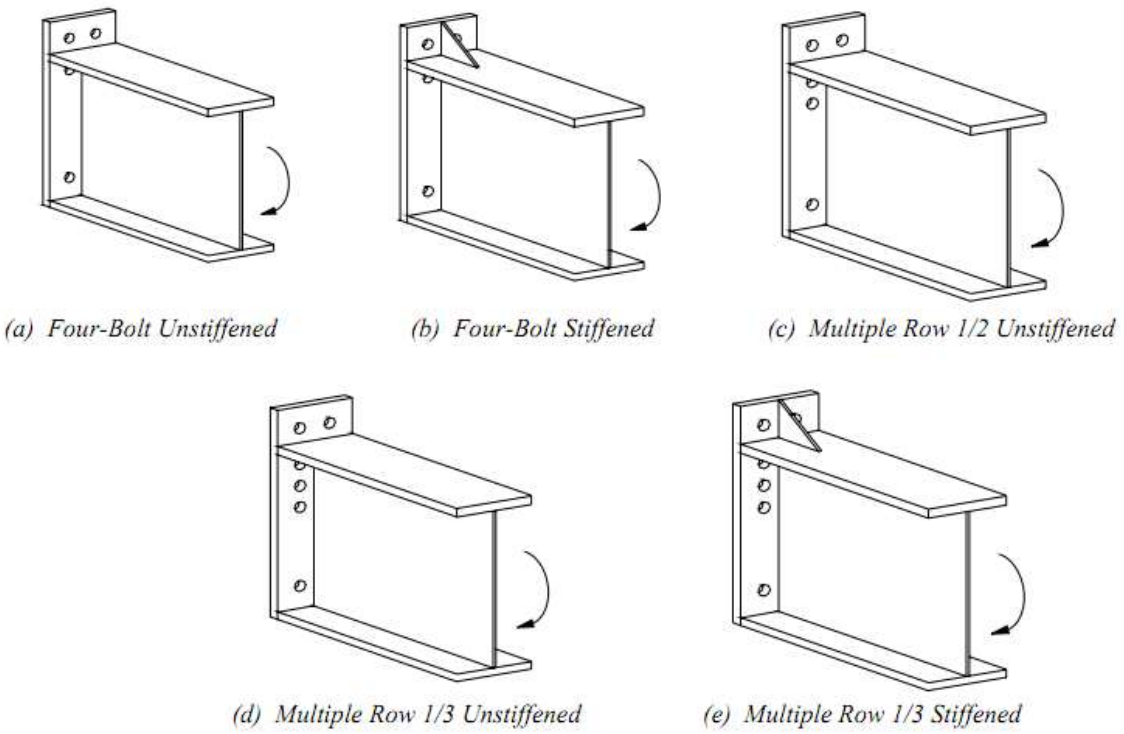

Figure 2-2 Extended End-Plate Connections (Murray, T. M., & Shoemaker, W. L. (2002). Flush and Extended Multiple-Row Moment End-Plate Connections. AISC, Used under fair use)

2.2 Design Methodology

The design procedure as mentioned in section 2.5 of the Design Guide 16 has been followed. The design procedure is divided into two categories:

2.2.1 **Design Steps for Thick End-Plate Behavior**

The design procedure for thick end-plate assumes that bolts rupture without any prying action or end-plate yielding. Thick end-plate design results in thicker end-plate and smaller diameter bolts. The design steps are:

1. Compute the required bolt diameter, $d_{b,reqd} = \sqrt{\frac{2M_u}{\pi\phi F_t\left(\sum d_n\right)}}$, and the moment capacity at bolt rupture without prying action, $M_{np} = \phi\left(2P_t\left(\sum d_n\right)\right)$

where, d_b = nominal bolt diameter

M_u = required flexural strength of the connection

F_t = nominal tensile strength of the bolt material

d_n = distance from the centerline of the nth tension bolt row to the center of the compression flange

$\phi = 0.75$

M_{np} = connection strength based on bolt tension rupture without prying

$P_t = \pi d_b^2 F_t / 4$

2. Find out the required thickness of end-plate, $t_{p,reqd} = \sqrt{\frac{\gamma \phi M_{np}}{0.9 \phi_b F_{py} Y}}$, and the moment capacity for end-plate yielding, $M_{pl} = F_{py} t_p^2 Y$

where, $\phi_b = 0.90$, bending resistance factor

$\gamma = 1.25$ for flush end-plates and 1.0 for extended end-plates

F_{py} = end-plate material yield stress

Y = yield-line mechanism parameter explained in Chapter 3

ϕM_{np} = design strength of the connection based on bolt tension rupture with no prying action

2.2.2 **Design Steps for Thin End-Plate Behavior**

The design procedure for thin end-plate assumes that end-plate yields first and then the bolts rupture with prying action. Thin end-plate design results in thinner end-plate with larger diameter bolts. The design steps are:

1. Compute the required end-plate thickness, $t_{p,reqd} = \sqrt{\frac{\gamma M_u}{\phi_b F_{py} Y}}$ and the end-plate yielding moment, $M_{pl} = F_{py} t_p^2 Y$
2. Select a trial bolt diameter, d_b, and calculate the maximum prying force.

A modified version of the Kennedy method (Kennedy, Vinnakota, & Sherbourne, 1981) was used to determine tension bolt forces and prying forces. The Kennedy method uses the split-tee analogy. At a lesser load, the end-plate behaves like a "thick plate", as if no plastic hinges have been formed. As the load increases and the bolts haven't failed yet, plastic hinges are formed at the intersection of the face of the web and centerline of the end-plate at the level of the bolts. This is called as the "intermediate plate behavior". As the connection is loaded even more and still the bolts haven't ruptured, two additional plastic hinges are formed at the intersection of the bolt centerline and end-plate centerline and after this point the end-plate behaves like a "thin plate". Prying force is generally assumed to be zero at the thick plate limit, increasing in the intermediate stage and then keeping constant in the last stage.

The prying force for bolts depends on whether they are inside the flange or outside the flange. Hence, it is divided into two categories as described below:

Case I: Bolts inside the flange.

This applies to all the bolts in a flush end-plate connection and the interior bolts of an extended end-plate connection. Maximum prying force for this condition is:

$$Q_{\max,i} = \frac{w' t_p^2}{4a_i}\sqrt{F_{py}^2 - 3\left(\frac{F_i'}{w' t_p}\right)^2}$$

where,

$$w' = b_p/2 - (d_b + 1/16)$$

$$a_i = 3.62\left(\frac{t_p}{d_b}\right)^3 - 0.085$$

$$F_i' = \frac{t_p^2 F_{py}\left(0.85\frac{b_p}{2} + 0.80w'\right) + \frac{\pi d_b^3 F_t}{8}}{4p_{f,i}}$$

Case II: Bolts outside the flange.

This applies to the bolts outside the flange in an extended end-plate connection. Maximum prying force for this condition is:

$$Q_{\max,o} = \frac{w' t_p^2}{4a_o}\sqrt{F_{py}^2 - 3\left(\frac{F_o'}{w' t_p}\right)^2}$$

where,

$w' = b_p/2 - (d_b + 1/16)$

$$a_o = \min\left|\begin{array}{l} 3.62\left(\frac{t_p}{d_b}\right)^3 - 0.085 \\ p_{ext} - p_{f,o} \end{array}\right.$$

$$F_o' = \frac{t_p^2 F_{py}\left(0.85\frac{b_p}{2} + 0.80w'\right) + \frac{\pi d_b^3 F_t}{8}}{4p_{f,o}}$$

3. Calculate the connection design strength for the limit state of bolt rupture with prying action

   a. For a flush connection:

$$\phi M_q = \max\left|\begin{array}{l} \phi\left[2\left(P_t - Q_{\max,i}\right)\left(d_1 + d_2\right)\right] \\ \phi\left[2\left(T_b\right)\left(d_1 + d_2\right)\right] \end{array}\right.$$

   b. For an extended connection:

$$\phi M_q = \max \begin{vmatrix} \phi\left[2\left(P_t - Q_{\max,o}\right)d_0 + 2\left(P_t - Q_{\max,i}\right)\left(d_1 + d_3\right) + 2T_b d_2\right] \\ \phi\left[2\left(P_t - Q_{\max,o}\right)d_0 + 2T_b\left(d_1 + d_2 + d_3\right)\right] \\ \phi\left[2\left(P_t - Q_{\max,i}\right)\left(d_1 + d_3\right) + 2T_b\left(d_0 + d_2\right)\right] \\ \phi\left[2T_b\left(d_0 + d_1 + d_2 + d_3\right)\right] \end{vmatrix}$$

where, $\varphi = 0.75$

$P_t = \pi d_b^2 F_t / 4$

d_i = distance from the centerline of each tension bolt row to the center of the compression flange

T_b = minimum bolt pretension specified in Table J3.1 of AISC LRFD

Y = yield-line mechanism parameter explained in Chapter 3

ϕM_{np} = design strength of the connection based on bolt tension rupture with no prying action

2.3 Typical Experimental Validation

Each configuration included in the Design Guide 16 had its design procedures validated by testing. A configuration was considered validated by examining the test data available in the literature and comparing this data with the calculated values for different limit states. For example, the configuration Multiple Row Extended 1/2 Unstiffened (MRE 1/2) was validated by using experimental data from eight different tests available in Abel and Murray (1992) and Sumner and Murray (2001). All these tests were subjected to monotonic loading and consisted of two built-up beams spliced together at the midspan using bolts. It was made sure that the test data used for validation was for a range of design variables such as the depth of the beam, bolt pitch, bolt gage etc. A general rule of thumb followed to validate a design configuration consisted of the following four possible combinations:

- Shallow beam with thin end-plate behavior
- Shallow beam with thick end-plate behavior

- Deep beam with thin end-plate behavior
- Deep beam with thick end-plate behavior

3 PROPOSED DESIGN PROCEDURES

The general design methodology has been presented in Chapter 2. This chapter deals with the design procedures used specifically for each of the four connection configurations investigated. The following sections focus on assumptions and equations pertaining to limit states of connection, namely, end-plate yield moment (M_{pl}), moment associated with bolt rupture without prying (M_{np}) and moment associated with bolt rupture with prying (M_q).

A likely yield line mechanism was identified for each configuration and analysis was carried out to determine the predicted yield strength of the end-plate. Also, bolt force models were developed for each configuration to predict the moments associated with bolt rupture with or without prying. Both of them are presented in following sections for the four configurations examined.

Thick end-plate behavior is characterized by bolt rupture without prying action. Thin end-plate behavior is characterized by end-plate yielding leading to bolt rupture with prying action. Tests should be conducted on a range of rafter depths for each type of behavior to show that the design procedure is valid over that range of rafter depths.

It is to be noted that while calculating the moment capacity for bolt rupture with prying action, M_q, the maximum value obtained from different equations has been used as M_q. This is counterintuitive, because generally the minimum value is used for design purposes. However, the minimum value for design purposes is used while comparing different limit states not within a single limit state. A possible explanation of using the maximum values out of the different equations could be: Before loading the specimen, the bolts are pre-tensioned to a certain specified value. As the bottom flange of the specimen is loaded in tension, the connection decompresses and as a result, fully overcomes the compression force in the connection due bolt pretension. This is one of the equation that is used in the bolt force model. When this stage is reached, the connection still has more strength and keeps on taking more load, engaging some other equations which take into account the

prying forces as well. At this stage, a bolt row undergoes prying because of end-plate yielding, and as the loading is increased, some other bolt rows also undergo prying and finally, the connection fails. The order of the stages, mentioned in the discussion, could be interchanged, but the connection won't fail until it has undergone through all the stages. Since, the connection fails at the maximum moment, therefore, it is logical to use the maximum value from different equations.

Another, important point to be noted while using these design procedures is that they have been formulated assuming that the connection carries only moment, and no shear. In practical applications, there would be shear forces in the connection, but this shear could be taken by the bolts on the compression side of the connection. To check the connection for shear separate calculations will have to be made.

3.1 Eight Bolt Extended Four Wide Unstiffened (8E-4W)

3.1.1 **Yield Line Analysis**

The yield line mechanism considered for the configuration is shown in Figure 3-1. The end-plate has been divided into six panels, formed due to yield lines. The rotation of each panel has been shown in Table 3-1 and energy stored in each yield line has been illustrated in Table 3-2.

The yield line mechanism shown is valid only if $p_{f,i}\ and\ s > e$, otherwise an alternate yield line mechanism would control. Also for the shown yield line mechanism to control, $h \gg 2p_{f,i}$, otherwise the yield lines will overlap with the row of bolts on the compression side.

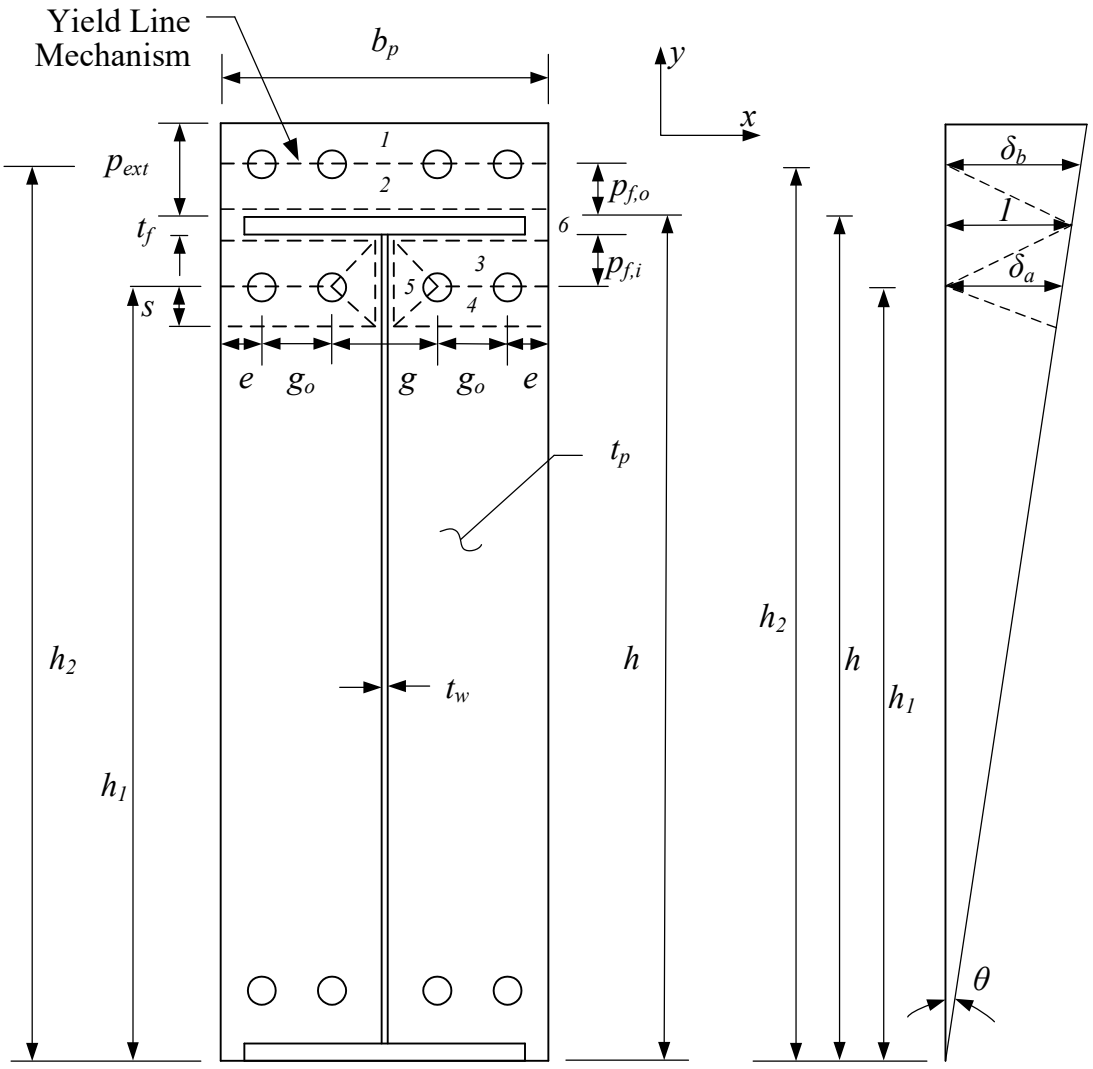

Figure 3-1 Yield Line Mechanism for 8E-4W configuration

Note: Four bolts shown on the compression side of the flange are just representative. In general, the number of bolts on the compression side will depend on the loading and calculations.

Table 3-1 Rotation of the Yield Line for 8E-4W configuration

Panel	θ_{nx}	θ_{ny}
1	0	0
2	$\frac{-(\delta_b - \theta(p_{f,o}))}{p_{f,o}}$	0
3	$\frac{-(\delta_a - \theta(p_{f,i}))}{p_{f,i}}$	0
4	$\frac{-(\delta_a - \theta s)}{s}$	0
5	θ	$\frac{2\delta_a - \theta(s - p_{f,i}))}{g}$
6	θ	0

Table 3-2 Energy Stored in Each Yield Line for 8E-4W Configuration

Yield Line	Energy Stored
$W_{i\text{-}1/2}$	$m_p b_p \left(\frac{\delta_b - \theta(p_{f,o})}{p_{f,o}}\right)$
$W_{i\text{-}2/6}$	$m_p b_p \left(\frac{\delta_b - \theta(p_{f,o})}{p_{f,o}} + \theta\right)$
$W_{i\text{-}6/3}$	$m_p \frac{(b_p)}{2}\left(\frac{\delta_a + \theta(p_{f,i})}{p_{f,i}} - \theta\right)$
$W_{i\text{-}3/4}$	$m_p \frac{(b_p - g)}{2}\left(\frac{\delta_a + \theta(p_{f,i})}{p_{f,i}} + \frac{\delta_a - \theta s}{s}\right)$
$W_{i\text{-}3/5}$	$m_p \frac{g}{2}\left(\frac{\delta_a + \theta(p_{f,i})}{p_{f,i}} - \theta\right) + m_p(p_{f,i})\left(\frac{2\delta_a - \theta(s - p_{f,i})}{g}\right)$
$W_{i\text{-}4/5}$	$m_p \frac{g}{2}\left(\theta + \frac{(\delta_a - \theta s)}{s}\right) + m_p(s)\left(\frac{2\delta_a - \theta(s - p_{f,i})}{g}\right)$
$W_{i\text{-}4/6}$	$m_p \frac{(b_p)}{2}\left(\theta + \frac{(\delta_a - \theta s)}{s}\right)$
$W_{i\text{-}5/6}$:	$m_p(p_{f,i} + s)\left(2\delta_a - \theta\frac{(s - p_{f,i})}{g}\right)$

Also, $\delta_a = h_1\,\theta$, $\delta_b = h_2\,\theta$, $1 = h\,\theta$

The sum of internal work done, $\sum W_i =$ total energy stored in the yield lines.

Therefore, on adding the equations presented in Table 3-2 and simplifying them,

$$\sum W_i = 2m_p b_p \theta\left(\frac{h_2}{p_{f,o}} + \frac{h_1}{p_{f,i}} + \frac{h_1}{s} - \frac{1}{2}\right) - 2m_p t_w \theta\left(\frac{h_1}{p_{f,i}} + \frac{h_1}{s}\right) + \frac{4m_p\theta}{g}\left(2h_1 - s - p_{f,i}\right)\left(p_{f,i} + s\right) \quad \textbf{(3-1)}$$

To determine the dimension s, differentiate $\sum W_i$ w.r.t. s

$$\Rightarrow \frac{d(\sum W_i)}{ds} = 0$$

$$\therefore s = \frac{1}{2}\sqrt{b_p g} \quad \textbf{(3-2)}$$

The plastic moment capacity of the end-plate is directly proportional to the yield line parameter, Y, and to calculate Y:

External Work done, $W_e = M_u\theta = M_n\theta$

Also, $m_p = F_y \frac{t_p^2}{4} \quad \Rightarrow W_i = 2F_y \frac{t_p^2}{4}\theta\ [Y]$

Equating $W_e = W_i$, and plugging in the value of s in W_i and finding out the yield line parameter, Y

$$Y = \frac{b_p}{2}\left[\frac{h_2}{p_{f,o}} + \frac{h_1}{p_{f,i}} + \frac{h_1}{s} - \frac{1}{2}\right] + 2(p_{f,i} + s)\left[\frac{h_1}{g}\right] \quad \textbf{(3-3)}$$

The yield line parameter equation matches that as predicted by Sumner and Murray (2001).

$$\phi M_{pl} = \phi F_{py} t_p^2 Y,\ \phi = 0.9 \quad \textbf{(3-4)}$$

3.1.2 **Bolt Force Model**

3.1.2.1 Thick Plate Model

The thick plate model simply considers the nominal tensile strength of the bolt times the lever arm.

$$\phi M_{np} = \phi[4P_t(d_0 + d_1)]\ ,\quad \phi = 0.75 \quad \textbf{(3-5)}$$

3.1.2.2 Thin Plate Model

The thin plate model considers a combination of prying forces at the bolt row levels and since there are two bolt rows which may or not go undergo prying action, we have four bolt force equations. Also, it has been experimentally observed that the outer bolts in a row as compared to the inner bolts, contribute lesser towards the moment capacity of the connection. This factor is taken into account by using bolt distribution factors, $\alpha\ and\ \beta$, which have been calibrated based on experimental results and the values of these are mentioned as below.

$$\phi M_q = max \begin{vmatrix} \phi \begin{bmatrix} \{2\alpha_1(P_t - Q_{max,o,1}) + 2\alpha_2(P_t - Q_{max,o,2})\}d_0 + \\ \{2\beta_1(P_t - Q_{max,i,1}) + 2\beta_2(P_t - Q_{max,i,2})\}d_1 \end{bmatrix} \\ \phi[\{2\alpha_1(P_t - Q_{max,o,1}) + 2\alpha_2(P_t - Q_{max,o,2})\}d_0 + \{2T_b(\beta_1 + \beta_2)\}d_1] \\ \phi[\{2T_b(\alpha_1 + \alpha_2)\}d_0 + \{2\beta_1(P_t - Q_{max,i,1}) + 2\beta_2(P_t - Q_{max,i,2})\}d_1] \\ \phi[2T_b\{(\alpha_1 + \alpha_2)d_0 + (\beta_1 + \beta_2)d_1\}] \end{vmatrix}$$

(3-6)

where,

$\phi = 0.75$

T_b = specified bolt pretension load

$\alpha_1 = 1.0$ (outside row, inner columns), $\alpha_2 = 0.5$ (outside row, outer columns)

$\beta_1 = 1.0$ (outside row, inner columns), $\beta_2 = 0.75$ (outside row, outer columns)

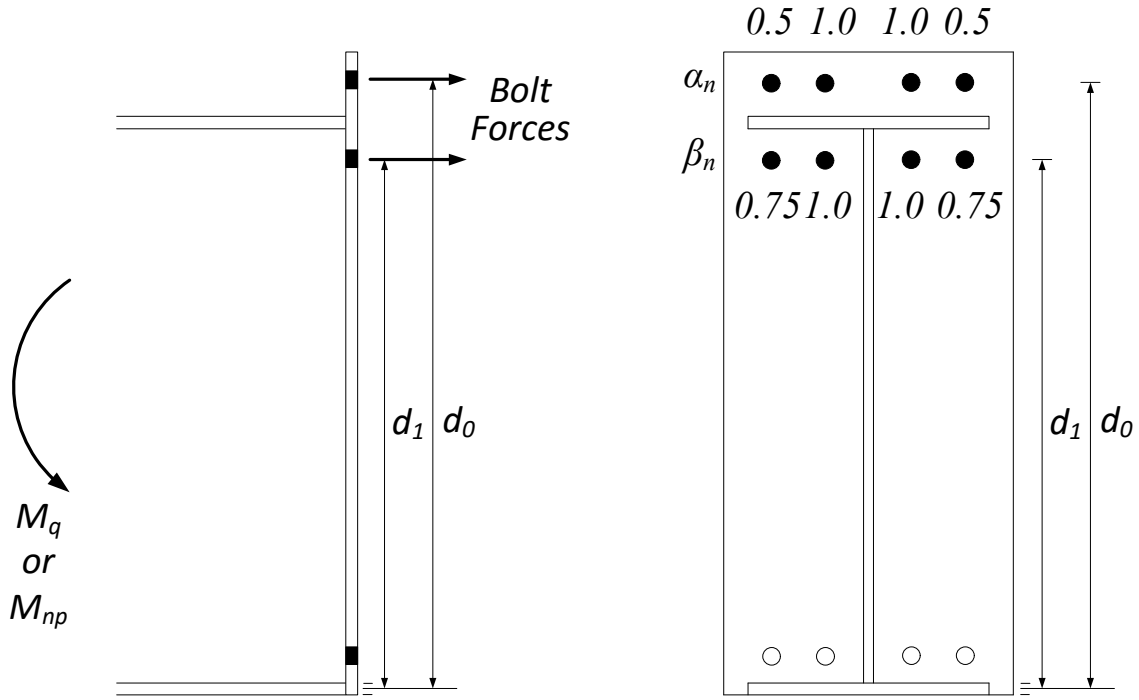

Figure 3-2 Bolt force model and contribution of each bolt for 8E-4W configuration

Note: Four bolts shown on the compression side of the flange are just representative. In general, the number of bolts on the compression side will depend on the loading and calculations.

The bolt force model that is assumed matches that as predicted by Sumner and Murray (2001). Table 3-3 presents a summary of the design procedures discussed for this configuration.

Table 3-3 Summary of Design Procedures for Eight Bolt Extended Four Wide Unstiffened

Yield Line Mechanism	Bolt Force Model
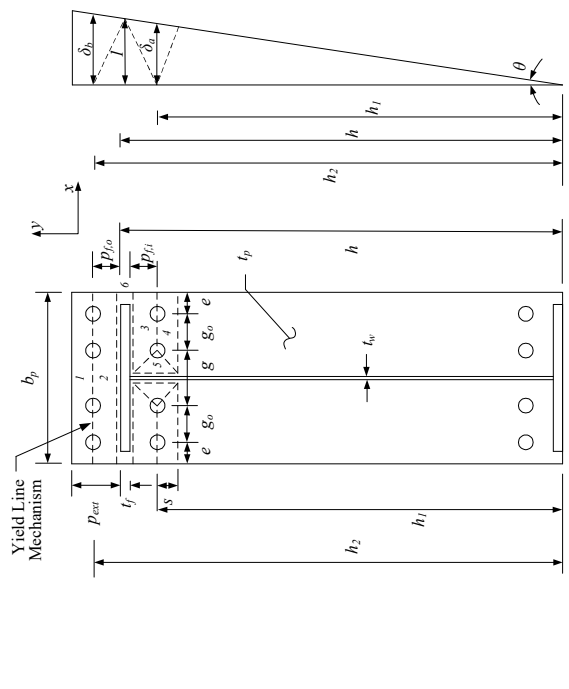	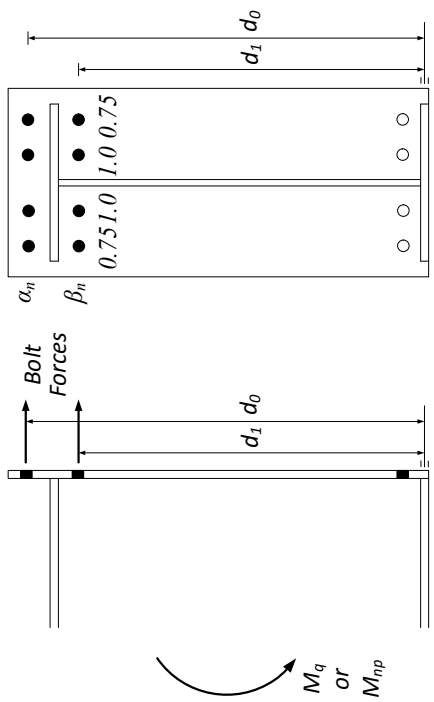

End-Plate Yield	$\phi M_n = \phi M_{pl} = \phi F_{py} t_p^2 Y$ $Y = \frac{b_p}{2}\left[\frac{h_2}{p_{f,o}} + \frac{h_1}{p_{fi}} + \frac{h_1}{s} - \frac{1}{2}\right] + 2\left(p_{f,i} + s\right)\left[\frac{h_1}{g}\right]$ $s = \frac{1}{2}\sqrt{b_p g}$	
Bolt Rupture with Prying Action	$\phi M_q = max \begin{vmatrix} \phi\left[\{2\alpha_1(P_t - Q_{max,o,1}) + 2\alpha_2(P_t - Q_{max,o,2})\}d_0 + \{2\beta_1(P_t - Q_{max,i,1}) + 2\beta_2(P_t - Q_{max,i,2})\}d_1\right] \\ \phi\left[\{2T_b(\alpha_1 + \alpha_2)\}d_0 + \{2\beta_1(P_t - Q_{max,i,1}) + 2\beta_2(P_t - Q_{max,i,2})\}d_1\right] \end{vmatrix}$ $\phi[2T_b\{(\alpha_1 + \alpha_2)d_0 + (\beta_1 + \beta_2)d_1\}]$ $\phi = 0.75,\ \alpha_1 = 1.0,\ \alpha_2 = 0.5, \beta_1 = 1.0,\ \beta_2 = 0.75$	
Bolt Rupture without Prying Action	$\phi M_{np} = \phi[4P_t(d_0 + d_1)],$ $\phi = 0.75$	

3.2 Eight Bolt Extended Stiffened (8ES)

The design procedures presented in this section are similar to Sumner et al. (2000) and are also similar to AISC 358-10 (AISC 2010).

3.2.1 **Yield Line Analysis**

The yield line mechanism considered for the configuration is shown in Figure 3-3. The end-plate has been divided into thirteen panels, formed due to yield lines. The rotation of each panel has been shown in Table 3-4 and the energy stored in each line has been shown in Table 3-5.

The yield line mechanism shown is valid only if $(p_{f,i}, p_{f,o},\ p_b\ and\ s) > e$, otherwise an alternate yield line mechanism would control. Also, for the shown yield line mechanism to control, $h \gg 2(p_{f,i} + p_b)$, otherwise the yield lines will overlap with the row of bolts on the compression side.

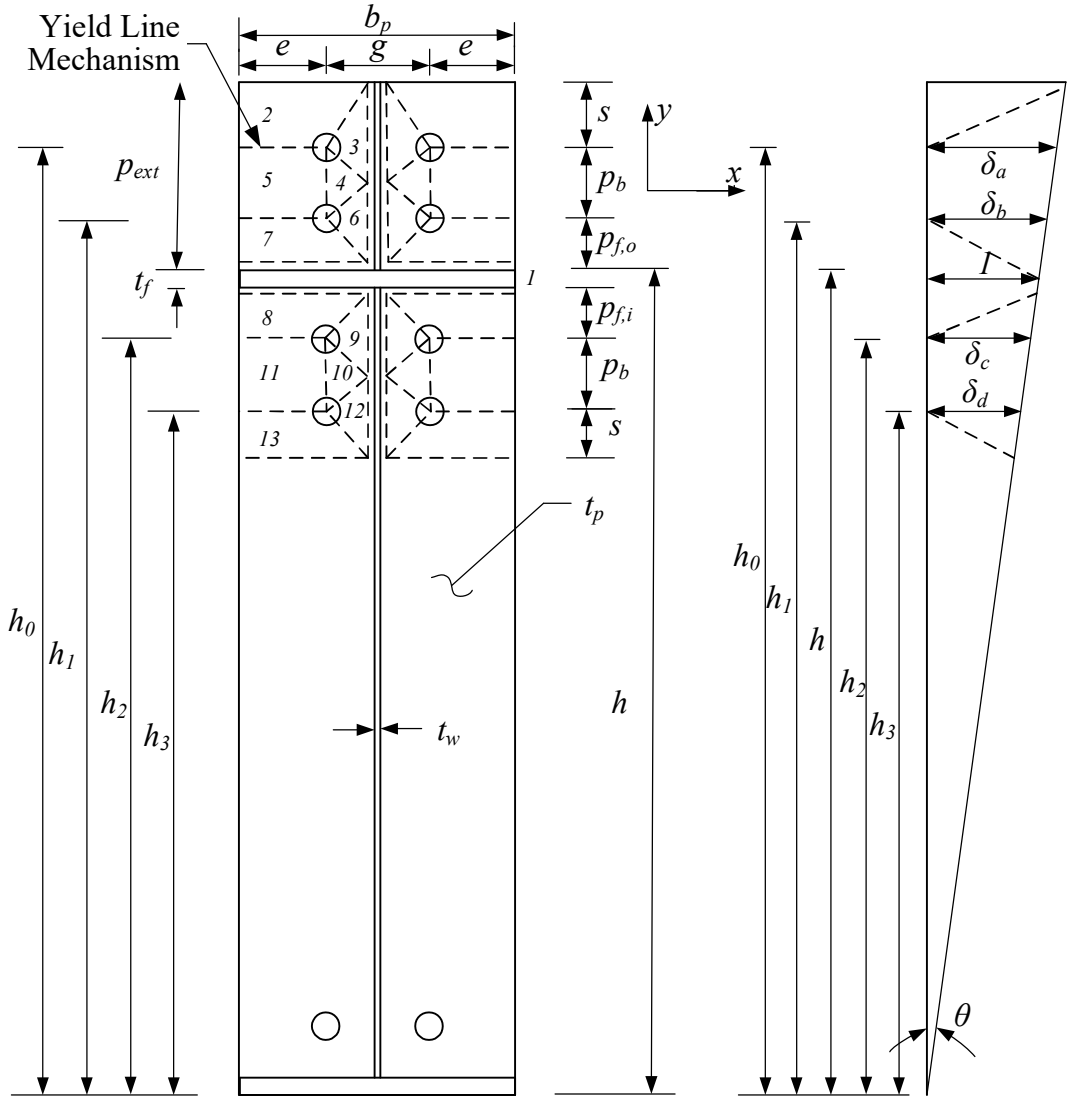

Figure 3-3 Yield Line Mechanism for 8ES Configuration

Note: Two bolts shown on the compression side of the flange are just representative. In the actual tests, the same pattern of bolts as the tension side was used on the compression side. In general, the number of bolts on the compression side will depend on the loading and calculations.

Table 3-4 Rotation of the Yield Line for 8ES Configuration

Panel	$\boldsymbol{\theta_{nx}}$	$\boldsymbol{\theta_{ny}}$
1	θ	0
2	$\frac{(\delta_a - s\theta)}{s}$	0
3	θ	$\frac{2\delta_a}{g}$
4	0	$\frac{(\delta_a + \delta_b)}{g}$
5	θ	0
6	θ	$\frac{2\delta_b}{g}$
7	$-\frac{(\delta_b - p_{f,o}\theta)}{p_{f,o}}$	0
8	$\frac{(\delta_c - p_{f,i}\theta)}{p_{f,i}}$	0
9	θ	$\frac{2\delta_c}{g}$
10	0	$\frac{(\delta_c + \delta_d)}{g}$
11	0	0
12	θ	$\frac{2\delta_d}{g}$
13	$-\frac{(\delta_d - s\theta)}{s}$	0

Table 3-5 Energy Stored in Each Yield Line for 8ES Configuration

Yield Line	Energy Stored
$W_{i\text{-}1/2}$	$\frac{m_p b_p}{2}\left(\frac{\delta_a}{s}\right)$
$W_{i\text{-}2/3}$	$\frac{m_p g}{2}\left(\frac{\delta_a}{s}\right) + m_p s\left(\frac{2\delta_a}{g}\right)$
$W_{i\text{-}2/5}$	$m_p\left(\frac{b_p - g}{2}\right)\left(\frac{\delta_a + s\theta}{s}\right)$
$W_{i\text{-}3/1}$	$m_p\left(s + \frac{p_b}{2}\right)\left(\frac{2\delta_a}{g}\right)$
$W_{i\text{-}3/4}$	$\frac{m_p g}{2}(\theta) + \frac{m_p p_b}{2}\left(\frac{\delta_a - \delta_b}{g}\right)$
$W_{i\text{-}4/5}$	$m_p p_b\left(\frac{\delta_a + \delta_b}{g}\right)$
$W_{i\text{-}4/6}$	$\frac{m_p g}{2}(\theta) + \frac{m_p b_p}{2}\left(\frac{\delta_a - \delta_b}{g}\right)$
$W_{i\text{-}6/1}$	$m_p\left(p_{f,o} + \frac{p_b}{2}\right)\left(\frac{2\delta_b}{g}\right)$
$W_{i\text{-}6/7}$	$\frac{m_p g}{2}\left(\frac{\delta_b}{p_{f,o}}\right) + m_p p_{f,o}\left(\frac{2\delta_b}{g}\right)$
$W_{i\text{-}7/5}$	$m_p\left(\frac{b_p - g}{2}\right)\left(\frac{\delta_b + p_{f,o}\theta}{p_{f,o}}\right)$
$W_{i\text{-}7/1}$	$\frac{m_p b_p}{2}\left(\frac{\delta_b}{p_{f,o}}\right)$
$W_{i\text{-}1/8}$	$\frac{m_p b_p}{2}\left(\frac{\delta_c}{p_{f,i}}\right)$
$W_{i\text{-}8/9}$	$\frac{m_p g}{2}\left(\frac{\delta_c}{p_{f,i}}\right) + m_p p_{f,i}\left(\frac{2\delta_c}{g}\right)$
$W_{i\text{-}8/11}$	$m_p\left(\frac{b_p - g}{2}\right)\left(\frac{\delta_c + p_{f,i}\theta}{p_{f,i}}\right)$
$W_{i\text{-}9/1}$	$m_p\left(p_{f,i} + \frac{p_b}{2}\right)\left(\frac{2\delta_c}{g}\right)$

$W_{i\text{-}9/10}$	$\frac{m_p g}{2}(\theta) + \frac{m_p p_b}{2}\left(\frac{\delta_c - \delta_d}{g}\right)$
$W_{i\text{-}10/11}$	$m_p p_b\left(\frac{\delta_c + \delta_d}{g}\right)$
$W_{i\text{-}10/12}$	$\frac{m_p g}{2}(\theta) + \frac{m_p p_b}{2}\left(\frac{\delta_c - \delta_d}{g}\right)$
$W_{i\text{-}11/13}$	$m_p\left(\frac{b_p - g}{2}\right)\left(\frac{\delta_d - s\theta}{s}\right)$
$W_{i\text{-}13/12}$	$\frac{m_p g}{2}\left(\frac{\delta_d}{s}\right) + m_p s\left(\frac{2\delta_d}{g}\right)$
$W_{i\text{-}12/1}$	$m_p\left(\frac{p_b}{2} + s\right)\left(\frac{2\delta_d}{g}\right)$
$W_{i\text{-}13/1}$	$\frac{m_p b_p}{2}\left(\frac{\delta_d}{s}\right)$

Also, $\delta_a = h_0\,\theta$, $\delta_b = h_1\,\theta$, $1 = h\,\theta$, $\delta_c = h_3\,\theta$, $\delta_d = h_4\,\theta$

The sum of internal work done, $\sum W_i =$ total energy stored in the yield lines.

Therefore, on adding the equations presented in Table 3-5 and simplifying them,

$$\sum W_i = 2m_p\theta\left[b_p\left(\frac{h_0}{s} + \frac{h_1}{p_{f,o}} + \frac{h_2}{p_{f,i}} + \frac{h_3}{s}\right) + \frac{1}{g}\left(h_0(4s + 3p_b) + h_1\left(4p_{f,o} + p_b\right) + h_2\left(4p_{f,i} + 3p_b\right) + h_3(4s + p_b)\right) + 2g\right] \quad \textbf{(3-7)}$$

To determine the dimension s, differentiate $\sum W_i$ w.r.t. s

$$\Rightarrow \frac{d(\sum W_i)}{ds} = 0$$

$$\therefore s = \frac{1}{2}\sqrt{b_p g} \quad \textbf{(3-8)}$$

The plastic moment capacity of the end-plate is directly proportional to the yield line parameter, Y, and to calculate Y:

External Work done, $W_e = M_u\theta = M_n\theta$

Also, $m_p = F_y\frac{t_p^2}{4} \quad \Rightarrow W_i = 2F_y\frac{t_p^2}{4}\theta\,[Y]$

Equating $W_e = W_i$, and plugging in the value of s in W_i and finding out the Yield Line Parameter,

$$Y = \frac{b_p}{2}\left[\frac{h_0}{s} + \frac{h_1}{p_{f,o}} + \frac{h_2}{p_{f,i}} + \frac{h_3}{s}\right] + \frac{2}{g}\left[h_0\left(s + \frac{3p_b}{4}\right) + h_1\left(p_{f,o} + \frac{p_b}{4}\right) + h_2\left(p_{f,i} + \frac{3p_b}{4}\right) + h_3(s + \frac{p_b}{4})\right] + g \quad \textbf{(3-9)}$$

The yield line parameter presented here is assumed to be correct but it is different from the one presented in Sumner et al. (2000).

$$\phi M_{pl} = \phi F_{py} t_p^2 Y \quad \textbf{(3-10)}$$

3.2.2 Bolt Force Model

3.2.2.1 Thick Plate Model

The thick plate model simply considers the nominal tensile strength of the bolt times the lever arm.

$$\phi M_{np} = \phi[2P_t(d_0 + d_1 + d_2 + d_3)]\,, \qquad \phi = 0.75 \quad \textbf{(3-11)}$$

3.2.2.2 Thin Plate Model

The thin plate model considers a combination of prying forces at the bolt row levels and there are four bolt rows which may or not go undergo prying action. Further, it is assumed that the rows closest to the flange have more probability to experience prying action and the outermost rows won't experience prying action without the rows closest to flange experiencing it. Also, there could be a chance that just one of the rows closest to the flange experiences prying and none of the other bolt rows undergo prying action.

$$\phi M_q = max\begin{vmatrix} \phi\begin{bmatrix} 2\alpha_1(P_t - Q_{max,\alpha,1})d_0 + 2\beta_1(P_t - Q_{max,\beta,1})d_1 \\ +2\gamma_1(P_t - Q_{max,\gamma,1})d_2 + 2\delta_1(P_t - Q_{max,\delta,1})d_3 \end{bmatrix} \\ \phi[2\alpha_1 T_b d_0 + 2\beta_1(P_t - Q_{max,\beta,1})d_1 + 2\gamma_1(P_t - Q_{max,\gamma,1})d_2 + 2\delta_1 T_b d_3] \\ \phi[2\alpha_1 T_b d_0 + 2\beta_1(P_t - Q_{max,\beta,1})d_1 + 2\gamma_1 T_b d_2 + 2\delta_1 T_b d_3] \\ \phi[2\alpha_1 T_b d_0 + 2\beta_1 T_b d_1 + 2\gamma_1(P_t - Q_{max,\gamma,1})d_2 + 2\delta_1 T_b d_3] \\ \phi[2T_b(\alpha_1 d_0 + \beta_1 d_1 + \gamma_1 d_2 + \delta_1 d_3)] \end{vmatrix}$$

(3-12)

$\phi = 0.75$

$\alpha_1 = 1.0$ (outermost row)

$\beta_1 = 1.0$ (outside row closest to flange)

$\gamma_1 = 1.0$ (inside row closest to flange)

$\delta_1 = 1.0$ (innermost row)

The bolt force model presented here matches that of Sumner et al. (2000).

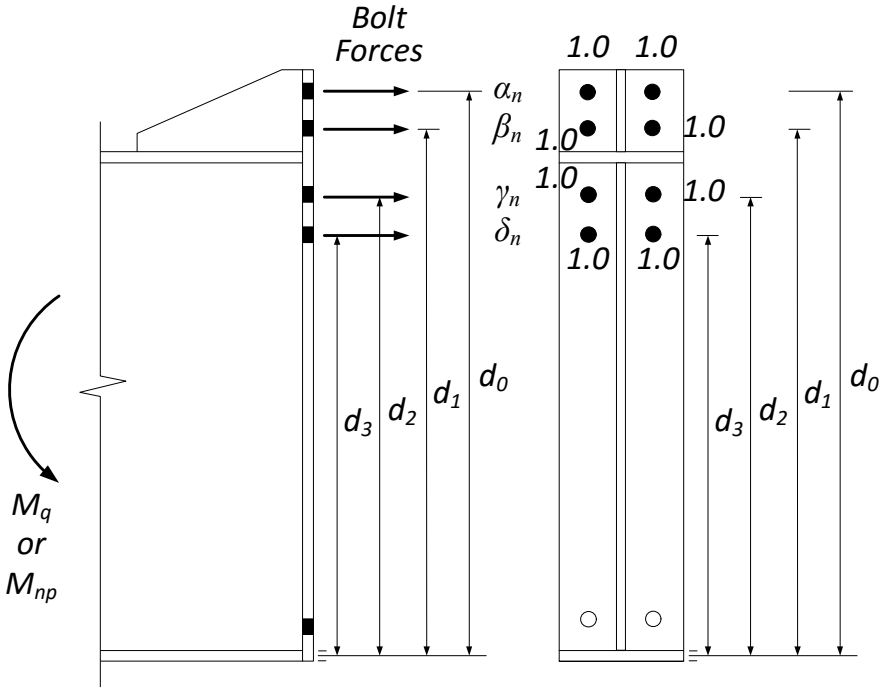

Figure 3-4 Bolt force model for 8ES configuration

Note: Two bolts shown on the compression side of the flange are just representative. In the actual tests, the same pattern of bolts as the tension side was used on the compression side. In general, the number of bolts on the compression side will depend on the loading and calculations.

Table 3-6 presents a summary of the design procedures discussed for this configuration.

Table 3-6 Summary of Design Procedures for Eight Bolt Extended Stiffened

	Yield Line Mechanism	Bolt Force Model
End-Plate Yield		$\phi M_n = \phi M_{pl} = \phi F_{py} t_p^2 Y$ $Y = \frac{b_p}{2}\left[\frac{h_0}{s} + \frac{h_1}{p_{f,o}} + \frac{h_2}{p_{f,i}} + \frac{h_3}{s}\right] + \frac{2}{g}\left[h_0\left(s + \frac{3p_b}{4}\right) + h_1\left(p_{f,o} + \frac{p_b}{4}\right) + h_2\left(p_{f,i} + \frac{3p_b}{4}\right) + h_3\left(s + \frac{p_b}{4}\right)\right] + g\,,$ $s = \frac{1}{2}\sqrt{b_p g}$
Bolt Rupture with Prying Action		$\phi M_q = max \begin{vmatrix} \phi\left[\begin{matrix} 2\alpha_1(P_t - Q_{max,\alpha,1})d_0 + 2\beta_1(P_t - Q_{max,\beta,1})d_1 \\ +2\gamma_1(P_t - Q_{max,\gamma,1})d_2 + 2\delta_1(P_t - Q_{max,\delta,1})d_3 \end{matrix}\right] \\ \phi\left[2\alpha_1 T_b d_0 + 2\beta_1(P_t - Q_{max,\beta,1})d_1 + 2\gamma_1(P_t - Q_{max,\gamma,1})d_2 + 2\delta_1 T_b d_3\right] \\ \phi\left[2\alpha_1 T_b d_0 + 2\beta_1(P_t - Q_{max,\beta,1})d_1 + 2\gamma_1 T_b d_2 + 2\delta_1 T_b d_3\right] \\ \phi\left[2\alpha_1 T_b d_0 + 2\beta_1 T_b d_1 + 2\gamma_1(P_t - Q_{max,\gamma,1})d_2 + 2\delta_1 T_b d_3\right] \\ \phi[2T_b(\alpha_1 d_0 + \beta_1 d_1 + \gamma_1 d_2 + \delta_1 d_3)] \end{vmatrix}$ $\phi = 0.75,\ \alpha_1 = 1.0,\ \beta_1 = 1.0,\ \gamma_1 = 1.0,\ \delta_1 = 1.0$
Bolt Rupture without Prying Action		$\phi M_{np} = \phi[2P_t(d_0 + d_1 + d_2 + d_3)]\,, \quad \phi = 0.75$

3.3 Six Bolt Flush Four Wide/Two Wide Unstiffened (6B-4W/2W)

3.3.1 **Yield Line Analysis**

The yield line mechanism considered for the configuration is shown in Figure 3-5. The end-plate has been divided into thirteen panels, formed due to yield lines. The rotation of each panel has been shown in Table 3-7 and the energy stored in each line has been shown in Table 3-8.

The yield line mechanism shown is valid only if $(p_f,\ p_b\ and\ s) > e$, otherwise an alternate yield line mechanism would control. Also, for the shown yield line mechanism to control, $h \gg 2(p_f + p_b)$, otherwise the yield lines will overlap with the row of bolts on the compression side.

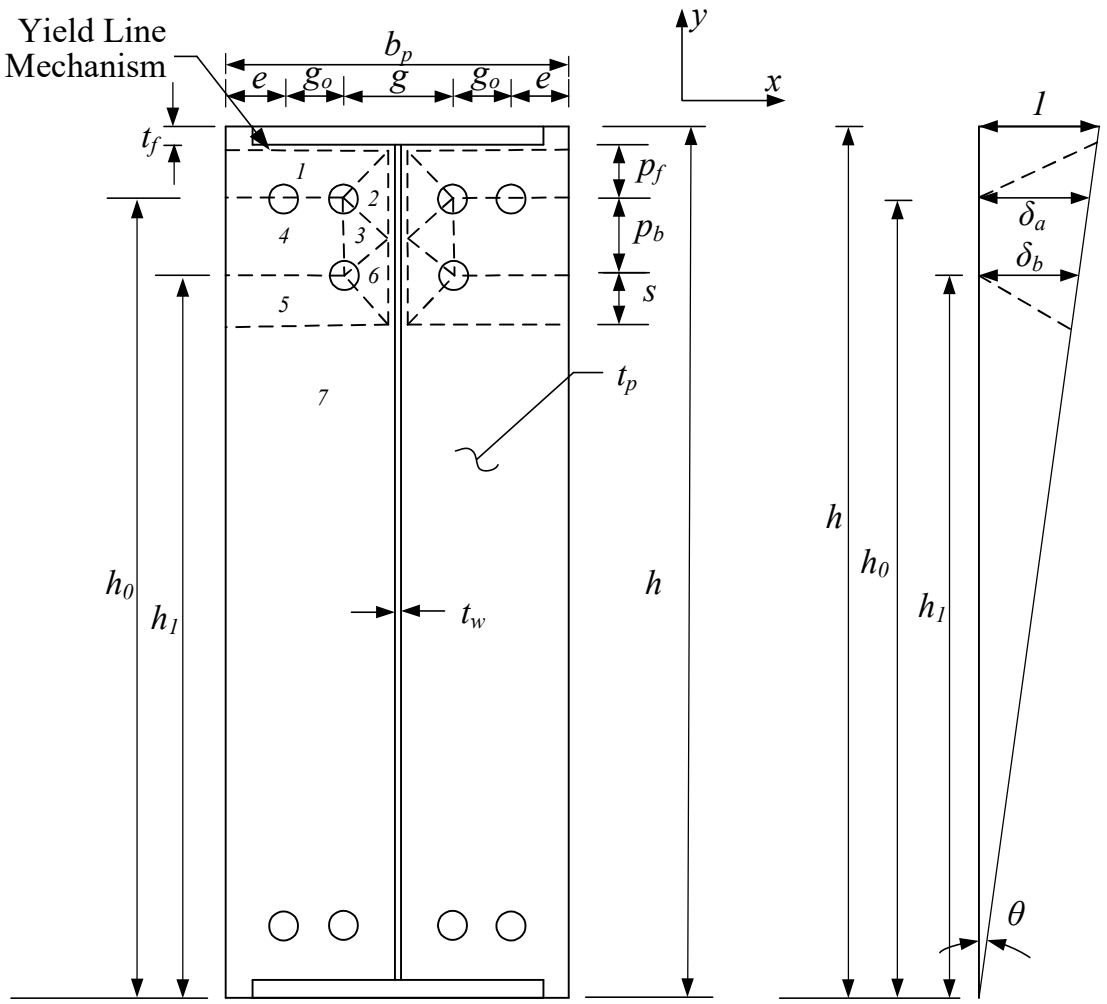

Figure 3-5 Yield Line Mechanism for 6B-4W/2W Configuration

Note: Four bolts shown on the compression side of the flange are just representative. In the actual tests, the same pattern of bolts as the tension side was used on the compression side. In general, the number of bolts on the compression side will depend on the loading and calculations.

Table 3-7 Rotation of the Yield Line for 6B-4W/2W Configuration

Panel	$\boldsymbol{\theta_{nx}}$	$\boldsymbol{\theta_{ny}}$
1	$\frac{(\delta_a - p_f\theta)}{p_f}$	0
2	θ	$\frac{2\delta_a}{g}$
3	0	$\frac{\delta_a + \delta_b}{g}$
4	0	0
5	$-\frac{(\delta_b - s\theta)}{s}$	0
6	θ	$\frac{2\delta_b}{g}$
7	θ	0

Table 3-8 Energy Stored in Each Yield Line for 6B-4W/2W Configuration

Yield Line	Energy Stored
$W_{i\text{-}7/1}$	$\frac{m_p b_p}{2}\left(\frac{\delta_a}{p_f}\right)$
$W_{i\text{-}1/2}$	$\frac{m_p g}{2}\left(\frac{\delta_a}{p_f}\right) + m_p p_f\left(\frac{2\delta_a}{g}\right)$
$W_{i\text{-}1/4}$	$m_p\left(\frac{b_p - g}{2}\right)\left(\frac{\delta_a + p_f\theta}{p_f}\right)$
$W_{i\text{-}2/7}$	$m_p\left(p_f + \frac{p_b}{2}\right)\left(\frac{2\delta_a}{g}\right)$
$W_{i\text{-}2/3}$	$\frac{m_p g}{2}(\theta) + \frac{m_p p_b}{2}\left(\frac{\delta_a - \delta_b}{g}\right)$
$W_{i\text{-}3/4}$	$m_p p_b\left(\frac{\delta_a + \delta_b}{g}\right)$
$W_{i\text{-}3/6}$	$\frac{m_p g}{2}(\theta) + \frac{m_p p_b}{2}\left(\frac{\delta_a - \delta_b}{g}\right)$
$W_{i\text{-}4/5}$	$m_p p_b\left(\frac{b_p - g}{2}\right)\left(\frac{\delta_b - s\theta}{s}\right)$
$W_{i\text{-}5/6}$	$\frac{m_p g}{2}\left(\frac{\delta_b}{s}\right) + m_p s\left(\frac{2\delta_b}{g}\right)$
$W_{i\text{-}5/7}$	$\frac{m_p b_p}{2}\left(\frac{\delta_b}{s}\right)$
$W_{i\text{-}6/7}$	$m_p\left(\frac{p_b}{2} + s\right)\left(\frac{2\delta_b}{g}\right)$

Energy Stored:

Also, $\delta_a = h_0\,\theta$, $\delta_b = h_1\,\theta$, $1 = h\,\theta$

The sum of internal work done, $\sum W_i =$ Total Energy Stored in the Yield Lines.

Therefore on adding the equations presented in Table 3-8 and simplifying them,

$$\sum W_i = 2m_p\theta\left[b_p\left(\frac{h_0}{p_f} + \frac{h_1}{s}\right) + \frac{1}{g}\left(4p_f h_0 + 3p_b h_0 + 4sh_1 + p_b h_1\right) + g\right] \quad \textbf{(3-13)}$$

To determine the dimension s, differentiate $\sum W_i$ w.r.t. s

$\Rightarrow \frac{d(\sum W_i)}{ds} = 0$

$$\therefore s = \frac{1}{2}\sqrt{b_p g} \quad \textbf{(3-14)}$$

The plastic moment capacity of the end-plate is directly proportional to the yield line parameter, Y, and to calculate Y:

External Work done, $W_e = M_u\theta = M_n\theta$

Also, $m_p = F_y\frac{t_p^2}{4} \quad \Rightarrow W_i = 2F_y\frac{t_p^2}{4}\theta\ [Y]$

Equating $W_e = W_i$, and plugging in the value of s in W_i and finding out the Yield Line Parameter,

$$Y = \frac{b_p}{2}\left[\frac{h_0}{p_f} + \frac{h_1}{s}\right] + \frac{2}{g}\left[h_0\left(p_f + \frac{3p_b}{4}\right) + h_1\left(s + \frac{p_b}{4}\right)\right] + \frac{g}{2} \quad \textbf{(3-15)}$$

$$\phi M_{pl} = \phi F_{py} t_p^2 Y \quad \textbf{(3-16)}$$

3.3.2 Bolt Force Model

3.3.2.1 Thick Plate Model

The thick plate model simply considers the nominal tensile strength of the bolt times the lever arm.

$$\phi M_{np} = \phi[2P_t(2d_1 + d_2)]\ ,\ \phi = 0.75 \quad \textbf{(3-17)}$$

3.3.2.2 Thin Plate Model

The thin plate model considers a combination of prying forces at the bolt row levels and since there are two bolt rows which may or not go undergo prying action, four bolt force equations are possible. Also, it has been experimentally observed that the outer bolts in a row as compared to the inner bolts, contribute lesser towards the moment capacity of the connection. Moreover, the bolt in the innermost row contribute lesser as compared to the bolts in the row closest to the flange. All these factors have been taken into account by using bolt distribution factors, $\beta\ and\ \gamma$, which have been calibrated based on experimental results and the values of these are mentioned as below.

$$\phi M_q = max \begin{vmatrix} \phi \begin{bmatrix} \{2\beta_1(P_t - Q_{max,\beta,1}) + 2\beta_2(P_t - Q_{max,\beta,2})\}d_1 \\ +\{2\gamma_1(P_t - Q_{max,\gamma,1})\}d_2 \end{bmatrix} \\ \phi[\{2\beta_1(P_t - Q_{max,\beta,1}) + 2\beta_2(P_t - Q_{max,\beta,2})\}d_1 + (2\gamma_1 T_b)d_2] \\ \phi[(2\beta_1 T_b)d_1 + (2\beta_2 T_b)d_1 + \{2\gamma_1(P_t - Q_{max,\gamma,1})\}d_2] \\ \phi[(2\beta_1 T_b)d_1 + (2\beta_2 T_b)d_1 + (2\gamma_1 T_b)d_2] \end{vmatrix}$$

(3-18)

where,

$\phi = 0.75$

T_b = specified bolt pretension load

$\beta_1 = 1.0$ (first inside row, inner columns), $\beta_2 = 0.75$ (first inside row, outer columns)

$\gamma_1 = 0.75$ (second inside row, inner columns)

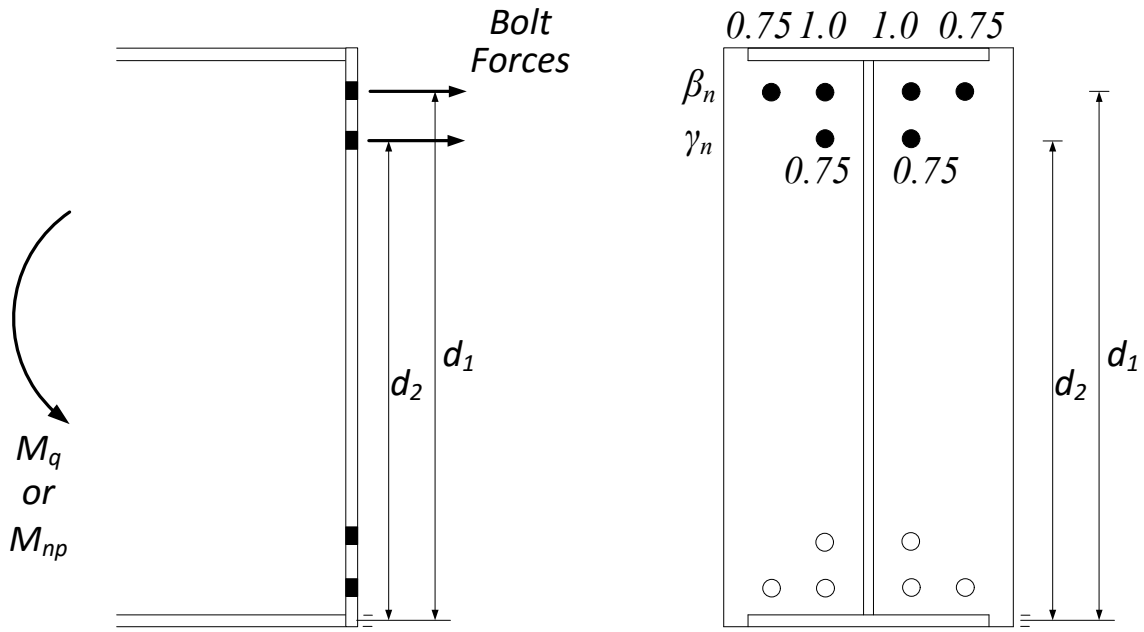

Figure 3-6 Bolt force model and contribution of each bolt for 6B-4W/2W configuration

Table 3-9 presents a summary of the design procedures discussed for this configuration.

Table 3-9 Summary of Design Procedures for Six Bolt Flush Four Wide/Two Wide Unstiffened

Yield Line Mechanism	Bolt Force Model	
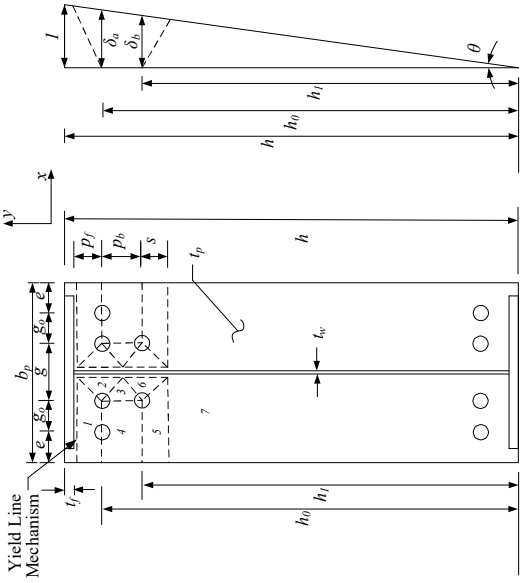	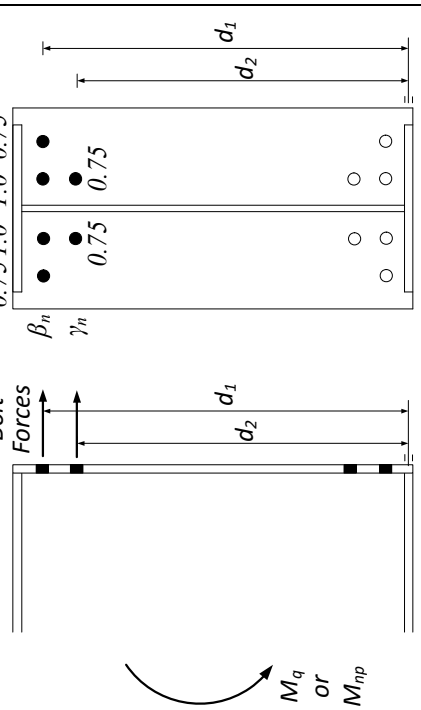	End-Plate Yield
		Bolt Rupture with Prying Action
		Bolt Rupture without Prying Action

$$\phi M_n = \phi M_{pl} = \phi F_{py} t_p^2 Y$$

$$Y = \frac{b_p}{2}\left[\frac{h_0}{p_f} + \frac{h_1}{s}\right] + \frac{2}{g}\left[h_0\left(p_f + \frac{3p_b}{4}\right) + h_1\left(s + \frac{p_b}{4}\right)\right] + \frac{g}{2}$$

$$s = \frac{1}{2}\sqrt{b_p g}$$

$$\phi M_q = max \begin{cases} \phi\left[\begin{matrix}\{2\beta_1(P_t - Q_{max,\beta,1}) + 2\beta_2(P_t - Q_{max,\beta,2})\}d_1 \\ +\{2\gamma_1(P_t - Q_{max,\gamma,1})\}d_2\end{matrix}\right] \\ \phi\left[\{2\beta_1(P_t - Q_{max,\beta,1}) + 2\beta_2(P_t - Q_{max,\beta,2})\}d_1 + (2\gamma_1 T_b)d_2\right] \\ \phi\left[(2\beta_1 T_b)d_1 + (2\beta_2 T_b)d_1 + \{2\gamma_1(P_t - Q_{max,\gamma,1})\}d_2\right] \end{cases}$$

$$\phi = 0.75,\ \beta_1 = 1.0,\ \beta_2 = 0.75,\ \gamma_1 = 0.75$$

$$\phi M_{np} = \phi[2P_t(2d_1 + d_2)], \qquad \phi = 0.75$$

3.4 Twelve Bolt Multiple Row Extended Four Wide/Two Wide Unstiffened (12B-MRE 1/3-4W/2W)

3.4.1 Yield Line Analysis

The yield line mechanism considered for the configuration is shown in Figure 3-7. The end-plate has been divided into ten panels, formed due to yield lines. The rotation of each panel has been shown in Table 3-10 and the energy stored in each line has been shown in Table 3-11.

The yield line mechanism shown is valid only if $(p_{f,i}, p_{f,o},\ p_b\ and\ s) > e$, otherwise an alternate yield line mechanism would control. Also, for the shown yield line mechanism to control, $h \gg 2(p_{f,i} + 2p_b)$, otherwise the yield lines will overlap with the row of bolts on the compression side.

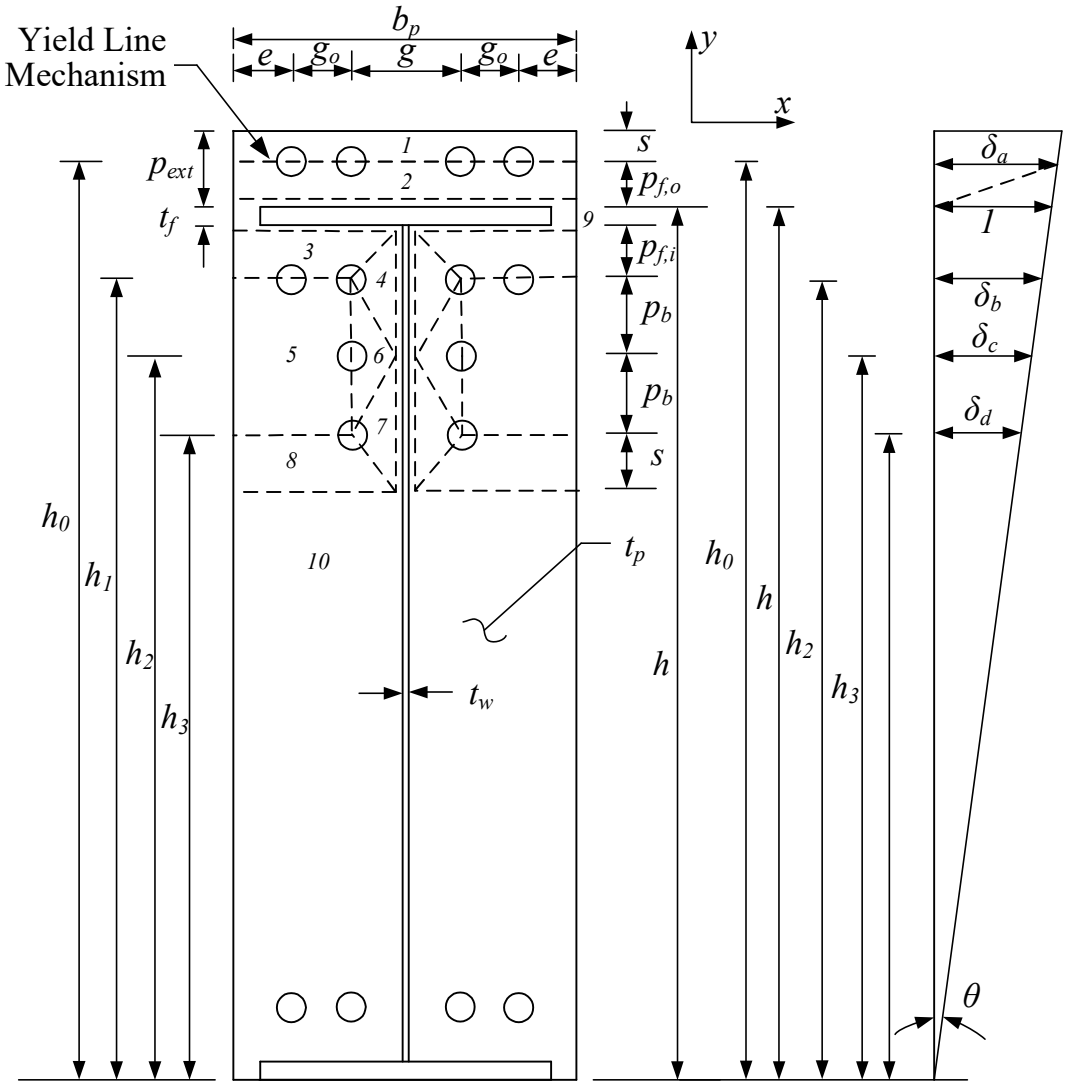

Figure 3-7 Yield Line Mechanism for 12B-MRE 1/3-4W/2W Configuration

Note: Four bolts shown on the compression side of the flange are just representative. In the actual tests, the same pattern of bolts as the tension side was used in the compression side. In general, the number of bolts on the compression side will depend on the loading and calculations.

Table 3-10 Rotation of the Yield Line for 12B-MRE 1/3-4W/2W Configuration

Panel	$\boldsymbol{\theta_{nx}}$	$\boldsymbol{\theta_{ny}}$
1	0	0
2	$-\frac{(\delta_a - p_{f,o}\theta)}{p_{f,o}}$	0
3	$\frac{(\delta_b + p_{f,i}\theta)}{p_{f,i}}$	0
4	θ	$\frac{2\delta_b}{g}$
5	0	0
6	0	$\frac{2\delta_c}{g}$
7	θ	$\frac{2\delta_d}{g}$
8	$-\frac{(\delta_c - s\theta)}{s}$	0
9	θ	0
10	0	0

Table 3-11 Energy Stored in Each Yield Line for 12B-MRE 1/3-4W/2W Configuration

Yield Line	Energy Stored
$W_{i\text{-}1/2}$	$\frac{m_p b_p}{2}\left(\frac{\delta_a - p_{f,o}\theta}{p_{f,o}}\right)$
$W_{i\text{-}2/9}$	$\frac{m_p b_p}{2}\left(\frac{\delta_a}{p_{f,o}}\right)$
$W_{i\text{-}9/3}$	$\frac{m_p p_b}{2}\left(\frac{\delta_b}{p_{f,i}}\right)$
$W_{i\text{-}3/4}$	$\frac{m_p g}{2}\left(\frac{\delta_b + p_{f,i}\theta}{p_{f,i}}\right) + m_p p_{f,i}\left(\frac{2\delta_b}{g}\right)$
$W_{i\text{-}3/5}$	$m_p\left(\frac{b_p - g}{2}\right)\left(\frac{\delta_a + p_{f,i}\theta}{p_{f,i}}\right)$
$W_{i\text{-}4/9}$	$m_p\left(\frac{2\delta_b}{g}\right)(p_{f,i} + p_b)$
$W_{i\text{-}4/6}$	$\frac{m_p g}{2}\theta + m_p p_b\left(\frac{2\delta_b - 2\delta_c}{g}\right)$
$W_{i\text{-}6/5}$	$2m_p p_b\left(\frac{2\delta_c}{g}\right)$
$W_{i\text{-}5/8}$	$\frac{m_p(b_p - g)}{2}\left(\frac{\delta_d - s\theta}{s}\right)$
$W_{i\text{-}6/7}$	$\frac{m_p g}{2}\theta + m_p p_b\left(\frac{2\delta_b - 2\delta_c}{g}\right)$
$W_{i\text{-}7/8}$	$\frac{m_p g}{2}\left(\frac{\delta_d}{s}\right) + m_p s\left(\frac{2\delta_d}{g}\right)$
$W_{i\text{-}7/9}$	$m_p(p_b + s)\left(\frac{2\delta_d}{g}\right)$
$W_{i\text{-}8/10}$	$\frac{m_p b_p}{2}\left(\frac{\delta_d - s\theta}{s}\right)$

Energy Stored:

Also, $\delta_a = h_0\theta$, $1 = h\theta$, $\delta_b = h_1\theta$, $\delta_c = h_2\theta$, $\delta_d = h_3\theta$ and $h_2 = \frac{h_1 + h_3}{2}$

The sum of internal work done, $\sum W_i$ = Total Energy Stored in the Yield Lines.

Therefore on adding the equations presented in Table 3-11 and simplifying them,

$$\sum W_i = 2m_p\theta\left[b_p\left(\frac{h_0}{p_{f,o}}+\frac{h_1}{p_{f,i}}+\frac{h_3}{s}-1\right)+\frac{1}{g}\left(4p_{f,i}h_1+4p_bh_1+4p_bh_2+4sh_3\right)+g\right] \quad \textbf{(3-19)}$$

To determine the dimension s, differentiate $\sum W_i$ w.r.t. s

$$\Rightarrow \frac{d(\sum W_i)}{ds}=0$$

$$\therefore s=\frac{1}{2}\sqrt{b_pg} \quad \textbf{(3-20)}$$

The plastic moment capacity of the end-plate is directly proportional to the yield line parameter, Y, and to calculate Y:

External Work done, $W_e = M_u\theta = M_n\theta$

Also, $m_p = F_y\frac{t_p^2}{4} \quad \Rightarrow W_i = 2F_y\frac{t_p^2}{4}\theta\,[Y]$

Equating $W_e = W_i$, and finding out the Yield Line Parameter,

$$\Rightarrow Y=\frac{b_p}{2}\left[\frac{h_0}{p_{f,o}}+\frac{h_1}{p_{f,i}}+\frac{h_3}{s}-1\right]+\frac{2}{g}\left[h_1\left(p_{f,i}+p_b\right)+h_2p_b+h_3s\right]+\frac{g}{2}$$

$$or\ \ Y=\frac{b_p}{2}\left[\frac{h_0}{p_{f,o}}+\frac{h_1}{p_{f,i}}+\frac{h_3}{s}-1\right]+\frac{2}{g}\left[h_1\left(p_{f,i}+1.5p_b\right)+h_3\left(s+\frac{p_b}{2}\right)\right]+\frac{g}{2} \quad \textbf{(3-21)}$$

$$\phi M_{pl}=\phi\ {}_{py}t_p^2Y \quad \textbf{(3-22)}$$

3.4.2 Bolt Force Model

3.4.2.1 Thick Plate Model

The thick plate model simply considers the nominal tensile strength of the bolt times the lever arm.

$$\phi M_{np}=\phi[2P_t(2d_0+2d_1+d_2+d_2)]\,,\qquad \phi=0.75 \quad \textbf{(3-23)}$$

3.4.2.2 Thin Plate Model

The thin plate model considers a combination of prying forces at the bolt row levels and there are four bolt rows which may or not go undergo prying action. It has been experimentally observed that "γ row" does not undergo prying. Also, it has been experimentally observed that the outer bolts in a row as compared to the inner bolts, contribute lesser towards the moment capacity of the connection. This factor is taken into account by using bolt distribution factors, $\alpha \; and \; \beta$, which have been calibrated based on experimental results and the values of these are mentioned as below. Moreover, the bolts further away from the flange contribute less to the moment capacity of the connection as compared to the bolts closest to the flange. This is taken into account by using the bolt calibration factors $\gamma \; and \; \delta$.

$$\phi M_q = \; max \left| \begin{array}{c} \phi \begin{bmatrix} 2\alpha_1(P_t - Q_{max,\alpha,1})d_0 + 2\alpha_2(P_t - Q_{max,\alpha,2})d_0 \\ +2\beta_1(P_t - Q_{max,\beta,1})d_1 + 2\beta_2(P_t - Q_{max,\beta,2})d_1 \\ +2\gamma_1(T_b)d_2 + 2\delta_1(P_t - Q_{max,\delta,1})d_3 \end{bmatrix} \\ \phi \begin{bmatrix} 2\alpha_1(T_b)d_0 + 2\alpha_2(T_b)d_0 + 2\beta_1(P_t - Q_{max,\beta,1})d_1 + \\ 2\beta_2(P_t - Q_{max,\beta,2})d_1 + 2\gamma_1(T_b)d_2 + 2\delta_1(P_t - Q_{max,\delta,1})d_3 \end{bmatrix} \\ \phi \begin{bmatrix} 2\alpha_1(P_t - Q_{max,\alpha,1})d_0 + 2\alpha_2(P_t - Q_{max,\alpha,2})d_0 + 2\beta_1(T_b)d_1 + \\ 2\beta_2(T_b)d_1 + 2\gamma_1(T_b)d_2 + 2\delta_1(T_b)d_3 \end{bmatrix} \\ \phi[2T_b\{(\alpha_1 + \alpha_2)d_0 + (\beta_1 + \beta_2)d_1 + (\gamma)d_2 + (\delta)d_3\}] \end{array} \right. \quad \textbf{(3-24)}$$

where,

$\phi = 0.75$

T_b = specified bolt pretension load

$\alpha_1 = 1.0$ (outside row, inner columns), $\alpha_2 = 0.5$ (outside row, outer columns)

$\beta_1 = 1.0$ (first inside row, inner columns), $\beta_2 = 0.75$ (outside row, outer columns)

$\gamma_1 = 0.75$ (second inside row, inner columns)

$\delta_1 = 0.5$ (third inside row, inner columns)

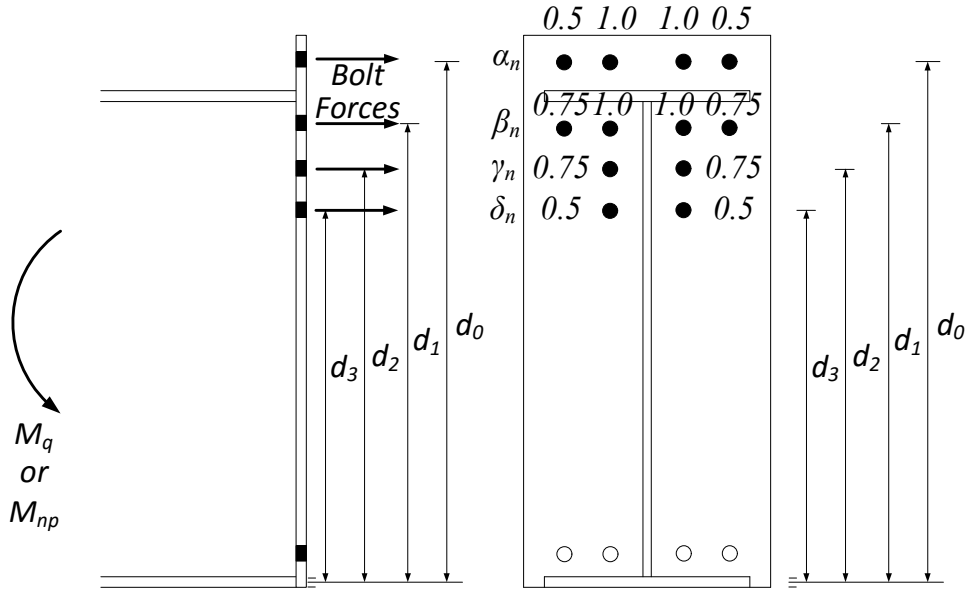

Figure 3-8 Bolt force model and contribution of each bolt for 12B-MRE 1/3-4W/2Wconfiguration

Note: Four bolts shown on the compression side of the flange are just representative. In the actual tests, the same pattern of bolts as the tension side was used in the compression side. In general, the number of bolts on the compression side will depend on the loading and calculations.

Table 3-12 presents a summary of the design procedures discussed for this configuration.

Table 3-12 Summary of Design Procedures for Twelve Bolt Multiple Row Extended Four Wide/Two Wide Unstiffened

Yield Line Mechanism	Bolt Force Model

End-Plate Yield	$\phi M_n = \phi M_{pl} = \phi F_{py} t_p^2 Y$ $Y = \frac{b_p}{2}\left[\frac{h_o}{p_{f,o}} + \frac{h_1}{p_{f,i}} + \frac{h_3}{s} - 1\right] + \frac{2}{g}\left[h_1(p_{f,i} + 1.5p_b) + h_3\left(s + \frac{p_b}{2}\right)\right] + \frac{g}{2}$ $s = \frac{1}{2}\sqrt{b_p g}$
Bolt Rupture with Prying Action	$\phi M_q = max \begin{cases} \phi\left[\begin{matrix} 2\alpha_1(P_t - Q_{max,\alpha,1})d_0 + 2\alpha_2(P_t - Q_{max,\alpha,2})d_0 \\ +2\beta_1(P_t - Q_{max,\beta,1})d_1 + 2\beta_2(P_t - Q_{max,\beta,2})d_1 \\ +2\gamma_1(T_b)d_2 + 2\delta_1(P_t - Q_{max,\delta,1})d_3 \end{matrix}\right] \\ \phi\left[\begin{matrix} 2\alpha_1(T_b)d_0 + 2\alpha_2(T_b)d_0 + 2\beta_1(P_t - Q_{max,\beta,1})d_1 + \\ 2\beta_2(P_t - Q_{max,\beta,2})d_1 + 2\gamma_1(T_b)d_2 + 2\delta_1(P_t - Q_{max,\delta,1})d_3 \end{matrix}\right] \\ \phi\left[\begin{matrix} 2\alpha_1(P_t - Q_{max,\alpha,1})d_0 + 2\alpha_2(P_t - Q_{max,\alpha,2})d_0 + 2\beta_1(T_b)d_1 + \\ 2\beta_2(T_b)d_1 + 2\gamma_1(T_b)d_2 + 2\delta_1(T_b)d_3 \end{matrix}\right] \\ \phi[2T_b\{(\alpha_1 + \alpha_2)d_0 + (\beta_1 + \beta_2)d_1 + (\gamma)d_2 + (\delta)d_3\}] \end{cases}$ $\phi = 0.75,\ \alpha_1 = 1.0,\ \alpha_2 = 0.5,\ \beta_1 = 1.0,\ \beta_2 = 0.75,\ \gamma_1 = 0.75,\ \delta_1 = 0.5$
Bolt Rupture without Prying Action	$\phi M_{np} = \phi[2P_t(2d_0 + 2d_1 + d_2 + d_2)], \quad \phi = 0.75$

4 VALIDATION OF CONNECTION CONFIGURATION BASED ON LITERATURE

As discussed in Chapter 1, there was a desire to include more connection configurations in Design Guide 16, and some of them could be validated by going through the previous literature. There was an interest in the behavior of the connection, whether the analytical models can predict the actual behavior of the connection and how different design parameters affect the behavior. This chapter deals only with the data from previous tests and no new tests have been discussed here. The configurations that have been reviewed here are the 8E-4W and 8ES configuration.

For the Eight Bolt Extended Four Wide Unstiffened configuration, the equations presented in the previous chapter for M_{pl}, M_{np} and M_{pl} appear to be accurate for a range of design variables including a depth ranging from 30 in. to 62 in. This has been presented in the Section 4.1 below.

For the Eight Bolt Extended Stiffened configuration, the equations presented in the previous chapter for M_{pl}, M_{np} and M_{pl} appear to be accurate for a range of design variables including a depth ranging from 24 in. to 30 in. This implies that correct predictions for the behavior of the connection could be made only for shallower depths. The test results for this configuration have been presented in the section 4.2 below.

4.1 Previous Testing on the Eight-Bolt Extended Four Wide Unstiffened Configuration

Research on the Eight-Bolt Extended Four Wide Unstiffened configuration has been reported by Sumner et al. (2000), Sumner and Murray (2001), and Sumner (2003). Based upon a review of the literature, as detailed in the following sections, it appears that the design equations for M_{pl}, M_{np} and M_{pl} proposed by Sumner et al. (2001) are accurate for a

range of design variables. Table 4-1 presents a summary of the experimental work that has been conducted thus far.

Table 4-1 Summary of Experimental Work

Specimen Identification*		Reference	Configuration	Loading	Depth (in)	Behavior
1	8E-4W-1.25-1.125-30	Sumner et al. (2000)	Beam – Column	Cyclic	30	NA
2	8E-4W-1.25-1-30	Sumner et al. (2000)	Beam – Column	Cyclic	30	Thin
3	8E-4W-1.25-1.375-36	Sumner et al. (2000)	Beam – Column	Cyclic	36	Thick
4	8E-4W-1.25-1.25-36	Sumner et al. (2000)	Beam – Column	Cyclic	36	Thin
5	8E-4W-1-1/2-62	Sumner & Murray (2001)	Splice	Mono.	62	Thin
6	8E-4W-3/4-3/4-62	Sumner & Murray (2001)	Splice	Mono.	62	Thick
7	8E-4W-3/4-3/4-62 (A490)	Sumner & Murray (2001)	Splice	Mono.	62	Thick

*Specimen Identification: "Connection type - Bolt diameter - End-plate thickness - Beam depth"

Four of the seven tests conducted will be used for verification of the design procedure. These were chosen in such a way that the design procedures could be verified for shallower and deeper specimens with both thick and thin end-plate behavior for a range of different design parameters. As identified in Table 4-1, the selected tests are boxed in with heavy lines. The tests used for verification are as follows: 8E-4W-1.25-1-30, 8E-4W-1.25-1.375-36, 8E-4W-1-1/2-62, and 8E-4W-3/4-3/4-62. 8E-4W-1.25-1-30 and 8E-4W-1.25-1.375-36

both utilized cyclic loading, while 8E-4W-1-1/2-62 and 8E-4W-3/4-3/4-62 were both conducted with monotonic loading. Regardless of loading conditions, the four tests demonstrate that the proposed design procedure is able to adequately predict the limit states associated with the connection configuration. Since adequate validation of the design procedures has been found in the literature, no further experimental work is necessary to include the Eight-Bolt Extended Four Wide Unstiffened in future editions of Design Guide 16.

It is important to address the difference between cyclic and monotonic loading and the way a specimen would behave when subjected to either type of loading. It is noted that the design procedures in Design Guide 16 are not intended for seismic loading and that monotonic testing has been used for the majority of experimental verification of the Design Guide 16 configurations. Though the tests performed by Sumner et al. (2000) utilized cyclic loading, it is assumed that cyclic tests will produce the same end-plate limit states with relatively similar yield and ultimate strength. For that reason, cyclic test data is considered to be applicable in validating the design procedures. Also, because of the following reasons it has been assumed that the way specimen is loaded won't affect the final results:

- Strain hardening in cyclic tests might cause larger apparent moments at a given level of rotation than monotonic tests. This may lead to a different post-yield stiffness, but it is expected that the yield moment won't change much.
- It is also possible that bolt fracture will occur at smaller rotations because of the repeated loading and unloading, but it appears that the bolt rupture would still occur at the same tension force as for monotonic loading.

The following sections demonstrate that previous experimental test results are in reasonable agreement with the limit states and values predicted by the design procedure proposed in Section 3.1.

4.1.1 **Shallow Section - Thin Plate Behavior**

Specimen 8E-4W-1.25-1-30 (cyclic) from Sumner et al. (2000) had a depth of 30 in. and can be considered relatively shallow for the amount of moment capacity that this configuration can generate. The specimen dimension and end-plate geometry is shown in Figure 4-1 and Figure 4-2 respectively.

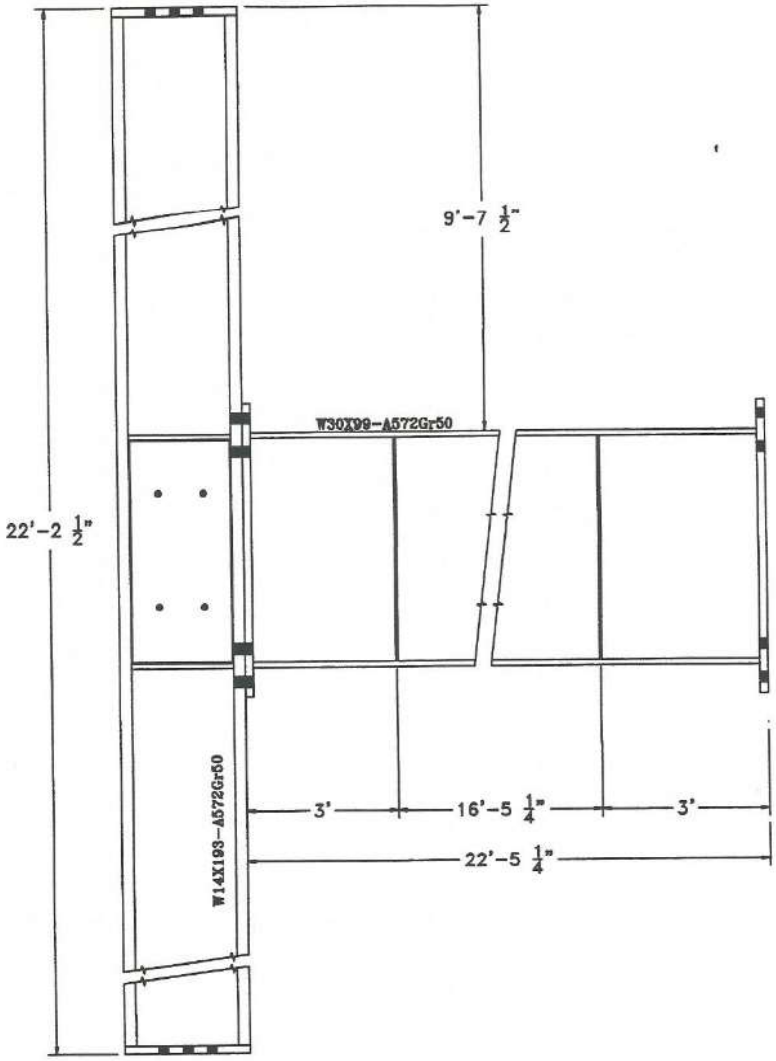

Figure 4-1 8E-4W-1.25-1-30 Specimen Dimensions [Sumner, E. A., Mays, T. W., & Murray, T. M. (2000). *Cyclic Testing of Bolted Moment End-Plate Connections. B*lacksburg, VA: Virginia Polytechnic Institute and State University, Used with Permission of T.M. Murray, 2015]

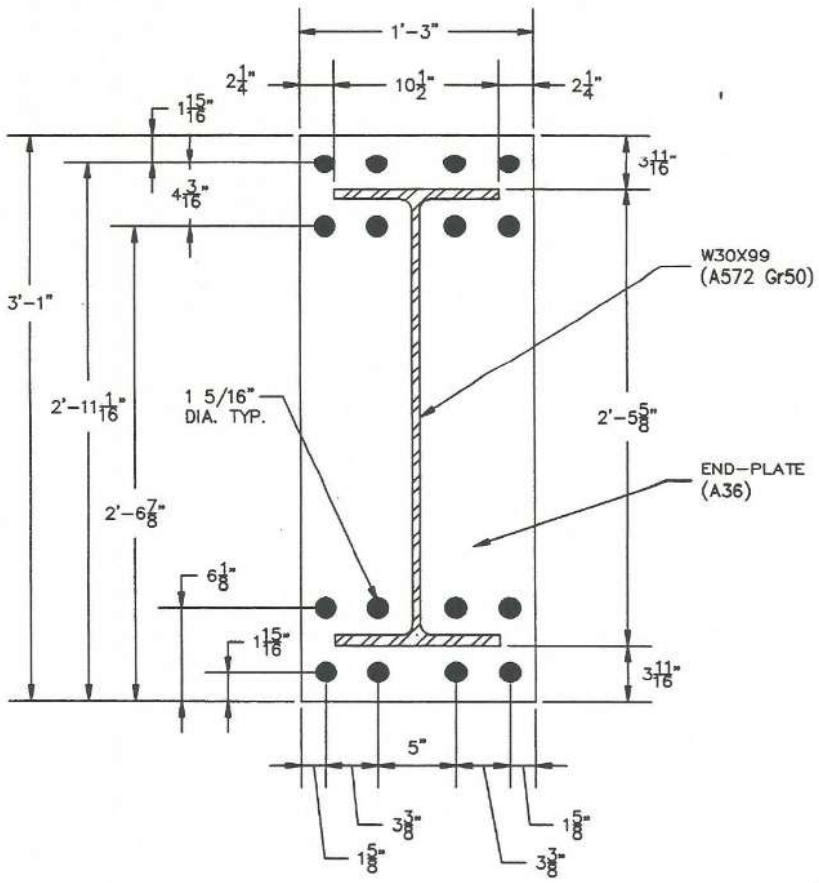

Figure 4-2 End Plate Layout for Specimen 8E-4W-1.25-1-30 [Sumner, E. A., Mays, T. W., & Murray, T. M. (2000). *Cyclic Testing of Bolted Moment End-Plate Connections.* Blacksburg, VA: Virginia Polytechnic Institute and State University, Used with Permission of T.M. Murray, 2015]

4.1.1.1 Limit State – Predictions and Progression

The design equations presented in Chapter 3, calculate moment capacity at bolt rupture without prying action, M_{np}, to be 25640 k-in and moment capacity for end-plate yielding, M_{pl}, of 15120 k-in. The design equations for M_{np} and M_{pl} presented in Chapter 3 for this connection configuration came from Sumner and Murray (2001), and calculated values match with those calculated by Sumner and Murray (2001). Moment capacity at bolt rupture with prying action, M_q, based on the equations presented in Chapter 3 was made to be 18840 k-in.

Based on the moment capacities, the end plate will yield first, then the bolts will rupture with prying action thereby exhibiting thin plate behavior. The specimen behaved as expected. End-plate yielding occurred followed by bolt rupture with prying action. The test was terminated after rupture of the two inner column bolts inside the bottom flange of the test specimen.

4.1.1.2 Experimental Results - Yield and Ultimate Moments

As reported in Sumner et al. (2000), a yield moment, M_y, of 14570 k-in and an ultimate moment, M_u, of 17980 k-in were experimentally obtained. Both are demonstrated graphically in Figure 4-3.

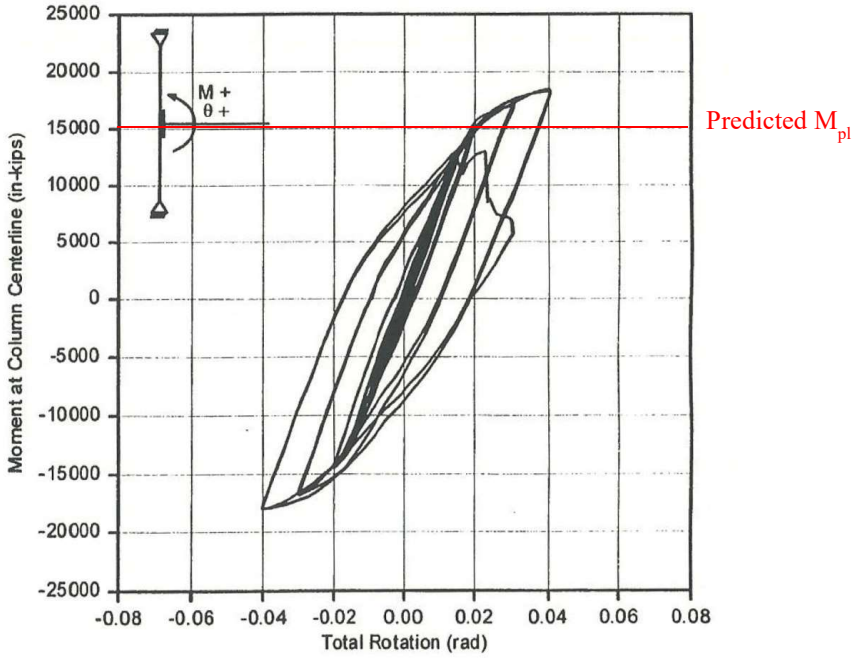

Figure 4-3 Load-deformation behavior for Specimen 8E-4W-1.25-1-30 [Sumner, E. A., Mays, T. W., & Murray, T. M. (2000). *Cyclic Testing of Bolted Moment End-Plate Connections.* Blacksburg, VA: Virginia Polytechnic Institute and State University, Used with Permission of T.M. Murray, 2015]

The moment associated with the controlling limit state, as reported by Sumner (2003), was then compared to the experimental moment capacity for end-plate yielding, M_y, and the experimental maximum moment applied, M_u, as reported by Sumner et al. (2000). This

comparison is presented in the form of a ratio such as M_{pl}/M_y and M_q/M_u. Values less than 1 for this ratio are considered conservative, indicating that the connection has capacity beyond the predicted value.

Though the ratios in Table 4-2 are slightly non-conservative (greater than 1.0), the experimental values are considered to be in reasonable agreement with predictions. Both predictions (yield and ultimate) are within 5% of experimental test results, indicating adequate correlation between the two sets of values.

Table 4-2 Predicted and Experimentally Obtained Moment Capacities for Specimen 8E-4W-1.25-1-30

Predicted (k-in)		Experimental (k-in)		Ratio	
M_{pl}	M_q	M_y	M_u	M_{pl}/M_y	M_q/M_u
15120	18840	14570	17980	1.04	1.05

4.1.1.3 Experimental Results - End-Plate Separation

Instrumented calipers were used during experimental testing to determine end-plate separation. Figure 4-4 displays end-plate separation in relation to moment at the column centerline. The plot verifies that thin plate behavior was achieved. This is evident from the occurrence of large separations once the end-plate began to yield. With thick plate behavior, end-plate separation would be smaller because the plate would not yield.

4.1.1.4 Experimental Results - Bolt Strains

Strain gages were installed in the shank of the bolts used in the experiment to determine bolt forces throughout the duration of the test.

As is shown in Figure 4-5, strains in Bolt 2 drastically increased past the point of end-plate yielding (approximately 14500 kip-in). This indicates prying forces and is consistent with thin end-plate behavior. This relationship between strain and moment was typical for all bolts in the test.

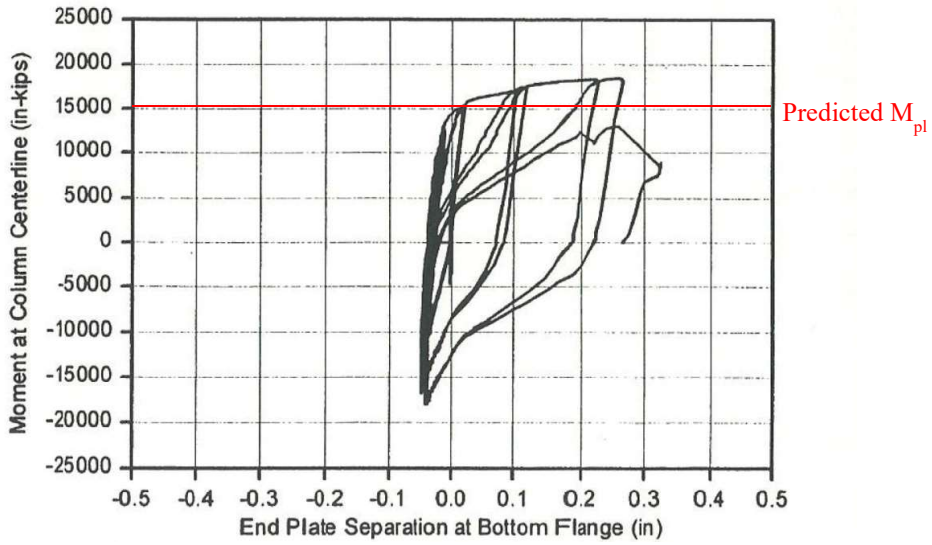

Figure 4-4 End-plate separation for Specimen 8E-4W-1.25-1-30 [Sumner, E. A., Mays, T. W., & Murray, T. M. (2000). *Cyclic Testing of Bolted Moment End-Plate Connections. B*lacksburg, VA: Virginia Polytechnic Institute and State University, Used with Permission of T.M. Murray, 2015]

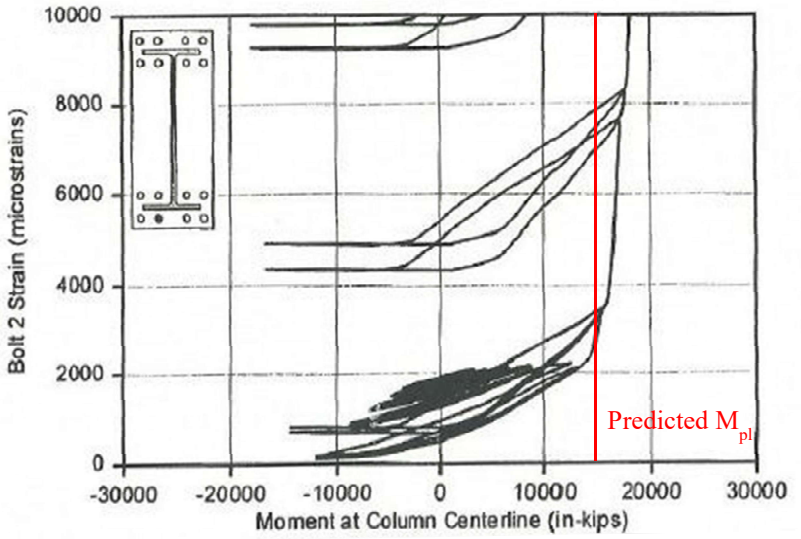

Figure 4-5 Bolt 2 strains for Specimen 8E-4W-1.25-1-30 [Sumner, E. A., Mays, T. W., & Murray, T. M. (2000). Cyclic Testing of Bolted Moment End-Plate Connections. Blacksburg, VA: Virginia Polytechnic Institute and State University, Used with Permission of T.M. Murray, 2015]

4.1.2 **Shallow Section - Thick Plate Behavior**

Specimen 8E-4W-1.25-1.375-36 (cyclic) from Sumner et al. (2000) had a depth of 36 in. and can be assumed to be shallow in relation to the moment capacity that this configuration can sustain. It was designed to exhibit thick end-plate behavior. The specimen dimension and geometry is shown in Figure 4-6 and Figure 4-7 respectively.

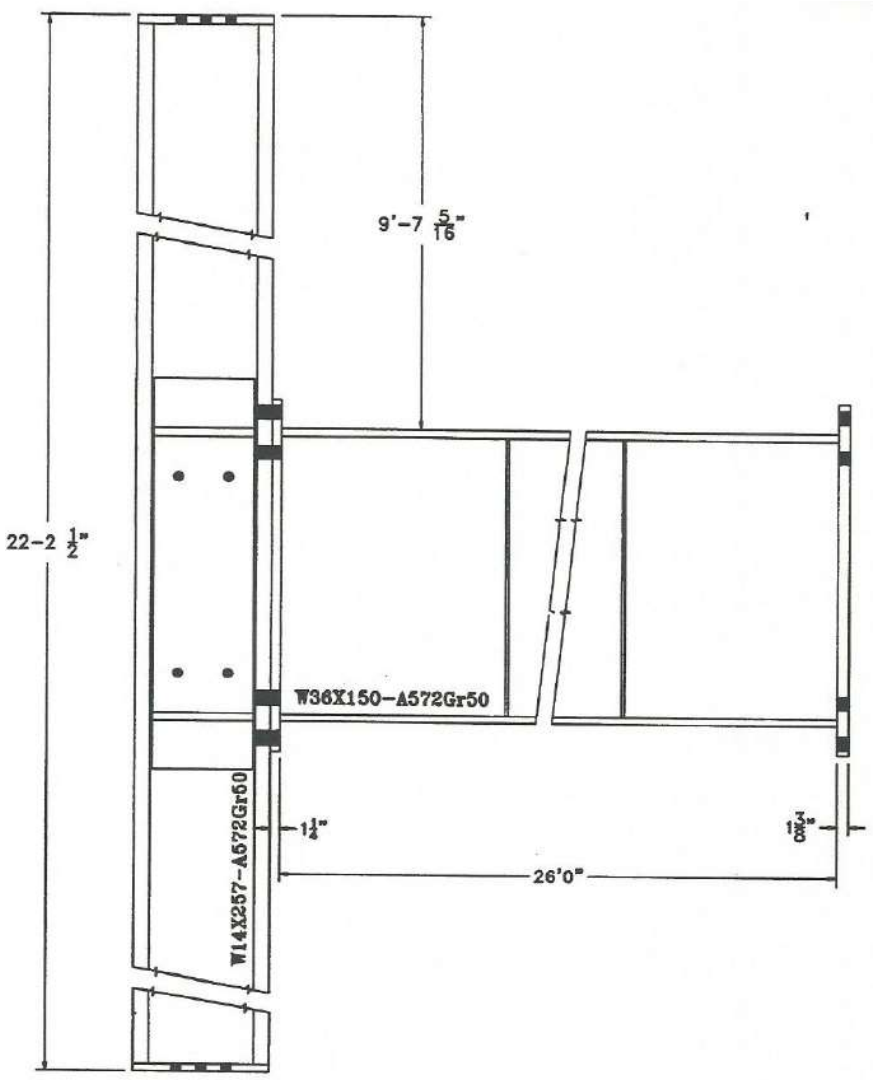

Figure 4-6 8E-4W-1.25-1.375-36 Specimen Dimensions [Sumner, E. A., Mays, T. W., & Murray, T. M. (2000). Cyclic Testing of Bolted Moment End-Plate Connections. Blacksburg, VA: Virginia Polytechnic Institute and State University, Used with Permission of T.M. Murray, 2015]

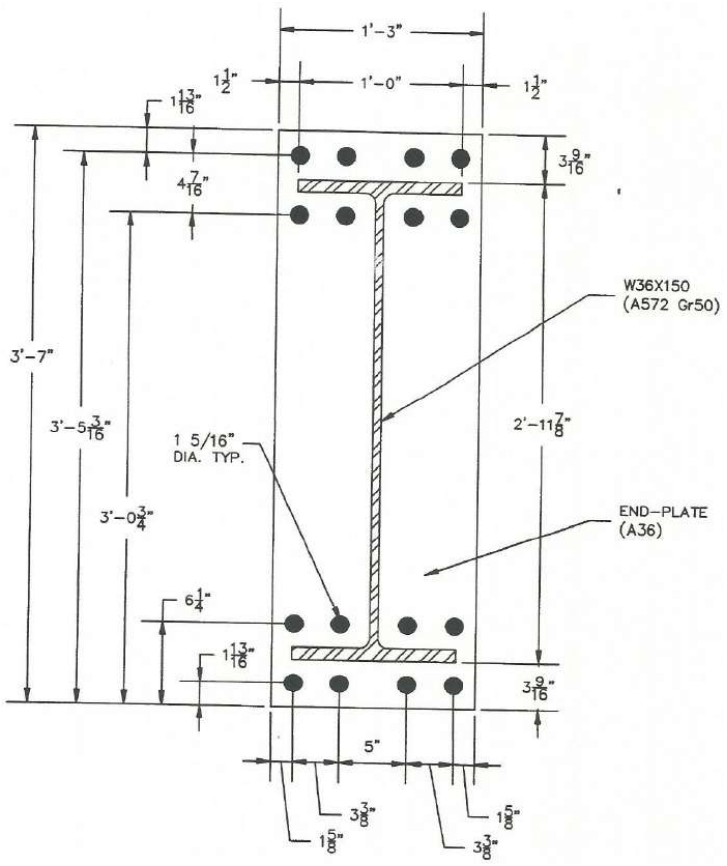

Figure 4-7 End Plate Layout for Specimen 8E-4W-1.25-1.375-36 [Sumner, E. A., Mays, T. W., & Murray, T. M. (2000). Cyclic Testing of Bolted Moment End-Plate Connections. Blacksburg, VA: Virginia Polytechnic Institute and State University, Used with Permission of T.M. Murray, 2015]

The specimen was tested with cyclic loading. Refer to the discussion in Section 4.1, which explains why cyclic tests would produce the same end-plate limit states with relatively similar yield and ultimate strength as monotonic tests.

4.1.2.1 Limit State – Predictions and Progression

Calculations using equations presented in Section 3.1, compute a moment capacity at bolt rupture without prying action, M_{np}, of 30900 k-in and a moment capacity for end-plate yielding, M_{pl}, to be 35100 k-in. These values match the values presented in Sumner and Murray (2001).

The expected limit state progression is bolt rupture without prying action, M_{np}, prior to any other limit state, thereby showing thick plate behavior. The specimen behaved as expected. Bolt rupture without prying action, M_{np}, controlled the strength of the connection while only minimal end-plate yielding occurred.

4.1.2.2 Experimental Results - Yield and Ultimate Moments

As reported in Sumner et al. (2000), a yield moment, M_y, of 29100 k-in and an ultimate moment, M_u, of 32800 k-in were experimentally obtained. Both are demonstrated graphically in Figure 4-8.

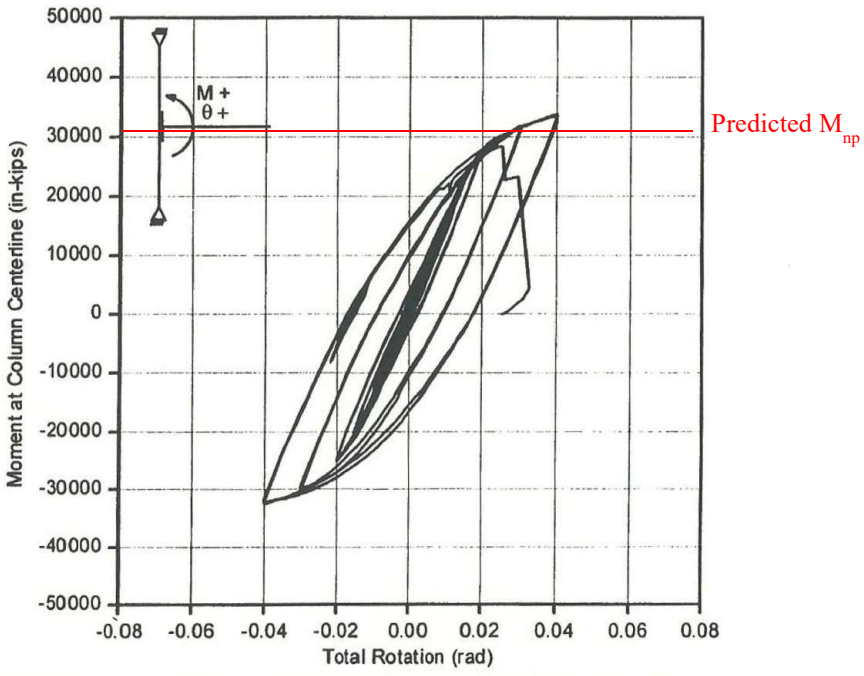

Figure 4-8 Load-deformation behavior for Specimen 8E-4W-1.25-1.375-36 [Sumner, E. A., Mays, T. W., & Murray, T. M. (2000). Cyclic Testing of Bolted Moment End-Plate Connections. Blacksburg, VA: Virginia Polytechnic Institute and State University, Used with Permission of T.M. Murray, 2015]

The ratios in the Table 4-3 compare the calculated limit states with experimentally observed limit states. If the ratio M_{np}/M_u is less than 1, then the calculated values are conservative.

Table 4-3 Predicted and Experimentally Obtained Moment Capacities for Specimen 8E-4W-1.25-1.375-36

Predicted (kip-in)		Experimental (kip-in)		Ratio	
M_{pl}	M_{np}	M_y	M_u	M_{pl}/M_y	M_{np}/M_u
35100	30900	29100	32800	-	0.94

Since M_{np}/M_u from Table 4-3 is less than 1.0, this implies a conservative prediction for the limit state of bolt rupture without prying action in relation to the experimentally obtained ultimate moment. The prediction was within 6% of the experimentally obtained strength, indicating adequate correlation between the two values.

4.1.2.3 Experimental Results - End-Plate Separation

Figure 4-9 displays end-plate separation in relation to moment at the column centerline. It suggests that thick plate behavior was achieved. Minimal end-plate separation was measured, indicating that the end-plate likely did not yield. Thus, the end-plate exhibited thick plate behavior.

4.1.2.4 Experimental Results - Bolt Strains

As is shown in Figure 4-10, the strain in Bolt 2 can be idealized to be a bilinear curve at any point during the test, not showing any exponential increase. Based on the shape of strain vs. moment it appears that there was no prying action, therefore, unlikely that end-plate yielded, implying thick plate behavior.

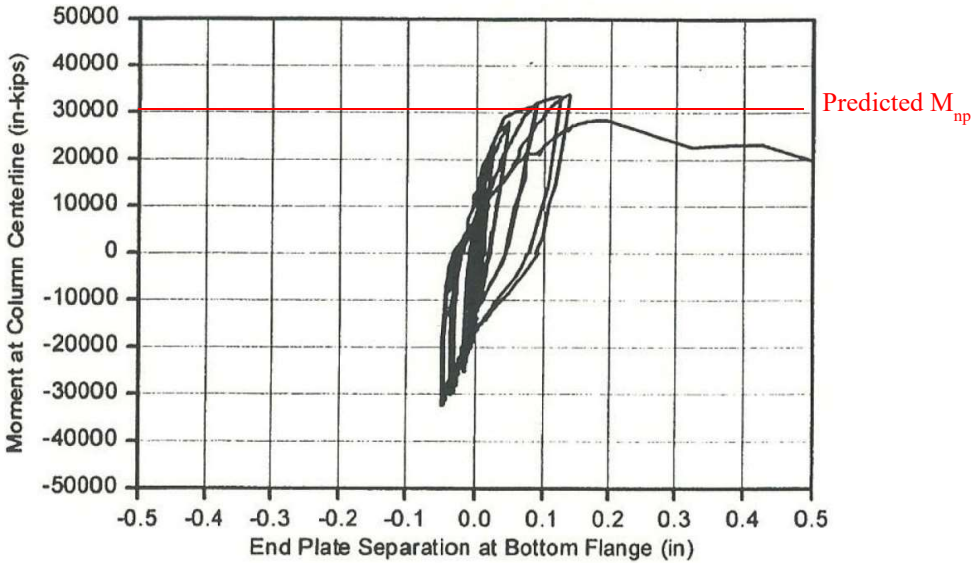

Figure 4-9 End-plate separation for Specimen 8E-4W-1.25-1.375-36 [Sumner, E. A., Mays, T. W., & Murray, T. M. (2000). Cyclic Testing of Bolted Moment End-Plate Connections. Blacksburg, VA: Virginia Polytechnic Institute and State University, Used with Permission of T.M. Murray, 2015]

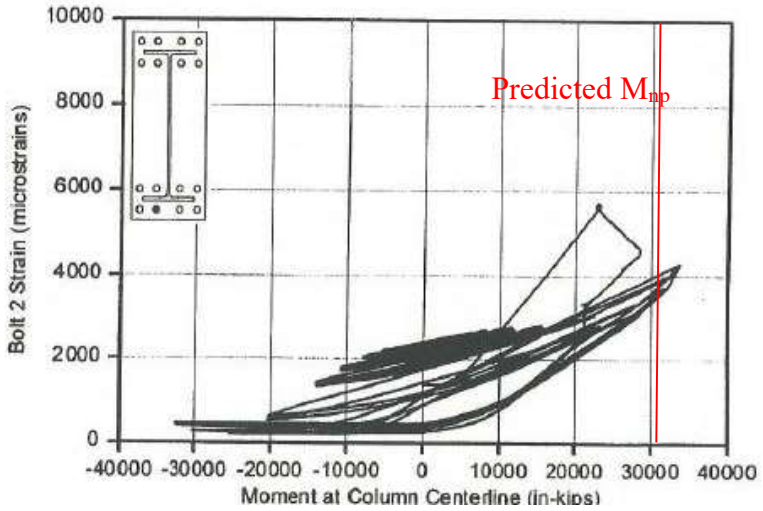

Figure 4-10 Bolt 2 strains for Specimen 8E-4W-1.25-1.375-36 [Sumner, E. A., Mays, T. W., & Murray, T. M. (2000). Cyclic Testing of Bolted Moment End-Plate Connections. Blacksburg, VA: Virginia Polytechnic Institute and State University, Used with Permission of T.M. Murray, 2015]

4.1.3 **Deep Section - Thin Plate Behavior**

Since the specimen 8E-4W-1-1/2-62 from Sumner and Murray (2001) had a higher moment carrying capacity for this type of configuration, it could be considered as a deep section (depth = 62 in.). Further, it was designed to exhibit thin end-plate behavior. The specimen geometry is shown in Figure 4-11 and the end-plate layout is shown in Figure 4-12.

4.1.3.1 Limit State – Predictions and Progression

Equations presented in Chapter 3 calculate a moment capacity at bolt rupture without prying action, M_{np}, of 2863 k-ft, moment capacity for end-plate yielding, M_{pl}, of 1034 k-ft, and moment capacity at bolt rupture with prying action, M_q, of 1707 k-ft. These values were verified with calculations based upon the design procedure proposed by Sumner and Murray (2001).

It is clear from the above mentioned moment capacities that end-plate will yield first, followed by bolts rupture with prying action. The specimen behaved as expected. End-plate yielding occurred followed by bolt rupture with prying action. The test was terminated prior to bolt rupture.

4.1.3.2 Experimental Results - Yield and Ultimate Moments

As reported in Sumner and Murray (2001), a yield moment, M_y, of 1075 k-ft was experimentally obtained and is demonstrated graphically in Figure 4-14. The test was stopped prior to bolt rupture and thus an ultimate moment, M_u, was not obtained. The maximum applied moment before the test was stopped was about 1540 k-ft (Figure 4-13).

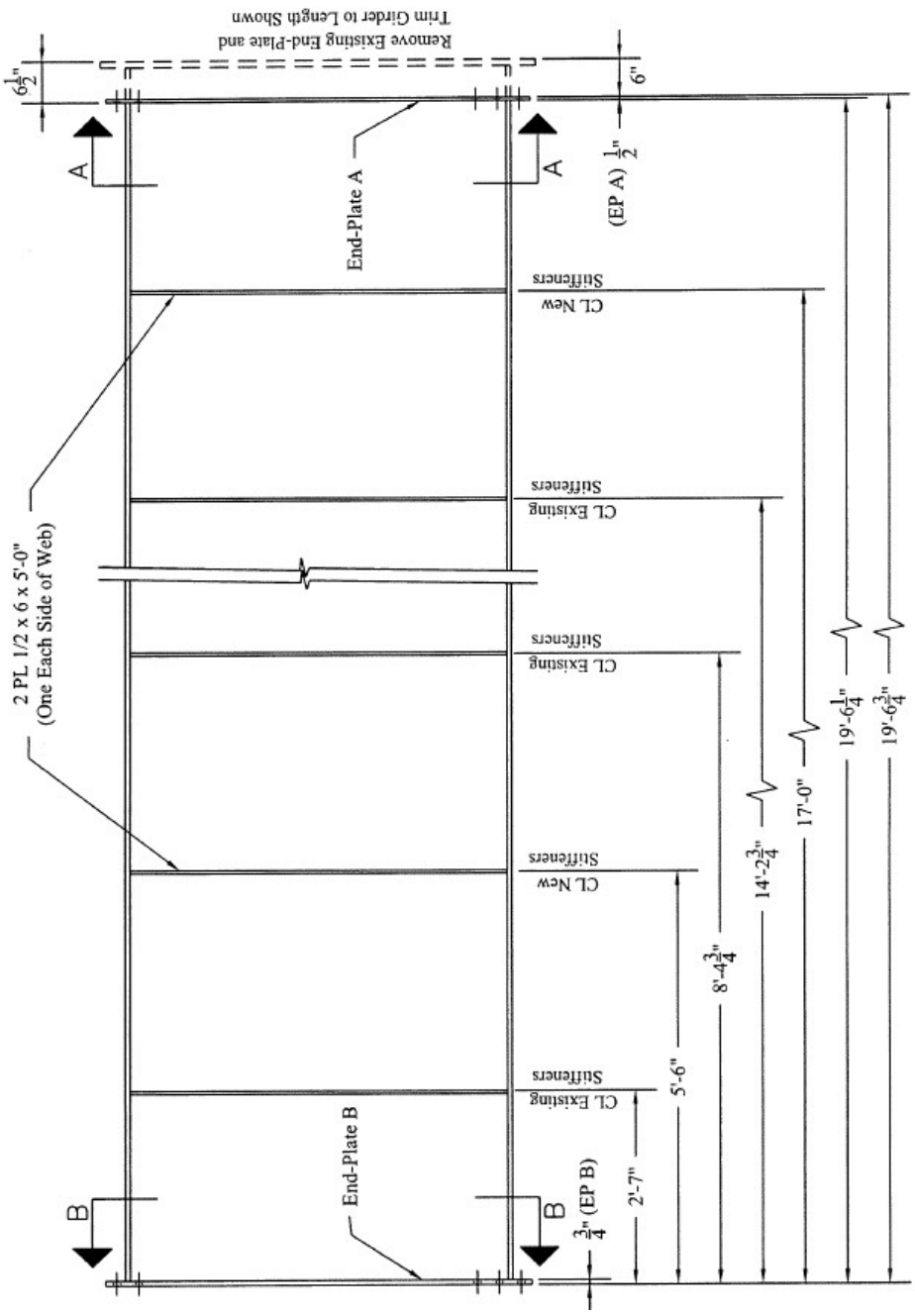

Figure 4-11 8E-4W-1-1/2-62 Specimen Dimensions [Sumner, E. A., & Murray, T. M. (2001). *Experimental Investigation of Four Bolt Wide Extended End-Plate Moment Connections.* Blacksburg, VA: Department of Civil Engineering, Virginia Polytechnic Institute and State University, Used with Permission of T.M. Murray, 2015]

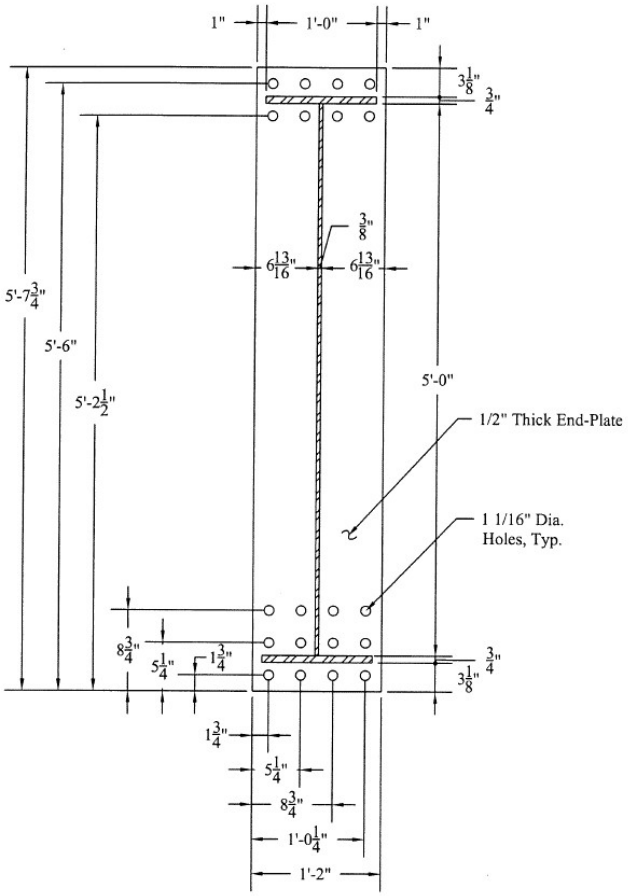

Figure 4-12 End Plate Layout for Specimen 8E-4W-1-1/2-62 [Sumner, E. A., & Murray, T. M. (2001). *Experimental Investigation of Four Bolt Wide Extended End-Plate Moment Connections.* Blacksburg, VA: Department of Civil Engineering, Virginia Polytechnic Institute and State University, Used with Permission of T.M. Murray, 2015]

The ratio M_{pl}/M_y in Table 4-4 implies a conservative prediction (ratio less than 1.0) for the limit state of end-plate yielding in relation to the experimentally obtained yield moment. The prediction was within 4% of the experimentally obtained strength, indicating adequate correlation between the two values.

The M_q/M_u ratio was unable to be calculated due to the experimental test being stopped prior to bolt rupture occurring.

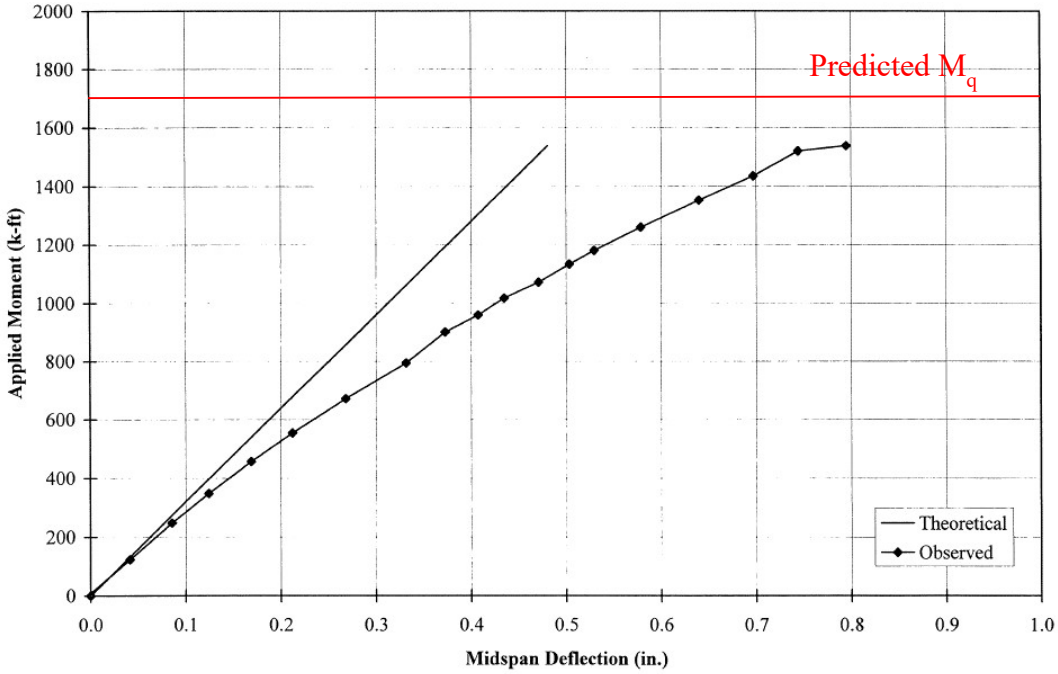

Figure 4-13 Load-deformation behavior for Specimen 8E-4W-1-1/2-62 [Sumner, E. A., & Murray, T. M. (2001). *Experimental Investigation of Four Bolt Wide Extended End-Plate Moment Connections.* Blacksburg, VA: Department of Civil Engineering, Virginia Polytechnic Institute and State University, Used with Permission of T.M. Murray, 2015]

Table 4-4 Predicted and Experimentally Obtained Moment Capacities for Specimen 8E-4W-1-1/2-62

Predicted (kip ft)		Experimental (kip ft)		Ratio	
M_{pl}	M_q	M_y	M_u^1	M_{pl}/M_y	M_q/M_u^1
1034	1707	1075	1540	0.96	0.90

M_u^1: Bolt Rupture not observed at this moment

4.1.3.1 Experimental Results - End-Plate Separation

As is evidenced by the relatively low slope of the initial section of Figure 4-14, end-plate yielding occurred during the test. This provides verification that thin plate behavior was achieved.

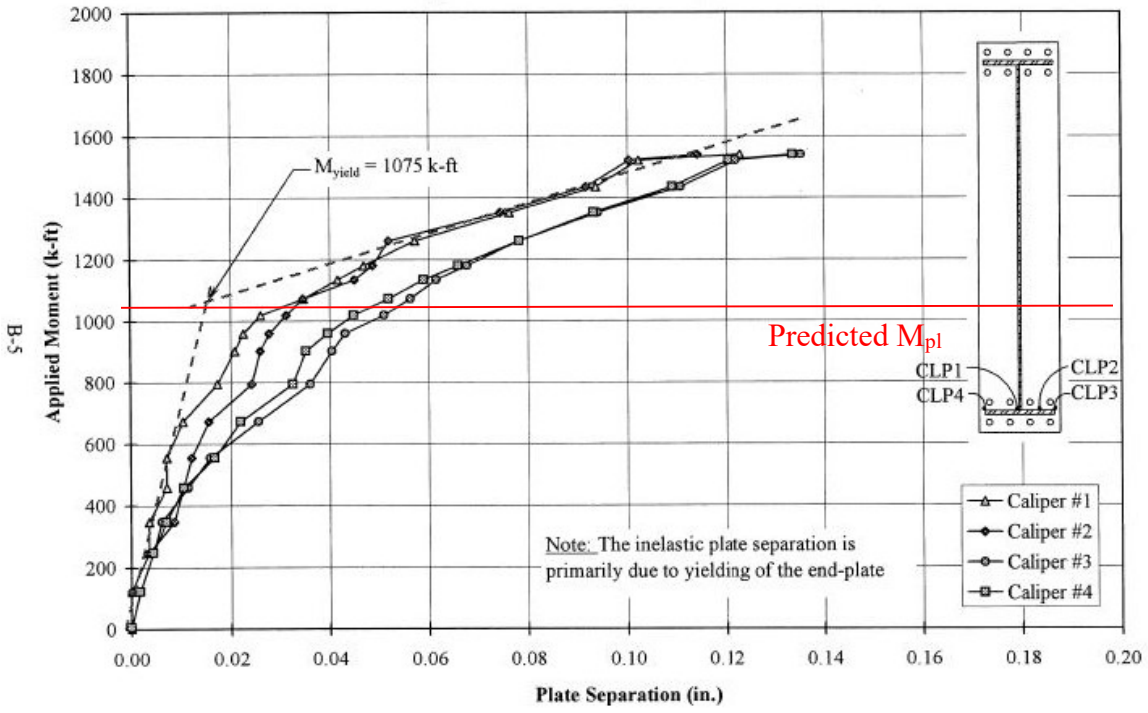

Figure 4-14 End-Plate Separation for Specimen 8E-4W-1-1/2-62 [Sumner, E. A., & Murray, T. M. (2001). *Experimental Investigation of Four Bolt Wide Extended End-Plate Moment Connections.* Blacksburg, VA: Department of Civil Engineering, Virginia Polytechnic Institute and State University, Used with Permission of T.M. Murray, 2015]

4.1.3.2 Experimental Results - Bolt Forces

As is shown in Figure 4-15, forces in the instrumented bolts drastically increased past the observed yield moment of 1075 kip-ft. This indicates substantial prying forces as a result of thin end-plate behavior. Furthermore, the bolt forces approached their ultimate force as the applied moment approached the predicted M_q value.

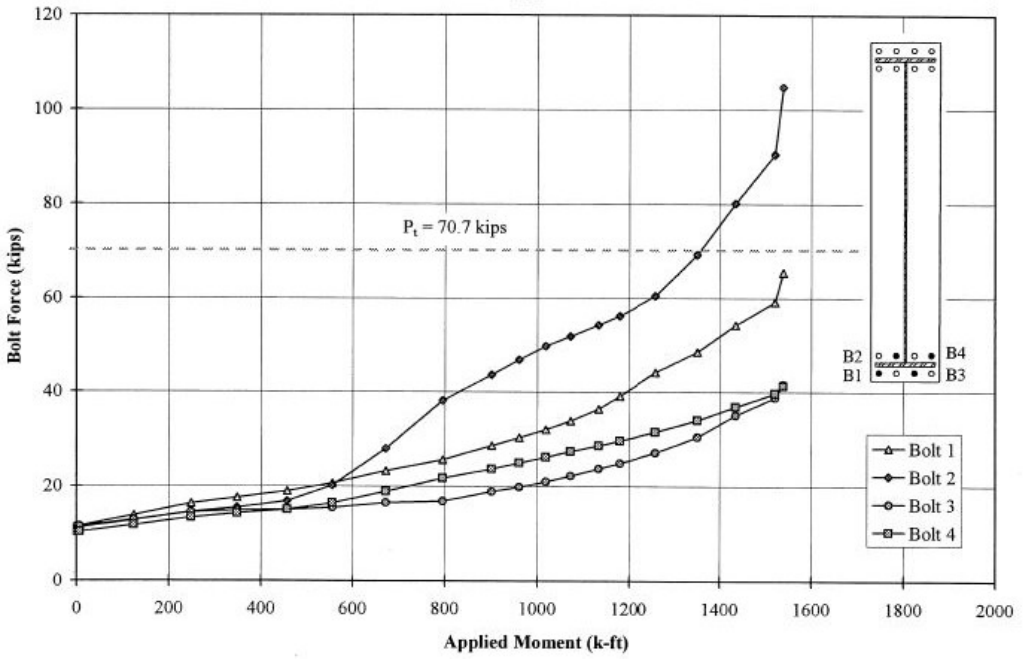

Figure 4-15 Bolt forces for Specimen 8E-4W-1-1/2-62 [Sumner, E. A., & Murray, T. M. (2001). *Experimental Investigation of Four Bolt Wide Extended End-Plate Moment Connections.* Blacksburg, VA: Department of Civil Engineering, Virginia Polytechnic Institute and State University, Used with Permission of T.M. Murray, 2015]

4.1.4 Deep Section - Thick Plate Behavior

Specimen 8E-4W-3/4-3/4-62 from Sumner and Murray (2001) was a 62 in deep built-up beam designed to exhibit thick end-plate behavior. Figure 4-16 shows the specimen diagram and Figure 4-17 illustrates the end-plate geometry.

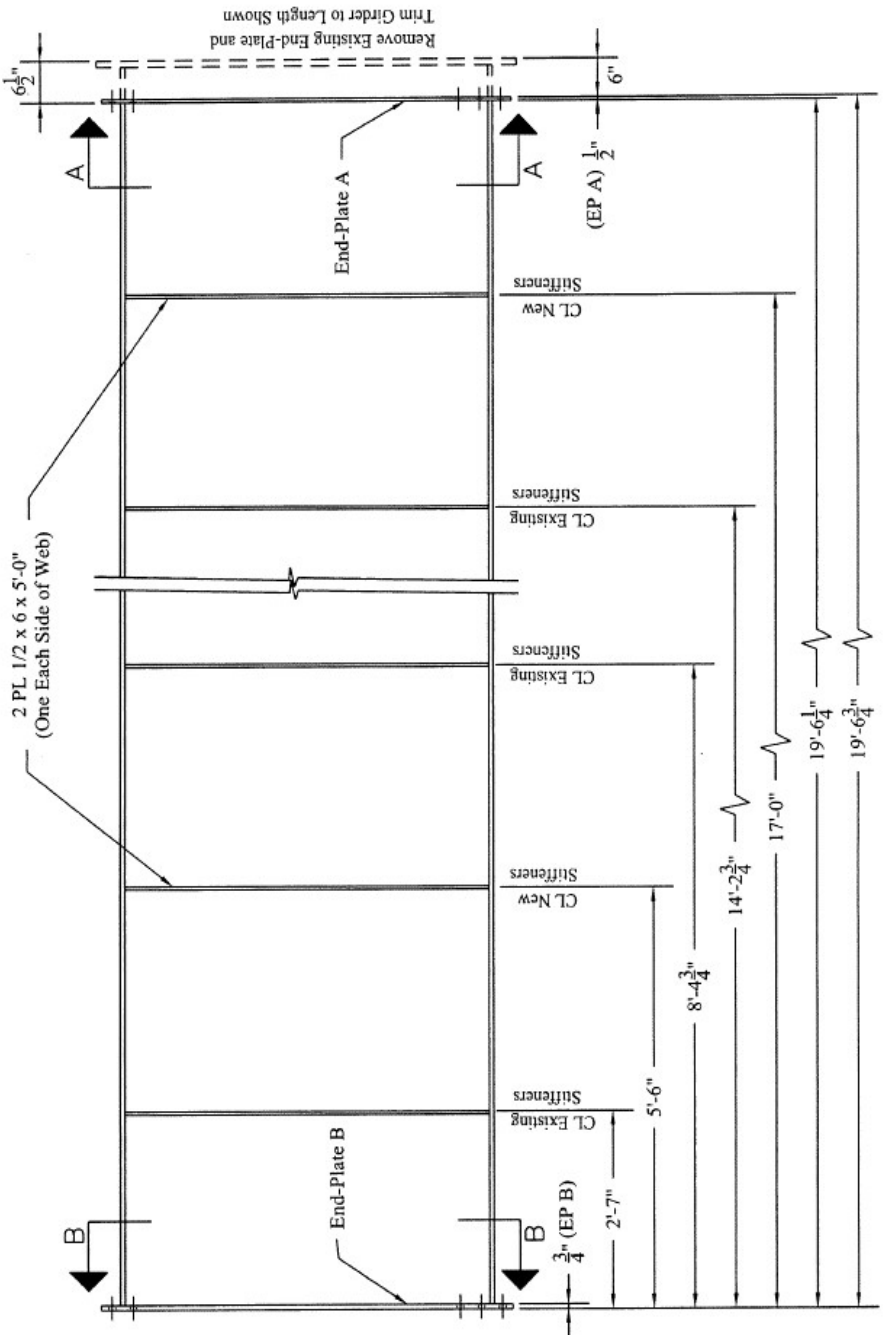

Figure 4-16 8E-4W-3/4-3/4-62 Specimen Dimensions [Sumner, E. A., & Murray, T. M. (2001). *Experimental Investigation of Four Bolt Wide Extended End-Plate Moment Connections.* Blacksburg, VA: Department of Civil Engineering, Virginia Polytechnic Institute and State University,
Used with Permission of T.M. Murray, 2015]

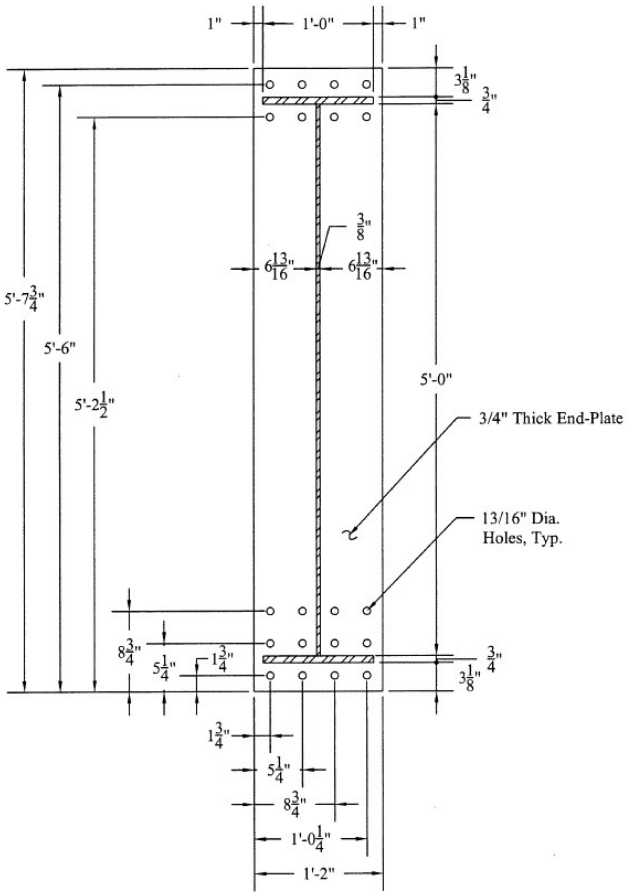

Figure 4-17 End Plate Layout for Specimen 8E-4W-3/4-3/4-62 [Sumner, E. A., & Murray, T. M. (2001). *Experimental Investigation of Four Bolt Wide Extended End-Plate Moment Connections.* Blacksburg, VA: Department of Civil Engineering, Virginia Polytechnic Institute and State University, Used with Permission of T.M. Murray, 2015]

4.1.4.1 Limit State – Predictions and Progression

Chapter 3 provides a moment capacity at bolt rupture without prying action, M_{np}, of 1612 k-ft and moment capacity for end-plate yielding, M_{pl}, of 2062 k-ft. These values were verified with calculations based upon the design procedure proposed by Sumner and Murray (2001). The expected limit state progression is that bolt rupture without prying action, M_{np}, will occur prior to any other limit state. The specimen behaved as expected. Bolt rupture without prying action, M_{np}, controlled the strength of the connection without any observed end-plate yielding.

4.1.4.2 Experimental Results - Yield and Ultimate Moments

As reported in Sumner and Murray (2001), a yield moment, M_y, of 1630 k-ft and an ultimate moment, M_u, of 1825 k-ft were experimentally obtained. The ultimate moment is shown in Figure 4-18 whereas the yield moment is demonstrated graphically in Figure 4-19.

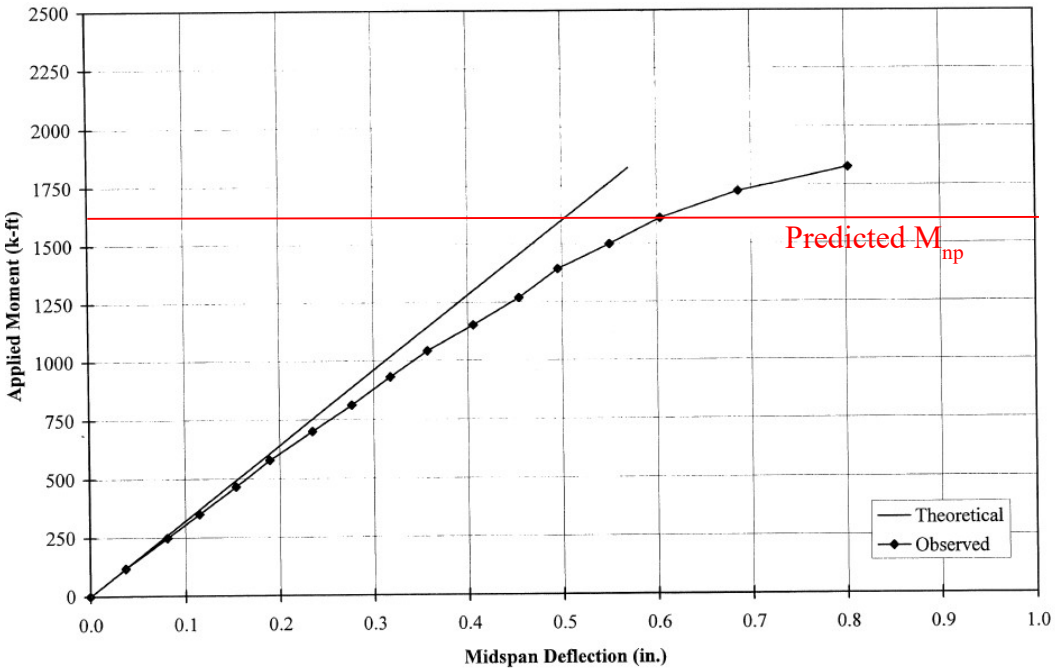

Figure 4-18 Load-deformation behavior for Specimen 8E-4W-3/4-3/4-62 [Sumner, E. A., & Murray, T. M. (2001). *Experimental Investigation of Four Bolt Wide Extended End-Plate Moment Connections.* Blacksburg, VA: Department of Civil Engineering, Virginia Polytechnic Institute and State University, Used with Permission of T.M. Murray, 2015]

Table 4-5 Predicted and Experimentally Obtained Moment Capacities for Specimen 8E-4W-3/4-3/4-62

Predicted (kip-ft)		Experimental (kip-ft)		Ratio	
M_{pl}	M_{np}	M_y	M_u	M_{pl}/M_y	M_{np}/M_u
2602	1612	1630	1825	-	0.88

The ratio in Table 4-5 implies a conservative prediction (less than 1.0) for the limit state of bolt rupture without prying action in relation to the experimentally obtained ultimate moment. The prediction was within 12% of the experimentally obtained strength, which is a greater differential than desired, but since it is a conservative prediction, the correlation between the two values (predicted and experimental) is adequate.

4.1.4.1 Experimental Results - End-Plate Separation

As is evidenced by the relatively stiff initial section of Figure 4-19 end-plate yielding did not occur in any significant amount during the test. This verifies that thick plate behavior was achieved and that the design procedure successfully provides a connection that behaves as intended.

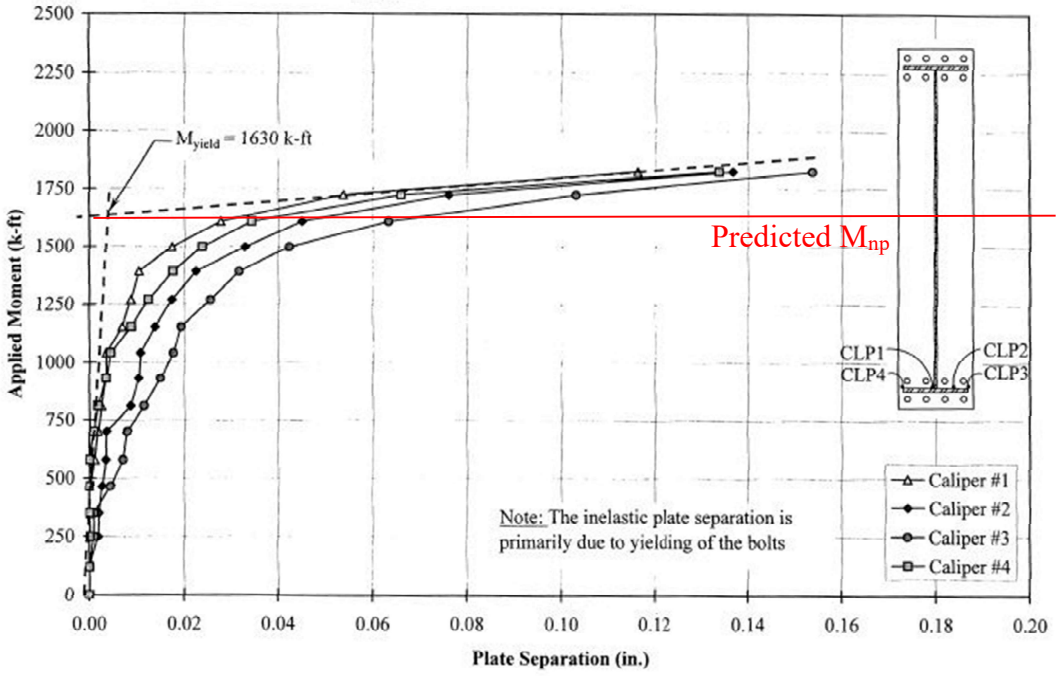

Figure 4-19 End-Plate Separation for Specimen 8E-4W-3/4-3/4-62 [Sumner, E. A., & Murray, T. M. (2001). *Experimental Investigation of Four Bolt Wide Extended End-Plate Moment Connections.* Blacksburg, VA: Department of Civil Engineering, Virginia Polytechnic Institute and State University, Used with Permission of T.M. Murray, 2015]

4.1.4.2 Experimental Results - Bolt Forces

As is shown in Figure 4-20, forces in the instrumented bolts did not drastically increase prior to their ultimate strength (data plotted past this point is considered invalid due to unaccounted for nonlinearity in the relationship between stress and strain). This indicates that prying forces were negligible. In other words, the end-plate did not yield, implying thick end-plate behavior. Furthermore, the bolt forces approached their ultimate force as the applied moment approached the predicted M_{np} value of 1612 k-ft.

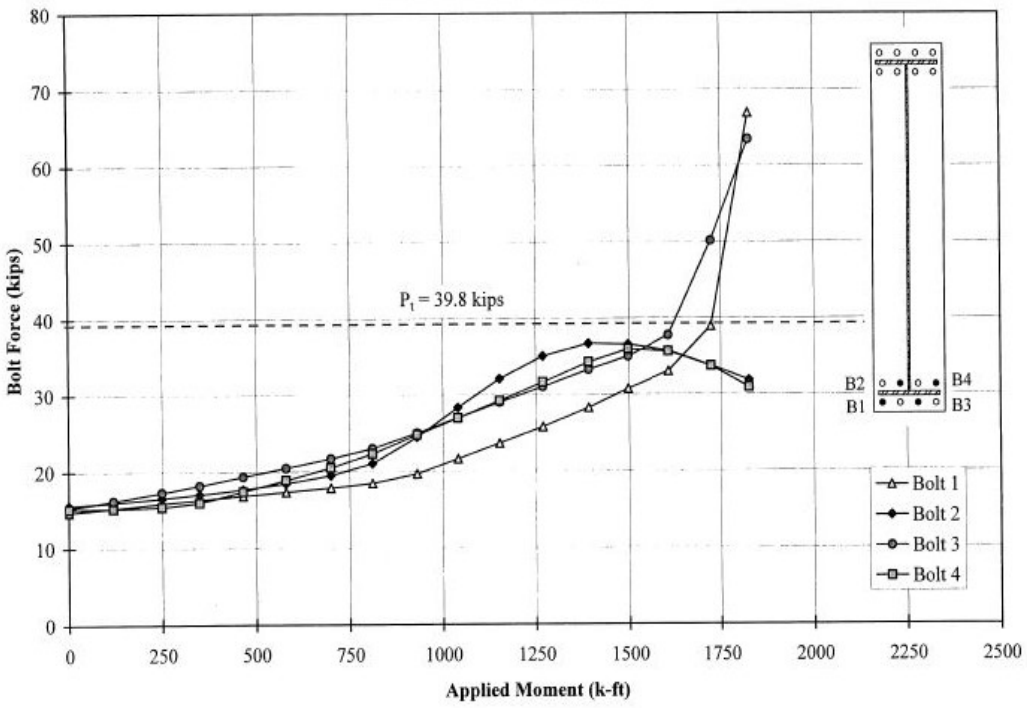

Figure 4-20 Bolt forces for Specimen 8E-4W-3/4-3/4-62 [Sumner, E. A., & Murray, T. M. (2001). *Experimental Investigation of Four Bolt Wide Extended End-Plate Moment Connections.* Blacksburg, VA: Department of Civil Engineering, Virginia Polytechnic Institute and State University,
Used with Permission of T.M. Murray, 2015]

4.1.5 Overall Summary of Eight Bolt Extended Four Wide Configuration and Recommendations

Table 4-6 shows a summary of the four specimens investigated herein. For thin plate specimens, M_{pl} was either 4% less or 4% more than the experimentally observed end-plate yield moment, M_y.

Table 4-6 Summary of the Four Test Specimens (from literature) of the Eight Bolt Extended Four Wide Configuration

Specimen Identification[1]		Reference	Depth (in.)	Behavior	Remarks[2]
2	8E-4W-1.25-1-30	Sumner et al. (2000)	30	Thin	M_{pl} was +4% of yield moment. M_q was +5% of the experimentally observed moment.
3	8E-4W-1.25-1.375-36	Sumner et al. (2000)	36	Thick	M_{np} was -6% of the experimentally observed moment
5	8E-4W-1-1/2-62	Sumner et and Murray (2001)	62	Thin	M_{pl} was -4% of yield moment. Bolt rupture not observed. Test stopped at
6	8E-4W-3/4-3/4-62	Sumner and Murray (2001)	62	Thick	M_{np} was -12% of the experimentally observed moment

[1]Specimen Identification: "Conn. type - Bolt diameter - End-plate thickness - Beam depth". Identification in parentheses was used in the reference.

Remarks[2]: A postive percentage means an unconservative calculation, whereas a negative percentage means a safe prediction.

Also, M_q for thin plate shallow specimen was 5% more than the experimental ultimate moment, which means that the calculations were a bit unconservative. Bolt rupture wasn't

observed for the thin plate deep specimen 8E-4W-1-1/2-62. End-plate yielding was seen for both the thin plate specimens and the experimentally observed end-plate separation was found to be in reasonable agreement with a typical thin plate behavior.

For the two thick plate specimens, 8E-4W-1.25-1.375-36 and 8E-4W-3/4-3/4-62, M_{np} was conservative by 6% and 12% respectively, indicating reserve capacity in the connection past which the design procedure predicts. The experimental limit state progression matched that which was predicted; bolt rupture without prying action occurring prior to any other limit state. Furthermore, experimentally measured end-plate separation was found to be consistent with thick end-plate behavior wherein the end-plate does not significantly yield prior to bolt fracture.

Hence, it could be said that the design procedures proposed in the previous chapter for 8E-4W appear to be validated.

4.2 Previous Testing on the Eight-Bolt Extended Stiffened Configuration

The eight bolt extended, stiffened end-plate connection is included in AISC 358-10 (AISC 2010) as a prequalified moment connection for special moment resisting frames. There have been several tests on the connection configuration, but many have focused on developing a plastic hinge in the beam prior to experiencing end plate yielding or bolt rupture. The references are reviewed in this section to investigate what data exists to validate design procedures for either thin plate or thick plate behavior.

Experimental programs on the Eight-Bolt Extended Stiffened configuration have been reported by Ghassemieh et al. (1983), Adey et al. (1997, 2000), Sumner et al. (2000), Sumner and Murray (2002), Sumner (2003) and Seek and Murray (2008). A summary of the previous tests on this connection configuration is given in Table 4-7.

Since many of the tests were intended for the development of seismic resisting moment connections, they consisted of beam-column test configurations subjected to cyclic

loading. Refer to discussion in Section 4.1 on why limit state moment capacities would be similar between monotonic and cyclic loading.

Table 4-7 Summary of Experiments on the Eight Bolt Extended Stiffened Configuration

Test Identification[1]		Reference	Configuration	Loading	Depth	Behavior[2]
1	8ES-0.875-0.75-24 (EP1)	Ghassemieh (1983)	Splice	Mono.	24	Thin
2	8ES-0.875-1-24 (EP2)	Ghassemieh (1983)	Splice	Mono.	24	Thick
3	8ES-1.125-0.75-18 (M5)	Adey et al. (1997)	Beam - Column	Cyclic	18	P.H. / Thin
4	8ES-1.125-0.75-18 (M7)	Adey et al. (1997)	Beam - Column	Cyclic	18	P.H. / Thin
5	8ES-1.125-0.75-18 (B5)	Adey et al. (1997)	Beam - Column	Cyclic	18	P.H. / Thin
6	8ES-1.25-1.75-30	Sumner et al. (2000)	Beam - Column	Cyclic	30	P.H.
7	8ES-1.25-1-30	Sumner et al. (2000)	Beam - Column	Cyclic	30	P.H. / Thin
8	8ES-1.25-2.5-36	Sumner et al. (2000)	Beam - Column	Cyclic	36	P.H.
9	8ES-1.25-1.25-36	Sumner et al. (2000)	Beam - Column	Cyclic	36	Thick
10	8ES-1.125-1.25-27	Seek and Murray (2008)	Beam - Column	Cyclic	27	P.H.

[1]Test Identification: "Connection type - Bolt diameter - End-plate thickness - Beam depth". Identification in parentheses was used in the reference.

[2]P.H. means plastic hinging of the beam.

In this section, test specimens 8ES-0.875-0.75-24, 8ES-0.875-1-24, 8ES-1.25-1-30, and 8ES-1.25-1.25-36, which are boxed in thicker lines in Table 4-7, will be examined. Specimens identified as having the most useful data for validating design procedures for thick and thin end plate behavior (not end plate connections designed to promote plastic hinging of the beam) were investigated.

4.2.1 Shallow Section - Thin Plate Behavior

4.2.1.1 Specimen 8ES-1.25-1-30 from Sumner et al. (2000)

Specimen 8ES-1.25-1-30 from Sumner et al. (2000) experienced both inelasticity in the beam and inelasticity in the end-plate due to similar moment capacities for the two limit states. The specimen dimension and end-plate layout is shown in Figure 4-21 and Figure 4-22.

4.2.1.1.1 Limit State – Predictions and Progression

Moment capacities were calculated based on the equations presented in Section 3.2 and the obtained values were within 7% of the values published in Sumner (2003). A beam plastic moment capacity, M_p of 16400 k-in (calculated using measured yield stress), end-plate yield moment capacity, M_{pl} of 17700 k-in (calculated using measured yield stress), moment capacity for bolt rupture with prying action, M_q = 19100 k-in and moment capacity for bolt rupture without prying action, M_{np} = 25700 k-in were calculated.

As reported in Sumner et al. (2000), the specimen first experienced yielding in the flanges of the beam at the base of the stiffeners, followed by yielding in the column web doubler plate and the end plate. During subsequent cycles, full yield of the beam flanges led to local flange buckling while inelasticity spread to many parts of the specimen: end plate, beam web, column web, end plate stiffeners. The test was stopped after cycles up to 0.055 rad after severe lateral displacements of the beam.

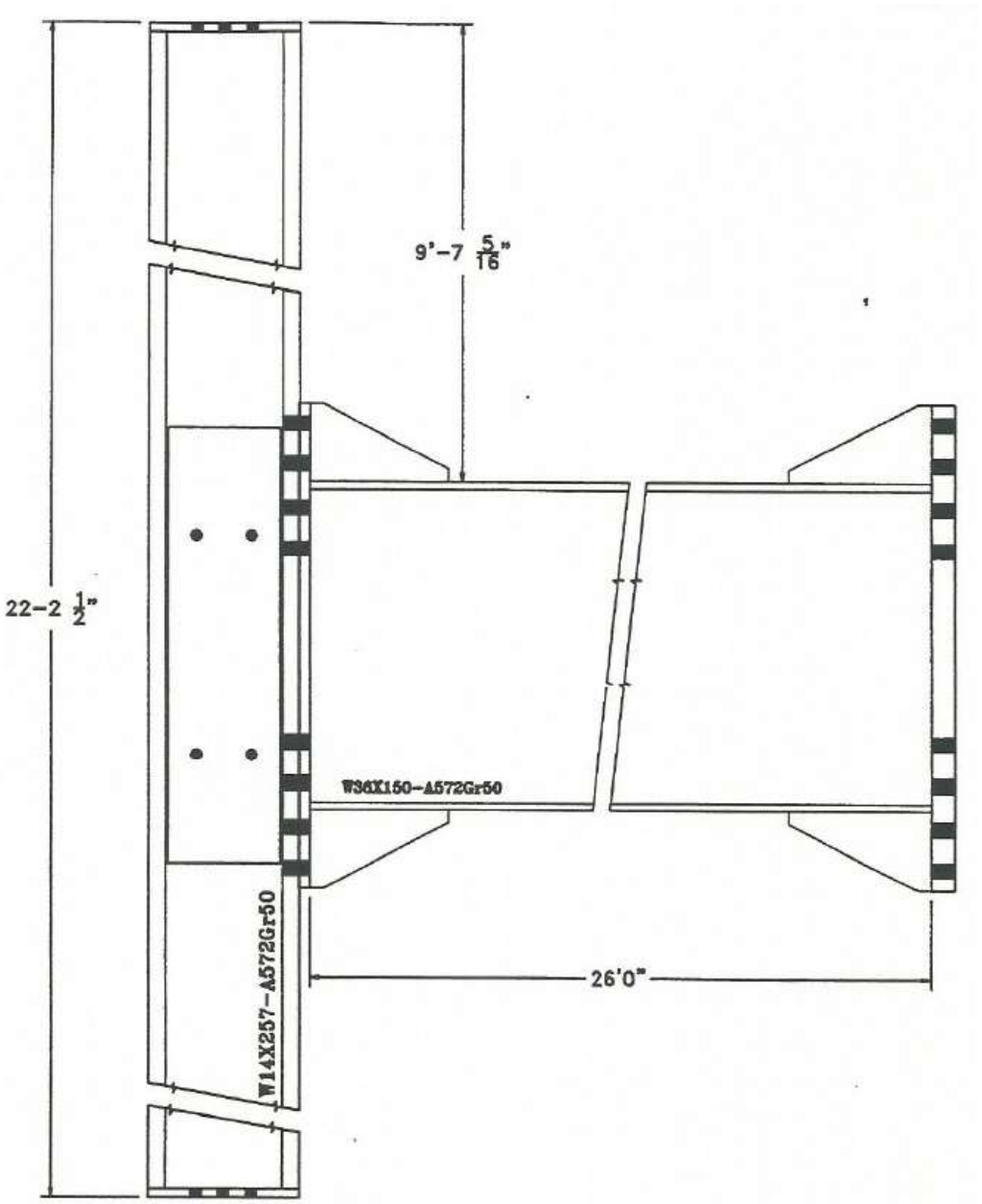

Figure 4-21 8ES-1.25-1-30 Specimen Dimensions [Sumner, E. A., Mays, T. W., & Murray, T. M. (2000). *Cyclic Testing of Bolted Moment End-Plate Connections.* Blacksburg, VA: Virginia Polytechnic Institute and State University, Used with Permission of T.M. Murray, 2015]

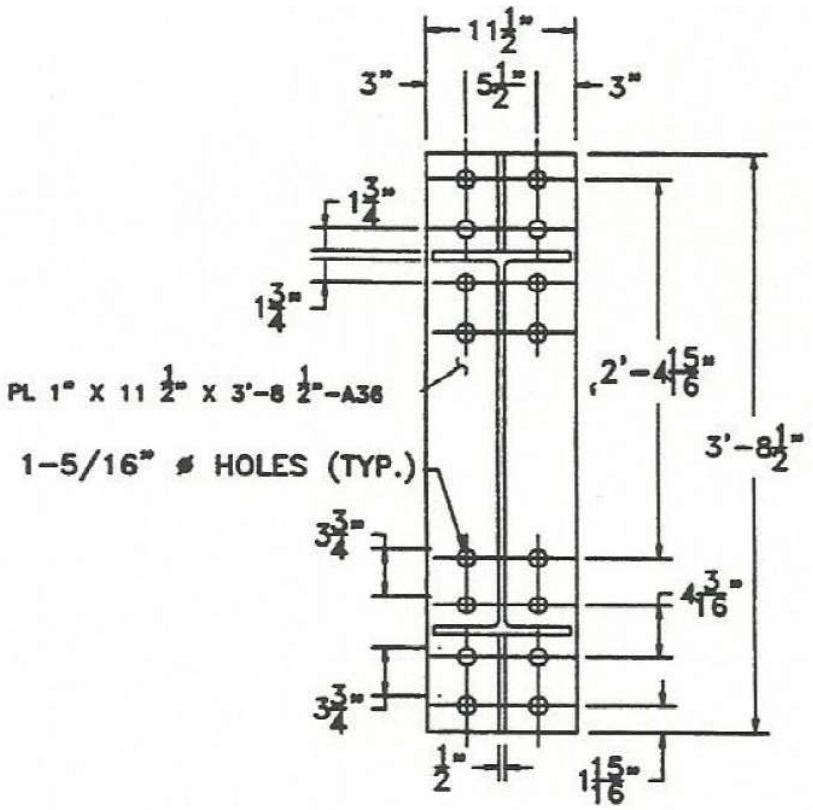

Figure 4-22 End-Plate Layout for Specimen 8ES-1.25-1-30 [Sumner, E. A., Mays, T. W., & Murray, T. M. (2000). *Cyclic Testing of Bolted Moment End-Plate Connections.* Blacksburg, VA: Virginia Polytechnic Institute and State University, Used with Permission of T.M. Murray, 2015]

4.2.1.1.1 Experimental Results – Yield and Ultimate Moments

As reported in Sumner et al. (2000), a yield moment, M_y, of 16900 k-in and an ultimate moment, M_u, of 20900 k-in were experimentally obtained. Figure 4-23 shows the moment rotation behavior for the specimen. The moment-rotation plot is difficult to interpret (in terms of validating the end plate moment capacity) because several limit states were occurring including plastic hinging of the beam.

Table 4-8 shows the comparison between the predicted and experimentally obtained moment capacities. The test reached an ultimate moment of 20900 k-in before local buckling caused degradation in the moment capacity. This was approximately 10% larger

than the calculated moment associated with bolt rupture with prying action, M_q. Since the specimen moment strength degraded, the moment capacity associated with bolt rupture was not experimentally obtained and may have been even larger.

Table 4-8 Predicted and Experimentally Obtained Moment Capacities 8ES-1.25-1-30

Predicted (k-in)		Experimental (k-in)		Ratio	
M_{pl}	M_q	M_y	M_u[1]	M_{pl}/M_y	M_q/M_u[1]
17700	19100	16900	20900	1.05	0.91

M_u[1]: Bolt rupture not observed at this moment, but this was the peak moment, before local buckling

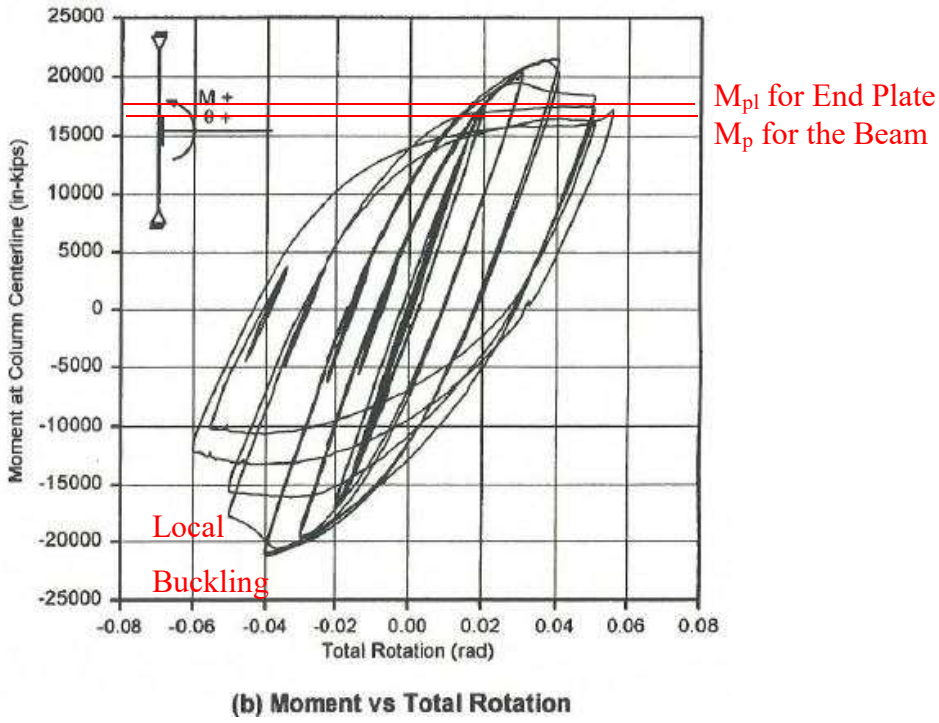

Figure 4-23 Load-deformation behavior for Specimen 8ES-1.25-1-30 [Sumner, E. A., Mays, T. W., & Murray, T. M. (2000). *Cyclic Testing of Bolted Moment End-Plate Connections.* Blacksburg, VA: Virginia Polytechnic Institute and State University, Used with Permission of T.M. Murray, 2015]

4.2.1.1.1 Experimental Results – End-Plate Separation

Figure 4-24 displays end-plate separation in relation to moment at the column centerline. The nonlinearity in the end plate separation shown in Figure 4-24 may be related to end plate yielding.

4.2.1.1.2 Experimental Results – Bolt Strains

Figure 4-25 shows the strain from Bolt 11. A rapid increase is seen in the strains past the experimental end-plate yield moment, M_y, which suggests prying action in the connection due to end-plate yielding.

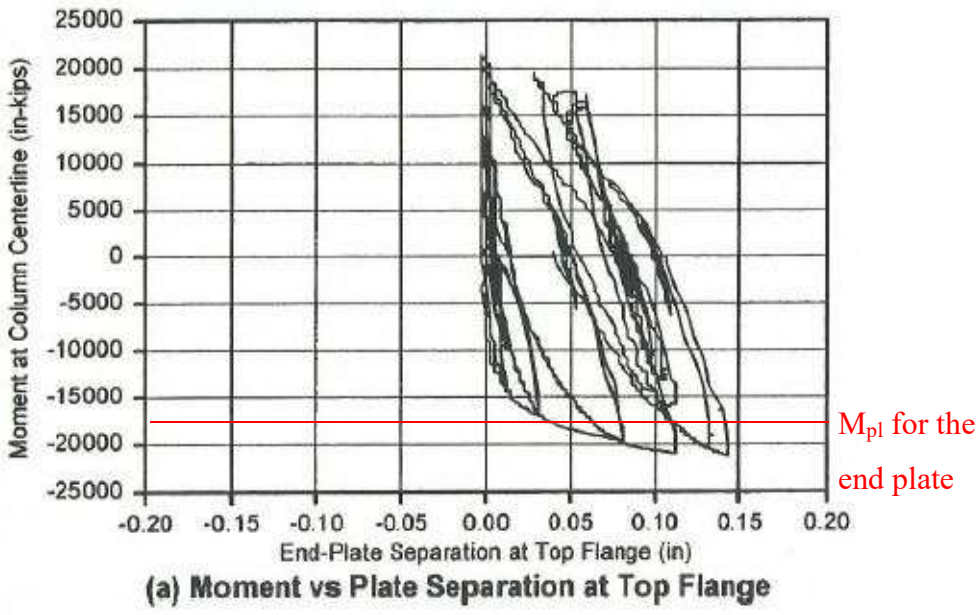

Figure 4-24 End-plate separation for Specimen 8ES-1.25-1-30 [Sumner, E. A., Mays, T. W., & Murray, T. M. (2000). *Cyclic Testing of Bolted Moment End-Plate Connections.* Blacksburg, VA: Virginia Polytechnic Institute and State University, Used with Permission of T.M. Murray, 2015]

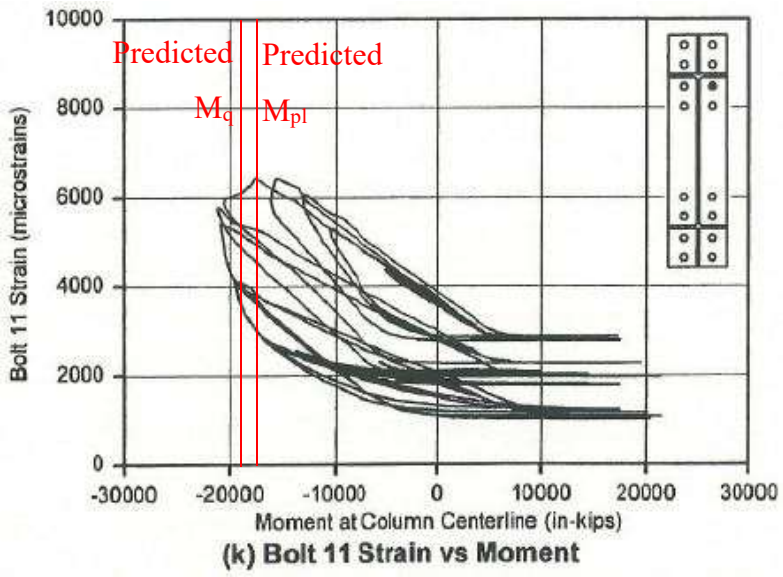

Figure 4-25 Bolt 11 strains for Specimen 8ES-1.25-1-30 [Sumner, E. A., Mays, T. W., & Murray, T. M. (2000). *Cyclic Testing of Bolted Moment End-Plate Connections.* Blacksburg, VA: Virginia Polytechnic Institute and State University, Used with Permission of T.M. Murray, 2015]

4.2.1.2 Specimen 8ES-0.875-0.75-24 from Ghassemieh et al. (1983)

There is little discussion provided in Ghassemieh et al. (2000) as to the types of limit states observed during the testing of specimen 8ES-0.875-0.75-24. See Figure 4-26 for specimen dimensions and Figure 4-27 for end-plate layout. It is stated that end-plate yielding was observed, but it is unclear when end plate yielding initiated.

4.2.1.2.1 Limit State – Predictions and Progression

Based on the predicted moment capacities, it was expected that end plate yielding would occur followed by bolt rupture with prying action. The specimen did experience end plate yielding, but the test was stopped prior to bolt rupture.

The predicted moment capacities are: bolt rupture with prying action, M_q = 648 k-ft and M_q = 578 k-ft (calculated using the AISC Manual) and bolt rupture without prying action, M_{np} = 853 k-ft. Also, end plate yield moment capacity, $M_{pl,}$ was calculated to be 788 k-ft (calculated using measured yield stress) and beam plastic moment capacity, $M_{p,}$ was computed to be 840 k-ft (calculated using nominal yield stress).

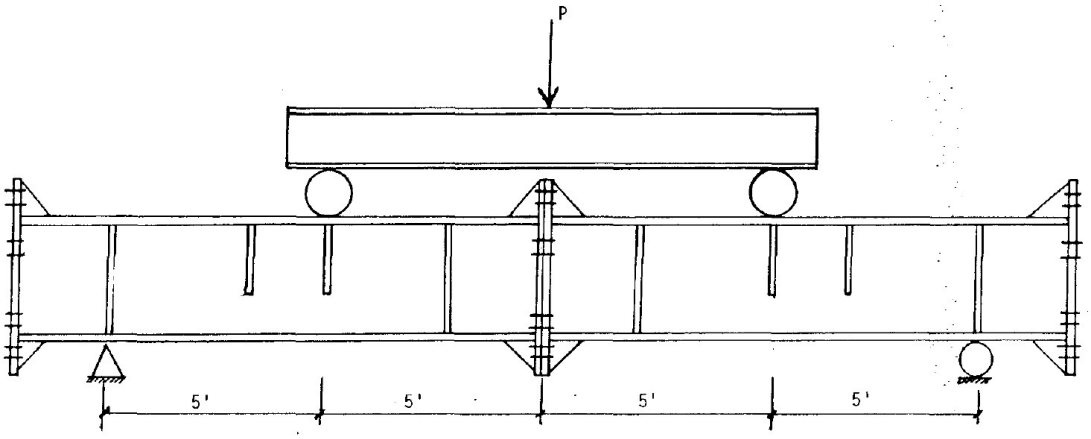

Figure 4-26 8ES-0.875-0.75-24 Specimen Dimensions [Ghassemieh, M., Kukreti, A., and Murray, T.M. (1983) *Inelastic Finite Element Analysis of Stiffened End-Plate Moment Connections*, Report No. FSEL/AISC 8302, School of Civil Engineering and Environmental Science, University of Oklahoma, Norman, OK, Used with Permission of T.M. Murray, 2015]

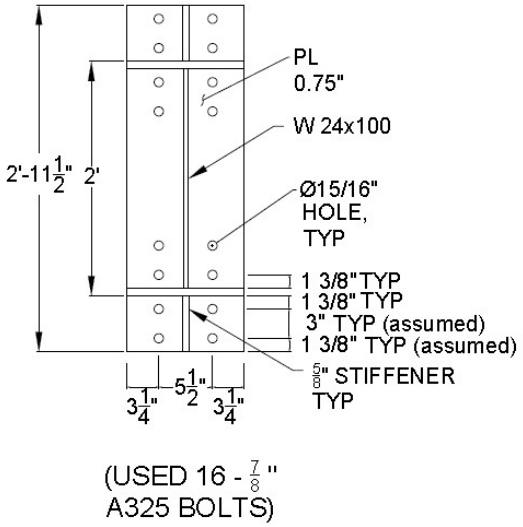

Figure 4-27 End-Plate Layout for Specimen 8ES-0.875-0.75-24 [redrawn from Ghassemieh, M., Kukreti, A., and Murray, T.M. (1983) *Inelastic Finite Element Analysis of Stiffened End-Plate Moment Connections*, Report No. FSEL/AISC 8302, School of Civil Engineering and Environmental Science, University of Oklahoma, Norman, OK, Used with Permission of T.M. Murray, 2015]

4.2.1.2.2 Experimental Results – Yield and Ultimate Moments

Figure 4-28 shows the moment-deflection behavior. Ghassemieh et al. (1983) reported nonlinearity starting at 350 k-ft, a yield moment of approximately 500 k-ft, and ultimate moment equal to 680 k-ft.

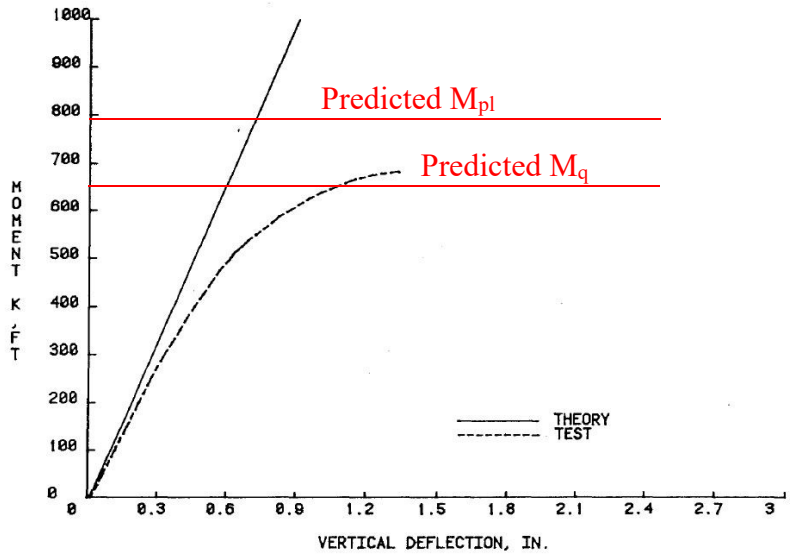

Figure 4-28 Moment-Deflection behavior for Specimen 8ES-0.875-0.75-24 [Ghassemieh, M., Kukreti, A., and Murray, T.M. (1983) *Inelastic Finite Element Analysis of Stiffened End-Plate Moment Connections*, Report No. FSEL/AISC 8302, School of Civil Engineering and Environmental Science, University of Oklahoma, Norman, OK, Used with Permission of T.M. Murray, 2015]

A comparison of the calculated and experimentally observed limit states is shown in Table 4-9. The calculated moment capacity for bolt rupture with prying action was found to be less than the end plate yield moment capacity. It is hypothesized that as soon as the bolt pretension force was overcome, end plate separation began which led to prying forces. As the prying forces increased, the bolts yielded (going off the plot in Figure 4-30). It is likely that the end plates didn't experience much yielding because bolt inelasticity was responsible for the softening of the connection.

Table 4-9 Predicted and Experimentally Obtained Moment Capacities 8ES-0.875-0.75-24

Predicted (k-ft)		Experimental (k-ft)		Ratio	
M_{pl}	M_q	M_y	M_u^1	M_{pl}/M_y	M_q/M_u^1
788	648	500	680	1.58	0.95

M_u^1: Bolt rupture not observed at this moment.

4.2.1.2.3 Experimental Results – End-Plate Separation

Figure 4-29 shows the end-plate separation for the specimen. It is stated in Ghassemieh et al. (1983) that end plate yielding was observed at 680 k-ft of moment (at the ultimate moment). This further supports the previous hypothesis.

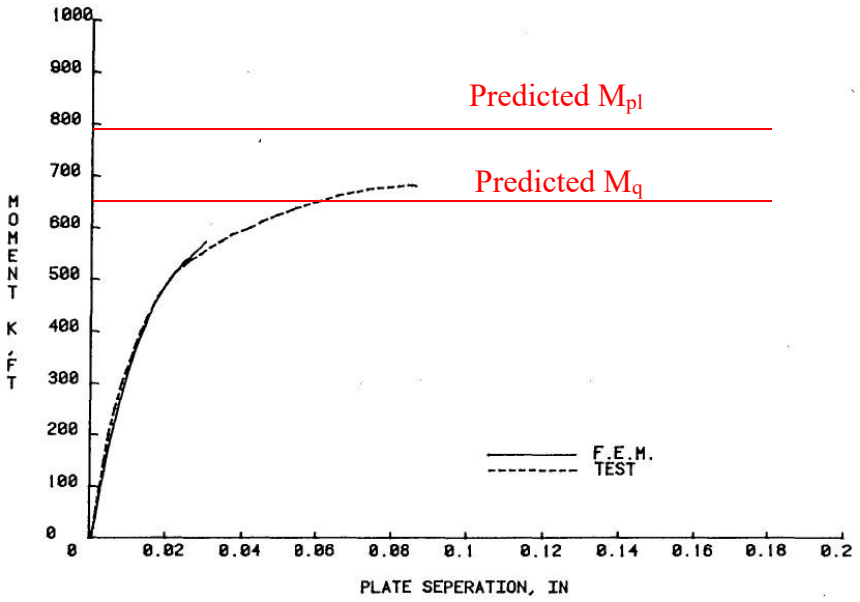

Figure 4-29 End-plate separation for Specimen 8ES-0.875-0.75-24 [Ghassemieh, M., Kukreti, A., and Murray, T.M. (1983) *Inelastic Finite Element Analysis of Stiffened End-Plate Moment Connections*, Report No. FSEL/AISC 8302, School of Civil Engineering and Environmental Science, University of Oklahoma, Norman, OK, Used with Permission of T.M. Murray, 2015]

4.2.1.2.1 Experimental Results – Bolt Forces

Figure 4-30 shows the bolt forces during the test. Although it appears from Ghassemieh et al. (1983) that the test was stopped prior to bolt fracture, based on the nonlinearity and excessive bolt forces, the predicted moment capacity for bolt rupture with prying action appears reasonable.

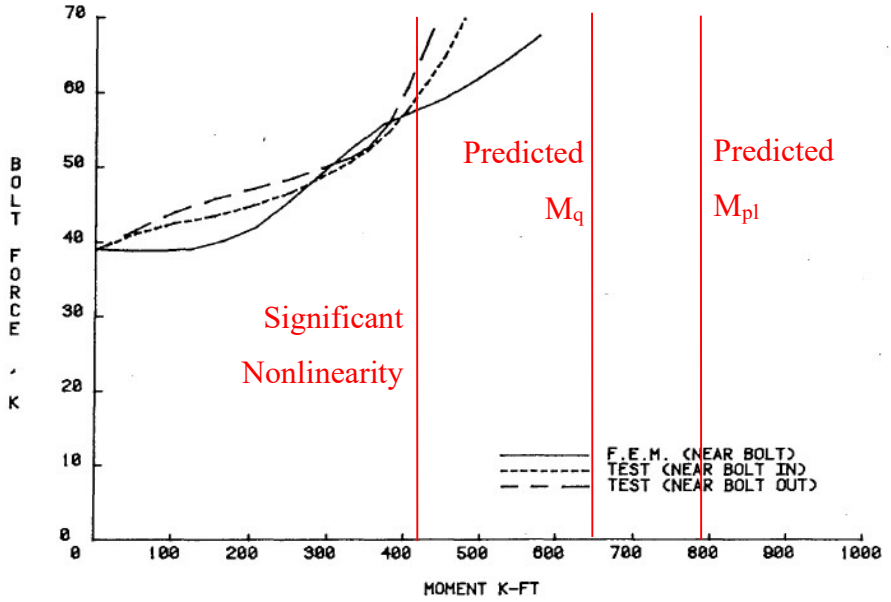

Figure 4-30 Bolt forces for 8ES-0.875-0.75-24 [Ghassemieh, M., Kukreti, A., and Murray, T.M. (1983) *Inelastic Finite Element Analysis of Stiffened End-Plate Moment Connections*, Report No. FSEL/AISC 8302, School of Civil Engineering and Environmental Science, University of Oklahoma, Norman, OK, Used with Permission of T.M. Murray, 2015]

4.2.2 Shallow Section - Thick Plate Behavior

4.2.2.1 Specimen 8ES-1.25-1.25-36 from Sumner et al. (2000)

Figure 4-31 shows the specimen dimensions and Figure 4-32 shows the end-plate layout for the specimen.

4.2.2.1.1 Limit State – Predictions and Progression

Calculations were made using the design procedures proposed in the previous chapter and were within 6% of the values published in Sumner (2003). Moment capacity for bolt rupture without prying action, M_{np}, was calculated to be 30800 k-in, beam plastic moment capacity, M_p, of 32500 k-in (calculated using measured yield strength) and end plate yield moment capacity, M_{pl}, was computed to be 36800 k-in.

Based on the predicted moment capacities for bolt rupture, beam plastic hinging, and end plate yield, it would be expected that the bolts would rupture prior to significant inelasticity in the beam or end plate. However, yielding in both the beam flanges and the end plate were observed starting at 0.010 rad story drift and continuing until bolt rupture at 0.04 rad story drift.

4.2.2.1.2 Experimental Results – Yield and Ultimate Moments

Sumner et al. (2000) reported a yield moment, M_y, of 23300 k-in and an ultimate moment, M_u, of 32700 k-in from the experiment. Figure 4-33 shows the moment-rotation behavior of the specimen.

End plate yielding occurred at approximately 23300 k-in or 63% of the predicted end plate moment, M_{pl} = 36800 k-in. There is a need to revisit the equations for end plate yielding. Table 4-10 compares the calculated and observed limit states.

If it is assumed that end plate yielding was not so large as to produce prying forces in the bolts, then the moment associated with bolt rupture can be compared to the predicted moment capacity without prying action, M_{np}. The moment associated with bolt rupture without prying action, M_{np} =30800 k-in, was 94% of the experimentally obtained moment at bolt rupture of 32700 k-in.

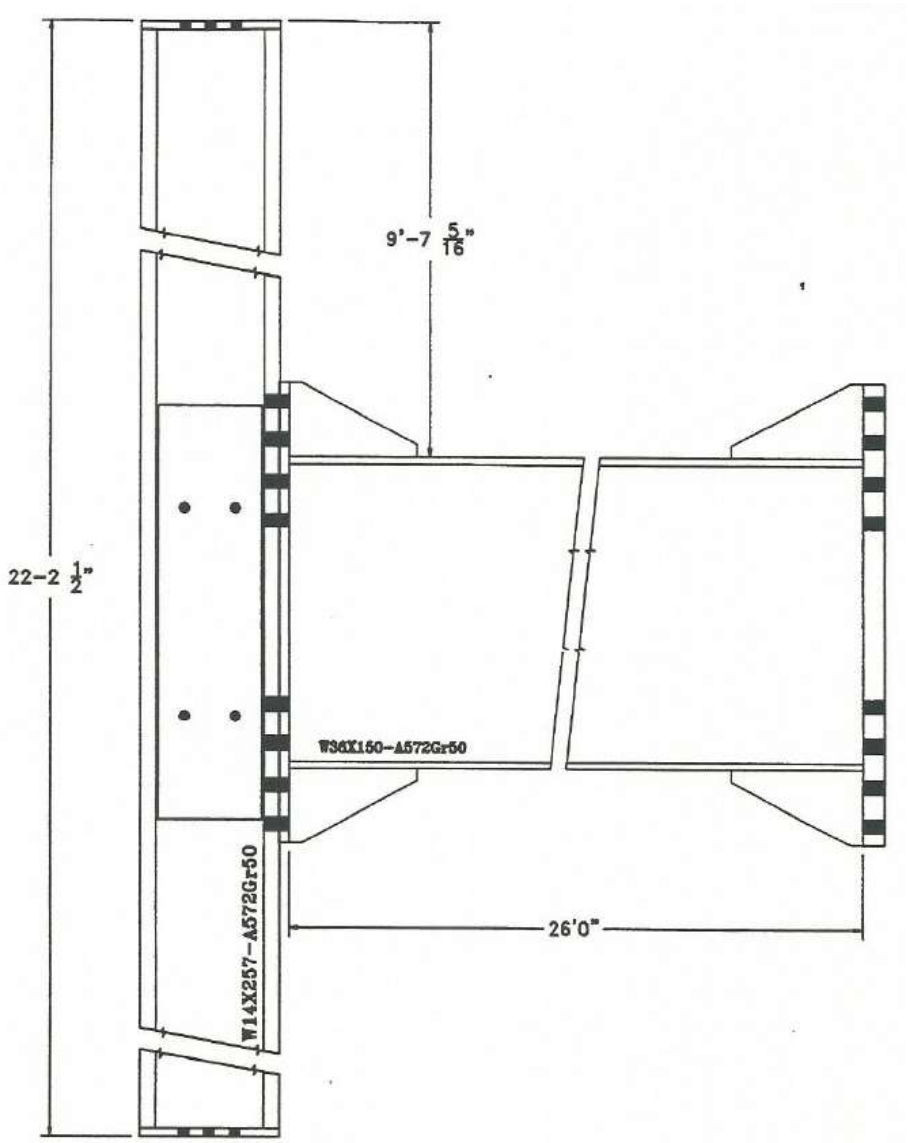

Figure 4-31 8ES-1.25-1.25-36 Specimen Dimensions [Sumner, E. A., Mays, T. W., & Murray, T. M. (2000). *Cyclic Testing of Bolted Moment End-Plate Connections.* Blacksburg, VA: Virginia Polytechnic Institute and State University, Used with Permission of T.M. Murray, 2015]

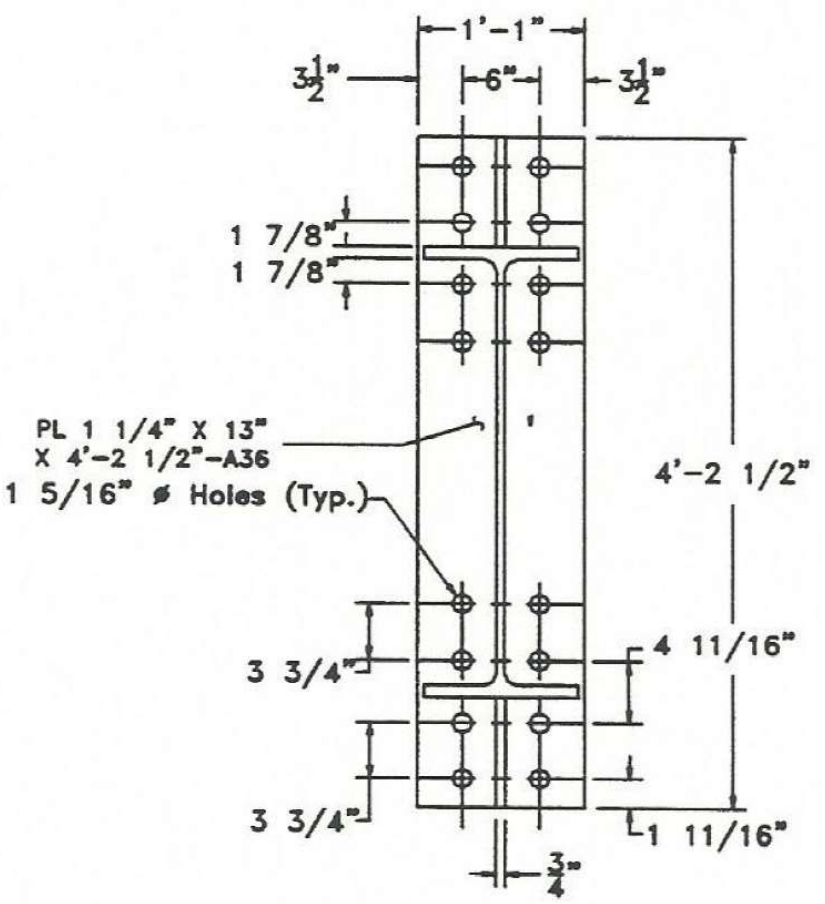

Figure 4-32 End-plate Layout for Specimen 8ES-1.25-1.25-36 [Sumner, E. A., Mays, T. W., & Murray, T. M. (2000). *Cyclic Testing of Bolted Moment End-Plate Connections.* Blacksburg, VA: Virginia Polytechnic Institute and State University, Used with Permission of T.M. Murray, 2015]

Table 4-10 Predicted and Experimentally Obtained Moment Capacities for Specimen 8ES-1.25-1.25-36

Predicted (k-in)		Experimental (k-in)		Ratio	
M_{pl}	M_{np}	M_y	M_u	M_{pl}/M_y	M_{np}/M_u
36800	30800	23300	32700	-	0.94

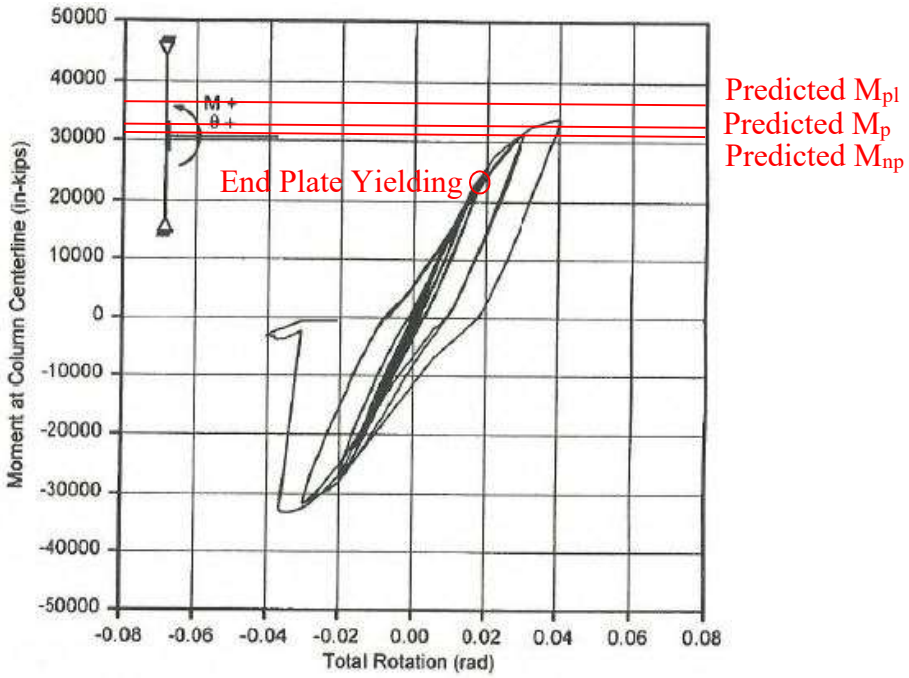

Figure 4-33 Load-deformation behavior for Specimen 8ES-1.25-1.25-36 [Sumner, E. A., Mays, T. W., & Murray, T. M. (2000). *Cyclic Testing of Bolted Moment End-Plate Connections.* Blacksburg, VA: Virginia Polytechnic Institute and State University, Used with Permission of T.M. Murray, 2015]

4.2.2.1.3 Experimental Results – End-Plate Separation

The large end plate separations shown in Figure 4-34 appear to be related to yielding of the bolts as demonstrated by large bolt strains in Figure 4-35. This supports the hypothesis that although the end plate suffered some yielding, that the plate may still have acted more as a thick plate with minor prying action.

4.2.2.1.4 Experimental Results – Bolt Strains

Figure 4-34 and Figure 4-35 also support the sharp increase in bolt strain and end plate separation as the predicted bolt rupture strength is approached. This could be considered to verify the prediction of bolt rupture for thick plates.

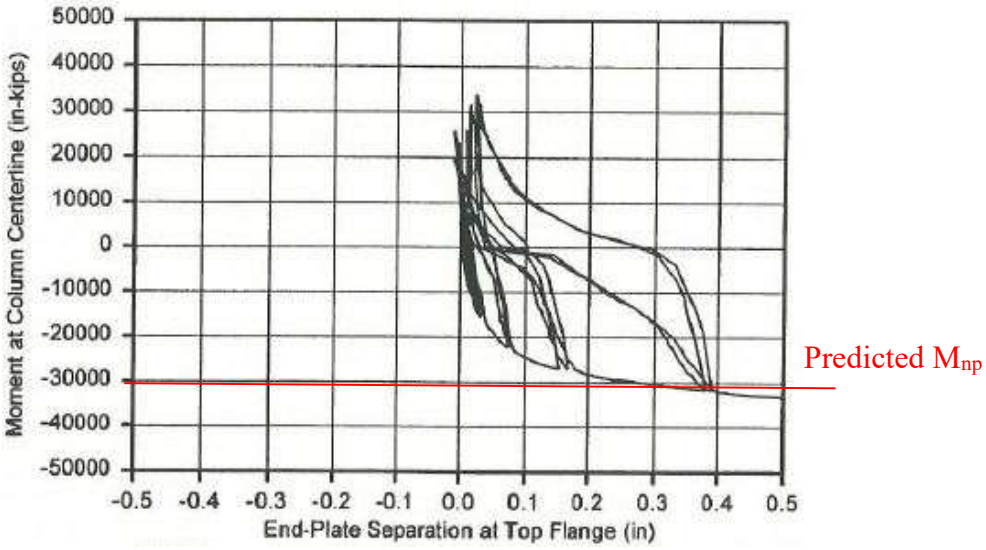

Figure 4-34 End-plate separation for Specimen 8ES-1.25-1.25-36 [Sumner, E. A., Mays, T. W., & Murray, T. M. (2000). *Cyclic Testing of Bolted Moment End-Plate Connections.* Blacksburg, VA: Virginia Polytechnic Institute and State University, Used with Permission of T.M. Murray, 2015]

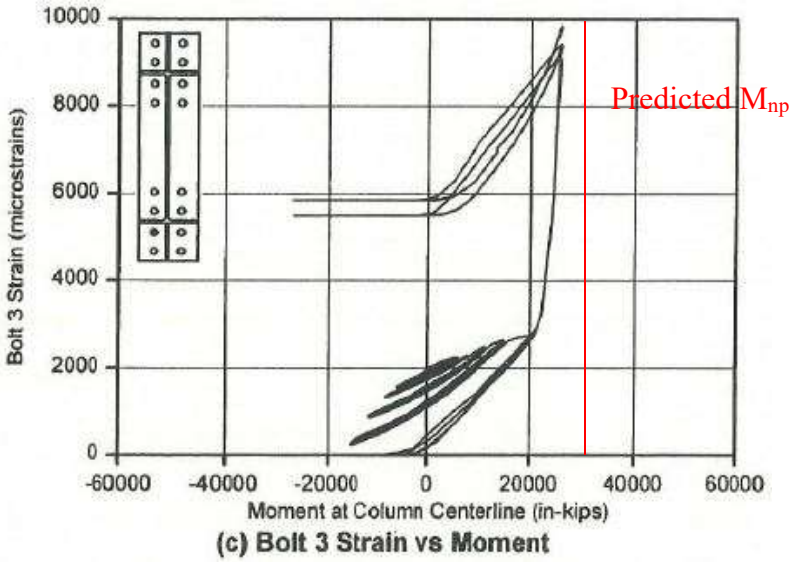

Figure 4-35 Bolt 3 strains for Specimen 8ES-1.25-1.25-36 [Sumner, E. A., Mays, T. W., & Murray, T. M. (2000). *Cyclic Testing of Bolted Moment End-Plate Connections.* Blacksburg, VA: Virginia Polytechnic Institute and State University, Used with Permission of T.M. Murray, 2015]

4.2.2.2 Specimen 8ES-0.875-1-24 from Ghassemieh et al. (1983)

Specimen 8ES-0.875-1-24 from Ghassemieh et al. (1983) was very similar to Specimen 8ES-0.875-0.75-24 with a 1 in. thick end plate instead of the 0.75 in. end plate used in 8ES-0.875-0.75-24. See Figure 4-36 for specimen dimensions and Figure 4-37 for end plate layout.

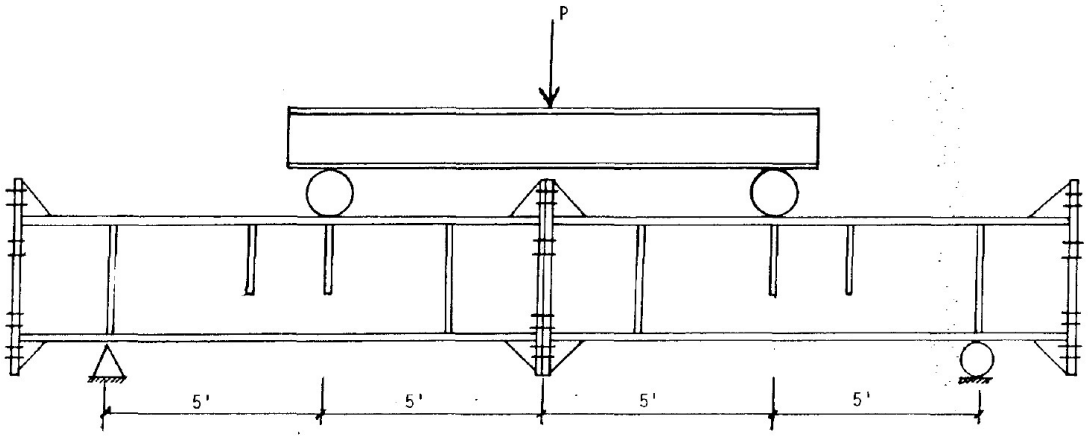

Figure 4-36 8ES-0.875-1-24 Specimen Dimensions [Ghassemieh, M., Kukreti, A., and Murray, T.M. (1983) *Inelastic Finite Element Analysis of Stiffened End-Plate Moment Connections*, Report No. FSEL/AISC 8302, School of Civil Engineering and Environmental Science, University of Oklahoma, Norman, OK, Used with Permission of T.M. Murray, 2015]

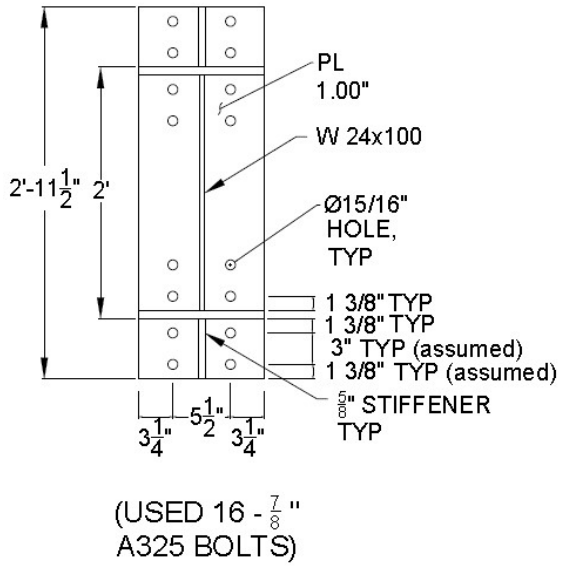

Figure 4-37 End-Plate Layout for Specimen 8ES-0.875-1-24 [redrawn from Ghassemieh, M., Kukreti, A., and Murray, T.M. (1983) *Inelastic Finite Element Analysis of Stiffened End-Plate Moment Connections*, Report No. FSEL/AISC 8302, School of Civil Engineering and Environmental Science, University of Oklahoma, Norman, OK, Used with Permission of T.M. Murray, 2015]

4.2.2.2.1 Limit State – Predictions and Progression

Beam plastic moment capacity, M_p, was calculated to be 840 k-ft (calculated using measured yield stress). Moment capacity for bolt rupture without prying action, M_{np}, was found out to be 853 k-ft and end plate yield moment capacity, M_{pl}, was 1460 k-ft.

Based on the predicted moment capacities, it is expected that beam inelasticity and bolt rupture would occur. Ghassemieh et al. (1983) does not describe the limit states actually observed. Because bolt rupture is not mentioned, it is assumed that the test was stopped prior to bolt rupture.

4.2.2.2.2 Experimental Results – Yield and Ultimate Moments

As reported in Ghassemieh et al. (1983), a yield moment, M_y, of 637 k-ft and an ultimate moment, M_u, of 750 k-ft were experimentally obtained. Figure 4-38 show the moment-deflection behavior. The moment reported when the test was stopped was 750 k-ft. This is

88% of the predicted moment capacity for bolt rupture without prying action. Based on Figure 4-38, it is unlikely that the specimen would have reached the predicted moment capacity even if the test was continued.

Table 4-11 Predicted and Experimentally Obtained Moment Capacities for Specimen 8ES-0.875-1-24

Predicted (k-ft)		Experimental (k-ft)		Ratio	
M_{pl}	M_{np}	M_y	M_u^1	M_{pl}/M_y	M_{np}/M_u^1
1460	853	-	750	-	1.13

M_u^1: Test Stopped prior to bolt rupture.

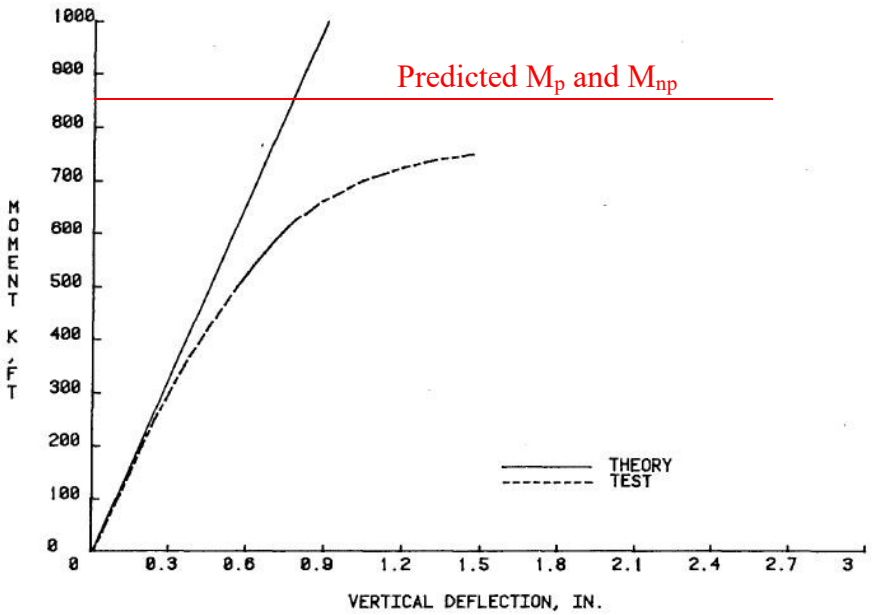

Figure 4-38 Load-deformation behavior for Specimen 8ES-0.875-1-24 [Ghassemieh, M., Kukreti, A., and Murray, T.M. (1983) *Inelastic Finite Element Analysis of Stiffened End-Plate Moment Connections*, Report No. FSEL/AISC 8302, School of Civil Engineering and Environmental Science, University of Oklahoma, Norman, OK, Used with Permission of T.M. Murray, 2015]

4.2.2.2.1 Experimental Results – End-Plate Separation

Figure 4-39 shows the end-plate separation. It shows small end plate separation which may imply that the end plate exhibited thick plate behavior and that nonlinearity was due to inelasticity in the bolts.

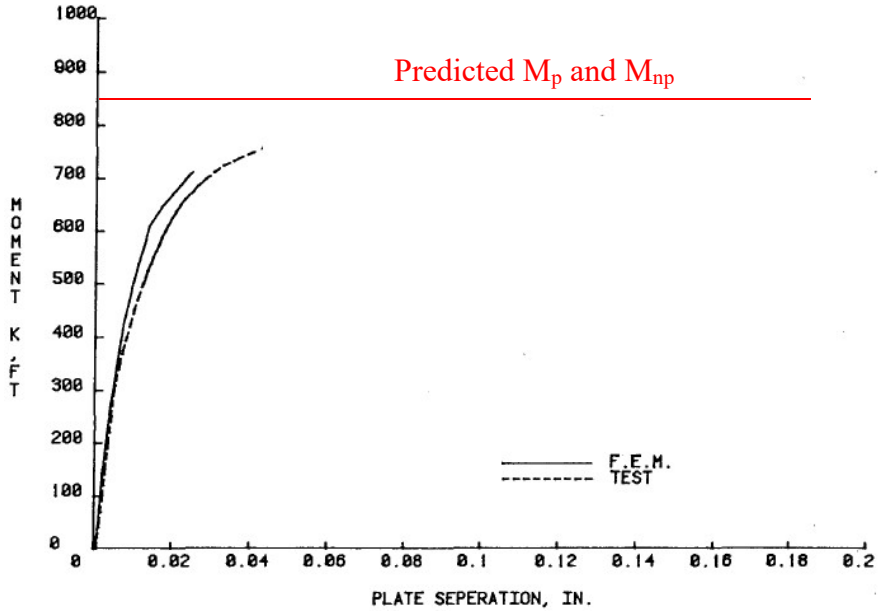

Figure 4-39 End-plate separation for Specimen 8ES-0.875-1-24 [Ghassemieh, M., Kukreti, A., and Murray, T.M. (1983) *Inelastic Finite Element Analysis of Stiffened End-Plate Moment Connections*, Report No. FSEL/AISC 8302, School of Civil Engineering and Environmental Science, University of Oklahoma, Norman, OK, Used with Permission of T.M. Murray, 2015]

4.2.2.2.1 Experimental Results – Bolt Forces

Figure 4-40 shows the typical bolt force. The bolt forces shown in the figure increase to the nominal tensile strength of the 7/8" A325 bolt (54 kips) by 300 k-ft to 400 k-ft for the bolts nearest the flange. The predicted end moment capacity without prying is 850 k-ft assuming all bolts are resisting their nominal tensile strength. It is possible that the top and bottom rows of bolts are not resisting as much load (supported by data in Sumner et al. (2000)) leading to a reduced moment capacity when the bolts start to yield.

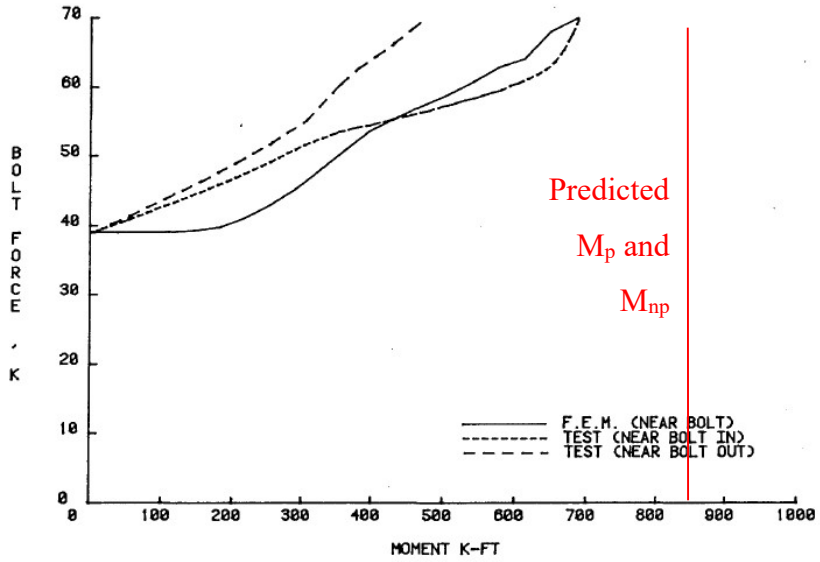

Figure 4-40 Bolt forces for Specimen 8ES-0.875-1-24 [Ghassemieh, M., Kukreti, A., and Murray, T.M. (1983) *Inelastic Finite Element Analysis of Stiffened End-Plate Moment Connections*, Report No. FSEL/AISC 8302, School of Civil Engineering and Environmental Science, University of Oklahoma, Norman, OK, Used with Permission of T.M. Murray, 2015]

4.2.3 Overall Summary of the Eight Bolt Extended Stiffened Configuration and Recommendations

As stated at the beginning of the section, ten tests on eight-bolt extended, stiffened end plates were included in four experimental programs. This section investigated four of these specimens identified as having the most useful data for validating design procedures for thick and thin end plate behavior (not end plate connections designed to promote plastic hinging of the beam).

Table 4-12 summarizes the four specimens investigated herein. The behavior of the four specimens were all quite different and the relationship between experimentally obtained end plate yield moment and predicted values varied.

Table 4-12 Summary of Four Test Specimens (from literature) of Eight Bolt Extended Stiffened Configuration

Specimen Identification[1]		Reference	Depth (in.)	Behavior[2]	Remarks[3]
7	8ES-1.25-1-30	Sumner et al. (2000)	30	Thin / P.H.	M_{pl} was +5% of yield moment. Bolt rupture not observed. Predicted M_q was -9% of the moment, at which the test was stopped
1	8ES-0.875-0.75-24 (EP-1)	Ghassemieh et al. (1983)	24	Thin	M_q was smaller than M_{pl} – bolts yielded before end plate. M_q -5% of M_u and M_{pl} +58% of M_y.
9	8ES-1.25-1.25-36	Sumner et al. (2000)	36	Thick	End plate yielding at 63% of M_{pl}. M_{np} was -6% of moment at bolt rupture.
2	8ES-0.875-1-24 (EP-2)	Ghassemieh et al. (1983)	24	Thick	Test stopped prior to bolt fracture. M_{np} was +13% of experimental maximum moment observed.

[1]Specimen Identification: "Conn. type - Bolt diameter - End-plate thickness - Beam depth". Identification in parentheses was used in the reference.

[2]P.H. means plastic hinging of the beam.

Remarks[3]: A positive percentage means an unconservative calculation, whereas a negative percentage means a safe prediction.

Although the predicted end plate yield moment capacity, M_{pl}, was within 5% of the experimental yield moment for Specimen 8ES-1.25-1-30 from Sumner et al. (2000), end plate yielding was observed in Specimen 8ES-1.25-1.25-36 at only 63% of the predicted moment, M_{pl}. Specimen 8ES-0.875-0.75-24 from Ghassemieh et al. (1983) produced a moment at the end of the test similar to the predicted M_q value, but Specimen 8ES-1.25-1-

30 reached 110% of M_q before the test was stopped without bolt fracture. Specimen 8ES-1.25-1.25-36 experienced bolt rupture at a moment that was within 6% of the predicted value, M_{np}, but it is unlikely that Specimen 8ES-0.875-1-24 would have reached the predicted M_{np} and was stopped at 88% of M_{np} after significant softening.

Out of the four tests discussed above for shallower beams, two of them were stopped before bolt rupture. The moment capacity calculation for end-plate yielding and bolt rupture with prying was conservative by 5% for the specimens 8ES-1.25-1-30 [Sumner et al. (2000)] and 8ES-0.875-0.75-24 [Ghassemieh et al. (1983)], respectively. Also, the moment capacity calculation for bolt rupture without prying action was conservative by 5% for the specimen 8ES-1.25-1.25-36 [Sumner et al. (2000)]. Taking these three conservative predictions into account, it could be argued that the design procedures proposed in the Section 3.2 are validated for shallower depths.

Further, two deeper specimens were tested and have been included in Section 6.3. By testing a deeper section (56 in. depth), the applicability of the connection configuration can extend to deeper built up rafters instead of just rolled sections as was the focus of testing to date.

5 EXPERIMENTAL TESTING

5.1 Test Specimens

A total of ten end-plate moment connection tests were performed. These include four tests each on 6B-4W/2W configuration and 12B-MRE 1/3-4W/2W configuration, and two tests on deep 8ES configuration.

Each test specimen consisted of two built-up beam sections spliced together at midspan using A325 bolts. Each built-up beam had an end-plate at each end so that it could be used for two tests. This was done by rotating the built-up beam by 180 degrees, such that the unused end came in the center and flipping it over, such that the bottom flange came on the top. The shallower built-up beam sections (shown in Figure 5-1 (a)) were 3 ft. deep with 3/4 in. by 12 in. flanges and a 1/4 in. thick web. Four such built-up beams were fabricated, two each for the 6B-4W/2W and 12B-MRE 1/3-4W/2W configurations.

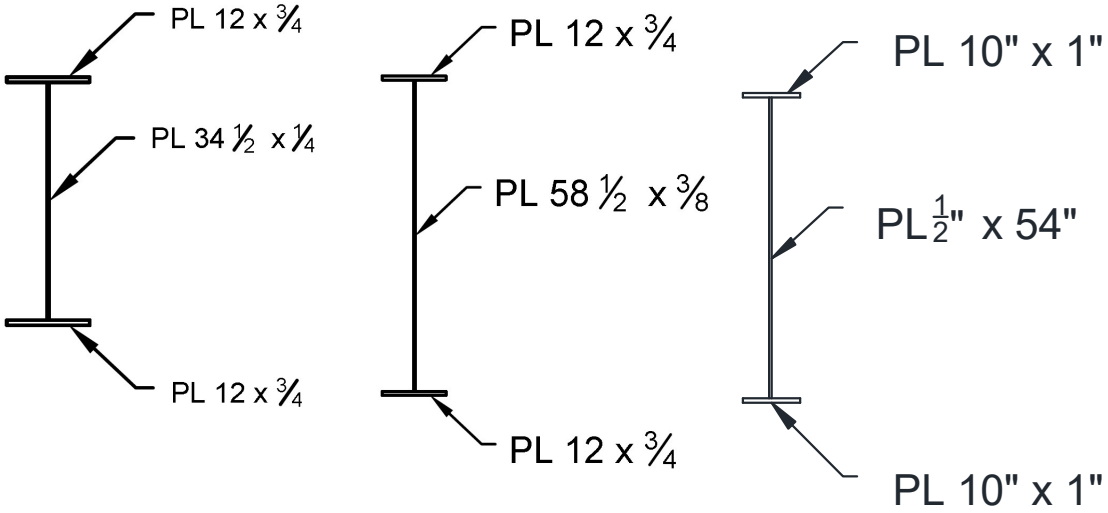

(a) 3 ft. deep beam (b) 5ft. deep beam (c) 56 in. deep beam

Figure 5-1 Sections of Beams Used for Testing

The deep built-up beams were of two types. Firstly, for the 6B-4W/2W and 12B-MRE 1/3-4W/2W configuration, beam section (shown in Figure 5-1 (b)) was 5 ft. deep with 3/4 in.

by 12 in. flanges and a 3/8 in. thick web. Four such deep built-up beams were fabricated, two each for the 6B-4W/2W and 12B-MRE 1/3-4W/2W configurations. Secondly, for the 8ES connection, beam section (shown in Figure 5-1 (c)) was 56 in. deep with 1 in. by 10 in. flanges and a 1/2 in. thick web. Refer to Appendix D for the drawings of the specimens.

End-plate width of 14 in. was used for 12B-MRE 1/3-4W/2W and 6B-4W/2W connection configurations. The thickness of end-plate was either 1 in. or 3/4 in. depending on whether it was a thick end-plate or a thin-end plate respectively. End-plate width of 10 in. was used for the 8ES configuration with the same thicknesses as the earlier mentioned configurations.

For the 12B-MRE 1/3-4W/2W and 6B-4W/2W configurations, inner bolt gage of 4 1/2 in. and outer bolt gage of 3 in. was used. Further, a vertical bolt to bolt pitch of 3 1/2 in. and a bolt to flange pitch of 2 1/4 in. was used. Whereas, for the 8ES configuration, bolt gage was 5 in. Also, bolt to bolt pitch of 3 1/2 in. and a bolt to flange pitch of 2 1/4 in. was used. The end-plates for the deeper beams of the three configurations are shown in Figure 5-2.

Refer to Appendix A for the mill test reports of the material used in the fabrication of the specimens.

Fully pretensioned A325 bolts were used with A563 nuts. No washers were used with the exception of washers being used for 8ES-1.25-0.75-56. This was done since the grip length of the bolts was more than the thickness of two end-plates combined.

The test matrix shown in Table 5-1 shows all the important parameters related to the built-up beam section and the bolted connections and the end-plate parameters are shown in Figure 5-3, Figure 5-4 and Figure 5-5. Refer to Appendix D and Appendix E for detailed drawings of the specimens and design calculations (including the specimens reviewed from past literature), respectively. The specimens were designed without using any ϕ factors.

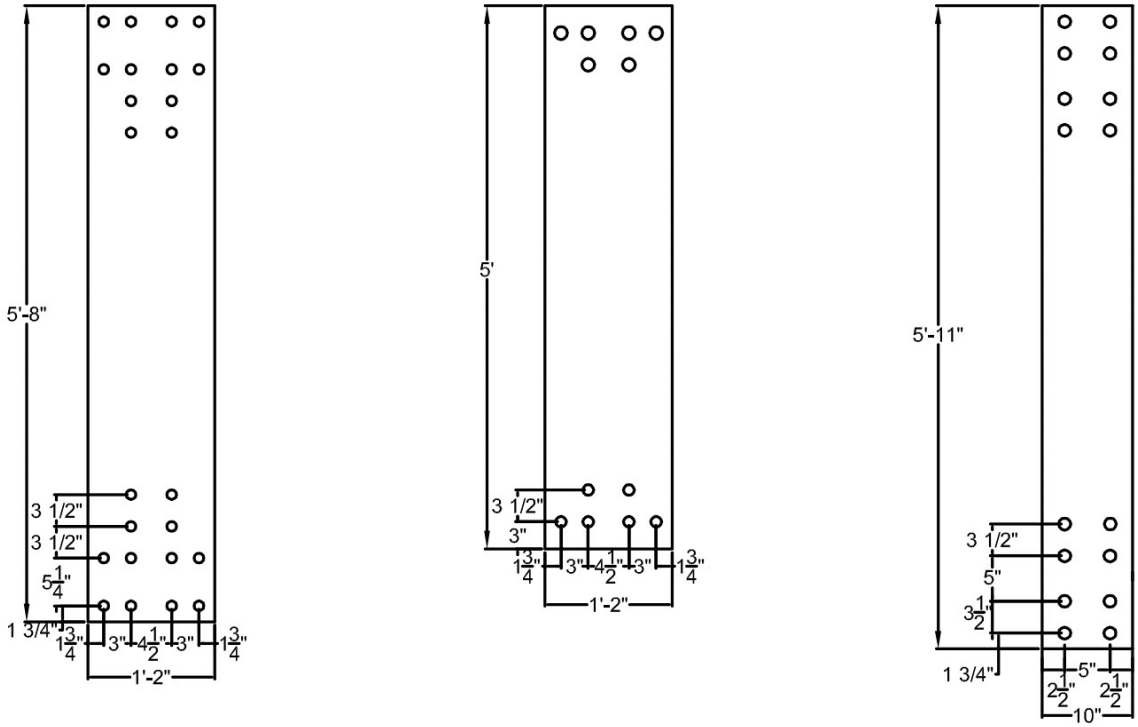

(a) 12B-MRE 1/3-4W/2W (b) 6B-4W/2W (c) 8ES

Figure 5-2 End-Plate for three configurations showing typical bolt to bolt pitch and gage distances

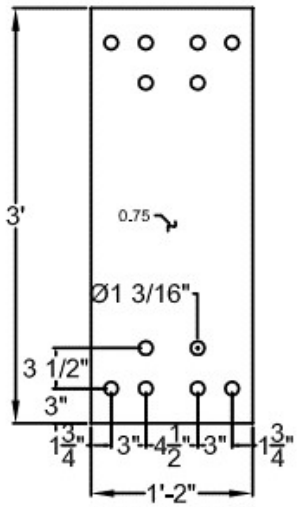

6B-4W/2W - 1.125 - 0.75 - 36

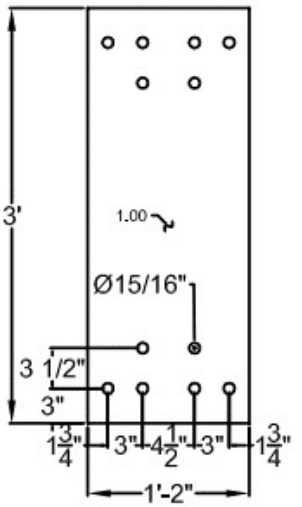

6B-4W/2W - 0.875 - 1.00 - 36

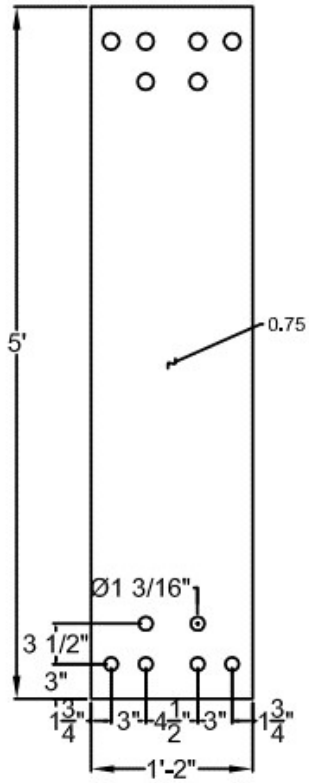

6B-4W/2W - 1.125 - 0.75 - 60

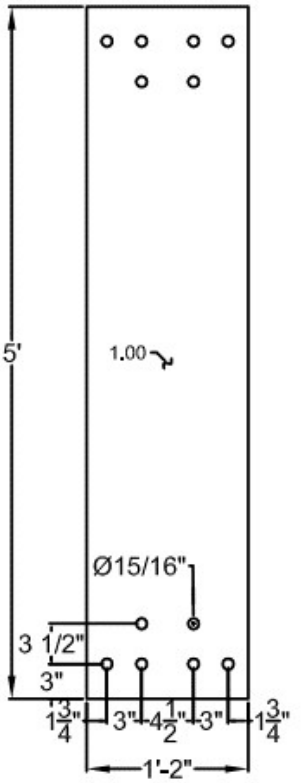

6B-4W/2W - 0.875 - 1.00 - 60

Figure 5-3 End-Plate Parameters for 6B-4W/2W Configuration

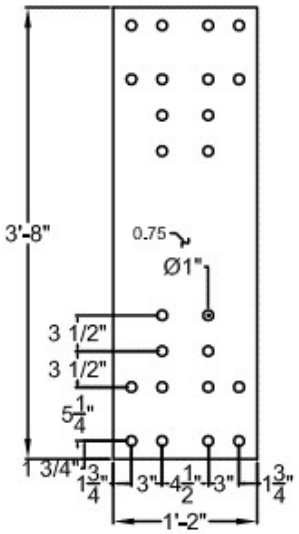

12B - MRE 1/3 - 4W/2W - 1.00 - 0.75 - 36

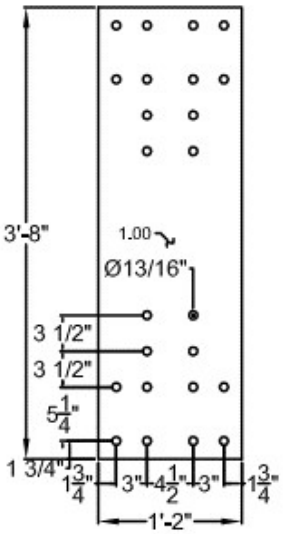

12B - MRE 1/3 - 4W/2W - 0.75 - 1.00 - 36

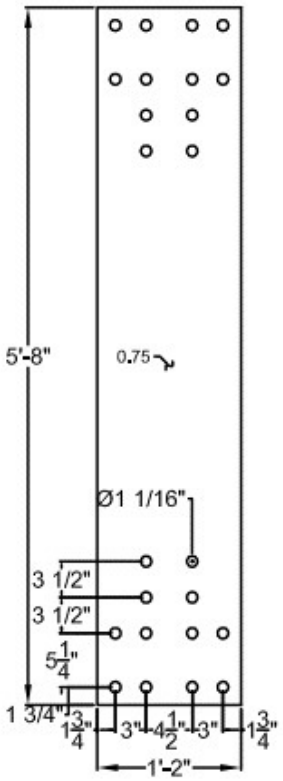

12B - MRE 1/3 - 4W/2W - 1.00 - 0.75 - 60

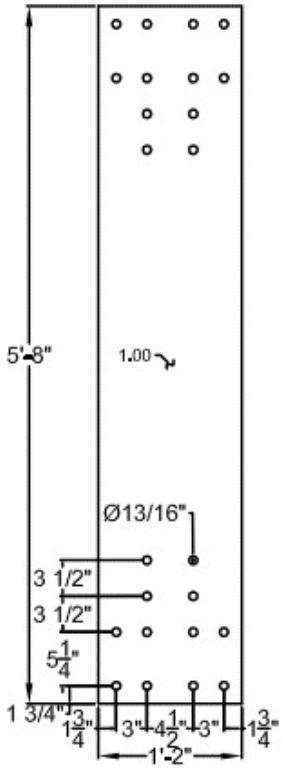

12B - MRE 1/3 - 4W/2W - 0.75 - 1.00 - 60

Figure 5-4 End-Plate Parameters for 12B-MRE 1/3-4W/2W Configuration

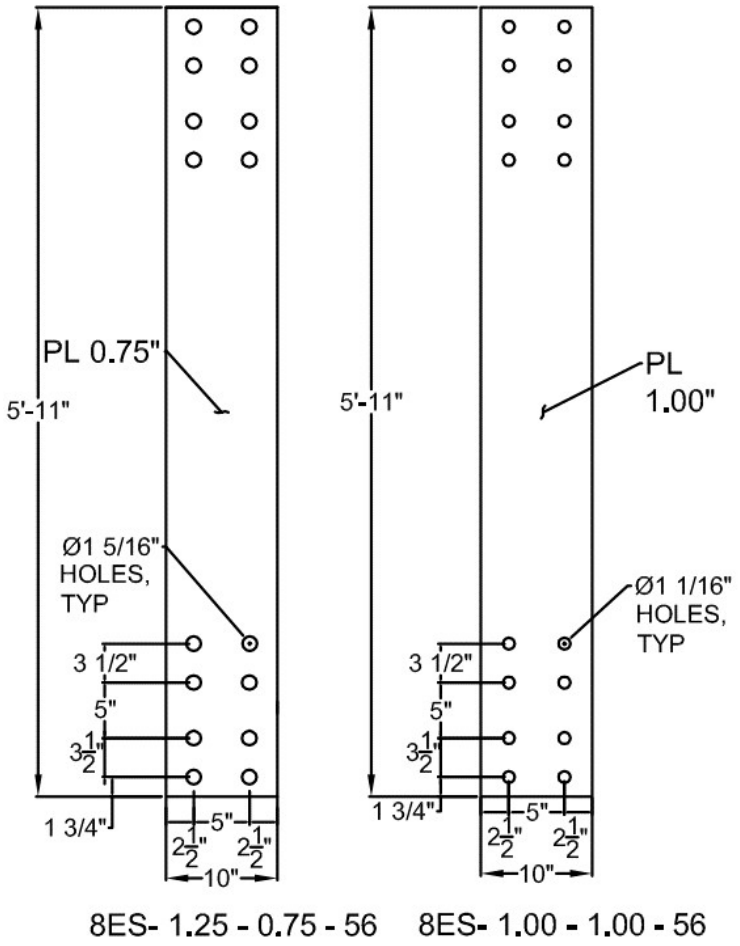

Figure 5-5 End-Plate Dimensions for 8ES Configuration

Table 5-1 Test Matrix

Specimen Identification	Bolt Dia., d_b (in.)	Bolt Grade	No. of Tension Bolts	End-Plate Thickness (in.)	Pitch, p_b (in.)	Gage, g, g_o (in.)	End-Plate Width, b_p (in.)	Flange Width, b_f (in.)	Beam Depth, d (in.)
6B-4W/2W-0.875-1.00-36	7/8	A325	6	1	3 1/2	4 1/2, 3	14	12	36
6B-4W/2W-1.125-0.75-36	1 1/8	A325	6	3/4	3 1/2	4 1/2, 3	14	12	36
6B-4W/2W-0.875-1.00-60	7/8	A325	12	1	3 1/2	4 1/2, 3	14	12	60
6B-4W/2W-1.125-0.75-60	1 1/8	A325	12	3/4	3 1/2	4 1/2, 3	14	12	60
12B- MRE 1/3 - 4W/2W-0.75-1.00-36	3/4	A325	6	1	3 1/2	4 1/2, 3	14	12	36
12B- MRE 1/3 - 4W/2W-1.00-0.75-36	1	A325	6	3/4	3 1/2	4 1/2, 3	14	12	36
12B- MRE 1/3 - 4W/2W-0.75-1.00-60	3/4	A325	12	1	3 1/2	4 1/2, 3	14	12	60
12B- MRE 1/3 - 4W/2W-1.00-0.75-60	1	A325	12	3/4	3 1/2	4 1/2, 3	14	12	60
8ES-1.00-1.00-56	1	A325	8	1	3 1/2	5	10	10	56
8ES-1.25-0.75-56	1 1/4	A325	8	3/4	3 1/2	5	10	10	56

5.2 Test Setup

The spliced built-up beams were simply supported by rollers at each end. Each end of the beam was supported by a stiffened steel beam connected to the reaction floor. The specimen was held down at the support using a ratchet and chain mechanism. Two MTS 201.80 actuators, supported by vertical reaction frames, were used to load the specimen symmetrically. The top flange of the specimen was connected to the actuators by four 1 1/4 dia bolts so that when the bolts rupture at the end of the test, the specimen never hits the floor. Each actuator is capable of applying 445 kip compressive (downward) force and a 300 kip tensile (upward) force.

The lateral braces were custom made in the structures lab. They were used as is. Reaction frames were erected onto which the lateral braces were supported. Each lateral brace consisted of a hinged link in the center and an adjustable (in length) mild steel rod on each side of the link. The link had three holes, one in the center and two at the end (which were bolted into the rods). The hole in the center made it possible to attach the bracing to a plate bolted onto the flange of the specimen. The plate had a bolt welded (on the head side) in the center and four holes on each end to grip the flange using more bolts and matching small plates. Each mild steel rod had eye shaped adjustable bolts (adjustable by about 6 in.) on both ends, with one end attached to the link and the other end attached to the reaction frame column using bolts. A picture of the lateral bracing is shown in Figure 5-10.

The specimens were braced laterally at ten brace points, with six brace points on the top flange and four brace points on the bottom flange. The bracing locations were kept as close as possible to the load point, near midspan and at about 7ft. from the support (see Figure 5-12). Lateral bracing design calculations are reported in Appendix F. The test setup for deep beam is shown in Figure 5-6 and Figure 5-7. The test setup for shallow beam is shown in Figure 5-8 and Figure 5-9.

5.3 Instrumentation

Three types of instrumentation were used to measure the specimen deflection, bolt forces and end-plate separation for each test. Also, the actuators had an in-built load cell and LVDT, the data from which was also recorded by the data acquisition system. Calibrated string potentiometer (wirepot) measured the deflection of the specimen at five points, namely the midspan, two load points and near the two supports. Bolt forces were measured using calibrated strain gaged bolts. Calibration of the bolts was done in a 300 kip SATEC universal testing machine to determine the elastic load-strain relationship. 120 ohm bolt strain gages (BTM-6C) were inserted in a 2 mm diameter hole drilled in the shank of the bolt and glued using bolt adhesive (A-2). Half of the bolts on the tension side were instrumented (strain gaged) bolts. They were placed in such a way that each bolt could also represent another non-instrumented bolt mirrored about the centerline of the web. The exact locations of the strain gaged bolts is shown in Figure 5-13.

Four calipers were used to measure end-plate separation. A caliper (shown in Figure 5-11) is an instrument used for measuring external dimensions, having two hinged legs with a strain gage at the end. It has two pointed ends which are capable of gripping an end-plate with the help of a spring. The calipers were calibrated using high precision machinist parallel blocks. Two calipers were placed towards the inside of the bottom flange (at the flange to end-plate weld) near each edge. Another caliper was placed at the same horizontal level but as close to the web, as possible. The fourth caliper was placed midway between the first inside bolt hole (near the web) and the second inside bolt hole (near the web). The location of calipers is shown in Figure 5-14

The instrumentation layout for both the shallow and deep beam is shown in Figure 5-12. Also, Figure 5-11 shows a picture of Calipers and String Potentiometers.

The data from the instrumented bolts was recorded using NI SCXI-1521 24 channel, 350-ohm quarter-bridge strain module in combination with a NI SCXI-1317 front-mounting

terminal block. Rest of the data was recorded using two NI SCXI-1520 8 channel universal strain/bridge in combination with a NI SCXI-1314 front-mounting terminal block.

5.4 Testing Procedure

Four holes were drilled in each built-up beam to connect the actuator bottom plate to the top flange. As discussed earlier this prevented the test specimen from hitting the floor after bolt rupture. Each test specimen was erected in the reaction frame. Since some of the built-up sections were not exactly square, the best possible vertical plumbness of the end plate on each end of the built-up beam was achieved by shimming thin plates under the roller supports. Also, it was ensured that the specimen was horizontally leveled throughout its span. All the bolts including the instrumented bolts in the connection were inserted. The instrumented bolts were connected to the data acquisition system and then all the bolts were tightened to a snug tight level. The tightening sequence followed was starting from the stiffest part of the connection and then moving towards the least stiff part of the connection. Multiple rounds of the tightening sequence were followed till all the bolts were snug tight. After this, each bolt end and the nut was match-marked and pretensioned using the turn of the nut method as described in the RCSC, 2009. These were cross checked with the readings from the instrumented bolts and necessary correction in the turn of the nut applied.

Then, the lateral bracings were set up according to Figure 5-12. The section of the specimen between the actuators was whitewashed to observe any yielding in the connection, especially the end-plates. Finally, the remaining instrumentation viz. calipers and string potentiometers, were set up as shown in Figure 5-14 and Figure 5-12 respectively.

Three cameras were setup, each of which captured a picture every two seconds through every test. Test Pictures from two shallow specimen tests were combined together at 24 frames per second into a time-lapse video. Typical time-lapse camera views are shown in Figure 5-15.

Figure 5-6 Picture of a Typical Deep Beam Test Setup

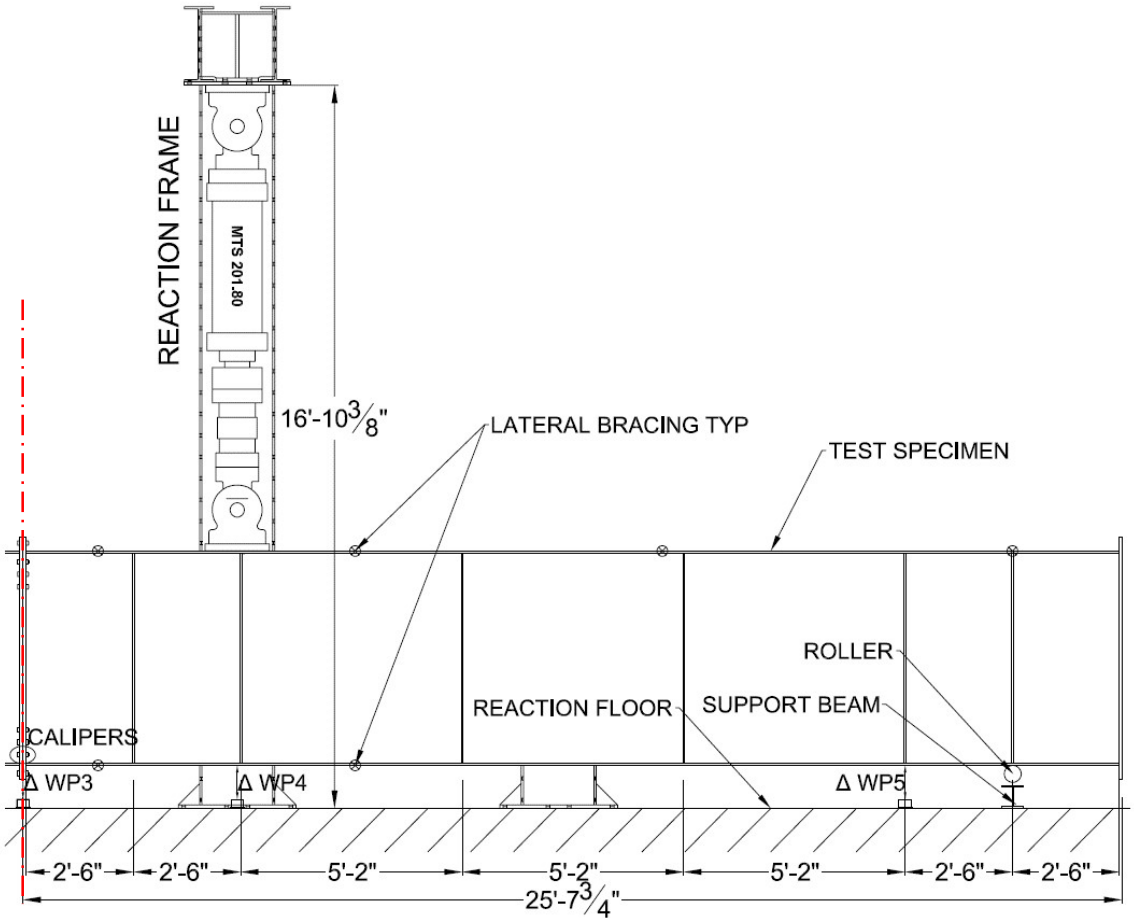

Note: The red dashed-dotted line denotes the line of symmetry

Figure 5-7 Half Diagram of Deep Beam Test Setup

The actuator displacements were zeroed before loading the specimens monotonically in the downward direction. Both the actuators used displacement control at a quasistatic rate of 0.10 in. /min. LabVIEW SignalExpress was used to record data points every 0.2 seconds. Since the actuators were displacement controlled, when the difference in the load between each actuator would reach 5 kips, displacement of one or both actuators was manually controlled until the loads were within approximately 1 kips.

The specimen was loaded until failure or until it stopped taking more load. All the results are described in detail in Chapter 6.

Figure 5-8 Picture of a Typical Shallow Beam Test Setup

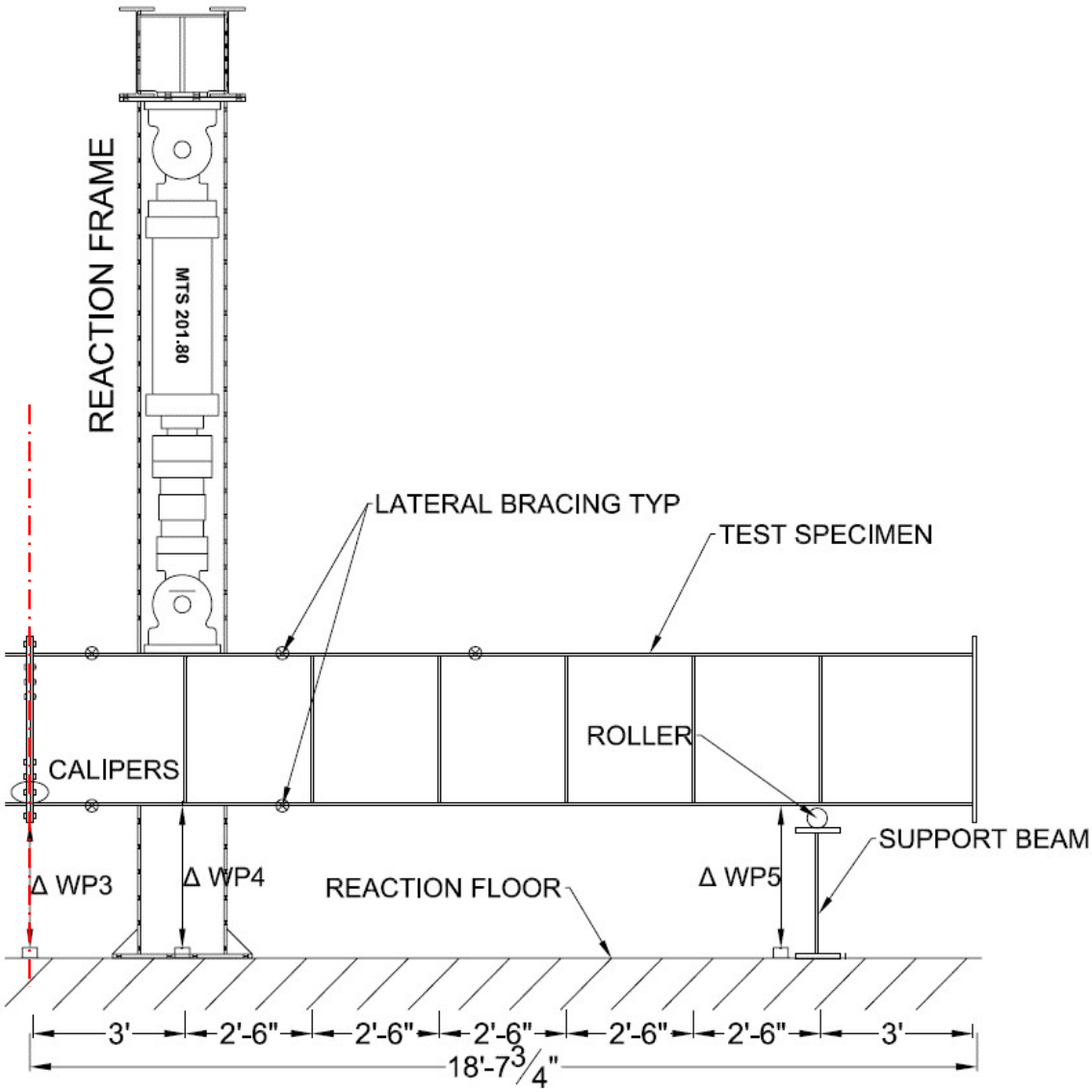

Note: The red dashed-dotted line denotes the line of symmetry

Figure 5-9 Half Diagram of Shallow Beam Test Setup

Figure 5-10 Typical Picture of Lateral Bracing

Figure 5-11 Picture Showing Calipers and String Potentiometer (Wirepot).

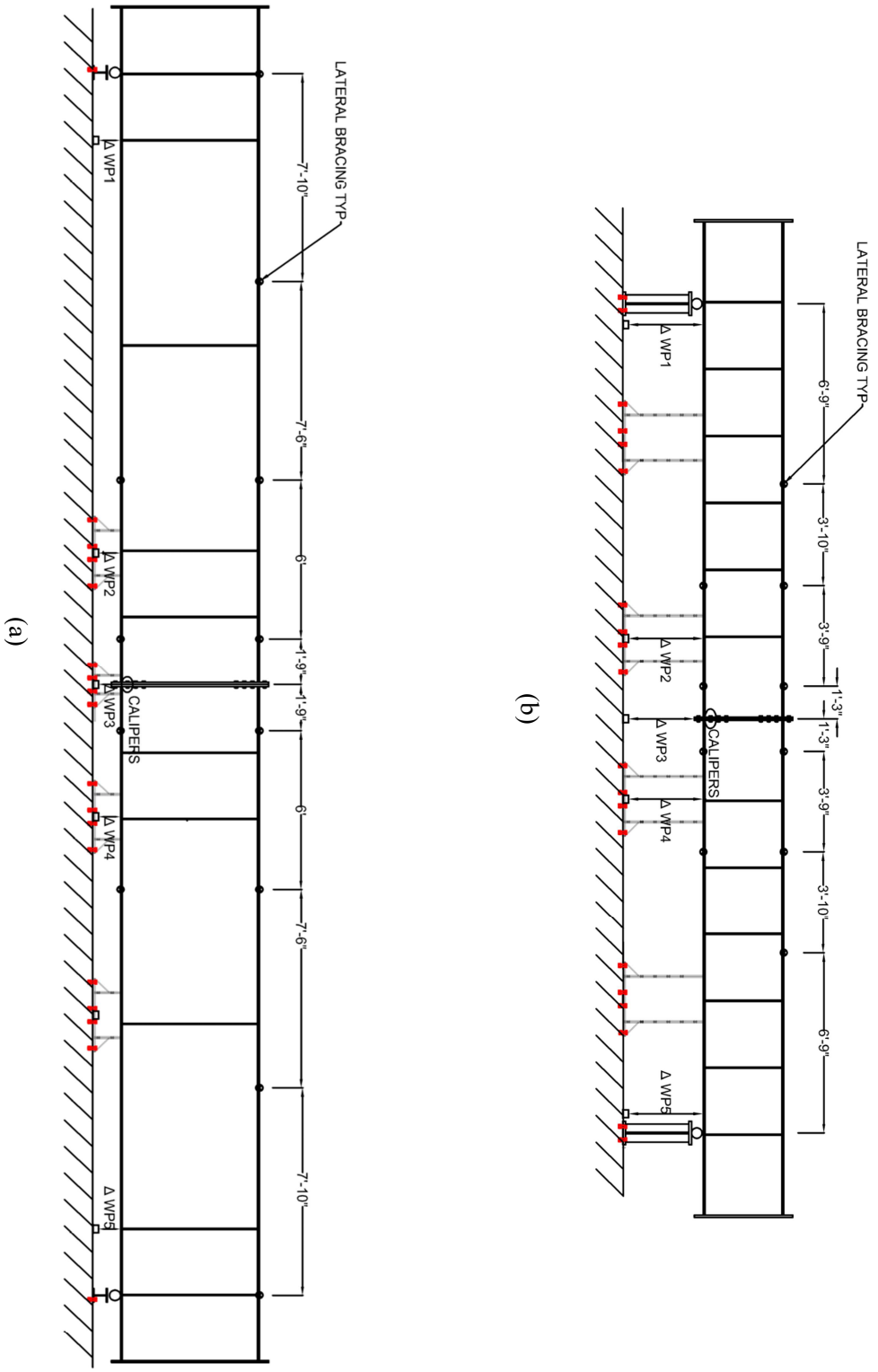

Figure 5-12 (a) Deep Beam Instrumentation Setup (b) Shallow Beam Instrumentation Setup

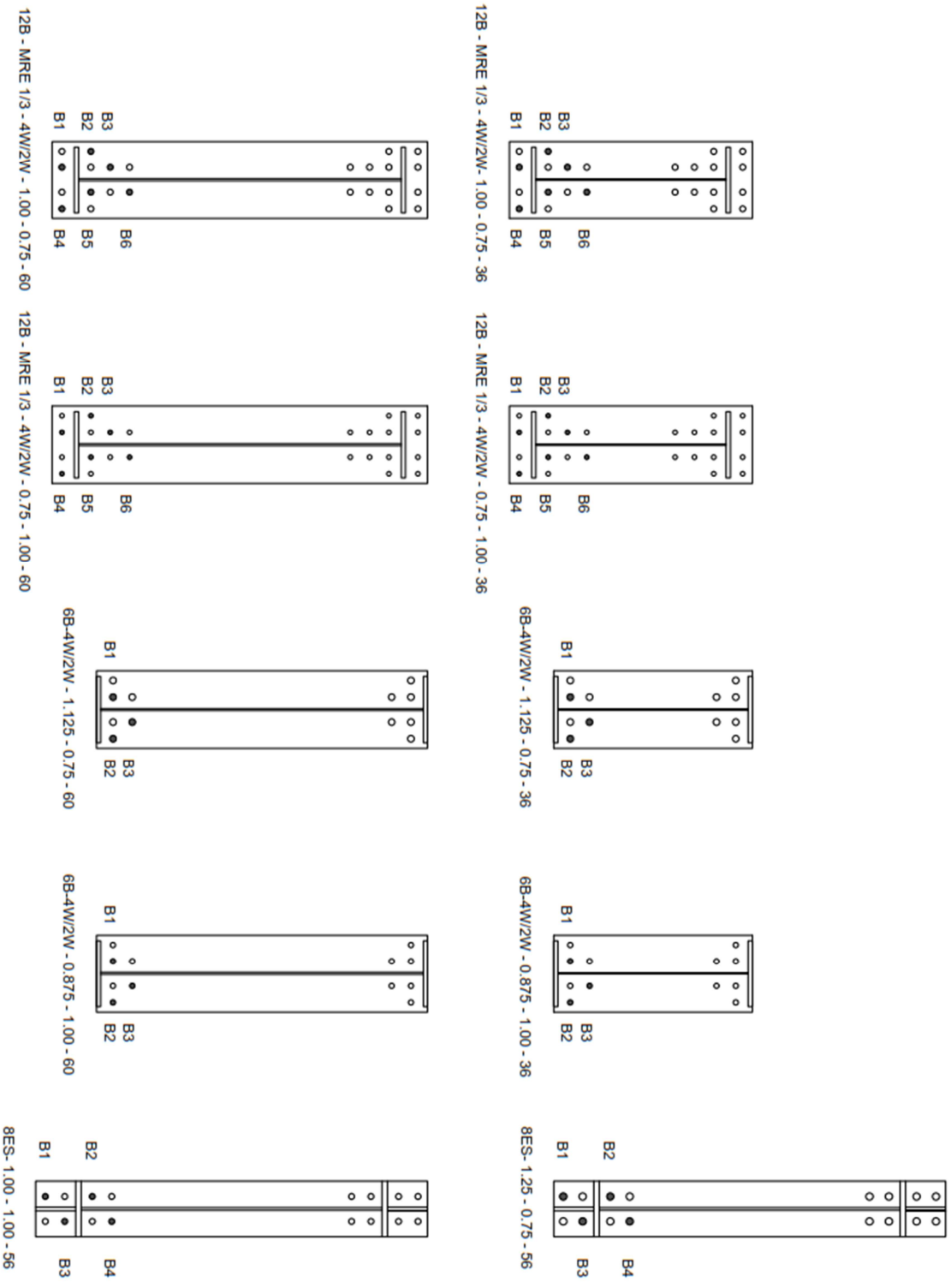

Figure 5-13 Location of Strain Gaged Bolts

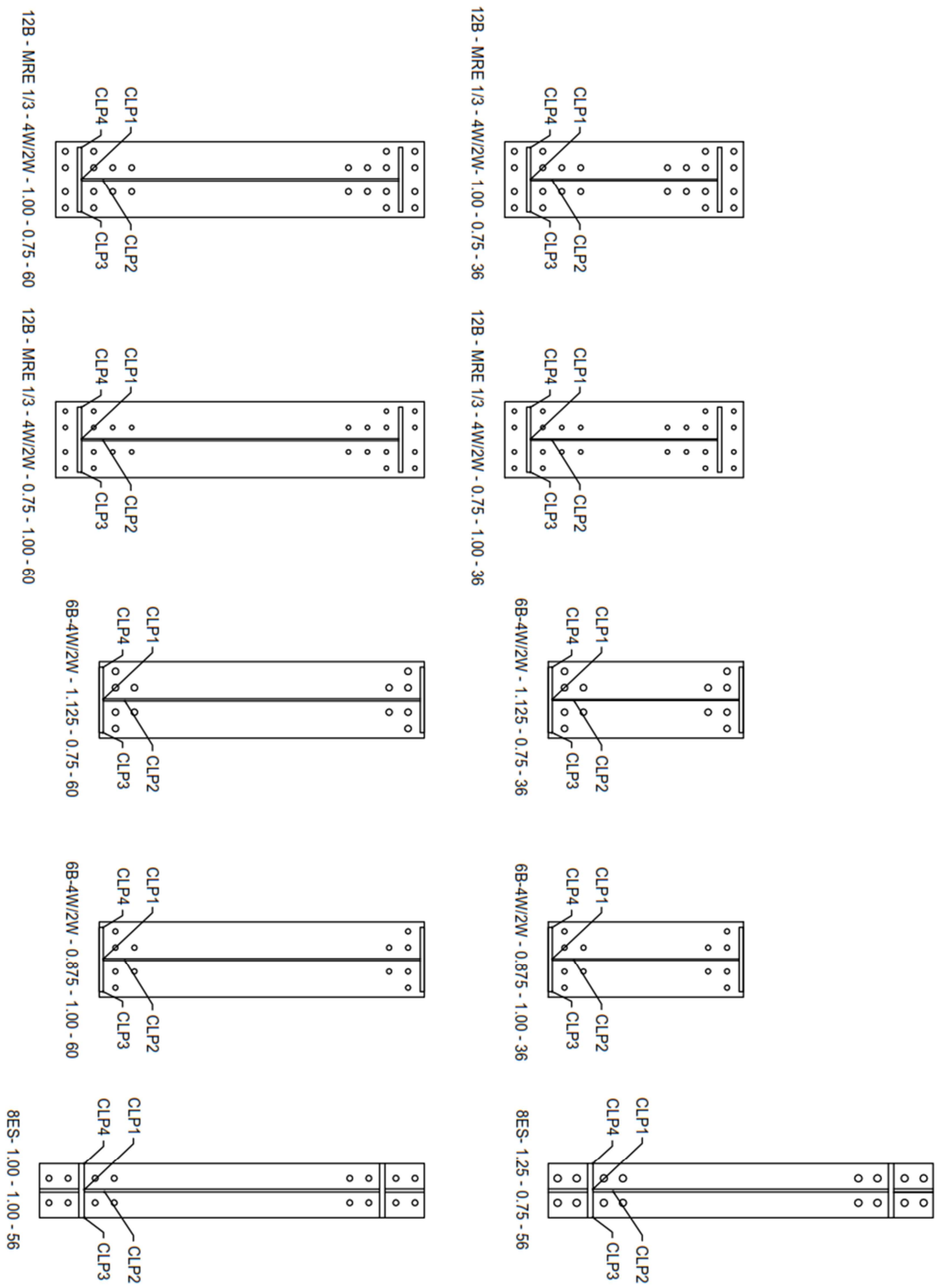

Figure 5-14 Location of Calipers

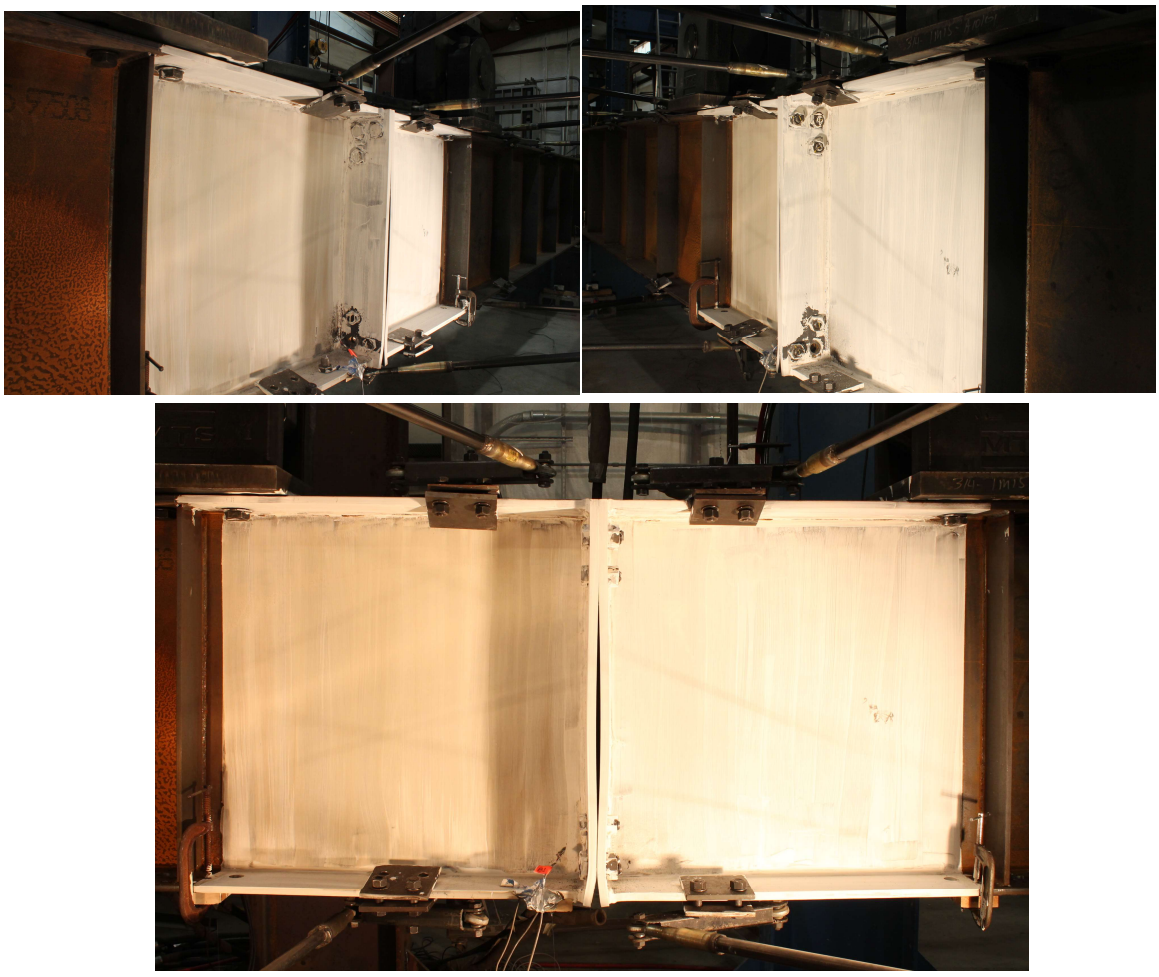

Figure 5-15 Typical Time-lapse Camera Views

5.5 Tensile Coupon Tests

Coupons from the same heat of material as used in the end-plates were cut and subjected to tensile loading in a 300 kip SATEC Universal Testing Machine. The 12B-MRE 1/3-4W/2W and 6B-4W/2W built-up beams were fabricated in such a way that the end-plates of the same thickness used the material from the same heat. Since, there were only two thicknesses of end-plates being used viz. 3/4 in. and 1 in., three coupons of each thickness were taken from each heat of the material. Also, for the 56 in. deep specimens, two coupons of each thickness (3/4 in. and 1 in.) were investigated. Therefore, in total ten tensile coupon tests were performed. All the test coupons and the testing procedure conformed to the

ASTM E8 - “Standard Test Methods for Tension Testing of Metallic Materials”. Refer to Table 5-2 for the summary of tensile coupon tests and, Figure 5-16, Figure 5-17, Figure 5-18 and Figure 5-19 for the results from all the coupons.

5.6 Bolt Rupture Reports

Mill test reports for the mechanical properties were obtained for the six bolt and twelve bolt configuration. No reports could be obtained for the bolts used for the 8ES configuration. The results from the material test reports are summarized in the Table 5-3 and the detailed reports are attached in Appendix B.

Table 5-2 Summary of Tensile Coupon Tests

Specimen	Coupon Number	Thickness (in.)	Yield Stress (ksi)	Tensile Stress (ksi)	Elongation, 8 in. Gage (%)	Average Yield Stress (ksi)
6B-4W/2W-0.875-1.00-36	1	1.004	59.3	83.7	24	59.3
6B-4W/2W-0.875-1.00-60	2	1.004	59.5	83.6	23	
12B- MRE 1/3 -4W/2W-0.75-1.00-36	3	1.003	59.0	83.2	26	
12B- MRE 1/3 -4W/2W-0.75-1.00-60						
6B-4W/2W-1.125-0.75-36	4	0.750	54.4	76.7	24	54.6
6B-4W/2W-1.125-0.75-60	5	0.748	54.7	76.5	24	
12B- MRE 1/3 -4W/2W-1.00-0.75-36	6	0.750	54.6	76.5	24	
12B- MRE 1/3 -4W/2W-1.00-0.75-60						
8ES-1.25-0.75-56	7	0.754	57.5	81.3	23	57.2
	8	0.754	56.9	80.0	25	
8ES-1.00-1.00-56	9	1.009	58.9	83.8	24	58.2
	10	1.004	57.5	85.2	23	

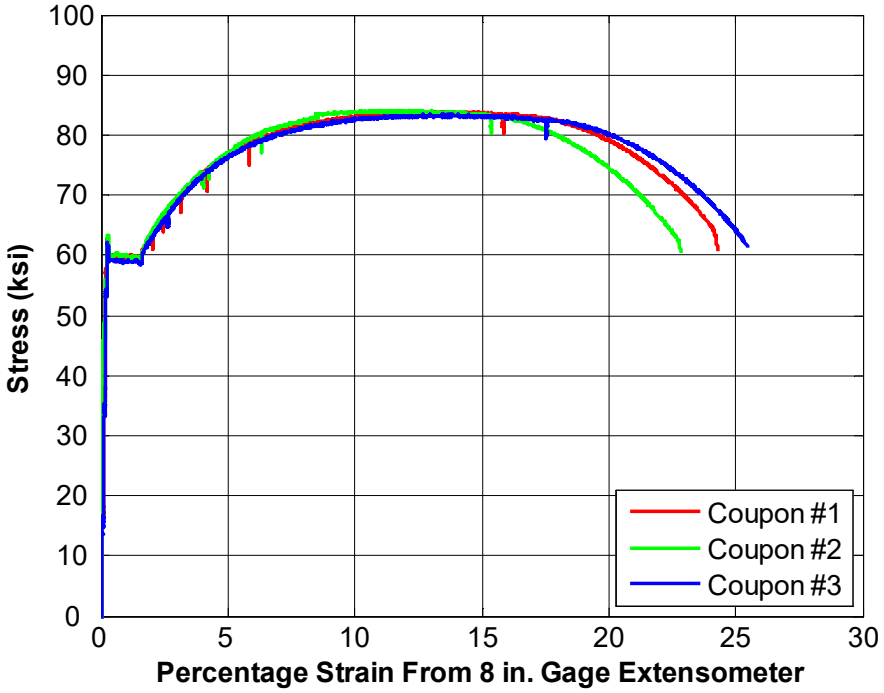

Figure 5-16 Results of Tensile Coupon Testing for 1 in. thick end-plate

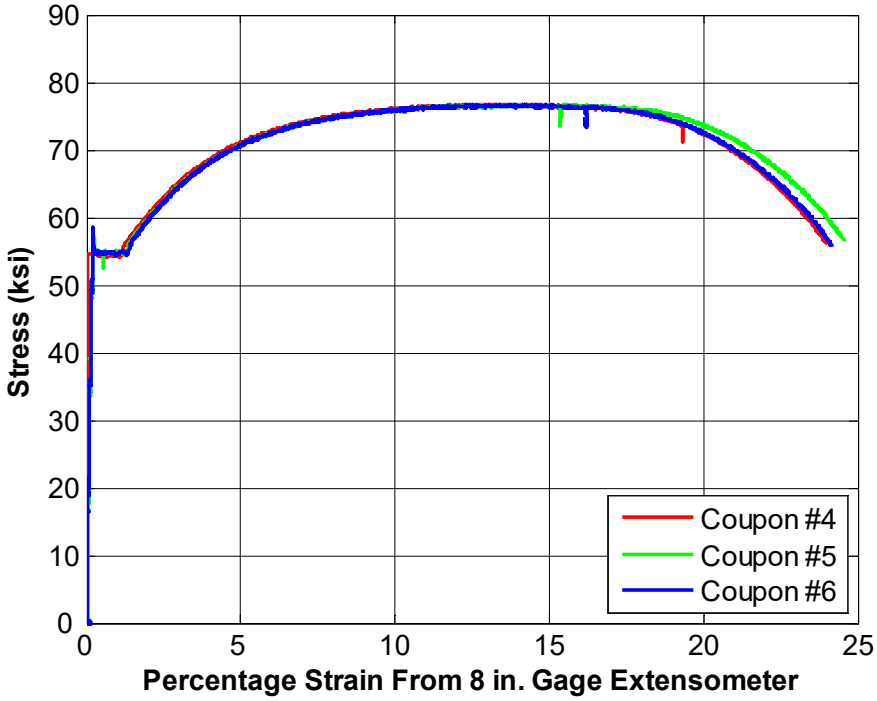

Figure 5-17 Results of Tensile Coupon Testing for 0.75 in. thick end-plate

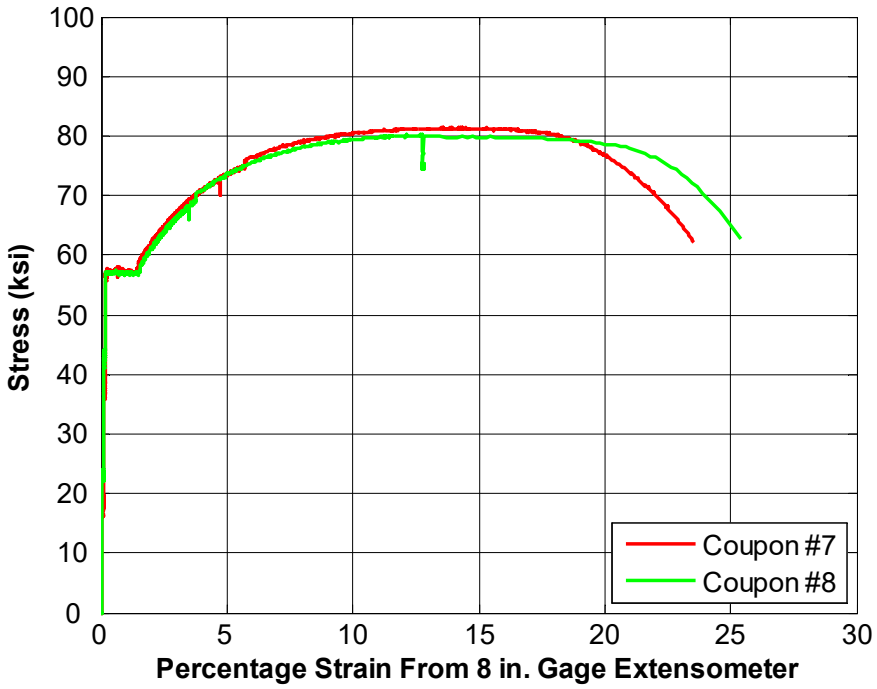

Figure 5-18 Results of Tensile Coupon Testing for 0.75 in. thick end-plate

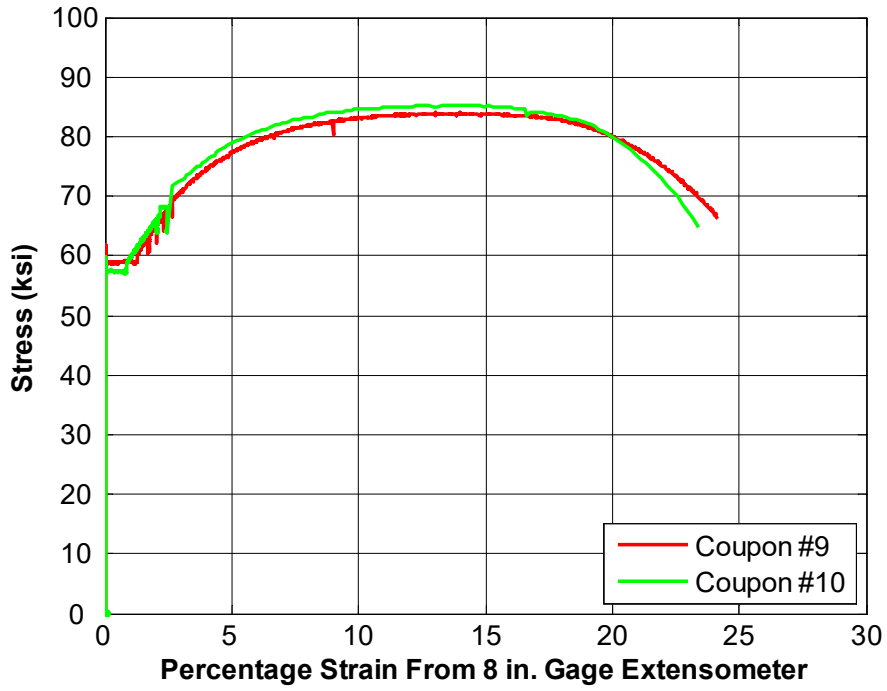

Figure 5-19 Results of Tensile Coupon Testing for 1.00 in. thick end-plate

Table 5-3 Summary of A325 Bolt Material Testing Reports

Specimen ID	Bolt Dia (in.)	Average Tensile Rupture Stress According to Mill Test Report (ksi)	No. of Samples	Specified Minimum Tensile Stress (ksi)
12B-MRE 1/3-4W/2W-**0.75**-1.00-36 12B-MRE 1/3-4W/2W-**0.75**-1.00-60	3/4	149	3	120
6B-4W/2W-**0.875**-1.00-36 6B-4W/2W-**0.875**-1.00-60	7/8	150	3	120
12B-MRE 1/3-4W/2W-**1.00**-0.75-36 12B-MRE 1/3-4W/2W-**1.00**-0.75-60	1	152	4	120
6B-4W/2W-**1.125**-0.75-36 6B-4W/2W-**1.125**-0.75-60	1 1/8	Too short to test	-	105
8ES-**1.00**-1.00-56	1	No report Provided	-	120
8ES-**1.25**-0.75-56	1 1/4	No report Provided	-	105

6 EXPERIMENTAL RESULTS

A total of ten tests were performed. These tests were aimed to introduce and validate two new configurations namely the 6B-4W/2W configuration and the 12B-MRE 1/3-4W/2W configuration. A total of four tests were done for each configuration, which included all the possible combinations of either a shallow beam (36 in. deep) or a deep beam (60 in. deep), with a thin end-plate and a thick end-plate. Also, two deep beam tests (56 in. deep), a thin end-plate test and thick end-plate test, were performed for the 8ES configuration. The results from all these tests are discussed in detail in the sections below.

All data points in the plots below have been down-sampled at the rate of one data point for every five hundred data points (except for the specimen 12B-MRE 1/3-4W/2W-1.00-0.75-60). This has been done for the clarity of plots and their easy interpretation. Also, the calculated moment capacity for end-plate yielding, M_{pl}, is based on the average tensile stress found out from the tensile coupon tests (Table 5-2). However, the moment capacity at bolt rupture with prying action, M_q, and moment capacity at bolt rupture without prying action, M_{np}, have been calculated based on the nominal tensile stress of the bolt (for A325 bolt = 90 ksi) and the nominal unthreaded body area of bolt. It is to be noted that the mill test reports (Table 5-3 and Appendix B) for the rupture stress of bolts predict about a 25% higher value than the specified minimum tensile stress of bolts.

To account for the above said higher bolt rupture stress, two more variables (M_q^{exp} and M_{np}^{exp}) have been shown in the following tables and plots, based on the stress of bolts obtained from the bolt test reports (Table 5-3). The actual tensile stress of some bolts, viz. 1 1/8 in., 1 1/4 in. and 1 in. (used for specimen 8ES-1.00-1.00-56) was not available. For the purpose of calculation of moment capacities involving these bolts an average value of 25% more than the specified minimum tensile stress (150 ksi for 1 in. diameter bolt and 131.25 ksi for 1 1/8 in. and 1 1/4in. diameter bolt) has been assumed. The basis for assuming a 25% higher stress of these bolts is that test reports for bolt diameter ranging from 3/4 in. to 1 in., were giving an average value of about 150 ksi which is 25% more

than the specified minimum tensile stress of 120 ksi. M_q^{exp} and M_{np}^{exp} have been calculated based on the expected bolt tensile stress (either from bolt test reports or assumed) and the net tensile area of the bolt (Table 7-17 of AISC Steel Construction Manual, 2011).

The green theoretical line in the applied moment vs midspan deflection plots has been calculated based on the stiffness of a simply supported beam with the same cross sectional properties as the specimen but assuming that the specimen is continuous at midspan without any connection.

The experimental end-plate yield moment (M_y) has been found out using the applied moment vs. end-plate separation plots. The curve has been assumed to be a bilinear curve, drawing two lines matching the initial and final slope of the curve. The point on the plot where these two lines meet has been considered to be the moment at which the end-plate yields.

6.1 Testing on the Six Bolt, Four-Wide/Two-Wide, Flush, Unstiffened (6B-4W/2W) Configuration

6.1.1 Shallow Section - Thin Plate Behavior

Specimen 6B-4W/2W-1.125-0.75-36 had a depth of 36 in. and can be assumed to be shallow in relation to the moment capacity of this configuration. It was designed to exhibit thin plate behavior.

6.1.1.1 Limit State – Predictions and Progression

Equations presented in Chapter 3 calculate a moment capacity at bolt rupture without prying action, M_{np}, of 1410 k-ft, moment capacity for end-plate yielding, M_{pl}, of 748 k-ft and moment capacity at bolt rupture with prying action, M_q, of 957 k-ft.

For thin plate behavior, the expected limit state progression is end-plate yielding at a moment equal to M_{pl} and then bolt rupture with prying action at a moment equal to M_q. The specimen behaved as expected. End-plate yielding occurred followed by bolt rupture

with prying action. The test was terminated after the rupture of the bottom inside bolt on one side (shown in Figure 6-5) and both the inside bolts on the other side.

6.1.1.2 Experimental Results - Yield and Ultimate Moments

A yield moment, M_y (from Figure 6-2) of 730 k-ft and an ultimate moment, M_u of 1110 k-ft were experimentally obtained. They are demonstrated graphically and compared with the predicted values in the Figure 6-1.

Though the ratio of M_{pl}/M_y in Table 6-1 is slightly non-conservative (greater than 1.0), but the prediction, M_{pl}, is within 2% of the experimental yield moment, M_y. Also, the ratio M_q/M_u in Table 6-1 is very conservative. This is due to the correction not applied to the bolt rupture strength. M_q has been predicted on the basis of a nominal tensile stress of 90 ksi for A325 bolts whereas they have been assumed to show about a 25% higher ultimate strength than the minimum specified tensile stress (105 ksi in this case) in bolt testing reports (Table 5-3). M_q^{exp} is within 1% of the ultimate moment observed. Hence, we can say that the ratio M_q/M_u is also in reasonable agreement with the equations presented in Section 3.3.

Table 6-1 Predicted and Experimentally Obtained Moment Capacities for Specimen 6B-4W/2W-1.125-0.75-36

Predicted (k-ft)			Experimental (k-ft)		Ratio		
M_{pl}	M_q	M_q^{exp}	M_y	M_u	M_{pl}/M_y	M_q/M_u	M_q^{exp}/M_u
748	957	1100	730	1110	1.02	0.86	0.99

Note: M_{pl}: Calculated based on measured material properties (tensile coupon tests)

M_q: Calculated based on nominal material properties

M_q^{exp}: Calculated based on expected material properties (bolt supplier's test report or assumption)

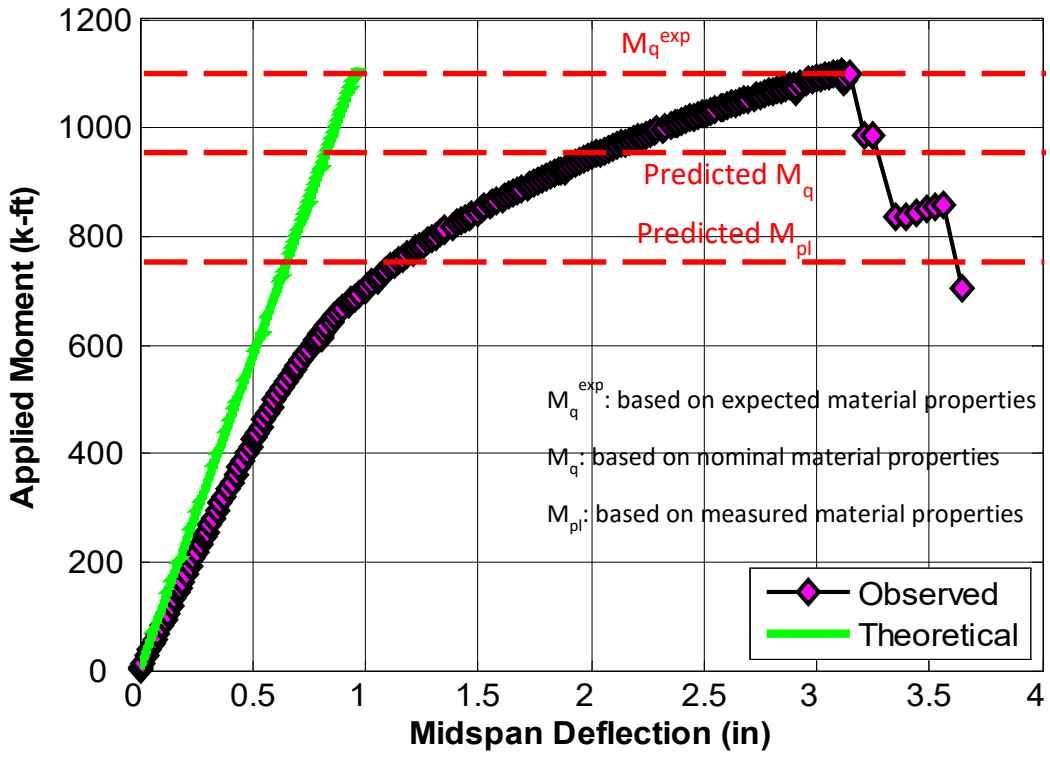

Figure 6-1 Applied Moment vs Midspan deflection for Specimen 6B-4W/2W-1.125-0.75-36

6.1.1.3 Experimental Results - End-Plate Separation

Instrumented calipers were used during experimental testing to determine end-plate separation. Figure 6-2 displays the end-plate separation in relation to the moment at the mid-span of the specimen.

The plot verifies that thin plate behavior was achieved. This is evident from the occurrence of large separations once the end-plate began to yield. With thick plate behavior, end-plate separation would be much smaller because the plate would not yield.

6.1.1.4 Experimental Results - Bolt Forces

Strain gages were installed in the shank of the bolts used in the experiment in order to determine bolt forces throughout the duration of the test. As shown in Figure 6-3, the bolt forces increased exponentially past the point of end-plate yielding which is approximately 730 k-ft.

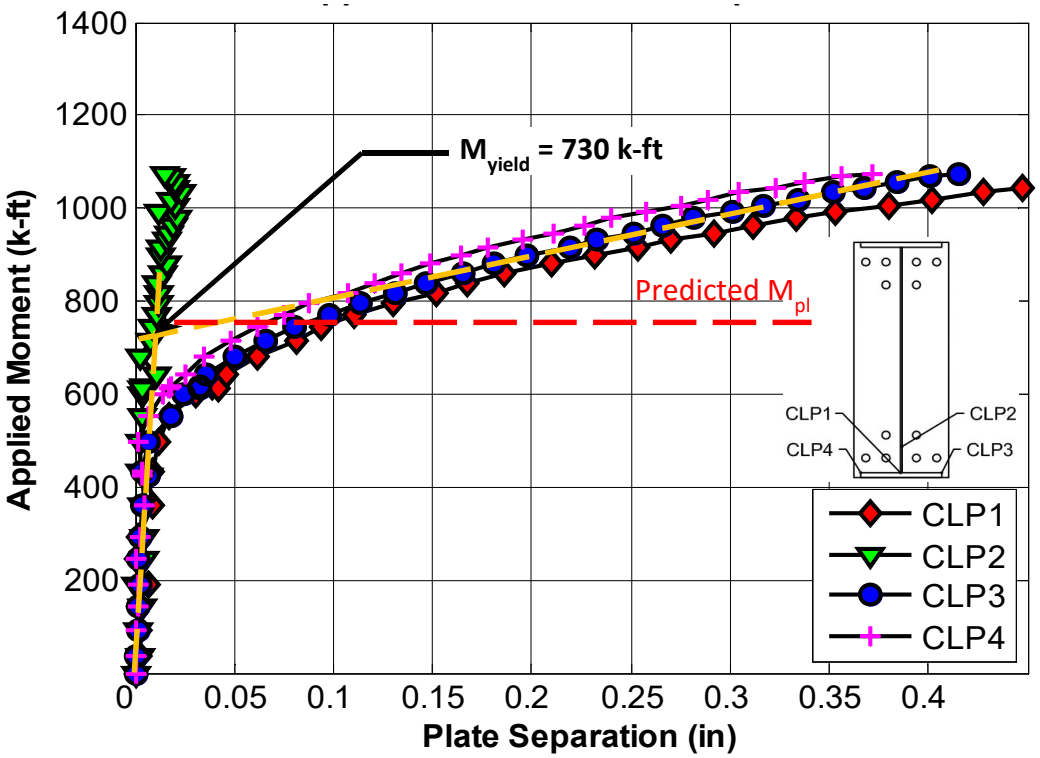

Figure 6-2 End-plate separation for Specimen 6B-4W/2W-1.125-0.75-36.

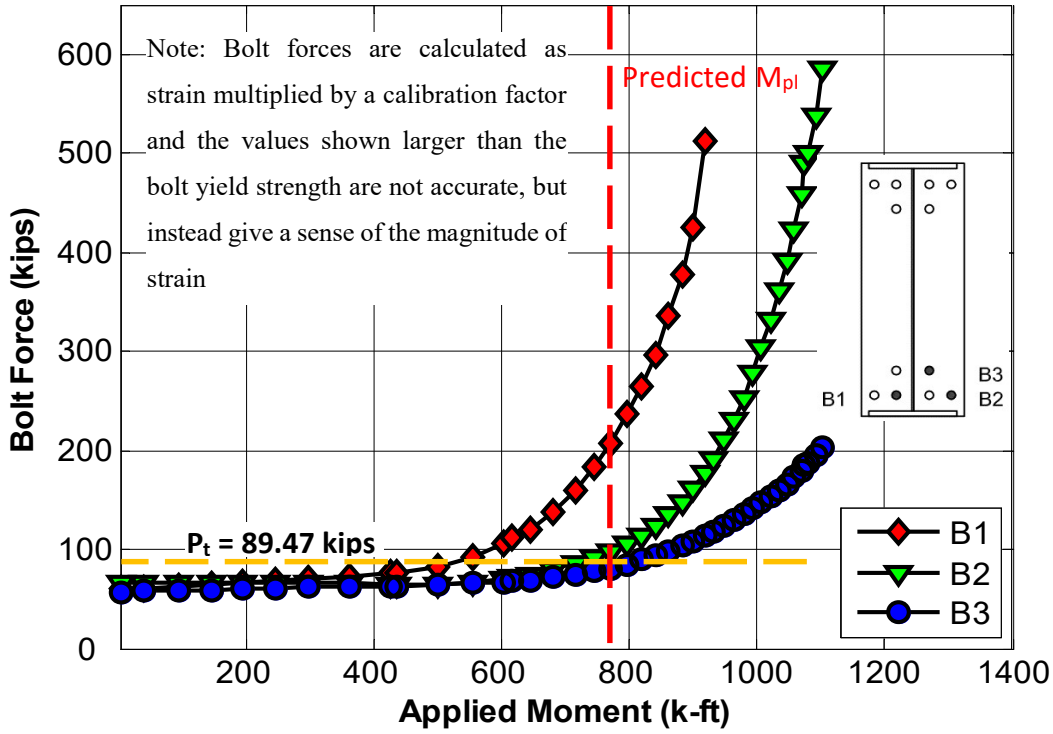

Figure 6-3 Bolt Forces for Specimen 6B-4W/2W-1.125-0.75-36

6.1.1.5 Experimental Results - Pictures of Specimen

Figure 6-4 and Figure 6-5 show the difference in the specimen at the start and the end of the test. From the pictures it is clear that there was end-plate yielding. Clearly, three yield lines, horizontal, vertical and diagonal, were seen on the end-plate on each side of the web. The first yield line to develop was the horizontal yield line at the bottom and then the vertical yield line started developing. The diagonal yield line started developing only after the bottom inside bolt had ruptured. Technically, the connection could be considered to have failed after the rupture of the bottom inside bolt and therefore, the diagonal yield line is not a part of the actual yield line mechanism considered in Chapter 3.

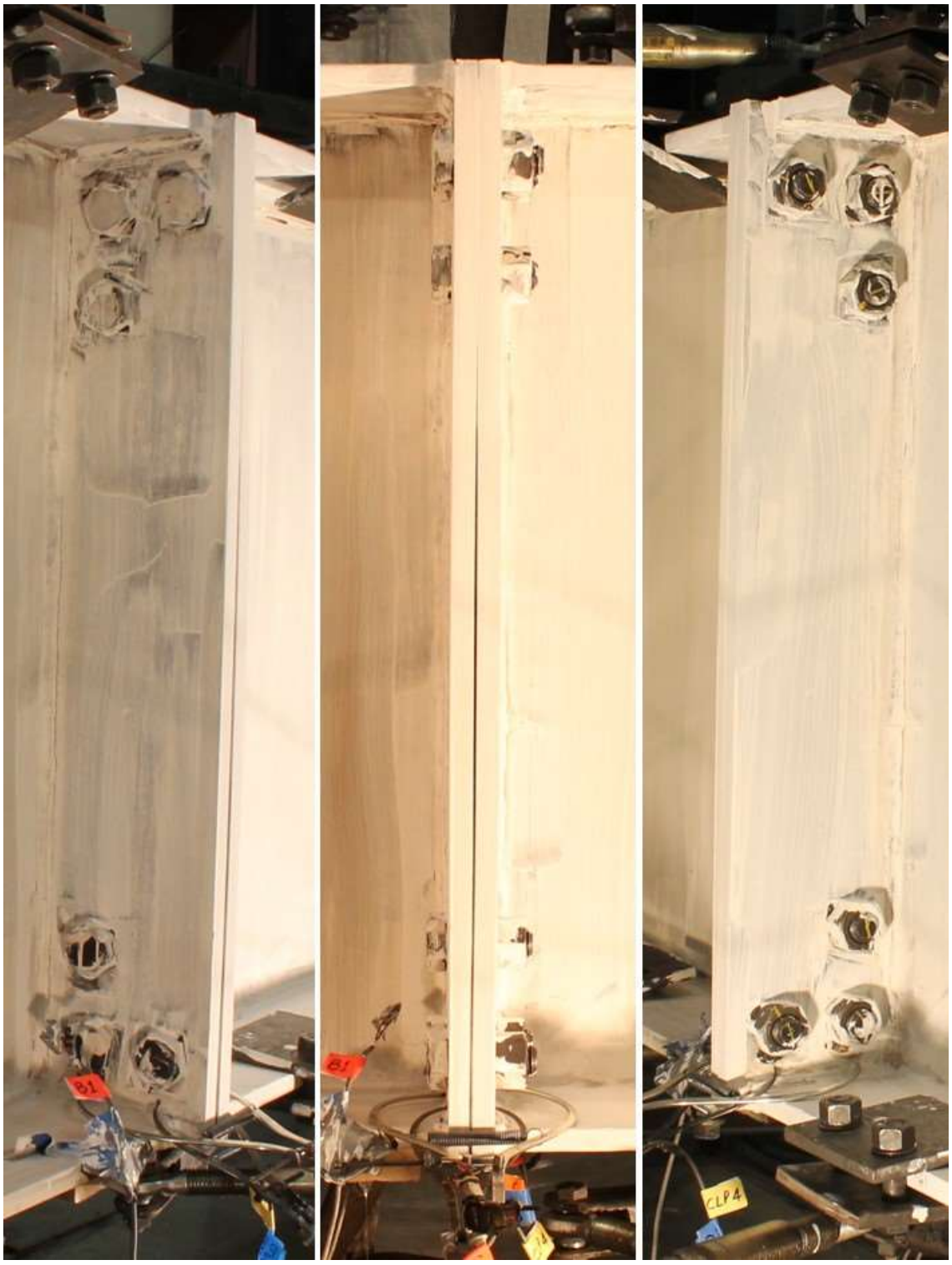

Figure 6-4 Three views of the Specimen 6B-4W/2W-1.125-0.75-36 at the start of the test

Figure 6-5 Three views of the specimen 6B-4W/2W-1.125-0.75-36 at the end of the test

6.1.2 **Shallow Section - Thick Plate Behavior**

Specimen 6B-4W/2W-0.875-1.00-36 had a depth of 36 in. and can be assumed to be shallow in relation to the moment capacity of this configuration. It was designed to exhibit thick end-plate behavior.

6.1.2.1 Limit State – Predictions and Progression

The predictions for bolt rupture without prying action, M_{np}, and moment capacity for end-plate yielding, M_{pl}, were 851 k-ft and 1440 k-ft, respectively. These values are based on equations proposed in Section 3.3.

For thick plate behavior, the expected limit state of progression is bolt rupture without prying action at a moment equal to M_{np}, without any end-plate plate yielding. The specimen behaved as expected. During the actual test, bolt rupture without prying action, M_{np}, controlled the strength of the connection. The six bolts on the tension side of the connection ruptured at once and no end-plate yielding was observed (shown in Figure 6-10).

6.1.2.2 Experimental Results - Yield and Ultimate Moments

A yield moment, M_y (shown in Figure 6-7) of 730 k-ft and an ultimate moment, M_u of 1030 k-ft were experimentally obtained. They are demonstrated graphically and compared with the predicted value, M_{np}, in the Figure 6-6.

The ratio M_{np}/M_u in Table 6-2 is conservative (less than 1.0). This is likely due to the correction not applied to the bolt rupture stress. M_q has been predicted on the basis of the nominal tensile stress of 90 ksi for A325 bolts whereas they have been observed to show about a 25% higher strength than the minimum specified tensile strength in material test reports (Table 5-3). To account for this overstrength in bolts M_{np}^{exp} was calculated and was found to be within 6% of the experimentally obtained moment capacity. Hence, we can also say that the ratio M_{np}/M_u is in reasonable agreement. Since, end-plate yielding was not observed, the ratio M_{pl}/M_y has been left blank.

Table 6-2 Predicted and Experimentally Obtained Moment Capacities for Specimen 6B-4W/2W-0.875-1.00-36

Predicted (k-ft)			Experimental (k-ft)		Ratio		
M_{pl}	M_{np}	M_{np}^{exp}	M_y	M_u	M_{pl}/M_y	M_{np}/M_u	M_{np}^{exp}/M_u
1440	851	1090	770	1030	-	0.83	1.06

Note: M_{pl}: Calculated based on measured material properties (tensile coupon tests)

M_{np}: Calculated based on nominal material properties

M_{np}^{exp}: Calculated based on expected material properties (bolt supplier's test report or assumption)

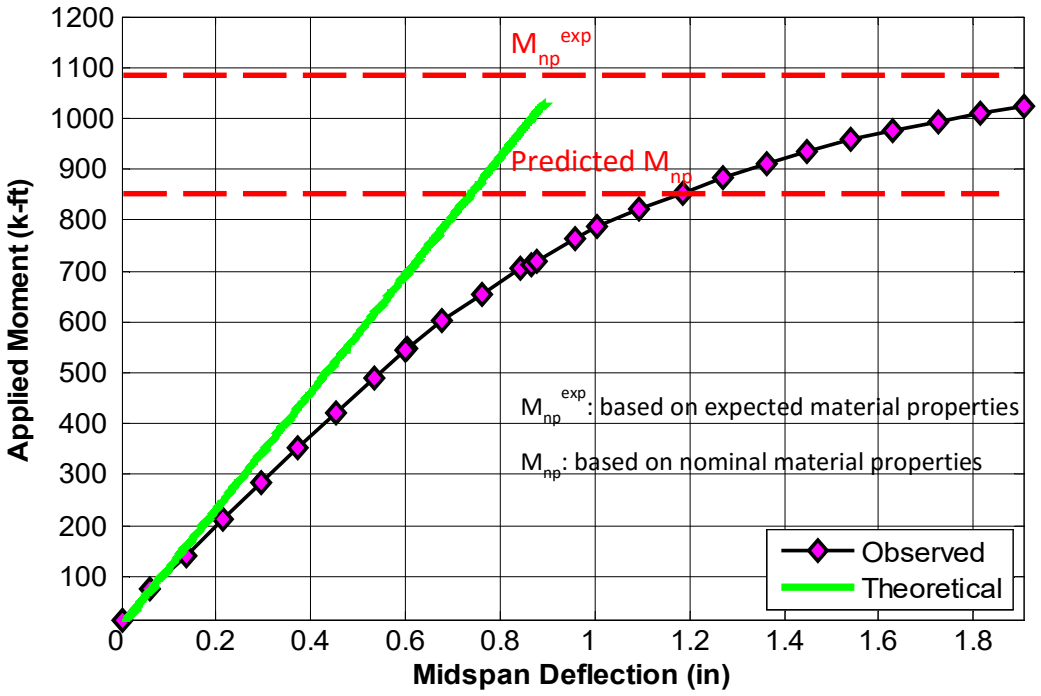

Figure 6-6 Applied Moment vs Midspan deflection for Specimen 6B-4W/2W-0.875-1.00-36

6.1.2.3 Experimental Results - End-Plate Separation

Figure 6-7 displays the end-plate separation in relation to the moment at the mid-span of the specimen.

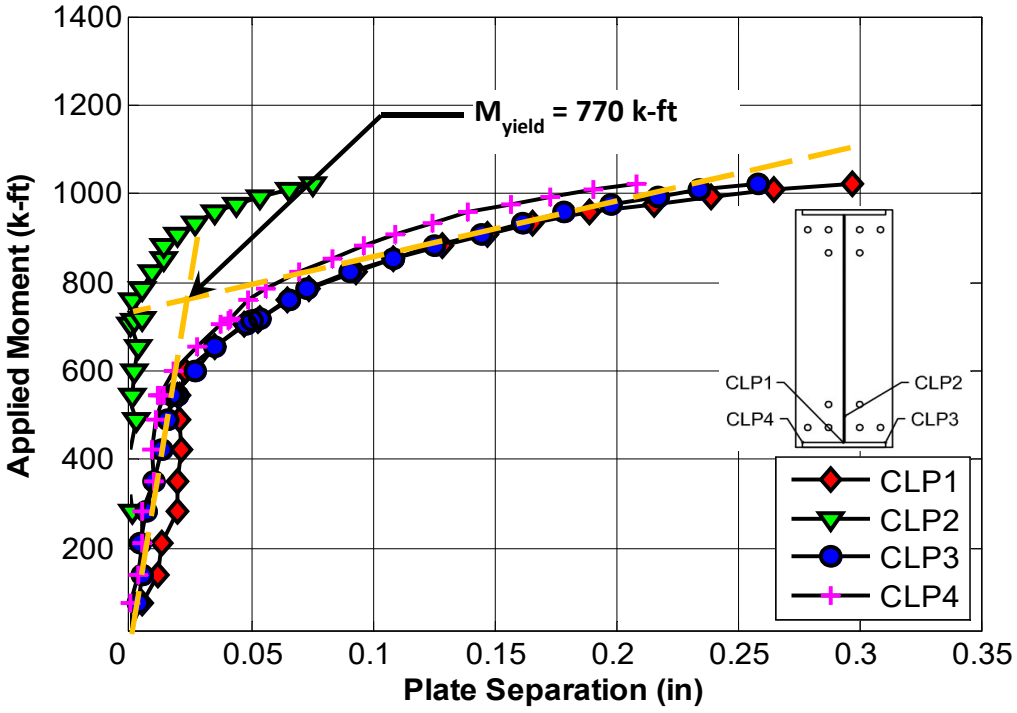

Figure 6-7 End-plate separation for Specimen 6B-4W/2W-0.875-1.00-36.

The plot shows that there was some yielding of the plate before the bolts actually went to rupture. This is evident from the occurrence of significant separations once the end-plate began to yield. It is also possible that this separation is due to the yielding of bolts. The pictures shown in Figure 6-10, prove that there was little yielding in the plates and hence, the behavior was of a thick plate.

6.1.2.4 Experimental Results - Bolt Forces

As is shown in Figure 6-8, the bolt forces did not increase significantly until they reached their nominal tensile strength (data plotted past this point is considered invalid due to unaccounted for nonlinearity in the relationship between stress and strain). This indicates that prying forces were negligible.

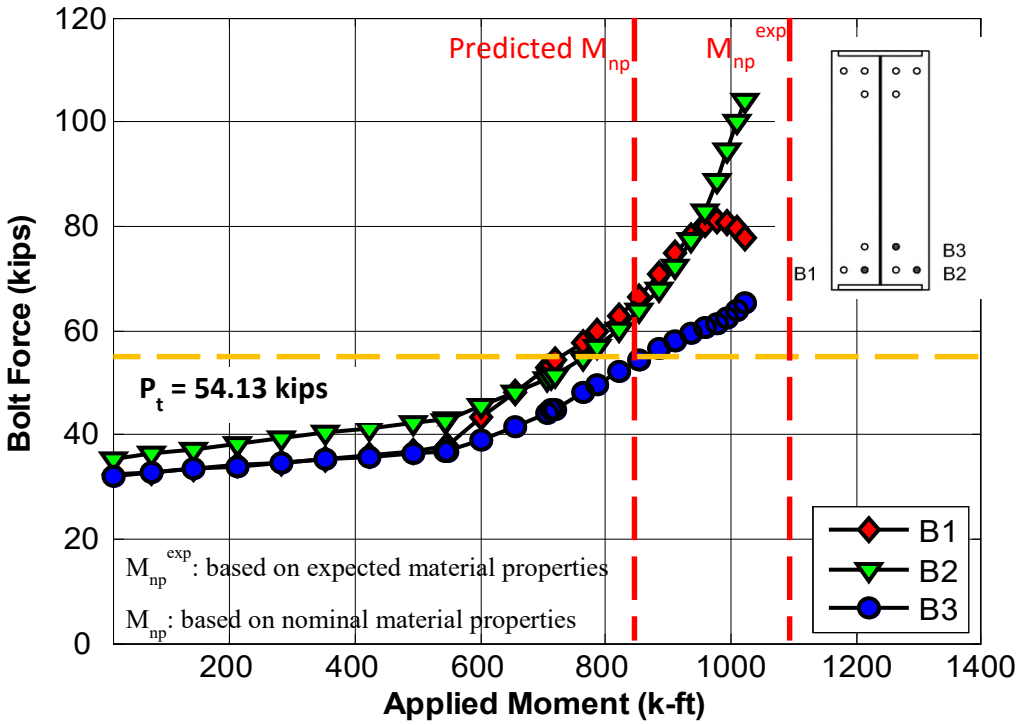

Note: Bolt forces are calculated as strain multiplied by a calibration factor and the values shown larger than the bolt yield strength are not accurate, but instead give a sense of the magnitude of strain

Figure 6-8 Bolt Forces for specimen 6B-4W/2W-0.875-1.00-36

6.1.2.5 Experimental Results - Pictures of Specimen

Figure 6-9 and Figure 6-10 show the difference in the specimen at the start and the end of the test. From the pictures it is clear that a horizontal yield line had just started to develop though it is evident that this was an incomplete yield line.

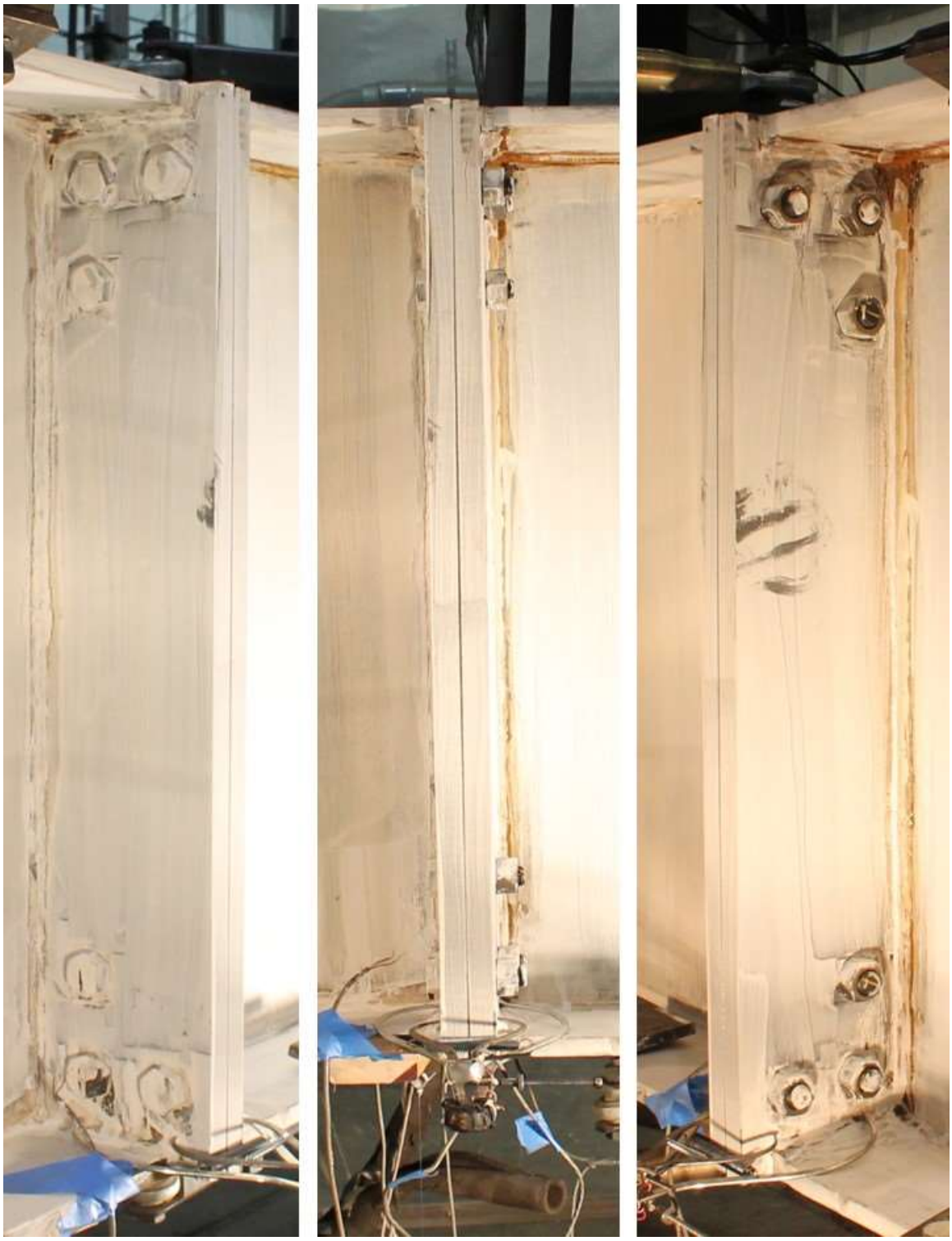

Figure 6-9 Three views of the Specimen 6B-4W/2W-0.875-1.00-36 at the start of the test

Figure 6-10 Three views of the specimen 6B-4W/2W-0.875-1.00-36 at the end of the test

6.1.3 **Deep Section - Thin Plate Behavior**

Specimen 6B-4W/2W-1.125-0.75-60 was a 60 in. deep section designed to exhibit thin end-plate behavior.

6.1.3.1 Limit State – Predictions and Progression

From the equations presented in Chapter 3, moment capacity at bolt rupture without prying action (M_{np}), moment capacity for end-plate yielding (M_{pl}), and moment capacity at bolt rupture with prying action (M_q) were 2480 k-ft, 1310 k-ft and 1680 k-ft, respectively.

For thin plate behavior, the expected limit state progression is end-plate yielding at a moment equal to M_{pl} and then bolt rupture with prying action at a moment equal to M_q. The specimen behaved as expected. End-plate yielding occurred followed by bolt rupture with prying action. The test was terminated after the rupture of the all the inside bolts on both sides of the web. The outer bolt on each side of the web didn't rupture (shown in Figure 6-15).

6.1.3.2 Experimental Results - Yield and Ultimate Moments

A yield moment, M_y (shown in Figure 6-12) of 1400 k-ft and an ultimate moment, M_u of 1980 k-ft were experimentally obtained. They are demonstrated graphically and compared with the predicted values in the Figure 6-11.

The ratio M_{pl}/M_y in Table 6-3 is conservative (less than 1.0) and the predicted, M_{pl}, is within 6% of the observed, M_y. Also, the ratio M_q/M_u in Table 6-3 is conservative. This is probably due to the correction not applied to the bolt yield strength. M_q has been predicted on the basis of a nominal tensile strength of 90 ksi for A325 bolts whereas they have been observed to show about a 25% higher strength than the specified minimum tensile strength (105 ksi, in this case) in the bolt material test reports (Table 5-3). To account for this, expected moment capacity at bolt rupture, M_q^{exp}, was computed to be 1930 k-ft. The ratio M_q^{exp}/M_u was conservative by 3%. Hence, we can say that the ratio M_q/M_u is also in reasonable agreement in equations presented in Chapter 3.

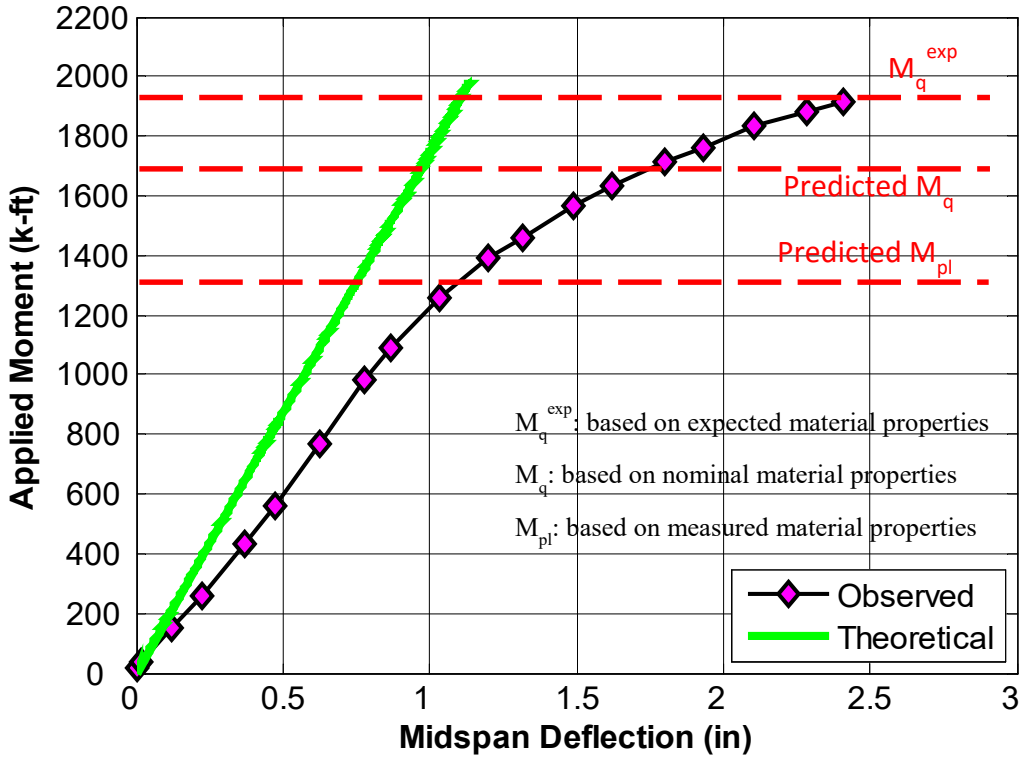

Figure 6-11 Applied Moment vs Midspan deflection for Specimen 6B-4W/2W-1.125-0.75-60

Table 6-3 Predicted and Experimentally Obtained Moment Capacities for Specimen 6B-4W/2W-1.125-0.75-60

Predicted (k-ft)			Experimental (k-ft)		Ratio		
M_{pl}	M_q	M_q^{exp}	M_y	M_u	M_{pl}/M_y	M_q/M_u	M_q^{exp}/M_u
1310	1680	1930	1400	1980	0.94	0.85	0.97

Note: M_{pl}: Calculated based on measured material properties (tensile coupon tests)

M_q: Calculated based on nominal material properties

M_q^{exp}: Calculated based on expected material properties (bolt supplier's test report or assumption)

6.1.3.3 Experimental Results - End-Plate Separation

Figure 6-12 displays the end-plate separation in relation to the moment at the mid-span of the specimen.

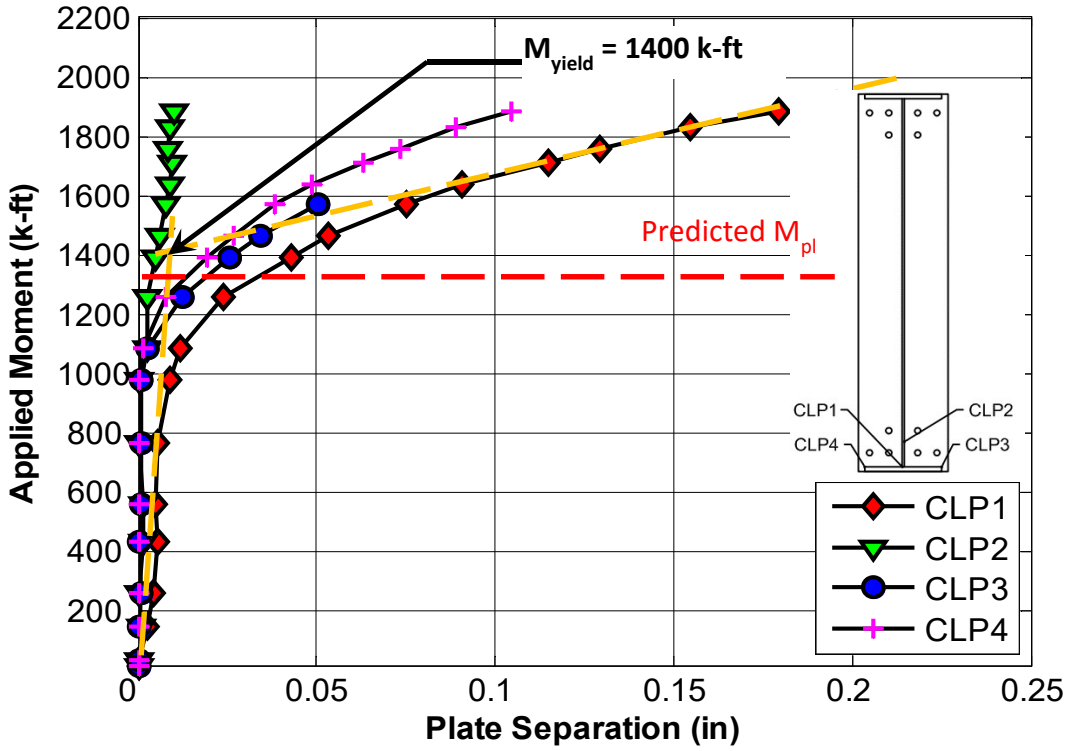

Figure 6-12 End-plate separation for Specimen 6B-4W/2W-1.125-0.75-60.

The plot verifies that thin plate behavior was achieved. This is evident from the occurrence of large separations once the end-plate began to yield. With thick plate behavior, end-plate separation would be much smaller because the plate would not yield.

6.1.3.4 Experimental Results - Bolt Forces

As shown in Figure 6-13, the bolt forces, especially in B1 and B3, increased drastically past the predicted end-plate yielding moment, which is 1310 k-ft. This indicates substantial prying forces as a result of thin end-plate behavior.

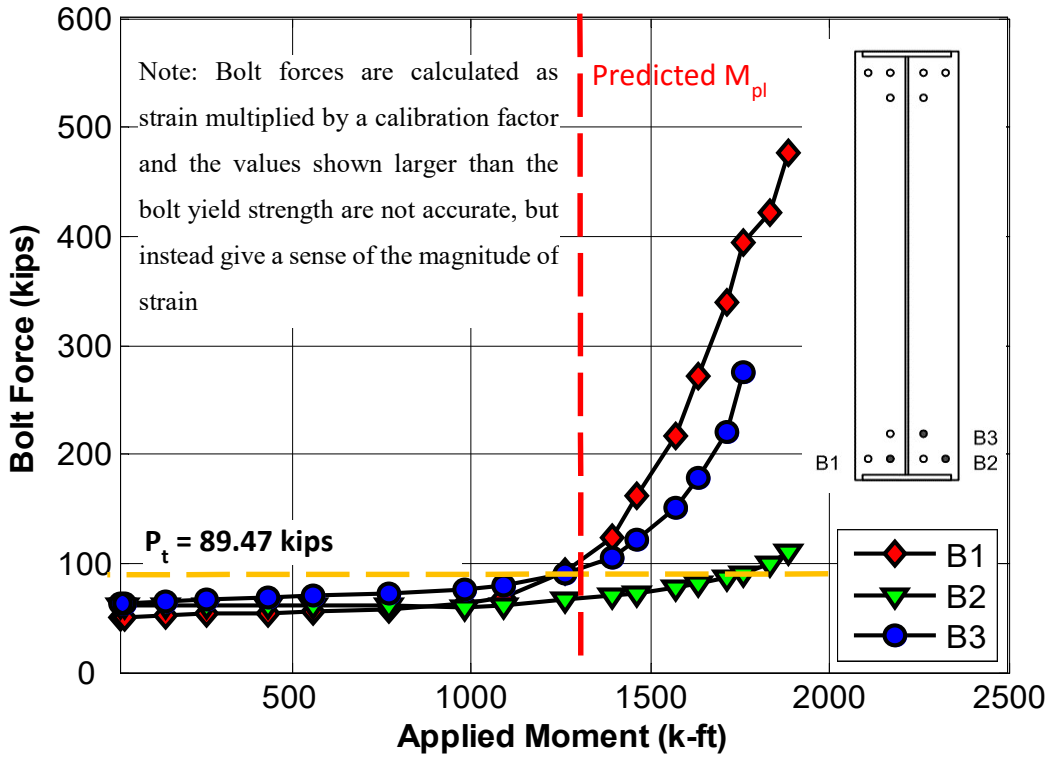

Figure 6-13 Bolt Forces for specimen 6B-4W/2W-1.125-0.75-60

6.1.3.5 Experimental Results - Pictures of Specimen

Figure 6-14 and Figure 6-15 show the difference in the specimen at the start and the end of the test. From the pictures it is clear that there was end-plate yielding. Clearly, three yield lines, horizontal, vertical and diagonal, were seen on the end-plate on each side of the web. The first yield line to develop was the horizontal yield line at the bottom and then the vertical yield line started developing. The diagonal yield line started developing only after the bottom inside bolt had ruptured. Technically, the connection could be considered to have failed after the rupture of the bottom inside bolt and therefore, the diagonal yield line is not a part of the actual yield line mechanism considered in Chapter 3. Also the profile of the end-plates as viewed from the side (middle picture in Figure 6-15) clearly shows that there was distortion in the end-plate.

Figure 6-14 Three views of the Specimen 6B-4W/2W-1.125-0.75-60 at the start of the test

Figure 6-15 Three views of the specimen 6B-4W/2W-1.125-0.75-60 at the end of the test

6.1.4 **Deep Section - Thick Plate Behavior**

Specimen 6B-4W/2W-0.875-1.00-60 was a 60 in. deep section designed to exhibit thick end-plate behavior.

6.1.4.1 Limit State – Predictions and Progression

Equations presented in Chapter 3 calculate a moment capacity at bolt rupture without prying action (M_{np}) and moment capacity for end-plate yielding (M_{pl}) to be 1500 k-ft and 2530 k-ft, respectively.

For thick plate behavior, the expected limit state of progression is bolt rupture without prying action at a moment equal to M_{np}, without any end-plate plate yielding. The specimen behaved as expected. During the actual test, bolt rupture without prying action, M_{np}, controlled the strength of the connection. The six bolts on the tension side of the connection ruptured at once and no end-plate yielding was observed (shown in Figure 6-20).

6.1.4.2 Experimental Results - Yield and Ultimate Moments

A yield moment, M_y (shown in Figure 6-17) of 1390 k-ft and an ultimate moment, M_u of 1730 k-ft were experimentally obtained. They are demonstrated graphically and compared with the predicted value, M_{np}, in the Figure 6-16.

The ratio M_{np}/M_u in Table 6-4 is conservative (less than 1.0). This is likely due to the correction not applied to the bolt tensile strength. M_{np} has been predicted on the basis of a nominal tensile strength of 90 ksi for A325 bolts whereas they have been observed to show about a 25% higher strength than the specified minimum tensile strength (120 ksi in this case) in the bolt material test reports (Table 5-3). To account for this M_{np}^{exp} was found out to be 1920 k-ft. It was found out that M_u lies between M_{np} and M_{np}^{exp}. Since, end-plate yielding was not observed, the ratio M_{pl}/M_y has been left blank.

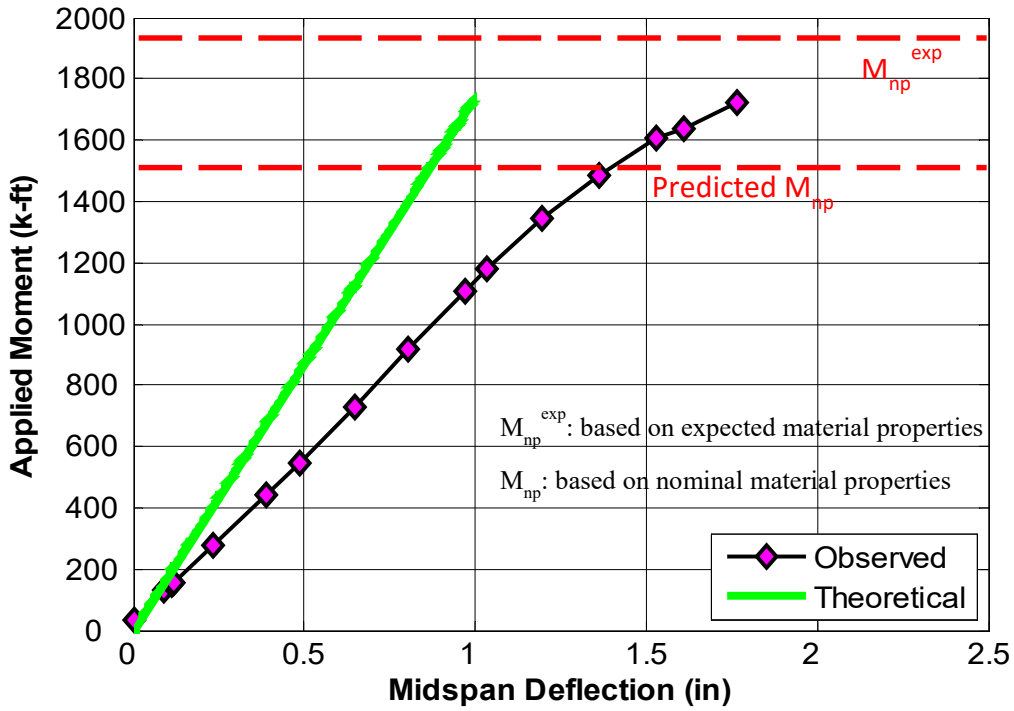

Figure 6-16 Applied Moment vs Midspan deflection for Specimen 6B-4W/2W-0.875-1.00-60

Table 6-4 Predicted and Experimentally Obtained Moment Capacities for Specimen 6B-4W/2W-0.875-1.00-60

Predicted (k-ft)			Experimental (k-ft)		Ratio		
M_{pl}	M_{np}	M_{np}^{exp}	M_y	M_u	M_{pl}/M_y	M_{np}/M_u	M_{np}^{exp}/M_u
2530	1500	1920	1390	1730	-	0.87	1.11

Note: M_{pl}: Calculated based on measured material properties (tensile coupon tests)

M_{np}: Calculated based on nominal material properties

M_{np}^{exp}: Calculated based on expected material properties (bolt supplier's test report or assumption)

6.1.4.3 Experimental Results - End-Plate Separation

Figure 6-17 displays the end-plate separation in relation to the moment at the mid-span of the specimen.

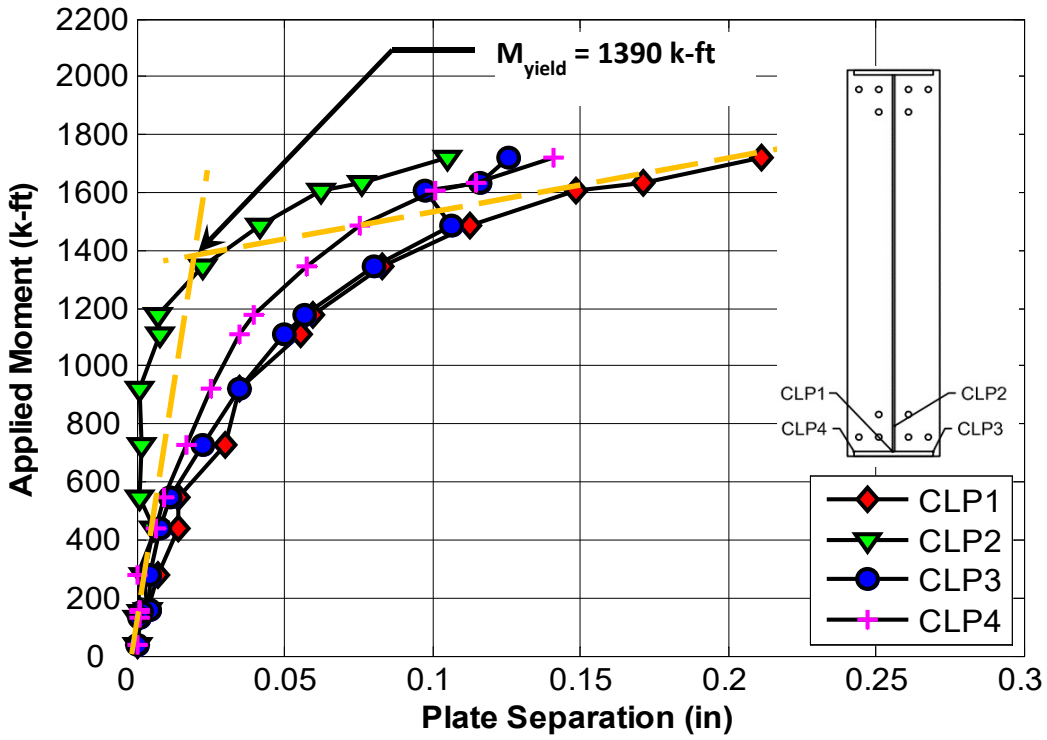

Figure 6-17 End-plate separation for Specimen 6B-4W/2W-0.875-1.00-60.

The plot shows that there may have been some yielding of the plate before the bolts actually ruptured. This is evident from the occurrence of significant separations once the end-plate began to yield. It is also possible that this separation is due to the yielding of bolts. But, the pictures shown in Figure 6-20, prove that there was no yielding in the plates and hence, the behavior was of a thick plate.

6.1.4.4 Experimental Results - Bolt Forces

As shown in Figure 6-18, the bolt forces did not increase significantly except for the bolt, B2 which had an exponential increase only towards the end. This indicates that was no prying in the connection.

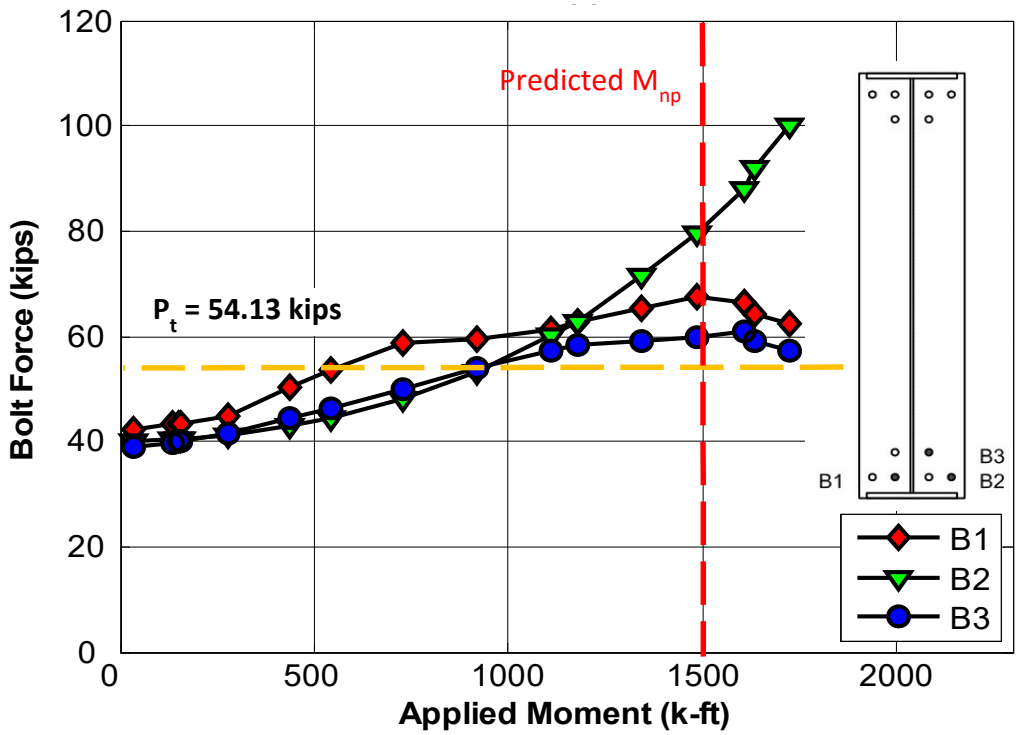

Note: Bolt forces are calculated as strain multiplied by a calibration factor and the values shown larger than the bolt yield strength are not accurate, but instead give a sense of the magnitude of strain

Figure 6-18 Bolt Forces for specimen 6B-4W/2W-0.875-1.00-60

6.1.4.5 Experimental Results - Pictures of Specimen

Figure 6-19 and Figure 6-20 show the difference in the specimen at the start and the end of the test. From the pictures it is clear that no yield lines, whatsoever, were seen. This validates that the specimen had the behavior of a thick plate.

Figure 6-19 Three views of the Specimen 6B-4W/2W-0.875-1.00-60 at the start of the test

Figure 6-20 Three views of the specimen 6B-4W/2W-0.875-1.00-60 at the end of the test

6.1.5 **Overall Summary of the Six Bolt Flush Configuration and Recommendations**

A total of four tests were conducted for the 6B-4W/2W configuration and all of them could be taken to bolt rupture. Table 6-5 summarizes the four specimens investigated herein.

Table 6-5 Summary of the Four Test Specimens of the Six Bolt Flush Unstiffened Configuration

Specimen Identification[1]	Depth (in.)	Behavior	Remarks[2]
6B-4W/2W-1.125-0.75-36	36	Thin	M_{pl} +2% of yield moment. M_q was -14% of the observed M_u. M_q^{exp} was -1% of the observed M_u. End-plate yielding observed.
6B-4W/2W-0.875-1.00-36	36	Thick	M_{np} was -17% of the observed M_u. M_{np}^{exp} was +6% of the observed M_u A bit of end-plate yielding observed.
6B-4W/2W-1.125-0.75-60	60	Thin	Predicted M_{pl} -6% of the observed yield moment, M_y. Predicted M_q was -13% of the observed M_u. M_q^{exp} was -3% of the observed M_u. End-plate yielding observed.
6B-4W/2W-0.875-1.00-60	60	Thick	M_{np} was -13% of the observed M_u. M_{np}^{exp} was +11% of the observed M_u. No end-plate yielding observed.

[1]Specimen Identification: "No. of bolts in the connection – No. of bolts in a row - Bolt diameter - End-plate thickness - Beam depth".

[2]Remarks: A postive percentage means an unconservative calculation, whereas a negative percentage means a safe prediction.

For the two thin plate tests, M_{pl} was either 2% more (unconservative) than the experimental yield moment (for shallow beam) or 6% less (safe) than the experimental yield moment

(for deep beam). M_q was 14% and 15% less (safe) than the observed M_u for shallow and deep beam, respectively. M_q^{exp} was 1% and 3% less (safe) than the observed M_u for shallow and deep beam, respectively. Furthermore, experimentally measured end-plate separation was found to be consistent with thin end-plate behavior wherein end-plate yielding allows end-plate separation prior to bolt fracture.

It could be said that the design procedures are validated for end-plate yielding and considering the M_q^{exp} values, the bolt force models for thin plate behavior for this configuration also appear to be correct.

For thick plate tests, the behavior of the two specimens was quite as expected. Just the specimen 6B-4W/2W-0.875-1.00-36, exhibited a bit of end-plate yielding. M_{np} was 17% and 13% less (safe) than the observed M_u for shallow and deep beam, respectively. M_{np}^{exp} was 6% and 11% more (unsafe) than the observed M_u for shallow and deep beam, respectively. The experimental moment capacity of the connection for both the cases was found to lie between the predicted moment capacity based on nominal material properties and the moment capacity of the connected based on expected material properties. Considering the former as the lower bound and the latter as the upper bound, it appears that the bolt force model for thick plate behavior appears to be reasonable.

6.2 Testing on the Twelve Bolt, Multiple Row Extended, Four-Wide/Two-Wide (12B-MRE 1/3-4W/2W), Unstiffened Configuration

6.2.1 Shallow Section - Thin Plate Behavior

Specimen 12B-MRE 1/3-4W/2W-1.00-0.75-36 could be considered to be a shallow section (depth = 36 in.) considering the moment capacity of this configuration. It was designed to exhibit thin end-plate behavior.

6.2.1.1 Limit State – Predictions and Progression

Equations presented in Chapter 3 calculate a moment capacity at bolt rupture without prying action (M_{np}), moment capacity for end-plate yielding (M_{pl}) and moment capacity at bolt rupture with prying action (M_q) to be 2310 k-ft, 1130 k-ft and 1420 k-ft, respectively.

For thin plate behavior, the expected limit state progression is end-plate yielding at a moment equal to M_{pl} and then bolt rupture with prying action at a moment equal to M_q. The specimen was designed accordingly, but the test had to be stopped prior to bolt rupture. This was due to the flange and web local buckling of the section, because the section had crossed its nominal moment capacity of 1630 k-ft (assuming a yield stress of 55 ksi for the whole section). Therefore, when it reached this stage, it couldn't take any more load and the test had to be stopped, because the thick end-plate side was yet to be tested. End-plate yielding was observed and is shown in Figure 6-25.

6.2.1.2 Experimental Results - Yield and Ultimate Moments

A yield moment, M_y (shown in Figure 6-22) of 1230 k-ft and an ultimate moment, M_u of 1640 k-ft (none of the bolts were ruptured) were experimentally obtained. They are demonstrated graphically and compared with the predicted values in the Figure 6-21.

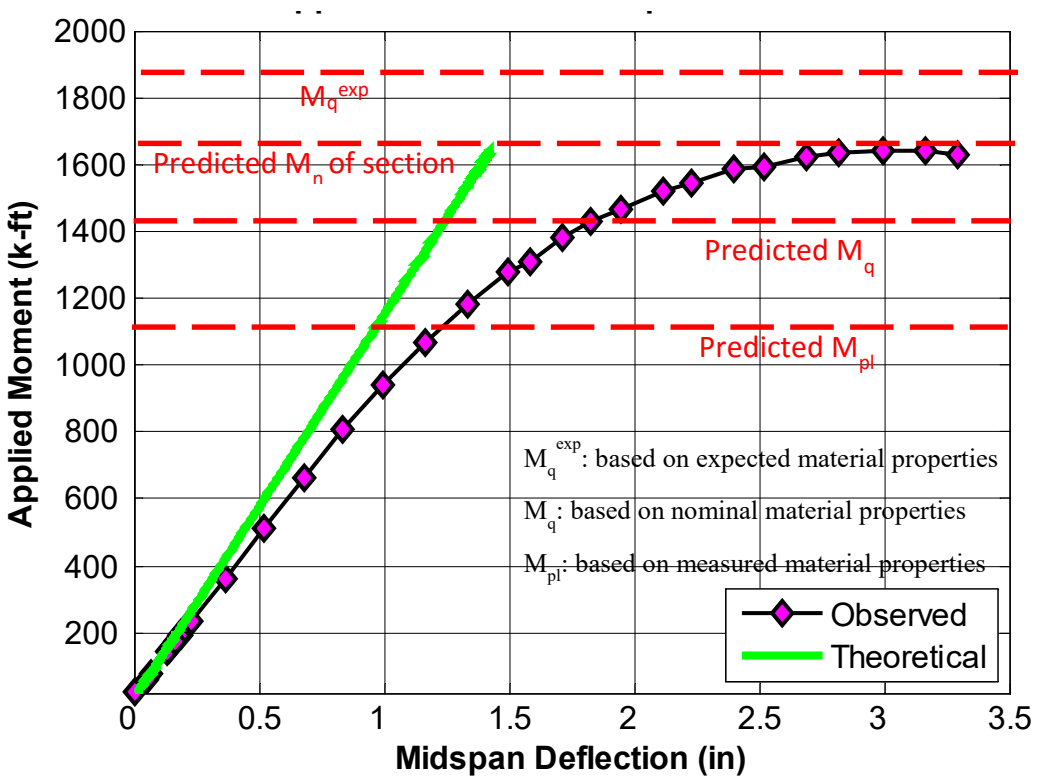

Figure 6-21 Applied Moment vs Midspan deflection for Specimen 12B-MRE 1/3-4W/2W-1.00-0.75-36

The ratio M_{pl}/M_y in Table 6-6 is conservative (less than 1.0) and it is within 8% of the predicted value. Also, the ratio M_q/M_u in Table 6-1 is conservative. M_q has been predicted on the basis of a nominal tensile strength of 90 ksi for A325 bolts whereas they have been observed to show about a 25% higher strength than the specified minimum tensile strength (120 ksi in this case) in the bolt material test reports (Table 5-3). To take this higher strength into account M_q^{exp} was computed and it was about 14% more than the maximum moment applied. It is to be noted that the test was stopped prior to bolt rupture.

6.2.1.1 Experimental Results - End-Plate Separation

Figure 6-22 displays the end-plate separation in relation to the moment at the mid-span of the specimen.

Table 6-6 Predicted and Experimentally Obtained Moment Capacities for Specimen 12B-MRE 1/3-4W/2W-1.00-0.75-36

Predicted (k-ft)			Experimental (k-ft)		Ratio		
M_{pl}	M_q	M_q^{exp}	M_y	M_u^1	M_{pl}/M_y	M_q/M_u^1	M_q^{exp}/M_u^1
1130	1420	1870	1230	1640	0.92	0.87	1.14

Note: M_u^1: Bolt rupture not observed at this moment and this was the maximum moment that the section could sustain.

M_{pl}: Calculated based on measured material properties (tensile coupon tests)

M_q: Calculated based on nominal material properties

M_q^{exp}: Calculated based on expected material properties (bolt supplier's test report or assumption)

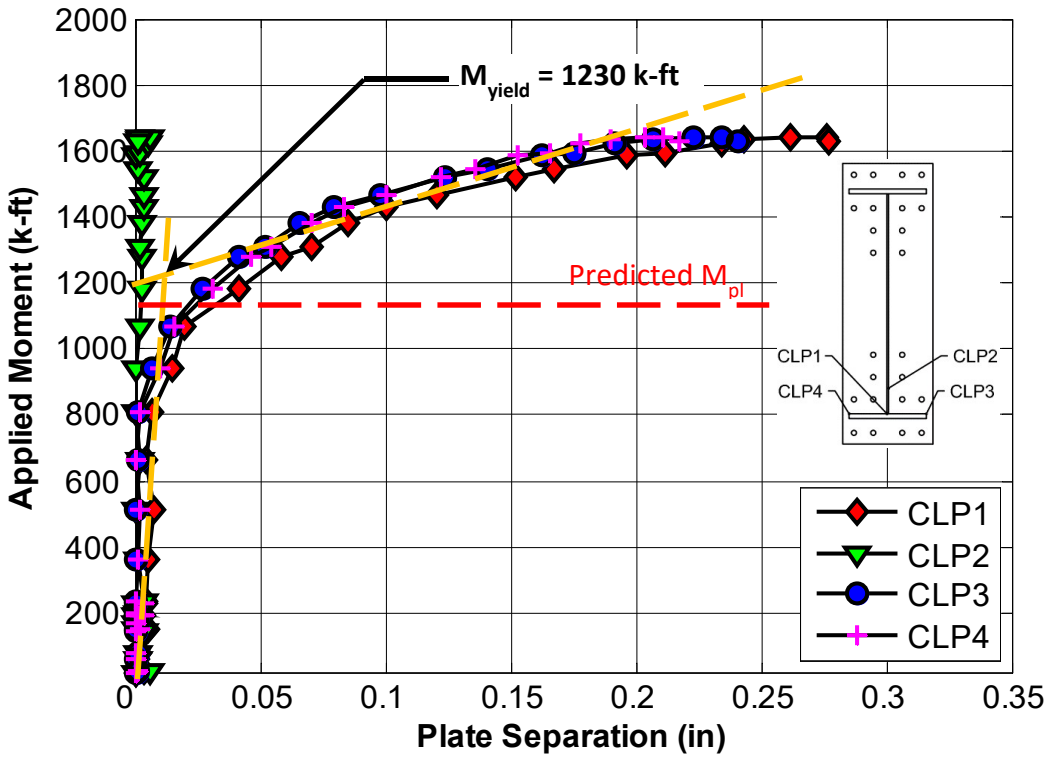

Figure 6-22 End-plate separation for Specimen 12B-MRE 1/3-4W/2W-1.00-0.75-36.

The plot verifies that thin plate behavior was achieved. This is evident from the occurrence of large separations once the end-plate began to yield. With thick plate behavior, end-plate separation would be much smaller because the plate would not yield.

6.2.1.2 Experimental Results - Bolt Forces

As shown in Figure 6-23, the bolt forces increased drastically, especially in bolts B1, B2, B4 and B5, past the point of end-plate yielding, which is approximately 1230 k-ft. This indicates substantial prying forces in the rows containing the above mentioned four bolts. Another important thing to be observed in the plot is that there was no exponential increase in the forces for bolt B3. This could be attributed to the absence of prying in this row of bolts.

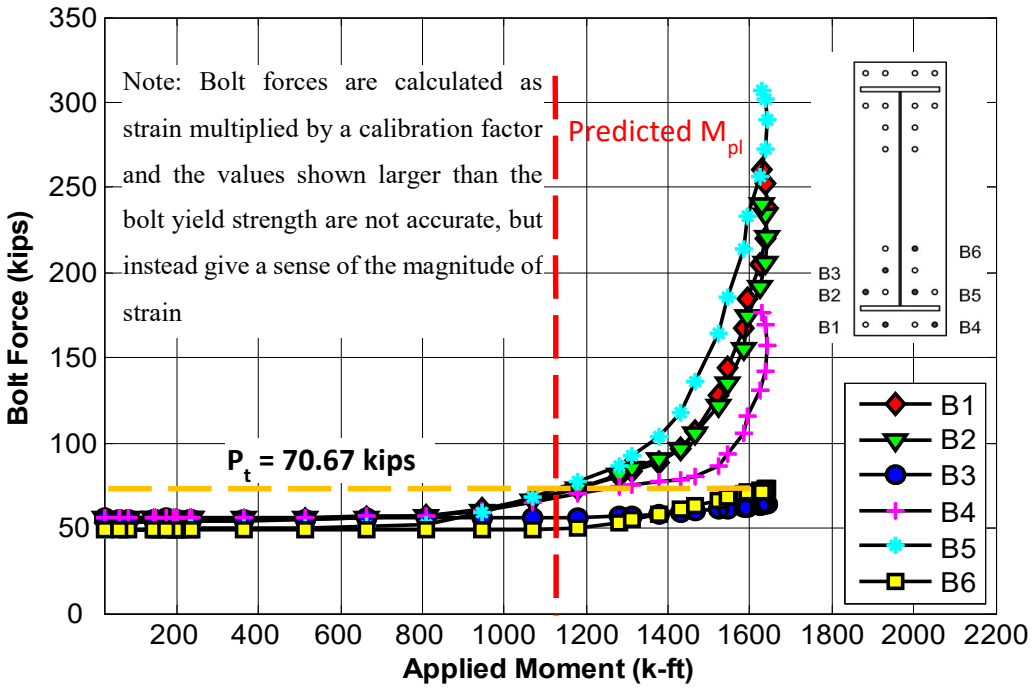

Figure 6-23 Bolt Forces for specimen 12B-MRE 1/3-4W/2W-1.00-0.75-36

6.2.1.3 Experimental Results - Pictures of Specimen

Figure 6-24 and Figure 6-25 show the difference in the specimen at the start and the end of the test. From the pictures it is clear that there was end-plate yielding. Clearly, two horizontal yield lines developed, one in the line of bolts outside the flange and the other in the line of bolts just inside of the flange.

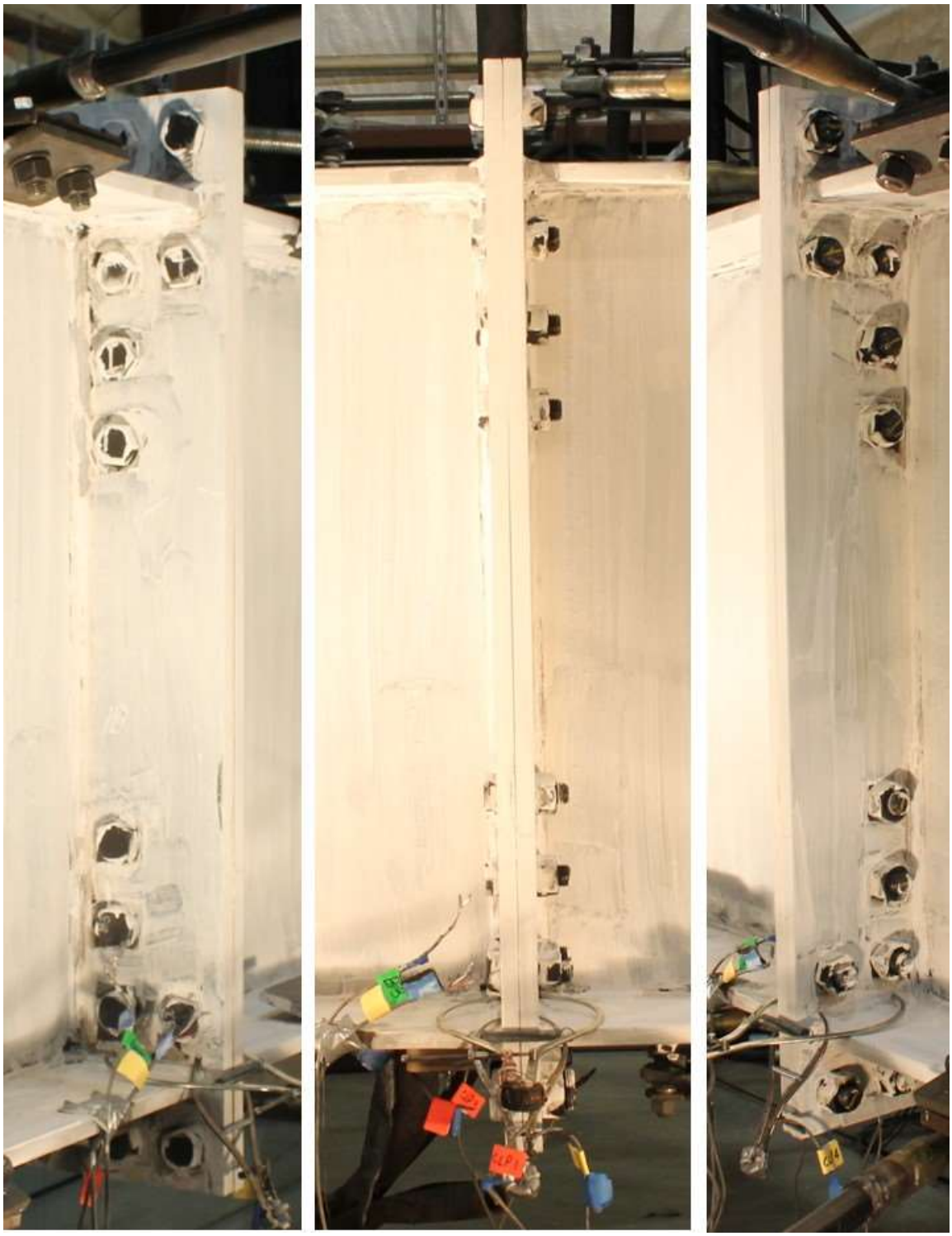

Figure 6-24 Three views of the Specimen 12B-MRE 1/3-4W/2W-1.00-0.75-36 at the start of the test

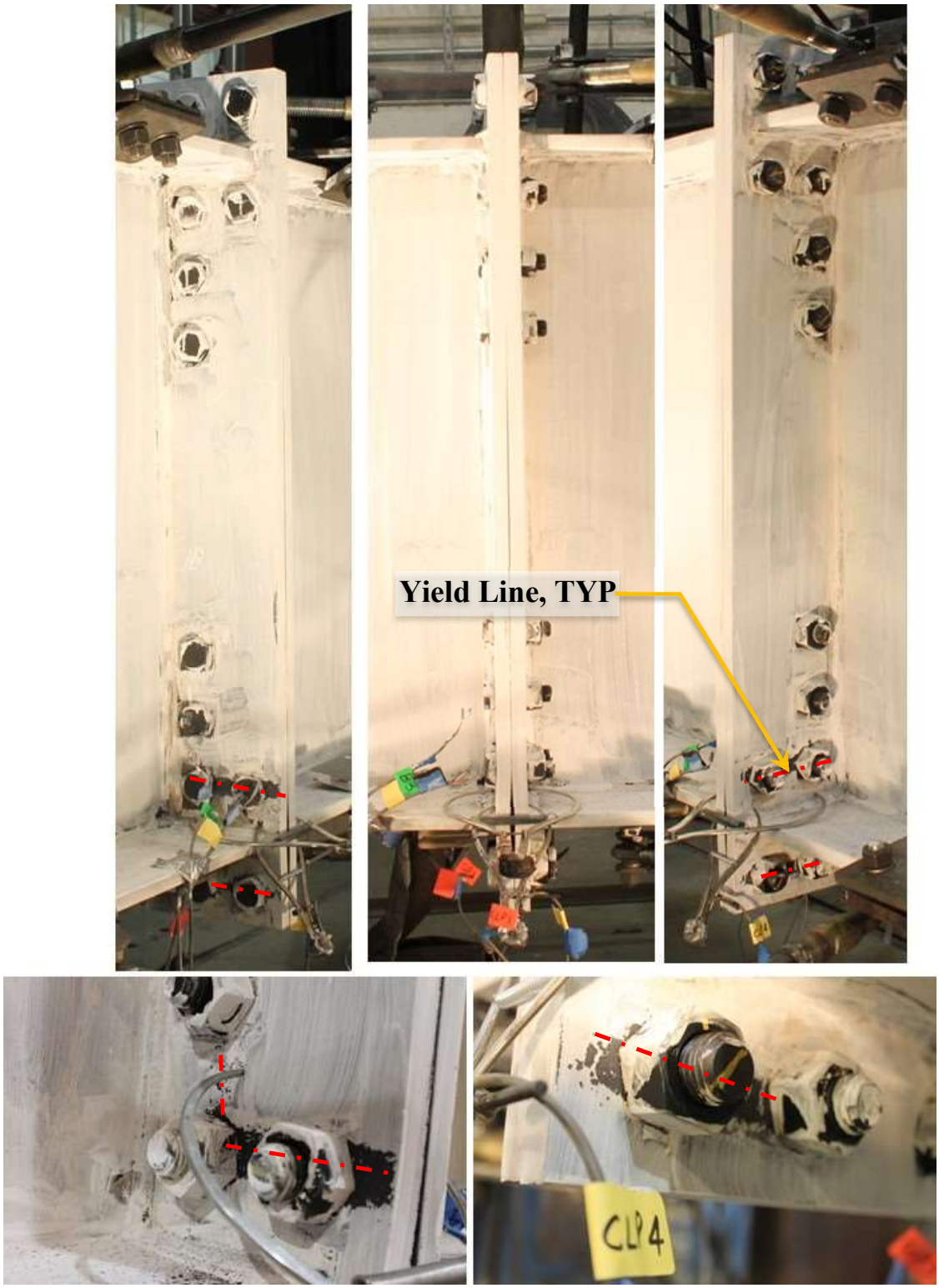

Figure 6-25 Three views of the specimen 12B-MRE 1/3-4W/2W-1.00-0.75-36 and the yield lines seen, at the end of the test

6.2.2 **Shallow Section - Thick Plate Behavior**

Since specimen 12B-MRE 1/3-4W/2W-0.75-1.00-36 could sustain a relatively lower moment, the beam section could be considered to be a shallow section (depth = 36 in.). It was designed to exhibit thick end-plate behavior.

6.2.2.1 Limit State – Predictions and Progression

Equations presented in Section 3.4 calculate a moment capacity at bolt rupture without prying action (M_{np}) and moment capacity for end-plate yielding (M_{pl}) of 1300 k-ft and 2190 k-ft, respectively.

For thick plate behavior, the expected limit state of progression is bolt rupture without prying action at a moment equal to M_{np}, without any end-plate plate yielding. The specimen behaved as expected. During the actual test, bolt rupture without prying action, M_{np}, controlled the strength of the connection. The six bolts on the tension side of the connection ruptured at once and no end-plate yielding was observed (shown in Figure 6-30).

6.2.2.2 Experimental Results - Yield and Ultimate Moments

A yield moment, M_y (Figure 6-27) of 960 k-ft and an ultimate moment, M_u of 1490 k-ft were experimentally obtained. They are demonstrated graphically and compared with the predicted value, M_{np}, in the Figure 6-26.

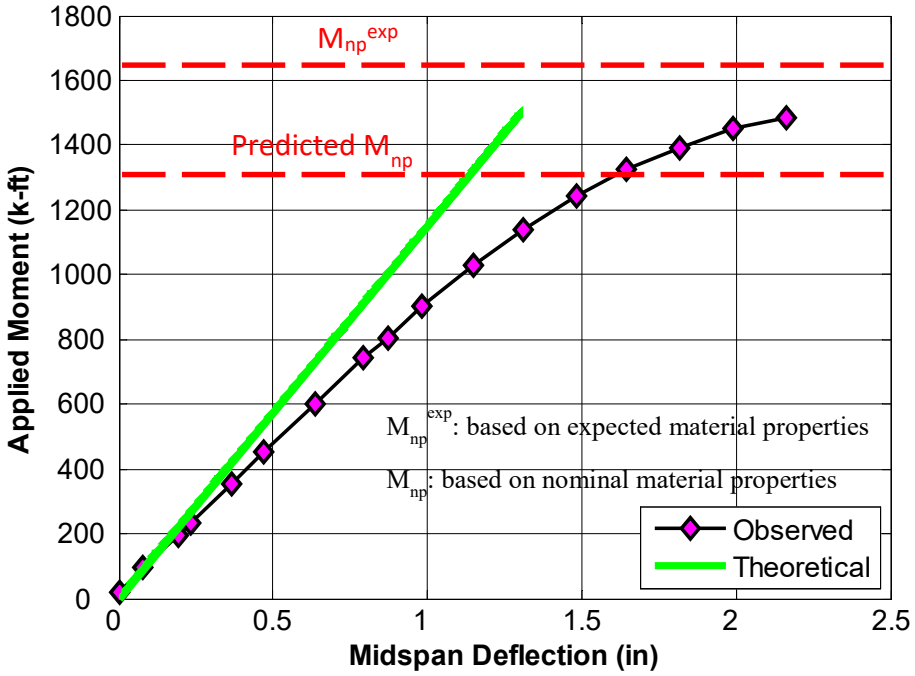

Figure 6-26 Applied Moment vs Midspan deflection for Specimen 12B-MRE 1/3-4W/2W-0.75-1.00-36

The ratio M_{np}/M_u in Table 6-7 is conservative (less than 1.0). This is likely due to the correction not applied to the bolt yield strength. M_{np} has been predicted on the basis of a nominal tensile strength of 90 ksi for A325 bolts whereas they have been observed to show about a 25% higher strength than the specified minimum tensile strength (120 ksi in this case) in the bolt material test reports (Table 5-3). To account for this M_{np}^{exp} was computed based on the expected material properties and was found out to be 9% more (unconservative) than the experimentally observed ultimate moment. Since, end-plate yielding was not observed, the ratio M_{pl}/M_y has been left blank.

6.2.2.3 Experimental Results - End-Plate Separation

Figure 6-27 displays the end-plate separation in relation to the moment at the mid-span of the specimen.

Table 6-7 Predicted and Experimentally Obtained Moment Capacities for Specimen 12B-MRE 1/3-4W/2W-0.75-1.00-36

Predicted (k-ft)			Experimental (k-ft)		Ratio		
M_{pl}	M_{np}	M_{np}^{exp}	M_y	M_u	M_{pl}/M_y	M_{np}/M_u	M_{np}^{exp}/M_u
2190	1300	1630	960	1490	-	0.87	1.09

Note: M_{pl}: Calculated based on measured material properties (tensile coupon tests)

M_{np}: Calculated based on nominal material properties

M_{np}^{exp}: Calculated based on expected material properties (bolt supplier's test report or assumption)

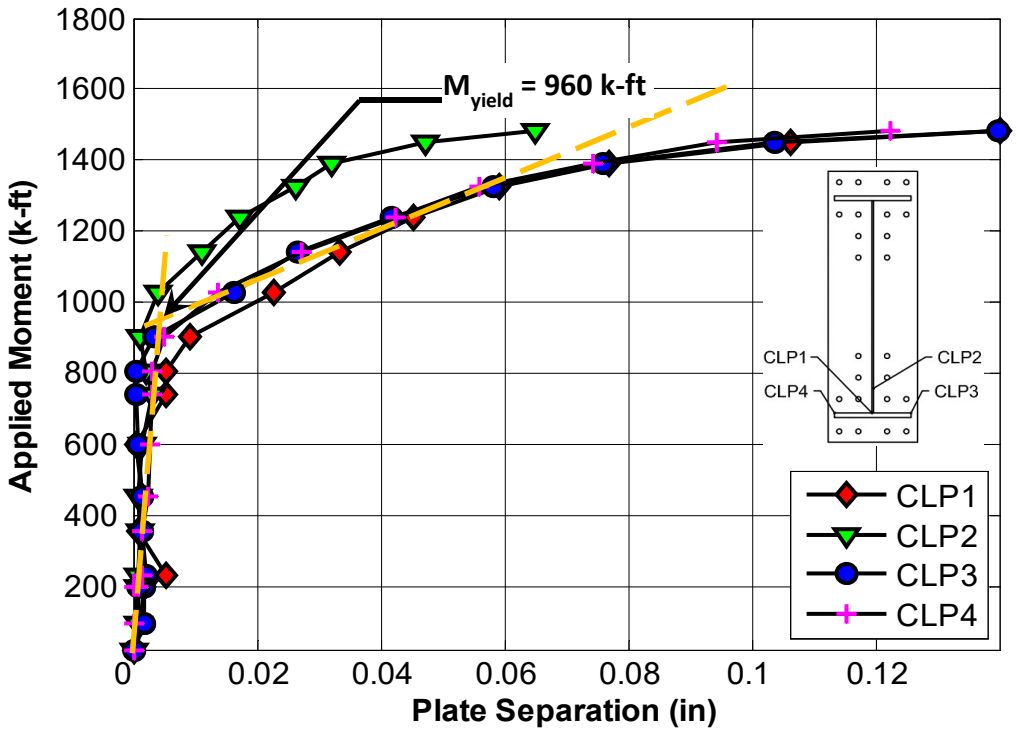

Figure 6-27 End-plate separation for Specimen 12B-MRE 1/3-4W/2W-0.75-1.00-36.

The plot shows that there was not much end-plate separation before the bolts ruptured, which is typical of a thick plate behavior. Also, the pictures shown in Figure 6-30, prove that there was no white wash spalling in the plates and hence, the end-plates didn't yield.

6.2.2.4 Experimental Results - Bolt Forces

As shown in Figure 6-28, the bolt forces did not increase significantly until they reached their nominal tensile strength (data plotted past this point is considered invalid due to unaccounted for nonlinearity in the relationship between stress and strain). This indicates that prying forces were negligible.

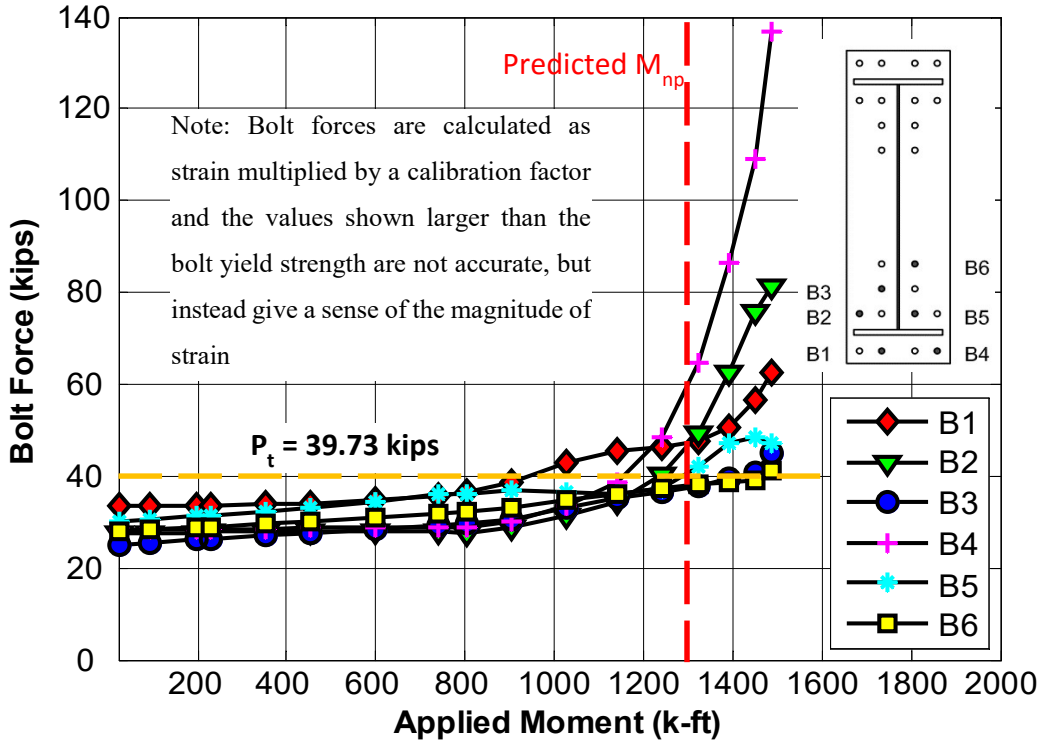

Figure 6-28 Bolt Forces for specimen 12B-MRE 1/3-4W/2W-0.75-1.00-36

6.2.2.5 Experimental Results - Pictures of Specimen

Figure 6-29 and Figure 6-30 show the difference in the specimen at the start and the end of the test. From the pictures it is clear that no yielding was observed. Also, the end-plate separation throughout the depth, was like a simple wedge with no distortions seen from the side view (middle picture in Figure 6-30), which is typical of thick plate behavior.

Figure 6-29 Three views of the Specimen 12B-MRE 1/3-4W/2W-0.75-1.00-36 at the start of the test

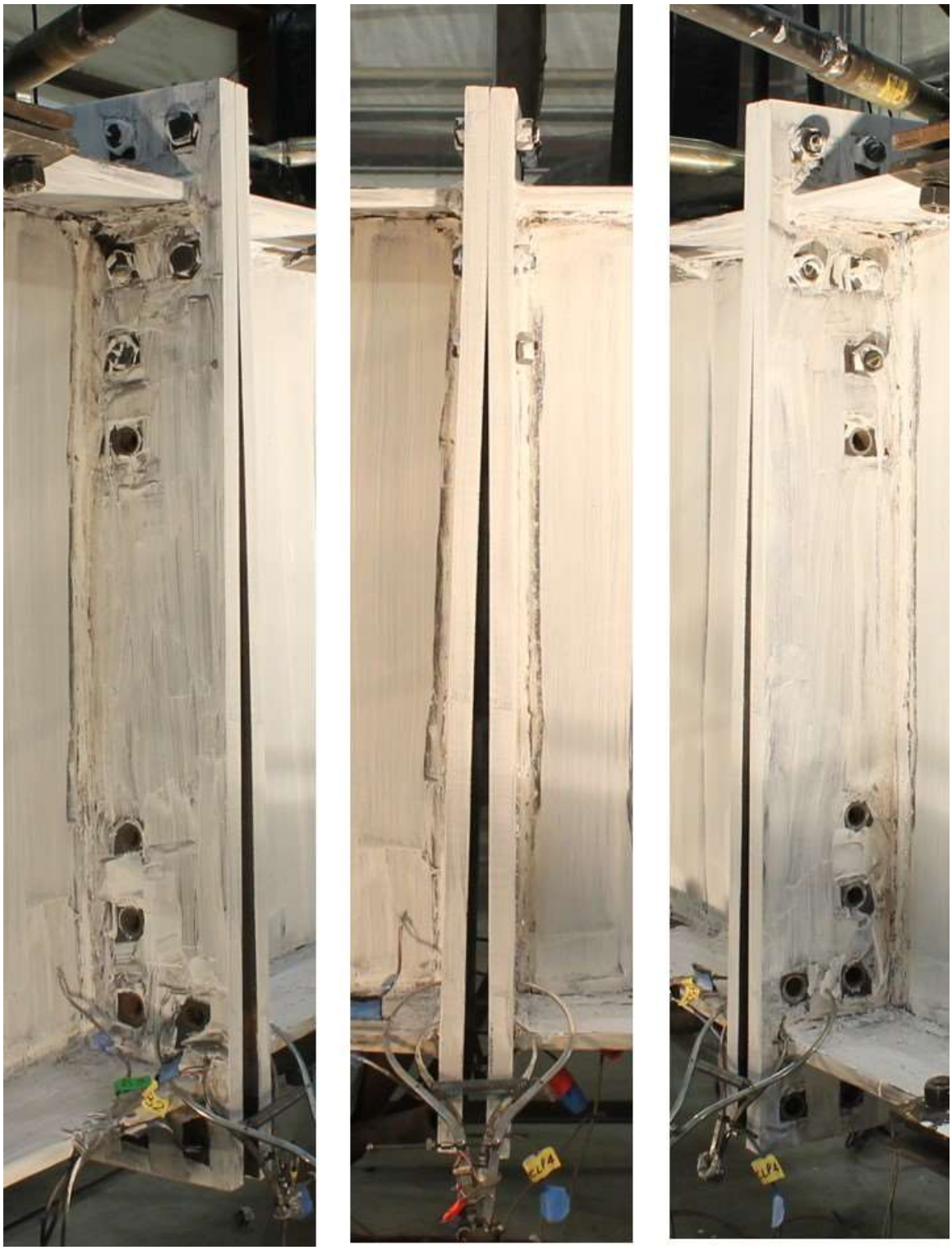

Figure 6-30 Three views of the specimen 12B-MRE 1/3-4W/2W-0.75-1.00-36 at the end of the test

6.2.3 **Deep Section - Thin Plate Behavior**

Specimen 12B-MRE 1/3-4W/2W-1.00-0.75-60 had a higher moment carrying capacity for this type of configuration, it could be considered as a deep section (depth = 60 in.) designed to exhibit thin end-plate behavior.

6.2.3.1 Limit State – Predictions and Progression

Equations presented in Chapter 3 calculate a moment capacity at bolt rupture without prying action (M_{np}), moment capacity for end-plate yielding (M_{pl}) and moment capacity at bolt rupture with prying action (M_q) of 4000 k-ft, 1980 k-ft and 2450 k-ft, respectively.

For thin plate behavior, the expected limit state progression is end-plate yielding at a moment equal to M_{pl} and then bolt rupture with prying action at a moment equal to M_q. The specimen was designed accordingly, but the test had to be stopped prior to bolt rupture. This was due to lateral torsional buckling for which the lateral bracing was insufficient to restrain, and this is shown in Figure 6-31. Therefore, when it reached this stage, it couldn't take any more load and the test had to be stopped, because the thick end-plate side was yet to be tested (it would have damaged the specimen and whole section would have been torqued, had the test been continued). Also, after unloading the specimen for the first time, another brace was added on to the specimen, and then loading continued. This is shown in the Figure 6-32. End-plate yielding was observed and is shown in Figure 6-38.

6.2.3.2 Experimental Results - Yield and Ultimate Moments

A yield moment, M_y (Figure 6-33 and Figure 6-34) of 2230 k-ft was experimentally obtained but the ultimate moment, M_u was not observed. The maximum applied moment was 2760 k-ft. They are demonstrated graphically and compared with the predicted values in the Figure 6-32.

Figure 6-31 Twisting of the Specimen Viewed from the two ends of the specimen

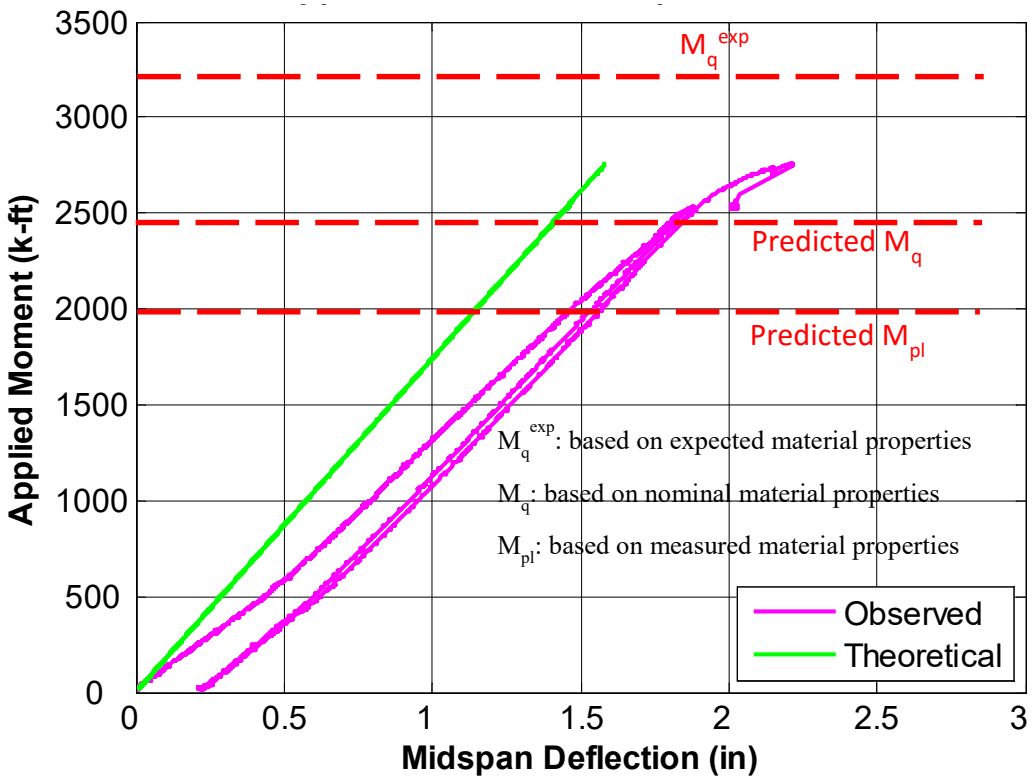

Figure 6-32 Applied Moment vs Midspan deflection for Specimen 12B-MRE 1/3-4W/2W-1.00-0.75-60

The ratio M_{pl}/M_y in Table 6-8 is conservative (less than 1.0) and the predicted, M_{pl}, is within 11% of the observed, M_y. Also, the ratio M_q/M_u in Table 6-8 is even more conservative. This is most probably due to the correction not applied to the bolt tensile strength. M_q has been predicted on the basis of a nominal tensile strength of 90 ksi for A325 bolts whereas they have been observed to show about a 25% higher strength than the specified minimum tensile strength (120 ksi in this case) in certified material test reports. (Table 5-3). M_q^{exp} was calculated to be 17% more (unconservative) than the observed ultimate maximum moment. It is to be noted that bolt rupture was not observed.

Table 6-8 Predicted and Experimentally Obtained Moment Capacities for Specimen 12B-MRE 1/3-4W/2W-1.00-0.75-60

Predicted (k-ft)			Experimental (k-ft)		Ratio		
M_{pl}	M_q	M_q^{exp}	M_y	M_u^1	M_{pl}/M_y	M_q/M_u^1	M_q^{exp}/M_u^1
1980	2450	3220	2230	2760	0.89	0.89	1.17

Note: M_u^1: Bolt rupture not observed at this moment and this was maximum moment before the section started twisting.

M_{pl}: Calculated based on measured material properties (tensile coupon tests)

M_q: Calculated based on nominal material properties

M_q^{exp}: Calculated based on expected material properties (bolt supplier's test report or assumption)

6.2.3.3 Experimental Results - End-Plate Separation

Figure 6-33 and Figure 6-34 display the end-plate separation in relation to the moment at the mid-span of the specimen. No significant conclusion can be drawn from the plots, since the end plate separation was about 0.1 in. Hence, it can't be said from the plots that the behavior was of a thin end-plate, but some end-plate yielding was seen and is shown in Figure 6-38.

6.2.3.4 Experimental Results - Bolt Forces

As shown in Figure 6-35 and Figure 6-36, the bolt forces, especially in B1 and B5, increased drastically past the observed end-plate yielding moment, which is 2230 k-ft. This indicates the presence of prying forces in these rows of the bolts, as a result of thin end-plate behavior.

6.2.3.5 Experimental Results - Pictures of Specimen

Figure 6-37 and Figure 6-38 show the difference in the specimen at the start and the end of the test. From the pictures it is clear that there was some end-plate yielding. Since the specimen couldn't be taken to bolt rupture, therefore not all the yield lines were observed. Only a horizontal yield line was seen in the row just inside of the flange, which is generally the first yield line to develop.

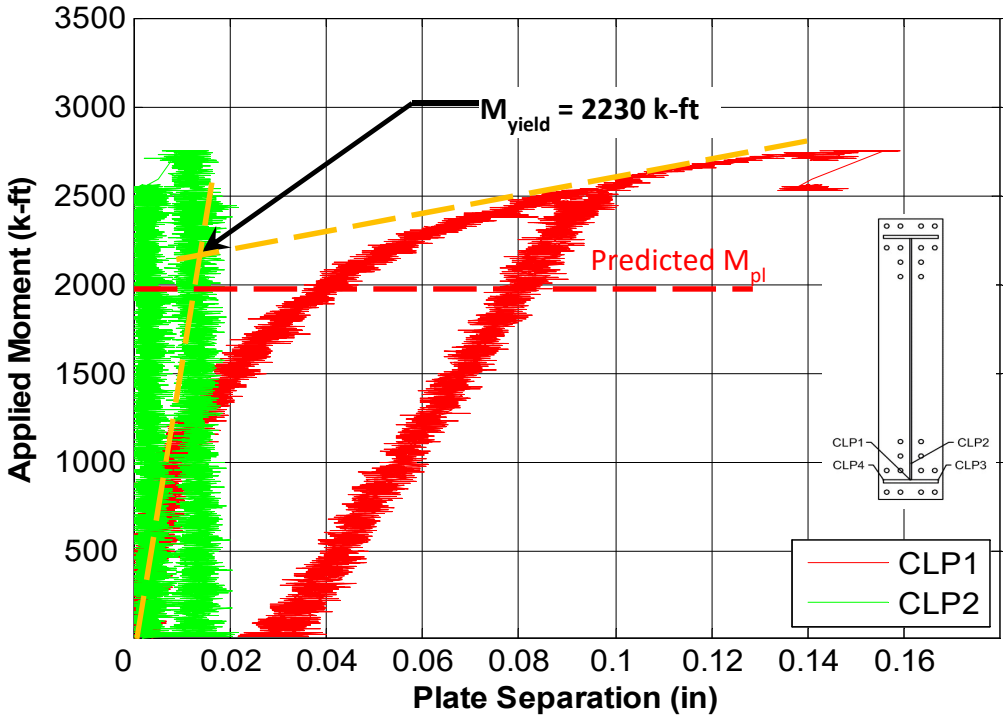

Figure 6-33 End-plate separation for Specimen 12B-MRE 1/3-4W/2W-1.00-0.75-60 (Caliper 1 and 2)

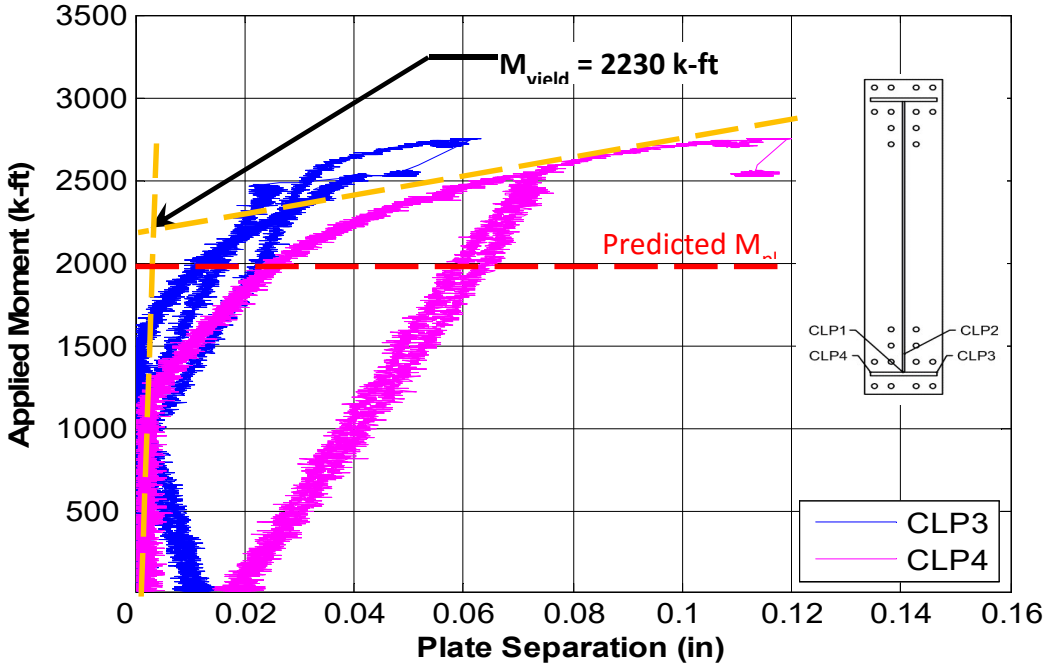

Figure 6-34 End-plate separation for Specimen 12B-MRE 1/3-4W/2W-1.00-0.75-60 (Caliper 3 and 4)

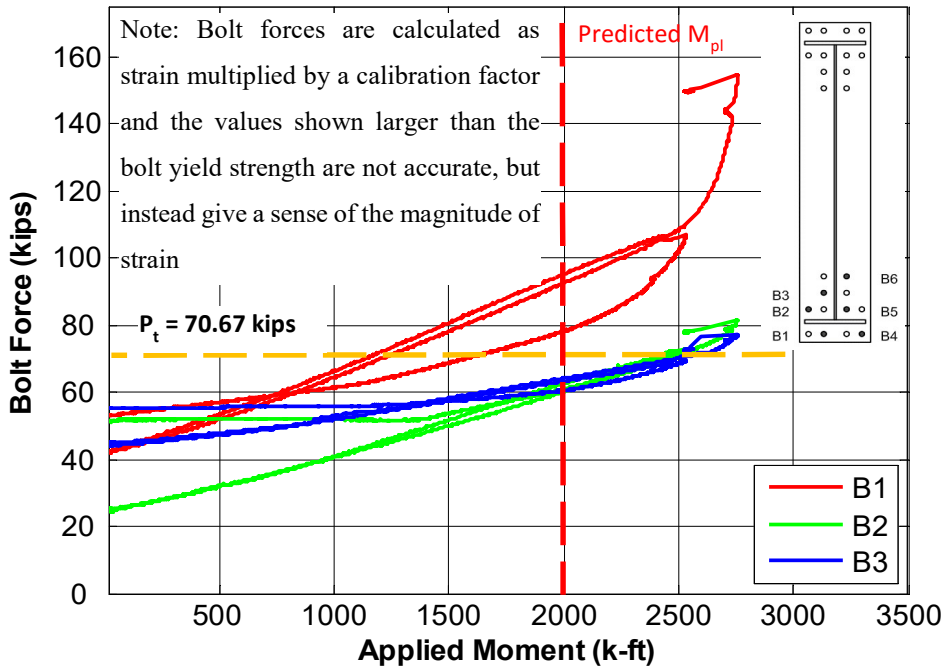

Figure 6-35 Bolt Forces for specimen 12B-MRE 1/3-4W/2W-1.00-0.75-60 (Bolt 1, 2 and 3)

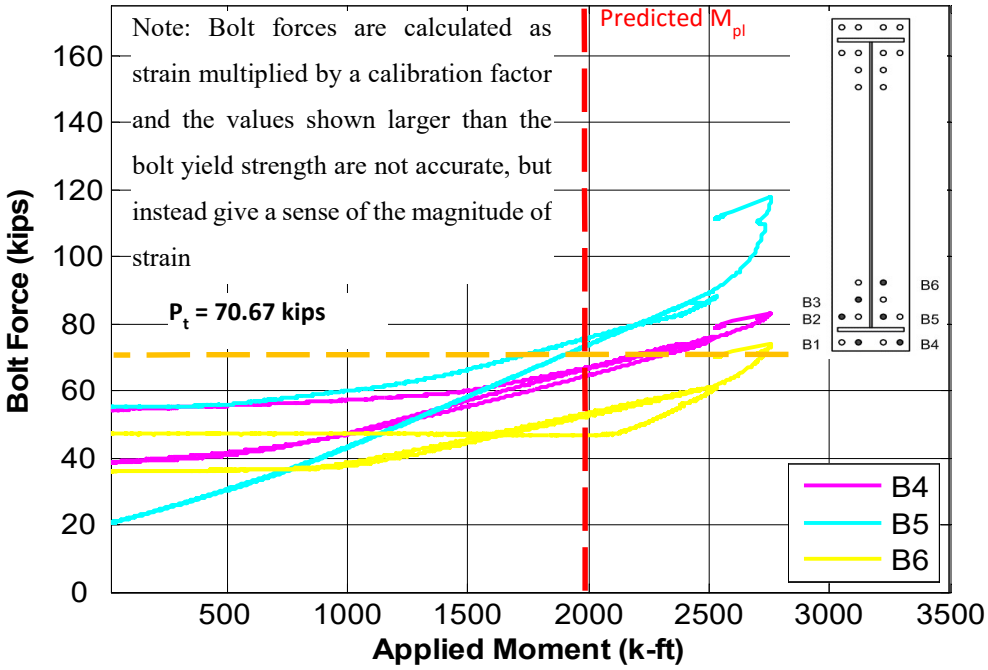

Figure 6-36 Bolt Forces for specimen 12B-MRE 1/3-4W/2W-1.00-0.75-60 (Bolt 4, 5 and 6)

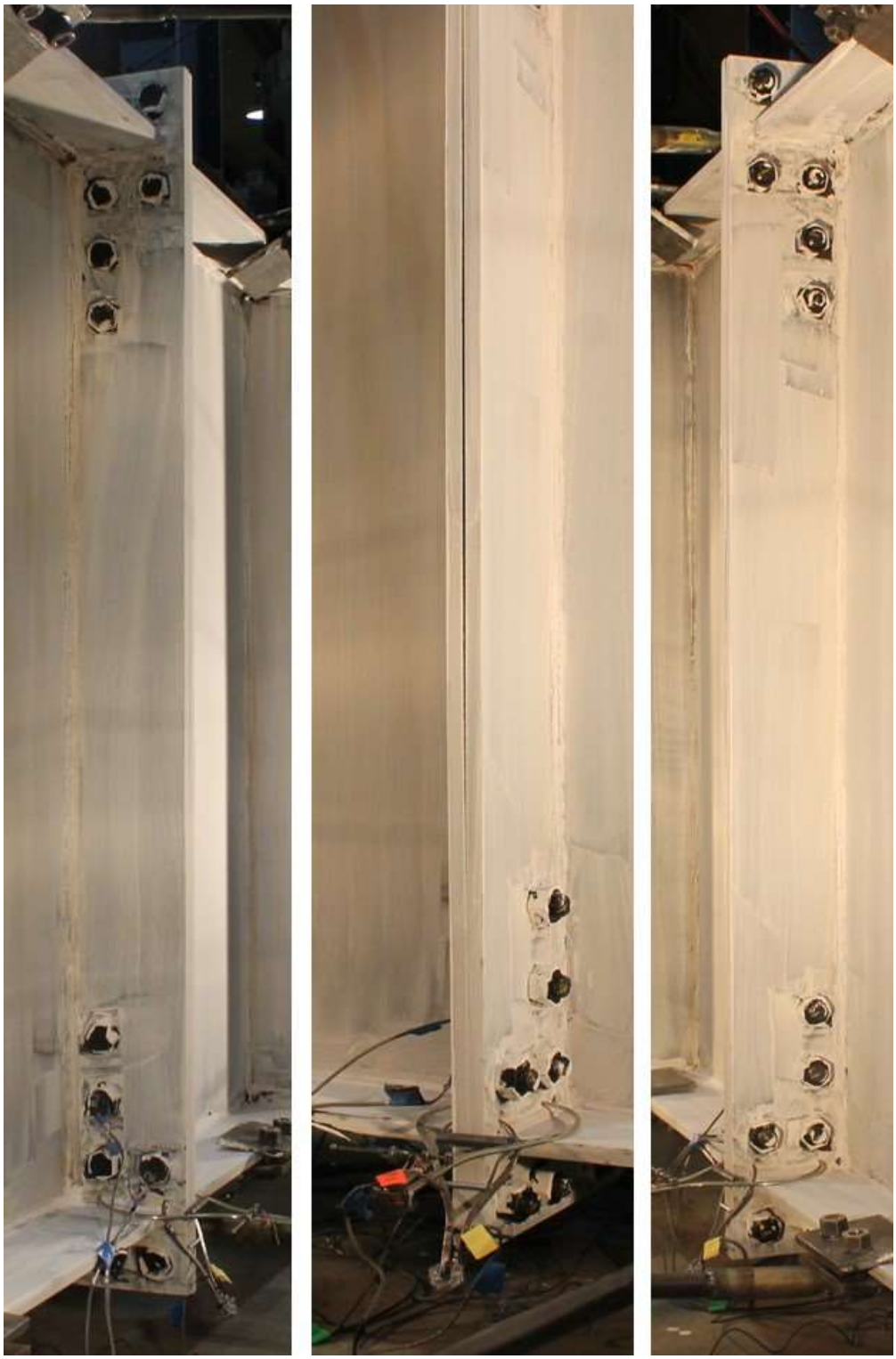

Figure 6-37 Three views of the Specimen 12B-MRE 1/3-4W/2W-1.00-0.75-60 at the start of the test

Figure 6-38 Three views of the specimen 12B-MRE 1/3-4W/2W-1.00-0.75-60 and zoomed in views of the connection to show any yield lines, at the end of the test

6.2.4 **Deep Section - Thick Plate Behavior**

Specimen 12B-MRE 1/3-4W/2W-0.75-1.00-60 was a 60 in. deep section designed to exhibit thick end-plate behavior.

6.2.4.1 Limit State – Predictions and Progression

The predictions for moment capacity at bolt rupture without prying action (M_{np}) and moment capacity for end-plate yielding (M_{pl}) were 2250 k-ft and 3830 k-ft, respectively. The values for M_{pl} and M_{np} are based on the discussion in Chapter 3.

For thick plate behavior, the expected limit state of progression is bolt rupture without prying action at a moment equal to M_{np}, without any end-plate plate yielding. The specimen behaved as expected. During the actual test, bolt rupture without prying action, M_{np}, controlled the strength of the connection. Twelve bolts on the tension side and two bottom bolts on the compression side of the connection, ruptured at once and no end-plate yielding was observed (shown in Figure 6-43).

6.2.4.2 Experimental Results - Yield and Ultimate Moments

A yield moment, M_y (Figure 6-40) of 2100 k-ft and an ultimate moment, M_u of 2490 k-ft were experimentally obtained. They are demonstrated graphically and compared with the predicted value, M_{np}, in the Figure 6-39.

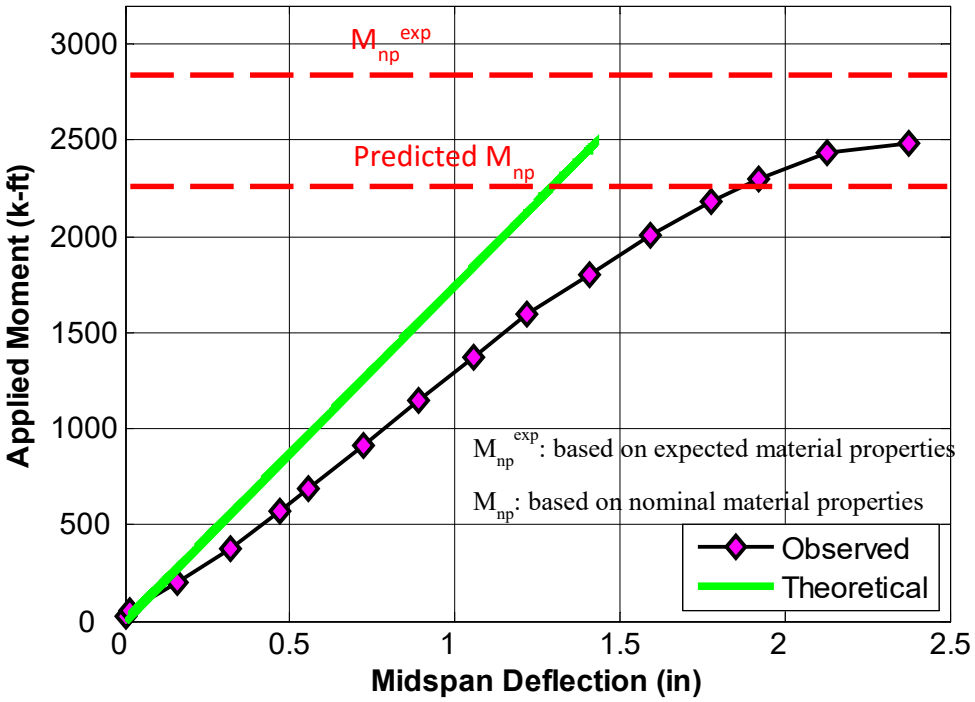

Figure 6-39 Applied Moment vs Midspan deflection for Specimen 12B-MRE 1/3-4W/2W-0.75-1.00-60

The ratio M_{np}/M_u in Table 6-9 is conservative (less than 1.0). This is likely due to the correction not applied to the bolt yield strength. M_{np}^{exp} was 13% more (unconservative) than the observed ultimate moment. Since, end-plate yielding was not observed, the ratio M_{pl}/M_y has been left blank.

Table 6-9 Predicted and Experimentally Obtained Moment Capacities for Specimen 12B-MRE 1/3-4W/2W-0.75-1.00-60

Predicted (k-ft)			Experimental (k-ft)		Ratio		
M_{pl}	M_{np}	M_{np}^{exp}	M_y	M_u	M_{pl}/M_y	M_{np}/M_u	M_{np}^{exp}/M_u
3830	2250	2820	2100	2490	-	0.90	1.13

Note: M_{pl}: Calculated based on measured material properties (tensile coupon tests)

M_{np}: Calculated based on nominal material properties

M_{np}^{exp}: Calculated based on expected material properties (bolt supplier's test report or assumption)

6.2.4.3 Experimental Results - End-Plate Separation

Figure 6-40 displays the end-plate separation in relation to the moment at the mid-span of the specimen.

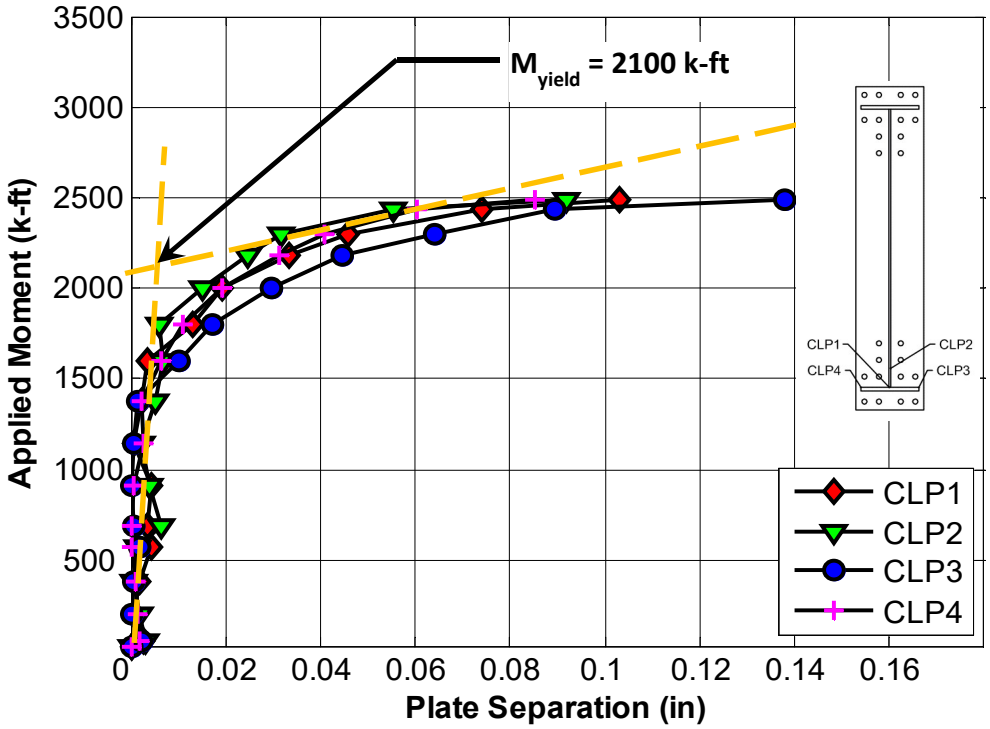

Figure 6-40 End-plate separation for Specimen 12B-MRE 1/3-4W/2W-0.75-1.00-60.

Since the end-plate separation in Figure 6-40 is negligible, it can be deduced that the there was no yielding of the end-plate. Also, the pictures shown in Figure 6-43, prove that there was no yielding in the plates and hence, the behavior was of a thick plate.

6.2.4.4 Experimental Results - Bolt Forces

As shown in Figure 6-41, the bolt forces, except for B1, remained linear well until the nominal tensile strength of the bolt. Even after that, except for B4, all the other bolts were fairly linear for most of the time. This is in line with thick plate behavior.

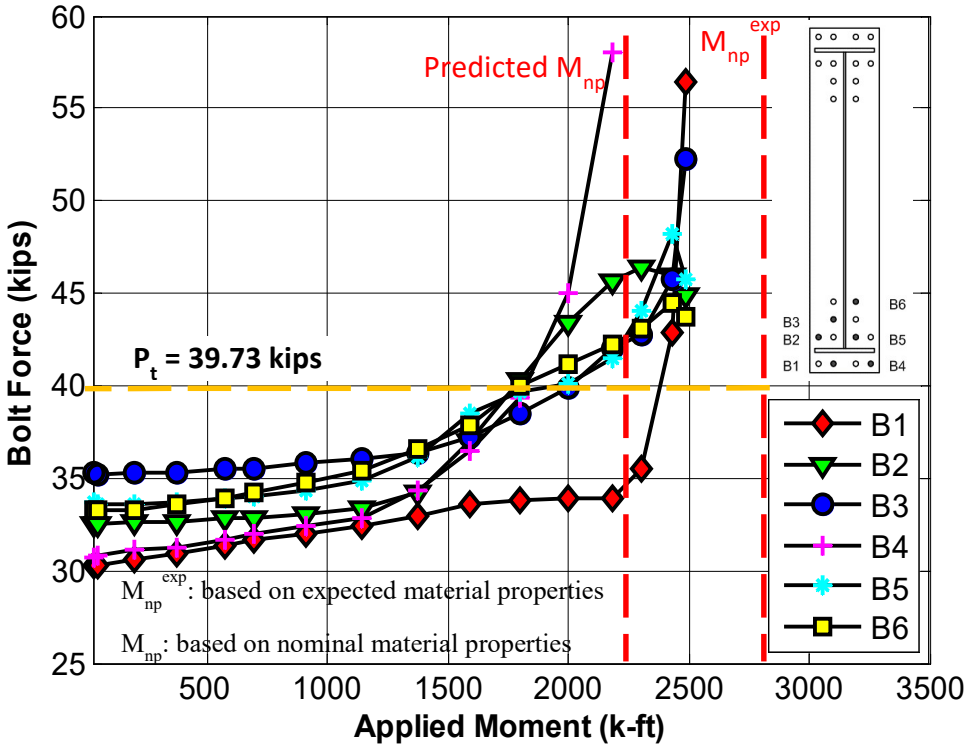

Note: Bolt forces are calculated as strain multiplied by a calibration factor and the values shown larger than the bolt yield strength are not accurate, but instead give a sense of the magnitude of strain

Figure 6-41 Bolt Forces for specimen 12B-MRE 1/3-4W/2W-0.75-1.00-60

6.2.4.5 Experimental Results - Pictures of Specimen

Figure 6-42 and Figure 6-43 show the difference in the specimen at the start and the end of the test. From the pictures it is clear that no yield lines, whatsoever, were seen. Also, no distortion was seen in the profile of the end-plates when seen from the side (center picture in Figure 6-43). This validates that the specimen had the behavior of a thick plate.

Figure 6-42 Three views of the Specimen 12B-MRE 1/3-4W/2W-0.75-1.00-60 at the start of the test

Figure 6-43 Three views of the specimen 12B-MRE 1/3-4W/2W-0.75-1.00-60 at the end of the test

6.2.5 Overall Summary of the Twelve Bolt Extended Unstiffened Configuration and Recommendations

Table 6-10 summarizes the four specimens investigated herein. Both the thin plate specimens could not be taken to bolt rupture, but the thick end-plate behaved as expected. Little yielding was seen in the thin plate specimens and the tests had to be discontinued after that.

Table 6-10 Summary of the Four Test Specimens of the Twelve Bolt Extended Unstiffened Configuration

Specimen Identification[1]	Depth (in.)	Behavior	Remarks[2]
12B-MRE 1/3-4W/2W-1.00-0.75-36	36	Thin	M_{pl} was -8% of yield moment. Predicted M_q -13% of the maximum applied moment. M_q^{exp} was +14% of the maximum applied moment. End-plate yielding observed. None of the bolts ruptured.
12B-MRE 1/3-4W/2W-0.75-1.00-36	36	Thick	M_{np} was -13% of the observed M_u. M_{np}^{exp} was +9% of M_u. No end-plate yielding seen
12B-MRE 1/3-4W/2W-1.00-0.75-60	60	Thin	Predicted M_{pl} -11% of the experimental yield moment, M_y. Predicted M_q was -11% of the observed M_u. M_q^{exp} was +17% of M_u. Some End-plate yielding observed. No bolts were ruptured.
12B-MRE 1/3-4W/2W-0.75-1.00-60	60	Thick	M_{np} -10% of the observed M_u. M_{np}^{exp} was +9% of M_u. No end-plate yielding observed.

[1]Specimen Identification: "No. of bolts in the connection - Multiple Row Extended with one bolt row outside the flange and three bolt rows inside the flange – No. of bolts in a row - Bolt diameter - End-plate thickness - Beam depth".

[2]Remarks: A postive percentage means an unconservative calculation, whereas a negative percentage means a safe prediction.

For the two thin plate tests, M_{pl} was either 8% less (conservative) than the experimental yield moment (for shallow beam) or 11% less (safe) than the experimental yield moment (for deep beam). M_q was 13% and 11% less (safe) than the observed M_u for shallow and deep beam, respectively. M_q^{exp} was 14% and 17% more (unconservative) than the observed M_u for shallow and deep beam, respectively. Furthermore, for shallow specimen, experimentally measured end-plate separation was found to be consistent with thin end-plate behavior wherein end-plate yielding allows end-plate separation prior to bolt fracture. Since, it is evident from Figure 6-22, that there was significant amount of end-plate yielding, it can further be hypothesized that the bolts were close to rupture.

For thin plate specimens, even though none of the specimens could be taken to bolt rupture, it was observed that the predicted M_q was at least 11% less than the maximum applied moment. Also, M_q^{exp} was at least 13% more than maximum applied moment. The predictions for M_q and M_q^{exp} could be considered to be the lower and upper bound respectively and it could be safely assumed that the actual moment at which the bolts would have ruptured, would lie somewhere between these two values. The procedures for end-plate yielding are validated and in light of the above discussion, the bolt force models for thin plate behavior for this configuration also appear to be correct.

For thick plate tests, the behavior of the two specimens was quite as expected. No end-plate yielding was seen. M_{np} was 13% and 10% less (safe) than the observed M_u for shallow and deep beam, respectively. M_{np}^{exp} was 9% and 13% more (unsafe) than the observed M_u for shallow and deep beam, respectively. The experimental moment capacity of the connection for both the cases was found to lie between the predicted moment capacity based on nominal material properties and the moment capacity of the connection based on expected material properties. Considering the former as the lower bound and the latter as the upper bound, it appears that the bolt force model for thick plate behavior appears to be reasonable.

6.3 Testing on the Eight Bolt Extended Stiffened (8ES) Configuration

6.3.1 **Deep Section - Thin Plate Behavior**

Specimen 8ES-1.25-0.75-56 was a 56 in. deep section designed to exhibit thin end-plate behavior. It is to be noted that for each bolt, one ASTM Grade F436 washer was used on the nut side. This was done because the grip length of the bolt was about 0.1 in. longer than the combined thickness (1.5 in) of the two end plates being connected.

6.3.1.1 Limit State – Predictions and Progression

The predictions for moment capacity at bolt rupture without prying action (M_{np}), moment capacity for end-plate yielding (M_{pl}) and moment capacity at bolt rupture with prying action (M_q) were 4110 k-ft, 2300 k-ft and 2650 k-ft, respectively. The values for M_{pl}, M_{np} and M_q based on discussion in Chapter 3.

For thin plate behavior, the expected limit state progression is end-plate yielding at a moment equal to M_{pl} and then bolt rupture with prying action at a moment equal to M_q. The test had to be stopped prior to bolt rupture. This was due to lateral torsional buckling for which the lateral bracing was insufficient to restrain, and this is shown in Figure 6-44. Therefore, when it reached this stage, it couldn't take any more load and the test had to be stopped. End-plate yielding was observed and is shown in Figure 6-49.

6.3.1.2 Experimental Results - Yield and Ultimate Moments

A yield moment, M_y, (Figure 6-46) of 2400 k-ft was experimentally obtained but the ultimate moment, M_u, was not observed. The maximum applied moment was 2920 k-ft. They are demonstrated graphically and compared with the predicted values in the Figure 6-45. It is to be noted that the test was stopped before the bolts could be ruptured.

The ratio M_{pl}/M_y in Table 6-11 is conservative and the predicted, M_{pl}, is within 4% of the observed, M_y. Also, the ratio M_q/M_u in Table 6-11 is a little more conservative. This is most probably due to the correction not applied to the bolt yield strength. M_q has been predicted on the basis of a nominal tensile strength of 90 ksi for A325 bolts whereas they

have been observed to show about a 25% higher strength than the specified minimum tensile strength (105 ksi in this case) in the bolt material test reports (Table 5-3). M_q^{exp} was found to be within 1% of the maximum applied moment.

Figure 6-44 Twisting of the Specimen Viewed from one end of the specimen

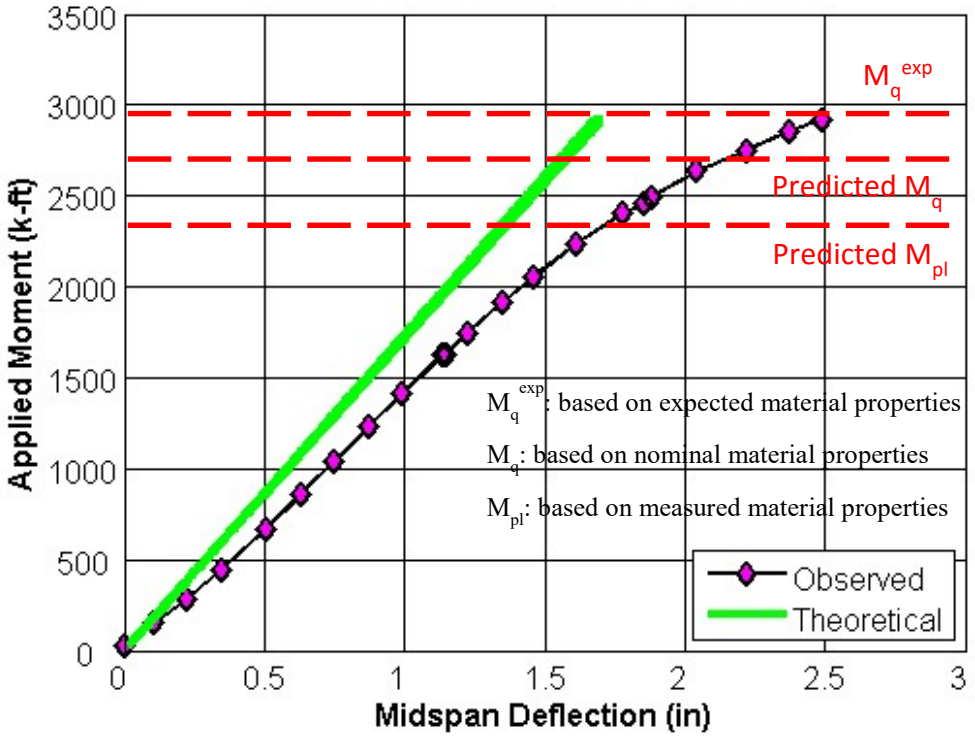

Figure 6-45 Applied Moment vs Midspan deflection for Specimen 8ES-1.25-0.75-56

Table 6-11 Predicted and Experimentally Obtained Moment Capacities for Specimen 8ES-1.25-0.75-56

Predicted (k-ft)			Experimental (k-ft)		Ratio		
M_{pl}	M_q	M_q^{exp}	M_y	M_u^1	M_{pl}/M_y	M_q/M_u^1	M_q^{exp}/M_u^1
2300	2650	2960	2400	2920	0.96	0.91	1.01

Note: M_u^1: Bolt rupture not observed at this moment and this was maximum moment before the section started twisting.

M_{pl}: Calculated based on measured material properties (tensile coupon tests)

M_q: Calculated based on nominal material properties

M_q^{exp}: Calculated based on expected material properties (bolt supplier's test report or assumption)

6.3.1.3 Experimental Results - End-Plate Separation

Figure 6-46 displays the end-plate separation in relation to the moment at the mid-span of the specimen.

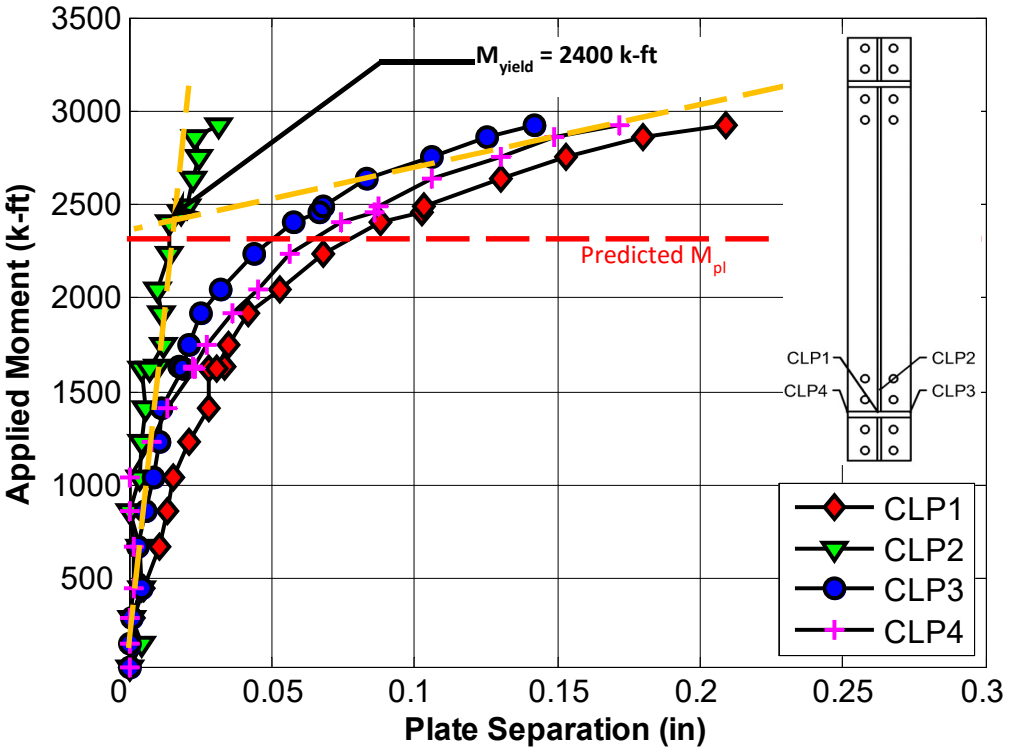

Figure 6-46 End-plate separation for Specimen 8ES-1.25-0.75-56

Significant end-plate separation was seen before the test was stopped. Hence, it can be said from the plots that the behavior was of a thin end-plate. With thick plate behavior, end-plate separation would be much smaller because the plate would not yield.

6.3.1.4 Experimental Results - Bolt Forces

As is shown in Figure 6-47, the bolt forces increased exponentially past the observed end-plate yielding moment, which is 2400 k-ft. This indicates the presence of prying forces in these rows of the bolts, as a result of thin end-plate behavior.

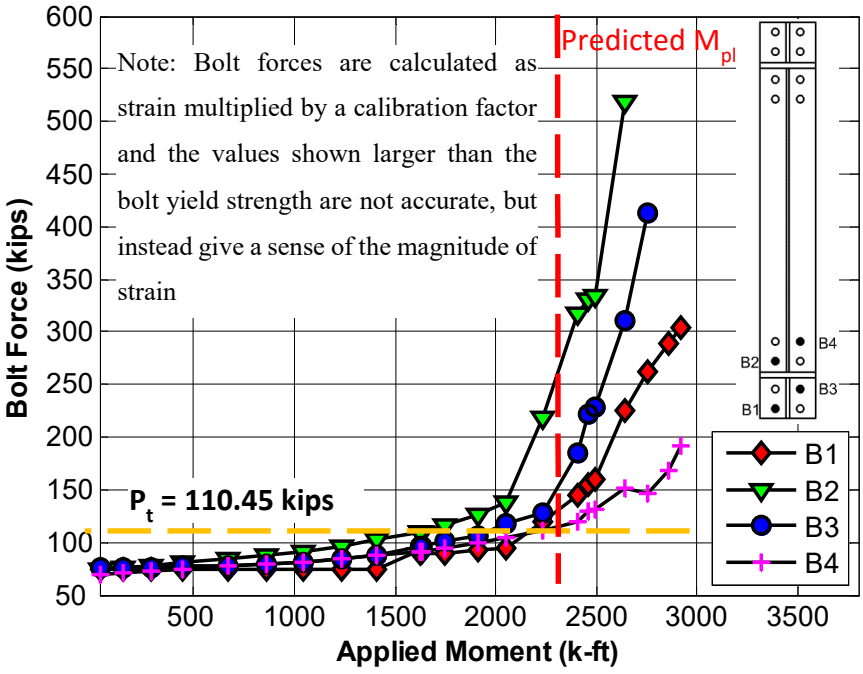

Figure 6-47 Bolt Forces for specimen 8ES-1.25-0.75-56

6.3.1.5 Experimental Results - Pictures of Specimen

Figure 6-48 and Figure 6-49 show the difference in the specimen at the start and the end of the test. From the pictures it is clear that there was end-plate yielding. White wash spalling was seen in in the top three horizontal bolt rows and also, along the vertical direction on both sides of the web. Also, when viewed from the side, end-plate distortion was seen, which further corroborates the yielding of end-plate.

Figure 6-48 Three views of the Specimen 8ES-1.25-0.75-56 at the start of the test

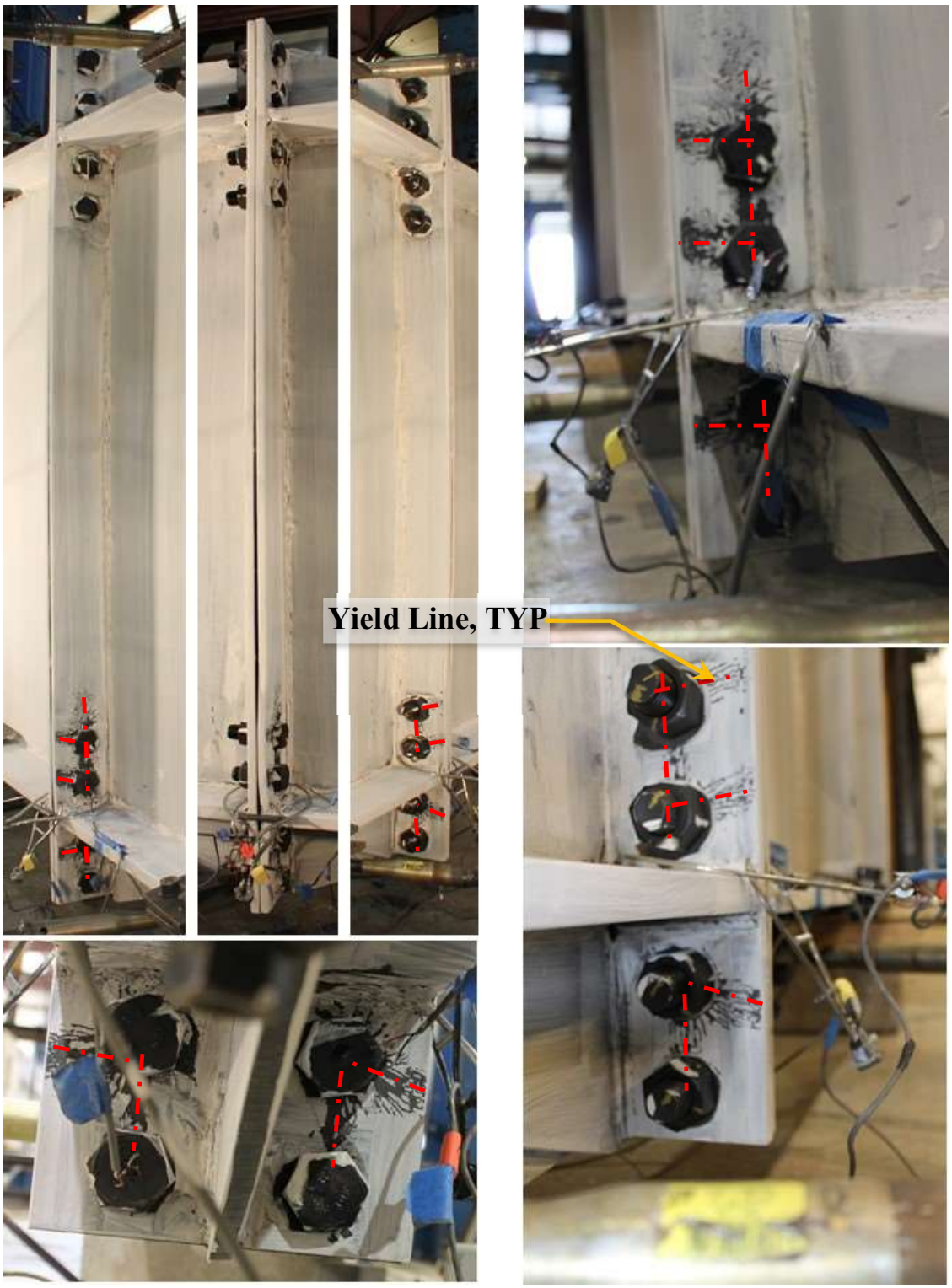

Figure 6-49 Three views of the specimen 8ES-1.25-0.75-56 and zoomed in views of the connection to show any yield lines, at the end of the test

6.3.2 **Deep Section - Thick Plate Behavior**

Specimen 8ES-1.00-1.00-56 was a 56 in. deep section designed to exhibit thick end-plate behavior.

6.3.2.1 Limit State – Predictions and Progression

Equations presented in Chapter 3 calculate a moment capacity at bolt rupture without prying action (M_{np}) and moment capacity for end-plate yielding (M_{pl}) of 2630 k-ft and 4160 k-ft, respectively.

For thick plate behavior, the expected limit state of progression is bolt rupture without prying action at a moment equal to M_{np}, without any end-plate plate yielding. The specimen behaved as expected. During the actual test, bolt rupture without prying action, M_{np}, controlled the strength of the connection. All eight bolts on the tension side, ruptured at once and marginal spalling of white wash was seen around the bolts (shown in Figure 6-54).

6.3.2.2 Experimental Results - Yield and Ultimate Moments

A yield moment, M_y (Figure 6-51) of 2520 k-ft and an ultimate moment, M_u of 3050 k-ft were experimentally obtained. They are demonstrated graphically and compared with the predicted value, M_{np}, in the Figure 6-50.

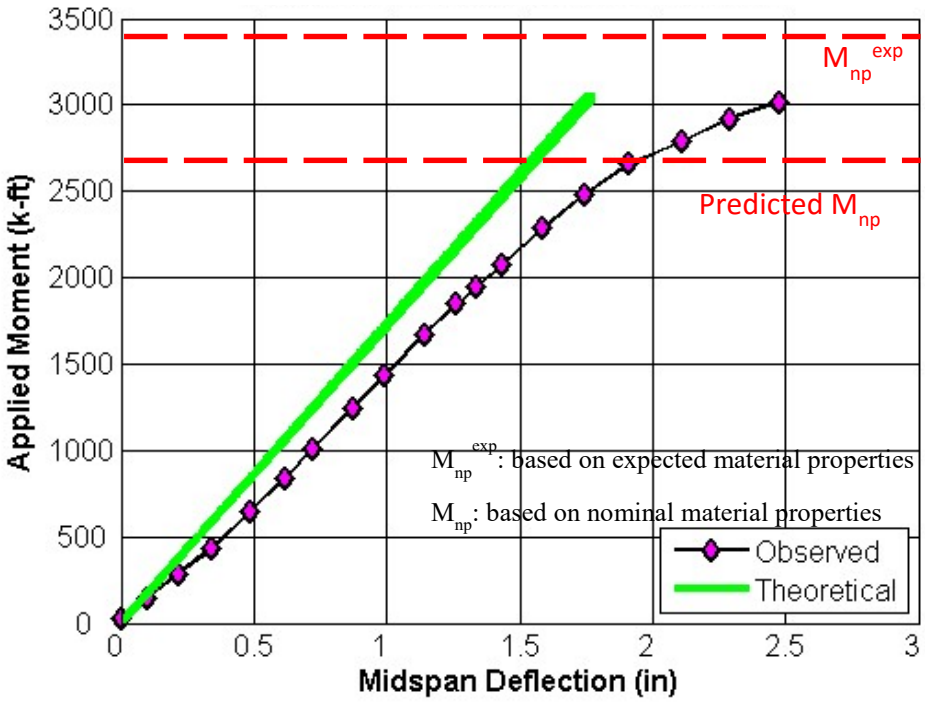

Figure 6-50 Applied Moment vs Midspan deflection for Specimen 8ES-1.00-1.00-56

The ratio M_{np}/M_u in Table 6-12 is conservative (less than 1.0). This is likely due to the correction not applied to the bolt yield strength. M_q has been predicted on the basis of a nominal tensile strength of 90 ksi for A325 bolts whereas they have been observed to show about a 25% higher strength than the specified minimum tensile strength (120 ksi) in the bolt material test reports (Table 5-3). M_{np}^{exp} was unconservative by 12%. Since, end-plate yielding was not observed, the ratio M_{pl}/M_y has been left blank.

Table 6-12 Predicted and Experimentally Obtained Moment Capacities for Specimen 8ES-1.00-1.00-56

Predicted (k-ft)			Experimental (k-ft)		Ratio		
M_{pl}	M_{np}	M_{np}^{exp}	M_y	M_u	M_{pl}/M_y	M_{np}/M_u	M_{np}^{exp}/M_u
4160	2630	3420	2520	3050	-	0.86	1.12

Note: M_{pl}: Calculated based on measured material properties (tensile coupon tests)

M_{np}: Calculated based on nominal material properties

M_{np}^{exp}: Calculated based on expected material properties (bolt supplier's test report or assumption)

6.3.2.3 Experimental Results - End-Plate Separation

Figure 6-51 displays the end-plate separation in relation to the moment at the mid-span of the specimen.

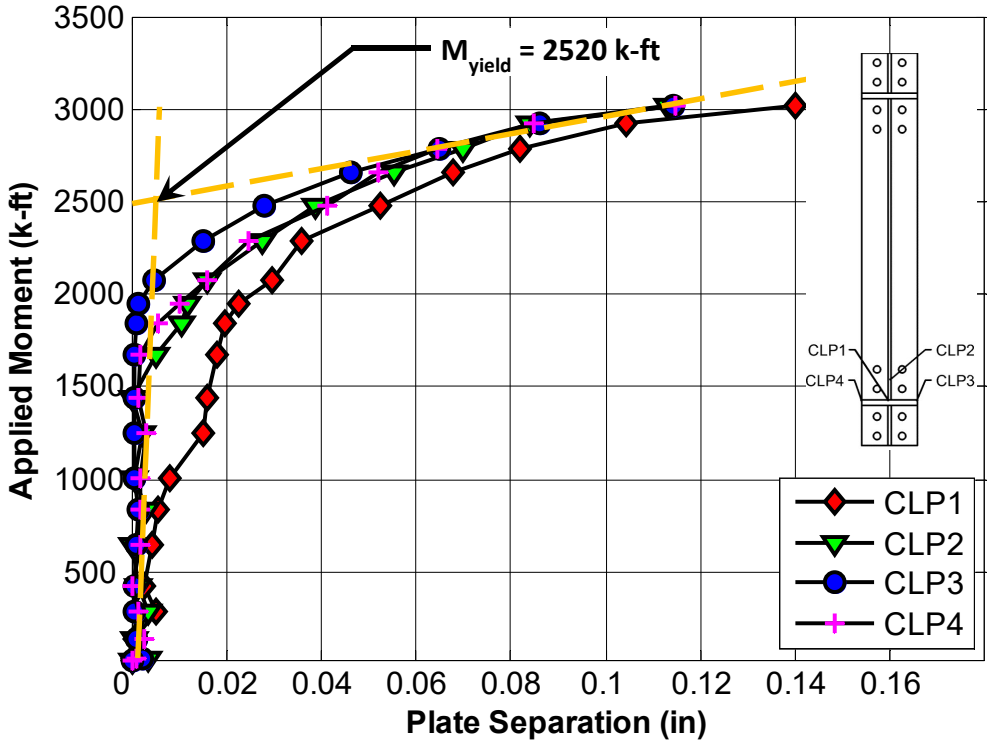

Figure 6-51 End-plate separation for Specimen 8ES-1.00-1.00-56.

Since the end-plate separation in Figure 6-51 is about 0.14 in., it can be deduced that the there was no yielding of the end-plate. Also, the pictures shown in Figure 6-54, prove that there was no yielding in the plates and hence, the behavior was of a thick plate.

6.3.2.4 Experimental Results - Bolt Forces

As shown in Figure 6-52, the bolt forces were fairly linear for most of the time with the bolt forces shooting up towards the end, but there was exponential increase particularly for bolt B1 towards the end. Also, the bolt B4 had maxed out because of a wrong signal input range. From the plot it seems that there may have been some prying forces in the bolts.

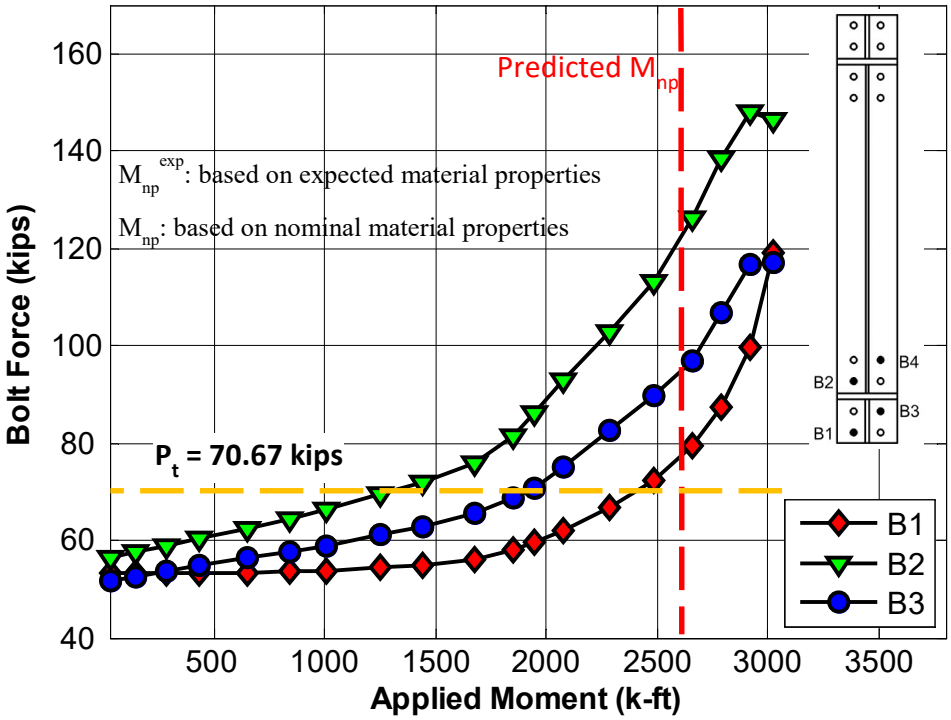

Note: Bolt forces are calculated as strain multiplied by a calibration factor and the values shown larger than the bolt yield strength are not accurate, but instead give a sense of the magnitude of strain

Figure 6-52 Bolt Forces for specimen 8ES-1.00-1.00-56

6.3.2.5 Experimental Results - Pictures of Specimen

Figure 6-53 and Figure 6-54 show the difference in the specimen at the start and the end of the test. From the pictures it is clear that was some local yielding around the bolts. But overall there was minimal yielding. Also, no distortion was seen in the profile of the end-plates when seen from the side (top center picture in Figure 6-54). This validates that the specimen had the behavior of a thick plate.

Figure 6-53 Three views of the Specimen 8ES-1.00-1.00-56 at the start of the test

Figure 6-54 Three views of the specimen 8ES-1.00-1.00-56 and zoomed in views to show local yielding around the bolts, at the end of the test

6.3.3 Overall Summary of the Eight Bolt Extended Configuration and Recommendations

Table 6-13 summarizes the two specimens investigated herein. The thin plate specimen could not be taken to bolt rupture, but the thick end-plate behaved as expected. End-plate yielding was clearly seen in the thin plate specimen, but the test had to be stopped prior to bolt failure. Also, the predicted bolt rupture moment (with or without prying), M_{np} and M_q, was always lower than the maximum applied moment, M_u. Predicted M_{np} was within 14% of the observed ultimate moment, M_u and predicted M_q was within 9% of the observed maximum moment, even though the bolts were not ruptured. This conservative prediction was due to the unaccounted over-strength of about 25% in the bolts. To take his into account, M_{np}^{exp} and M_q^{exp} were computed and they were found out to be 12% more and 1% more (unconservative) than the maximum applied moment, respectively. The predicted yield moment for thin end-plate behavior conservative by 4% (of the observed yield moment), which is close enough to validate the equations for M_{pl}.

Table 6-13 Summary of the Two Test Specimens of the Eight Bolt Extended Unstiffened Configuration

Specimen Identification[1]	Depth (in.)	Behavior	Remarks[2]
8ES-1.25-0.75-56	56	Thin	Predicted M_{pl} -4% of the observed yield moment, M_y. Predicted M_q was -9% of the maximum applied moment. M_q^{exp} was +1% of the maximum applied moment. End-plate yielding observed. No bolts were ruptured.
8ES-1.00-1.00-56	56	Thick	M_{np} -14% of the observed M_u. M_{np}^{exp} was +12% of M_u. Minimal end-plate yielding observed.

[1]Specimen Identification: "No. of bolts in the connection - Bolt diameter - End-plate thickness - Beam depth".

[2]Remarks: A postive percentage means an unconservative calculation, whereas a negative percentage means a safe prediction.

It could be again argued that the bolt force model for a deep thick plate specimen could be validated if we consider the moment capacity based on nominal material properties, M_{np} to be the lower bound and the moment capacity based on expected material properties, M_{np}^{exp} to be the upper bound value.

For deep thin plate specimen, the design procedure for end plate yelding seems to be accurate since the predicted M_{pl} is conservative by just 4%. For, the case of M_q, even though the bolts didn't go to rupture, the predicted moment was less than by 9% of the experimentally attained maximum moment whereas M_q^{exp} was 1% more than the maximum applied moment.

7 SUMMARY AND CONCLUSIONS

7.1 Summary

7.1.1 **8E-4W Configuration**

A total of four tests from the literature (Sumner et. al 2000, Sumner and Murray 2001) were examined for this configuration (Section 4.1). These were chosen in such a way that the design procedures could be verified for shallower and deeper specimens with both thick and thin end-plate behavior for a range of different design parameters. It is to be noted that rolled sections (30 in. and 36 in. deep) were used for the shallow specimens whereas built-up sections (both 61.5 in. deep) were used for testing. For the two thick plate tests, the ratio M_{np}/M_u was always conservative (less than 1.0) having values of 0.94 and 0.88 for the shallow and deep beam respectively. For the two thin plate tests, M_{pl}/M_y was close to 1.0 (1.04 for shallow and 0.96 for deep). M_q/M_u was 1.05 for the shallow-thin specimen whereas the deep-thin specimen couldn't be taken to bolt rupture, but the moment at which the test was stopped was 89% of the calculated M_q.

7.1.2 **8ES Configuration**

A total of six tests, four from the literature (Ghassemieh 1983, Sumner et. al 2000) and two new tests, were examined for this configuration (Section 4.2 and 6.3).

The behavior of the four specimens from the literature was all quite different and the relationship between experimentally obtained end plate yield moment and predicted values varied. Although the predicted end plate yield moment capacity, M_{pl}, was within 5% of the experimental yield moment for Specimen 8ES-1.25-1-30 from Sumner et al. (2000), end plate yielding was observed in Specimen 8ES-1.25-1.25-36 at only 63% of the predicted moment, M_{pl}. Specimen 8ES-0.875-0.75-24 from Ghassemieh et al. (1983) produced a moment at the end of the test similar to the predicted M_q value, but Specimen 8ES-1.25-1-30 reached 110% of M_q before the test was stopped without bolt fracture. Specimen 8ES-1.25-1.25-36 experienced bolt rupture at a moment that was within 6% of

the predicted value, M_{np}, but it is unlikely that Specimen 8ES-0.875-1-24 would have reached the predicted M_{np} and was stopped at 88% of M_{np} after significant softening.

For the two new tests (56 in. deep), the thin plate specimen could not be taken to bolt rupture, but the thick end-plate specimen behaved as expected. End-plate yielding was clearly seen in the thin plate specimen, but the test had to be stopped prior to bolt failure. Also, the calculated moment at bolt rupture (with or without prying), M_{np} and M_q, was always lower than the maximum applied moment, M_u. Calculated M_{np} was within 14% of the observed ultimate moment, M_u and predicted M_q was within 9% of the observed maximum moment, even though the bolts were not ruptured. This conservative prediction was due to the unaccounted over-strength of about 25% in the bolts. M_{np}^{exp} almost matched the experimentally observed value whereas M_q^{exp} was 12% more than the maximum applied moment, even though bolts were not ruptured at this stage. The calculated moment capacity for end-plate yielding for thin end-plate behavior was conservative and was within 4% of the observed yield moment.

7.1.3 **6B-4W/2W Configuration**

A total of four new tests were done for this configuration (Section 6.1). The specimens were either a thin end-plate or a thick-end plate welded onto either a deeper (60 in. deep) or shallower (36 in. deep) beam. This was done so that the procedures could be validated for a range of end-plate depths. The behavior of the four specimens was quite as expected.

For thin plate specimens, the calculated moment capacity for end-plate yielding was either 6% lower (deep beam) or 2 % higher (shallow beam) than actual yield moment. Also, the calculated moment at bolt rupture with prying action, M_q, was always lower than the maximum applied moment, M_u. It varied from 13% to 14%, which was due to the unaccounted over-strength in the bolts. But M_q^{exp} was within 3% of the ultimate moment, M_u. Experimentally measured end-plate separation (0.22 in to 0.45 in.) was found to be consistent with thin end-plate behavior wherein end-plate yielding allows end-plate separation prior to bolt fracture. Also, clear yield lines were seen on the specimen.

For thick plate specimens, the expected limit state of progression is bolt rupture without prying action at a moment equal to M_{np}, without any end-plate plate yielding. Just the specimen 6B-4W/2W-0.875-1.00-36, exhibited a bit of end-plate yielding, but there was no distortion in the profile of the end-plate when viewed from side. Also, the calculated moment at bolt without prying, M_{np}, was always lower than the maximum applied moment, M_u. It varied from 13% to 17%, which was due to the unaccounted over-strength in the bolts. M_{np}^{exp} was 6% to 11% higher than M_u which was unconservative.

7.1.4 **12B-MRE 1/3-4W/2W Configuration**

A total of four new tests were done for this configuration (Section 6.2). The specimens were either a thin end-plate or a thick-end plate welded onto either a deeper (60 in. deep) or shallower (36 in. deep) beam. This was done so that the procedures could be validated for a range of end-plate depths.

Both the thin plate specimens could not be taken to bolt rupture. Little yielding was seen in the thin plate specimens and the tests had to be discontinued after that. Also, the calculated moment capacity at bolt rupture with prying, M_q, was always lower than the maximum applied moment, M_u. They varied from 13% for the shallow specimen to 11% and still, was not the maximum moment at which the bolts would go to rupture. This conservative prediction was due to the unaccounted over-strength of about 25% in the bolts. M_q^{exp}/M_u varied from 1.14 to 1.17 (none of the bolts were ruptured) which suggests that the values would be lesser had the bolts ruptured. The predicted yield moment for thin end-plate behavior was between 8% to 11% (both on a conservative side) of the actual yield moment.

Both the thick plate specimens were taken to bolt rupture and behaved as expected. M_{np} was always lower than M_u by at least 10%. But M_{np}^{exp}/M_u varied from 1.09 (shallow) to 1.13 (deep), which suggests that the design was unconservative.

7.2 Conclusions

7.2.1 **8E-4W Configuration**

The end-plate separation for all the tests was found to be consistent with their expected behavior. The key ratios were all approximately within 10% of the calculated values. The calculated M_{np} was conservative (less than M_u) for the thick plate specimens. Also, M_{pl}/M_y was within 4% whereas the M_q/M_u was a little non –conservative and was off by about 10%. Considering all these factors, it could be assumed that the proposed design procedures presented in Section 3.1 are validated.

7.2.2 **8ES Configuration**

For two thin plate specimens out of three, calculated moment capacity for end-plate yielding was within 5% of the observed capacity. Also, for two specimens, the calculated moment capacity at bolt rupture without prying action, M_q, was about 10% less than the maximum applied moment and still bolt rupture was not observed. This means that the calculations for M_q were conservative. But M_q^{exp} was 12% higher than M_u which goes on the unconservative side. It could be safely assumed that M_q^{exp} would be the upper bound and M_q would be the lower bound for the purpose of design calculations. End-plate yielding was clearly seen on the new specimen tested. Hence, the procedures proposed in Section 3.2 for thin plate behavior seem to be validated.

For thick plate behavior, the new deeper specimen behaved as expected. Minimal end-plate yielding was seen. M_{np} was less than (conservative) the observed moment capacity at bolt rupture without prying action by about 14%. M_{np}^{exp} had an accuracy of 99%. For 8ES-1.25-1.25-36, M_{np} was again on a conservative side by 6%. Hence, the design procedures for thick plate behavior for 8ES configuration appear to be validated.

7.2.3 **6B-4W/2W Configuration**

The calculated moment capacity for end-plate yielding is close enough to the observed yield moment, to validate the equations for M_{pl}. The calculated M_q and M_{np} were

conservative by 13% to 17% which could be attributed to the overstrength in bolts. M_q^{exp}/M_u ranged from 0.97 to 0.98 which validates the bolt force models for this configuration. But, M_{np}^{exp}/M_u was unconservative by 6% to 11%. Still, the design procedures could be considered to be validated for this configuration assuming M_q^{exp} and M_{np}^{exp} to be the upper bound for design calculations.

7.2.4 **12B-MRE 1/3-4W/2W Configuration**

Both the thin end-plate couldn't be taken to bolt rupture. But, it is to be noted that the calculated moment capacity at bolt rupture with prying action was at least 10% less (safe) than the maximum applied moment. This could be attributed to the overstrength in bolts. M_q^{exp}/M_u was within 1.14 and 1.17, which is unconservative. Also, M_{pl} was again conservative by about 10% for both the thin plate specimens, but it still makes a case for the validation of the yield line analysis of the configuration.

The design procedures for thick plate behavior could be validated on the basis of the conservative prediction of the moment capacity at bolt rupture without prying, M_{np}. But M_{np}^{exp}/M_u was from 1.09 to 1.13, which is on the unconservative side. Again M_{np}^{exp} could be considered to be the upper bound value for design purposes.

References

Adey, B.T., Grondin, G.Y., and Cheng, J.J.R. (1997) *Extended End Plate Moment Connections Under Cyclic Loading*, Structural Engineering Report No. 216, University of Alberta Department of Civil and Environmental Engineering.

Adey, B.T., Adey, B.T., Grondin, G.Y., and Cheng, J.J.R. (2000) "Cyclic Loading of End Plate Moment Connections", *Canadian Journal of Civil Engineering*, Vol. 27, pp. 683-701.

Borgsmiller, J. T., & Murray, T. M. (1995). *Simplified Method for the Design of Moment End-Plate Connections.* Blacksburg, VA: Department of Civil Engineering, Virginia Polytechnic Institute and State University.

Ghassemieh, M., Kukreti, A., and Murray, T.M. (1983) *Inelastic Finite Element Analysis of Stiffened End-Plate Moment Connections*, Report No. FSEL/AISC 83-02, School of Civil Engineering and Environmental Science, University of Oklahoma, Norman, OK.

Kennedy, N. A., Vinnakota, S., & Sherbourne, A. N. (1981). The Split-Tee Anlogy in Bolted Splices and Beam-Column Connections. *Proceedings of the International Conference on Joints in Structural Steelwork*, (pp. 2.138-2.157).

Kulak, G.L., Fisher, J.W., Struik, J.H.A., (2001) "Guide to Design Criteria for Bolted and Riveted Joints", *American Institute of Steel Construction*, Chicago, IL

Murray, T. M. (1988). Recent Developments for the Design of Moment End-Plate Connections. *Journal of Constructional Steel Research*, 133-162.

Murray, T. M., & Shoemaker, W. L. (2002). Flush and Extended Multiple-Row Moment End-Plate Connections. *AISC*.

Seek, M.W., and Murray, T.M., (2008) "Seismic Strength of Moment End-Plate Connections with Attached Concrete Slab", *Proceedings of the Connections in Steel Structures VI Workshop*, Chicago, Il. June 23-25.

Specification for Structural Joints Using High-Strength Bolts. (2009). *Research Council on Structural Connections (RCSC)*.

Sumner, E. A. (2003). *Unified Design of Extended End-Plate Moment Connections Subject to Cyclic Loading.* Blacksburg, VA: Department of Civil Engineering, Viriginia Polytechnic Institute and State University.

Sumner, E. A., & Murray, T. M. (2001). *Experimental Investigation of Four Bolt Wide Extended End-Plate Moment Connections.* Blacksburg, VA: Department of Civil Engineering, Virginia Polytechnic Institute and State University.

Sumner, E. A., Mays, T. W., & Murray, T. M. (2000). *Cyclic Testing of Bolted Moment End-Plate Connections.* Blacksburg, VA: Virginia Polytechnic Institute and State University.

Appendix A Mill Test Report for Beam Material

6B-4W/2W-0.875-1.00-36
6B-4W/2W-0.875-1.00-60
12B- MRE 1/3 -4W/2W-0.75-1.00-36
12B- MRE 1/3 -4W/2W-0.75-1.00-60

NUCOR
PLATE MILL
P.O.Box 279
Winton, NC 27986
(252) 356-3700

Mill Test Report

NUCOR It's our Nature.

Issuing Date : 08/18/2012 B/L No. : 334335 Load No. : 336264 Our Order No. : 103114/2 Cust. Order No. : PPC516
Vehicle No: TTPX 804776
Specification : 1.0000" x 120.000" x 480.000"
ASTM A572 Grade 50-12/ASTM A709 Grade 50-11/AASHTO M270-50
Type 2

Sold To : METALS USA PLATES AND SHAPES NORTHEAST LP 2025 GREENTREE RD PITTSBURGH,PA 15220

Ship To : METALS USA C/O HARTWELL WAREHOUSE 5 N WILSON AVE BRISTOL,PA 19007

Marking :

Heat No	C	Mn	P	S	Si	Cu	Ni	Cr	Mo	Al(tot)	V	Nb	Ti	N	Ca	B	Sn	CEQ	PCM
2505623	0.20	1.20	0.023	0.004	0.18	0.13	0.05	0.10	0.01	0.036	0.043	0.002	0.002		0.0009	0.0002	0.007	0.44	0.28

Tensile Test								Charpy Impacts											
Plate Serial No	Pieces	Tons	Dir.	(psi) Yield	(psi) Tensile	Elongation % in 2"	Elongation % in 8"	Dir.	(ft-lbs) 1	(%) shear	(ft-lbs) 2	(%) shear	(ft-lbs) 3	(%) shear	(ft-lbs) Ave.	(%) shear	Size	Temp (°F)	Min Ave.
2505623-05	2	16.33	T	56,800	83,200		21.1	H-L	34.8		46.6		20.6		34.0		10mm	-22	15
			T	51,400	81,200		22.5	H-L	67.1		63.0		41.8		57.3		10mm	-22	15

NFCM, T1 and T2, 15ft-lbs @ +40 F (20J @ +4 C), H frequency. Temperature reduced by 15 F for each 10 ksi over 65 ksi;

Manufactured to fully killed fine grain practice by Electric Arc Furnace. Welding or weld repair was not performed on this material. Mercury has not been used in the direct manufacturing of this material. Produced as continuous cast discrete plate as-rolled, unless otherwise noted in Specification.
Yield by 0.5EUL method unless otherwise specified. Ceq = C+(Mn/6)+((Cr+Mo+V)/5)+((Cu+Ni)/15)
Pcm = C+(Si/30)+(Mn/20)+(Cu/20)+(Ni/60)+(Cr/20)+(Mo/15)+(V/10)+5B
Melted and manufactured in the USA. ISO 9001:2008 certified (#008063) by SRI Quality System Registrar (#0985-09). PED 97/23/EC 7/2 Annex 1, Para. 4.3 Compliant.
DIN 50049 3.1.B/EN 10204 3.1B(2004), DIN EN 10204 3.1(2005) compliant. For ABS grades only, Quality Assurance certificate 14-MMPOA-723

We hereby certify that the contents of this report are accurate and correct. All test results and operations performed by the material manufacturer are in compliance with the applicable specifications, including customer specifications.

T. A. Depretis

T. A. Depretis, Metallurgist

08/20/2012 8:54:04 AM

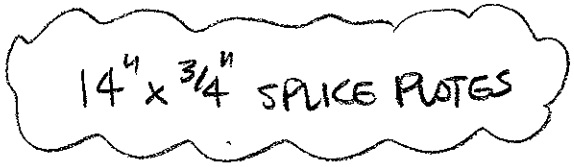

6B-4W/2W-1.125-0.75-36
6B-4W/2W-1.125-0.75-60
12B- MRE 1/3 -4W/2W-1.00-0.75-36
12B- MRE 1/3 -4W/2W-1.00-0.75-60

NUCOR
PLATE MILL

P.O.Box 279
Winton, NC 27986
(252) 356-3700

Mill Test Report

Page 2

NUCOR
It's our Nature.

Issuing Date : 06/30/2011 B/L No. : 297636 Load No. : 299124 Our Order No. : 91906/3 Cust. Order No. : VA-35442

Vehicle No: 7312

Specification : 0.7500" x 96.000" x 480.000"
ASTM A572 Grade 50/345-07/A709 Grade 50-10/ AASHTO M270 50 97
Type 2

Sold To : INFRAMETALS CO PETERSBURG
580 MIDDLETON BLVD STE D100
LANGHORNE,PA 19047

Ship To : INFRA - METALS
1900 BESSEMER RD
PH 8049575900
PETERSBURG,VA 23805

Marking :

Heat No	C	Mn	P	S	Si	Cu	Ni	Cr	Mo	Al(tot)	V	Nb	Ti	N	Ca	B	Sn	CEQ	PCM
1504480	0.17	1.17	0.010	0.002	0.17	0.21	0.08	0.10	0.02	0.034	0.043	0.001	0.002		0.0000	0.0002	0.008	0.41	0.26

Tensile Test

Plate Serial No	Pieces	Tons	Dir.	(psi) Yield	(psi) Tensile	Elongation % in 2"	Elongation % in 8"
1504480-07	2	9.80	T	52,700	80,900		19.2
			T	63,100	86,700		20.0

Charpy Impacts

Dir.	1	(%) shear	2	(%) shear	3	(%) shear	Ave.	(%) shear	Size	Temp	Min Ave.

Manufactured to fully killed fine grain practice by Electric Arc Furnace. Welding or weld repair was not performed on this material. Mercury has not been used in the direct manufacturing of this material. Produced as continuous cast discrete plate as-rolled, unless otherwise noted in Specification.

Yield by 0.5EUL method unless otherwise specified. Ceq = C+(Mn/6)+((Cr+Mo+V)/5)+((Cu+Ni)/15)

Pcm = C+(Si/30)+(Mn/20)+(Cu/20)+(Ni/60)+(Cr/20)+(Mo/15)+(V/10)+5B

Melted and manufactured in the USA. ISO 9001:2008 certified (#008063) by SRI Quality System Registrar (#0985-09). PED 97/23/EC 7/2 Annex 1, Para. 4.3 Compliant. DIN 50049 3.1.B/EN 10204 3.1B(2004), DIN EN 10204 3.1(2005) compliant. For ABS grades only, Quality Assurance certificate 14-MMPQA-723

We hereby certify that the contents of this report are accurate and correct. All test results and operations performed by the material manufacturer are in compliance with the applicable specifications, including customer specifications.

T. A. Depretis

T. A. Depretis, Metallurgist

06/30/2011 1:27:19 PM

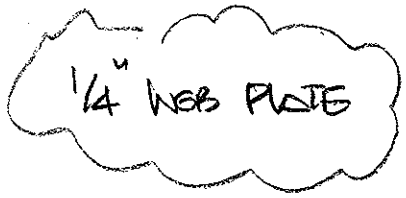

6B-4W/2W-1.125-0.75-36
6B-4W/2W-1.125-0.75-60
6B-4W/2W-0.875-1.00-36
6B-4W/2W-0.875-1.00-60

Report - Of - Information

FERALLOY CORPORATION

OWNER:

SHIP TO:
AMERICAN BUILDINGS CO
GOLDEN EAGLE DRIVE
LA CROSSE , VA 23950

DATE: 6/12/14

BILL OF LADING: 607 - 131481 - 10
HEAT/MILL COIL: 2404585 2404585-3
SKID NO: 256763
TAG NUMBER: 97508 - 01
PROCESSED AS: ASTM A529 HR C-Mn Steel Plate, Gr 55
REFERENCING: ASTM A-529 High Strength C-Mn Structural Steel

PART NO: 1/4X60X241 - *
SIZE: .2400 X 60.000 X 241.000
PRODUCT: HR PL55 A529
CUSTOMER PO NUMBER: 1-20198 051414

Element	C	Mn	P	S	Si	Cu	Ni	Cr	Mo	Sn
Weight %	.2600	1.1300	.0110	.0020	.2100	.0700	.0300	.0300	.0100	.0050
Element	Al	B	Nb	V	Ti	N	CA	H	O	
Weight %	.0270	.0000	.0010	.0060	.0010	.0060	.0020			

Location	Yield (PSI)	Tensile (PSI)	Elongation(% in 2")
HEAD	67600	91100	25.0
CENTER	69500	93000	25.0

Bend Test	n Value	Hardness	r Value	
	.000	88RB	.00	

NOTICE: FERALLOY MAKES NO REPRESENTATION OR WARRANTY AS TO THE INFORMATION CONTAINED IN THIS REPORT. The values published on this 'report-of-information' are transcribed from information provided by the owner and the owner's suppliers including mills, testing laboratories, etc. This is NOT a certificate of specification, inspection, or grade.

This material processed at & shipped from:
FERALLOY CHARLESTON
CHARLESTON DIVISION
1020 NORTH STEEL CIRCLE
HUGER , SC 29450

3/8" WEB PLATE

12B- MRE 1/3 -4W/2W-0.75-1.00-36
12B- MRE 1/3 -4W/2W-0.75-1.00-60
12B- MRE 1/3 -4W/2W-1.00-0.75-36
12B- MRE 1/3 -4W/2W-1.00-0.75-60

Report - Of - Information

FERALLOY CORPORATION

OWNER:

SHIP TO:
AMERICAN BUILDINGS CO
GOLDEN EAGLE DRIVE

LA CROSSE , VA 23950

DATE: 6/16/14

BILL OF LADING: 607 - 131547 - 10
HEAT/MILL COIL: 2404762 2404762-3
SKID NO: 257429
TAG NUMBER: 97552 - 01
PROCESSED AS: ASTM A529 HR C-Mn Steel Plate, Gr 55
REFERENCING: ASTM A-572 HSLA Cb-V Structural Steel

PART NO: 3/8X60X241 - *
SIZE: .3650 X 60.000 X 241.000
PRODUCT: HR PL55 A572
CUSTOMER PO NUMBER: 1-20200 051514

Element	C	Mn	P	S	Si	Cu	Ni	Cr	Mo	Sn
Weight %	.0500	1.4100	.0130	.0050	.3300	.0900	.0300	.0300	.0100	.0070
Element	Al	B	Nb	V	Ti	N	CA	H	O	
Weight %	.0380	.0000	.0400	.0060	.0020	.0080	.0020			

Location	Yield (PSI)	Tensile (PSI)	Elongation(% in 2")
HEAD	69900	82000	37.0
CENTER	69800	81600	39.0

Bend Test	n Value	Hardness	r Value	
	.000		.00	

NOTICE: FERALLOY MAKES NO REPRESENTATION OR WARRANTY AS TO THE INFORMATION CONTAINED IN THIS REPORT. The values published on this 'report-of-information' are transcribed from information provided by the owner and the owner's suppliers including mills, testing laboratories, etc. This in NOT a certificate of specification, inspection, or grade.

This material processed at & shipped from:
FERALLOY CHARLESTON
CHARLESTON DIVISION
1020 NORTH STEEL CIRCLE

HUGER , SC 29450

NUCOR
NUCOR CORPORATION
NUCOR STEEL TEXAS

Mill Certification
4/15/2014

MTR #: 0000020634
8812 Hwy 79 W
Jewett, TX 75846
(903) 626-4461
Fax: (903) 626-6290

Sold To: AMERICAN BUILDINGS CO
PO BOX 800
EUFAULA, AL 36027-0000
(334) 688-2276
Fax: (334) 687-9733

Ship To: AMERICAN BUILDINGS CO
501 GOLDEN EAGLE DR
LA CROSSE, VA 23950-0000
(000) 000-0000

Customer P.O.	1-20145	Sales Order	200741.3
Product Group	Merchant Bar Quality	Part Number	53750C004805300
Grade	ASTM A529/A529M-05 GR 55	Lot #	JW1410158251
Size	3/4x12" Flat	Heat #	JW14101582
Product	3/4x12" Flat 40' A529 Gr55	B.L. Number	J1-668160
Description	A529 Gr55	Load Number	J1-272301
Customer Spec		Customer Part #	

I hereby certify that the material described herein has been manufactured in accordance with the specifications and standards listed above and that it satisfies those requirements.

Roll Date: 2/22/2014 **Melt Date: 2/20/2014** **Qty Shipped LBS: 19,600** **Qty Shipped Pcs: 16**

C	Mn	P	S	Si	Cu	Ni	Cr	Mo	V	Cb	CEA529	CBV	MN/C
0.14%	1.12%	0.009%	0.024%	0.24%	0.25%	0.16%	0.11%	0.050%	0.0830%	0.001%	0.44%	0.080%	08.00%

CEA529: A529 CARBON EQUIVALENT
CBV: CB+V
MN/C: MN / C

Yield 1: 61,300psi (423MPa) Tensile 1: 78,900psi (544MPa) Elongation: 19% in 8"(% in 203.3mm)
Yield 2: 61,600psi (425MPa) Tensile 2: 80,900psi (558MPa) Elongation 18% in 8"(% in 203.3mm)

Specification Comments:

Comments: E-mail: websales@nstexas.com

ALL MANUFACTURING PROCESSES OF THE STEEL MATERIALS IN THIS PRODUCT, INCLUDING MELTING, HAVE OCCURRED WITHIN THE UNITED STATES. ALL PRODUCTS PRODUCED ARE WELD FREE. MERCURY, IN ANY FORM, HAS NOT BEEN USED IN THE PRODUCTION OR TESTING OF THIS MATERIAL.

12" x 3/4" FLANGES

6B-4W/2W-1.125-0.75-36
6B-4W/2W-1.125-0.75-60
6B-4W/2W-0.875-1.00-36
6B-4W/2W-0.875-1.00-60
12B- MRE 1/3 -4W/2W-0.75-1.00-36
12B- MRE 1/3 -4W/2W-0.75-1.00-60
12B- MRE 1/3 -4W/2W-1.00-0.75-36
12B- MRE 1/3 -4W/2W-1.00-0.75-60

Kim Pritchard
Division Metallurgist

NBMG-10 January 1, 2012

NUCOR

NUCOR CORPORATION
NUCOR STEEL SOUTH CAROLINA

Mill Certification

1/9/2014

MTR #: 0000001200
300 Steel Mill Road
DARLINGTON, SC 29540
(843) 393-5841
Fax: (843) 395-8701

Sold To: AMERICAN BUILDINGS CO
PO BOX 800
EUFAULA, AL 36027-0000
(888) 307-4338
Fax: (334) 688-2275

Ship To: AMERICAN BUILDINGS CO
501 GOLDEN EAGLE DR
LA CROSSE, VA 23950-0000
(434) 757-2220
Fax: (334) 688-2275

Customer P.O.	1-20122	Sales Order	195339.2
Product Group	Merchant Bar Quality	Part Number	535005004805300
Grade	ASTM A529/A529M-05 GR 55	Lot #	DL1310508901
Size	1/2x5" Flat	Heat #	DL13105089
Product	1/2x5" Flat 40' A529 Gr55	B.L. Number	C1-622195
Description	A529 Gr55	Load Number	C1-302384
Customer Spec		Customer Part #	

I hereby certify that the material described herein has been manufactured in accordance with the specifications and standards listed above and that it satisfies those requirements.

Roll Date: 9/7/2013 Melt Date: 8/25/2013 Qty Shipped LBS: 8,847 Qty Shipped Pcs: 26

C	Mn	P	S	Si	Cu	Ni	Cr	Mo	V	Cb
0.24%	1.22%	0.009%	0.035%	0.14%	0.37%	0.10%	0.13%	0.020%	0.0130%	0.003%

Yield 1: 57,000psi (393MPa) Tensile 1: 85,000psi (586MPa) Elongation: 26% in 8"(% in 203.3mm)
Yield 2: 58,000psi (400MPa) Tensile 2: 85,000psi (586MPa) Elongation 26% in 8"(% in 203.3mm)

Specification Comments:

1. WELDING OR WELD REPAIR WAS NOT PERFORMED ON THIS MATERIAL
2. MELTED AND MANUFACTURED IN THE USA
3. MERCURY, RADIUM, OR ALPHA SOURCE MATERIALS IN ANY FORM HAVE NOT BEEN USED IN THE PRODUCTION OF THIS MATERIAL

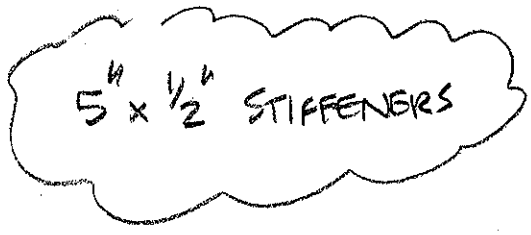

6B-4W/2W-1.125-0.75-36
6B-4W/2W-1.125-0.75-60
6B-4W/2W-0.875-1.00-36
6B-4W/2W-0.875-1.00-60
12B- MRE 1/3 -4W/2W-0.75-1.00-36
12B- MRE 1/3 -4W/2W-0.75-1.00-60
12B- MRE 1/3 -4W/2W-1.00-0.75-36
12B- MRE 1/3 -4W/2W-1.00-0.75-60

James H. Blew
Division Metallurgist

NBMG-10 January 1, 2012

CERTIFIED MATERIAL TEST REPORT

GERDAU

US-ML-CARTERSVILLE
384 OLD GRASSDALE ROAD NE
CARTERSVILLE, GA 30121
USA

CUSTOMER SHIP TO	CUSTOMER BILL TO
BLUESCOPE BUILDINGS NORTH AMER 1274 CHURCH AVE RAINSVILLE,AL 35986-6230 USA	BLUESCOPE BUILDINGS N AMERICA KANSAS CITY,MO 64141-6917 USA

GRADE	SHAPE / SIZE	LENGTH	WEIGHT	HEAT / BATCH
A529-55M	Flat / 1 X 8	40'00"	8,704 LB	**55036396**/04

SALES ORDER	CUSTOMER MATERIAL Nº
1477282/000040	092040

SPECIFICATION / DATE or REVISION
1-ASTM A529 GR55-05
2-BUTLER SPEC 10004.20 GR 55

CUSTOMER PURCHASE ORDER NUMBER	BILL OF LADING	DATE
252990	1323-0000037378	11/03/2014

CHEMICAL COMPOSITION

C %	Mn %	P %	S %	Si %	Cu %	Ni %	Cr %	Mo %	V %	Nb %	N %	Pb %
0.18	0.95	0.011	0.027	0.19	0.31	0.09	0.09	0.077	0.030	0.000	0.0110	0.0010

CHEMICAL COMPOSITION

Sn %
0.011

MECHANICAL PROPERTIES

Elong. %	G/L Inch	UTS PSI	UTS MPa	YS 0.2% PSI	YS MPa
18.60	8.000	83200	574	61900	427
18.10	8.000	85000	586	60300	416

COMMENTS / NOTES

MB
11/7/14

The above figures are certified chemical and physical test records as contained in the permanent records of company. We certify that these data are correct and in compliance with specified requirements. This material, including the billets, was melted and manufactured in the USA. CMTR complies with EN 10204 3.1.

BHASKAR YALAMANCHILI
QUALITY DIRECTOR

YAN WANG
QUALITY ASSURANCE MGR.

CERTIFIED MATERIAL TEST REPORT

GERDAU

US-ML-CARTERSVILLE
384 OLD GRASSDALE ROAD NE
CARTERSVILLE, GA 30121
USA

CUSTOMER SHIP TO	CUSTOMER BILL TO
BLUESCOPE BUILDINGS NORTH AMER 1274 CHURCH AVE RAINSVILLE,AL 35986-6230 USA	BLUESCOPE BUILDINGS N AMERICA KANSAS CITY,MO 64141-6917 USA

GRADE	SHAPE / SIZE
A529-55M	Flat / 1 X 8

LENGTH	WEIGHT	HEAT / BATCH
40'00"	8,704 LB	**55036396**/04

SALES ORDER	CUSTOMER MATERIAL N°
1477282/000040	092040

SPECIFICATION / DATE or REVISION
1-ASTM A529 GR55-05
2-BUTLER SPEC 10004.20 GR 55

CUSTOMER PURCHASE ORDER NUMBER	BILL OF LADING	DATE
252990	1323-0000037378	11/03/2014

CHEMICAL COMPOSITION

C %	Mn %	P %	S %	Si %	Cu %	Ni %	Cr %	Mo %	V %	Nb %	N %	Pb %
0.18	0.95	0.011	0.027	0.19	0.31	0.09	0.09	0.077	0.030	0.000	0.0110	0.0010

CHEMICAL COMPOSITION

Sn %
0.011

MECHANICAL PROPERTIES

Elong. %	G/L Inch	UTS PSI	UTS MPa	YS 0.2% PSI	YS MPa
18.60	8.000	83200	574	61900	427
18.10	8.000	85000	586	60300	416

COMMENTS / NOTES

11/7/14

The above figures are certified chemical and physical test records as contained in the permanent records of company. We certify that these data are correct and in compliance with specified requirements. This material, including the billets, was melted and manufactured in the USA. CMTR complies with EN 10204 3.1.

BHASKAR YALAMANCHILI
QUALITY DIRECTOR

YAN WANG
QUALITY ASSURANCE MGR.

GERDAU

CERTIFIED MATERIAL TEST REPORT

US-ML-CARTERSVILLE
384 OLD GRASSDALE ROAD NE
CARTERSVILLE, GA 30121
USA

CUSTOMER SHIP TO	CUSTOMER BILL TO
BLUESCOPE BUILDINGS NORTH AMER 1274 CHURCH AVE RAINSVILLE,AL 35986-6230 USA	BLUESCOPE BUILDINGS N AMERICA KANSAS CITY,MO 64141-6917 USA

GRADE	SHAPE / SIZE
A529-55M	Flat / 1 X 10

LENGTH	WEIGHT	HEAT / BATCH
40'00"	8,160 LB	**55033984**/04

SALES ORDER	CUSTOMER MATERIAL N°
1477282/000030	092042

SPECIFICATION / DATE or REVISION
1-ASTM A529 GR55-05
2-BUTLER SPEC 10004.20 GR 55

CUSTOMER PURCHASE ORDER NUMBER	BILL OF LADING	DATE
252990	1323-0000037378	11/03/2014

CHEMICAL COMPOSITION

C %	Mn %	P %	S %	Si %	Cu %	Ni %	Cr %	Mo %	V %	Nb %	N %	Pb %
0.20	0.97	0.013	0.031	0.17	0.30	0.09	0.07	0.025	0.030	0.002	0.0110	0.0060

CHEMICAL COMPOSITION

Sn %
0.017

MECHANICAL PROPERTIES

Elong. %	G/L Inch	UTS PSI	UTS MPa	YS 0.2% PSI	YS MPa
20.00	8.000	84500	583	62700	432
18.20	8.000	84700	584	61900	427

COMMENTS / NOTES

MB
11/7/14

The above figures are certified chemical and physical test records as contained in the permanent records of company. We certify that these data are correct and in compliance with specified requirements. This material, including the billets, was melted and manufactured in the USA. CMTR complies with EN 10204 3.1.

BHASKAR YALAMANCHILI
QUALITY DIRECTOR

YAN WANG
QUALITY ASSURANCE MGR.

CERTIFIED MATERIAL TEST REPORT

GERDAU

US-ML-CARTERSVILLE
384 OLD GRASSDALE ROAD NE
CARTERSVILLE, GA 30121
USA

CUSTOMER SHIP TO	CUSTOMER BILL TO
BLUESCOPE BUILDINGS NORTH AMER 1274 CHURCH AVE RAINSVILLE,AL 35986-6230 USA	BLUESCOPE BUILDINGS N AMERICA KANSAS CITY,MO 64141-6917 USA

GRADE	SHAPE / SIZE	LENGTH	WEIGHT	HEAT / BATCH
A529-55M	Flat / 1 X 10	40'00"	16,320 LB	**55035144**/04

SALES ORDER	CUSTOMER MATERIAL N°
1477282/000030	092042

SPECIFICATION / DATE or REVISION
1-ASTM A529 GR55-05
2-BUTLER SPEC 10004.20 GR 55

CUSTOMER PURCHASE ORDER NUMBER	BILL OF LADING	DATE
252990	1323-0000037378	11/03/2014

CHEMICAL COMPOSITION

C %	Mn %	P %	S %	Si %	Cu %	Ni %	Cr %	Mo %	V %	Nb %	N %	Pb %
0.21	1.00	0.013	0.031	0.19	0.40	0.09	0.07	0.034	0.033	0.002	0.0110	0.0030

CHEMICAL COMPOSITION

Sn %
0.013

MECHANICAL PROPERTIES

Elong. %	G/L Inch	UTS PSI	UTS MPa	YS 0.2% PSI	YS MPa
20.30	8.000	85100	587	61800	426
20.40	8.000	84800	585	61300	423

COMMENTS / NOTES

MB
11/7/14

The above figures are certified chemical and physical test records as contained in the permanent records of company. We certify that these data are correct and in compliance with specified requirements. This material, including the billets, was melted and manufactured in the USA. CMTR complies with EN 10204 3.1.

BHASKAR YALAMANCHILI
QUALITY DIRECTOR

YAN WANG
QUALITY ASSURANCE MGR.

OLYMPIC STEEL
5080 RICHMOND ROAD
BEDFORD HEIGHTS, OH 44146 USA
PHONE: 216-292-3800

METALLURGICAL TEST REPORT

>>>>>> CERTIFICATE OF ANALYSIS AND TESTS <<<<<<

Sold To: OLYMPIC STEEL - SOUTHERN
587 BARROW PARK DRIVE
WINDER, GA 30680

Ship To: BLUESCOPE BUILDINGS
1274 CHURCHILL AVE.
RAINSVILLE, AL 35986

Sales Order:	316975 - 01	B/L No:	519304	Release:	3
Reference:	KATZ, NEIL (11473)	2nd B/L:		Cus Ord #:	282960
				Cus Name:	OLYMPIC STEEL - SOUTHERN

Date: 25-Aug-2014

Description of Material and Specification

DOMESTIC PO 243135/ASTM A572 GR. 55
.5" x 60" x 241"

93393 REV O

TAG#: 23166906,23166907,23166909,23166910,23166911

HEAT#: 178933/NORTH STAR BLUESCOPE STEEL LLC

MC # 22923073

Chem Elem Symbol / Elem Content Value:

<C : .05> <MN : .81> <P : .013> <S : .004> <SI : .02> <AL : .02> <V : .057> <CU : .11> <NI : .04> <CR : .06>
<MO : .01> <N : .01> <TI : .001> <B : 0> <CA : .002> <SN : .01> <NB : 0>

Melted and manufactured in the USA

YIELD STRENGTH	MIN:	62790 PSI	MAX	62790 PSI
TENSILE STRENGTH	MIN:	72920 PSI	MAX	72920 PSI
ELONGATION 2"	MIN:	31.6 %	MAX	31.6 %

We hereby certify the above is correct as contained in the records of the corporation

8/29/14

Branch Certification Manager

USER: REPORTS@SEMSPRD
REPORT: ST_MSR_OSI

25-Aug-2014 12:37
Page 1 of 1

Certified Test Report

NORTH STAR BLUESCOPE STEEL LLC
6767 County Road 9
Delta, Ohio 43515
Telephone: (888) 822-2112

Customer:
Olympic Steel Inc.
5080 Richmond Road
Cleveland, OH 44146

Customer P.O.: 644796

Cust. Ref/Part # A1018 / HSLAS55

Order Number 306169
Line Item Number 1
Heat Number 178933
Coil Number 1412240

Ordered Width (mm/in) 1524.000 / 60.000
Ordered Gauge (mm/in) 12.446 / 0.490
Material Description ASTM A1018-55-1-10, For Conversion to ASTM A572-55-12
Production Date/Time May 6 2014 9:51PM

Heat Chemical Analysis (wt%)

Type	C	Mn	P	S	Si	Al	Cu	Cr	Ni	Mo	Sn	N	B	V	Nb	Ti	Ca
Heat	0.05	0.81	0.013	0.004	0.02	0.02	0.11	0.06	0.04	0.01	0.01	0.010	0.0000	0.057	0.000	0.001	0.002

Mechanical Test Report

All mechanical tests are performed on a sample from the tail of a coil.

Yield Strength	Tensile Strength	% Elongation in 2 inches
62,790 psi	72,920 psi	31.6%

This material has been produced to conform to EN 10204:2005. This material has been produced and tested in accordance with each of the following applicable standards: ASTM E 1806-96, ASTM E 415-99a, ASTM A 751-01, ASTM A 370-03a, JIS Z2201:1998, JIS Z 2241:1998. This report certifies that the above test results are representative of those contained in the records of North Star BlueScope Steel LLC for the material identified in this test report and is intended to comply with the requirements of the material description. North Star BlueScope Steel LLC is not responsible for the inability of this material to meet specific applications. Any modifications to this certification as provided negates the validity of this test report. All reproductions must have the written approval of North Star BlueScope Steel. This product was manufactured, melted, cast, and hot-rolled (min. 3:1 reduction ratio), entirely within the U.S.A at North Star BlueScope Steel LLC, Delta, Ohio. This material was not exposed to Mercury or any alloy which is liquid at ambient temperature during processing or while in North Star BlueScope Steel LLC possession. Test equipment calibration certificates are available upon request. NIST traceability is established through test equipment calibration certificates which are available upon request. Uncertainty calculations are calculated in accordance with NIST standards and are maintained at a 4:1 ratio in accordance with NIST standards. Uncertainty data is available upon request.

Tim Mitchell **Manager Quality Assurance and Technology**

Date Issued: May 15, 2014 16:00:10
Revision#: 01

8/29/14

OLYMPIC STEEL
5080 RICHMOND ROAD
BEDFORD HEIGHTS, OH 44146 USA
PHONE: 216-292-3800

METALLURGICAL TEST REPORT

>>>>>> CERTIFICATE OF ANALYSIS AND TESTS <<<<<<

Sold To: OLYMPIC STEEL - SOUTHERN
587 BARROW PARK DRIVE
WINDER, GA 30680

Ship To: BLUESCOPE BUILDINGS
1274 CHURCHILL AVE.
RAINSVILLE, AL 35986

Sales Order:	316975 - 01	B/L No:	519304	Release:	3
Reference:	KATZ, NEIL (11473)	2nd B/L:		Cus Ord #:	282960
				Cus Name:	OLYMPIC STEEL - SOUTHERN

Date: 25-Aug-2014

Description of Material and Specification

DOMESTIC PO 243135/ASTM A572 GR. 55
.5" x 60" x 241"

93393 REV O

TAG#: 23166906,23166907,23166909,23166910,23166911

HEAT#: 178933/NORTH STAR BLUESCOPE STEEL LLC

MC # 22923073

Chem Elem Symbol / Elem Content Value:

<C : .05> <MN : .81> <P : .013> <S : .004> <SI : .02> <AL : .02> <V : .057> <CU : .11> <NI : .04> <CR : .06>
<MO : .01> <N : .01> <TI : .001> <B : 0> <CA : .002> <SN : .01> <NB : 0>

Melted and manufactured in the USA

YIELD STRENGTH	MIN:	62790 PSI	MAX	64000 PSI
TENSILE STRENGTH	MIN:	71700 PSI	MAX	72920 PSI
ELONGATION 2"	MIN:	25.0 %	MAX	31.6 %
CARBON EQUIV	MIN:	.24	MAX	.24

We hereby certify the above is correct as contained in the records of the corporation

8/29/14

Branch Certification Manager

USER: REPORTS@SEMSPRD
REPORT: ST_MSR_OSI

26-Aug-2014 3:42 PM
Page 1 of 1

Appendix B Mill Test Report for Bolts

NUCOR
FASTENER DIVISION

LOT NO.
335852A

12B- MRE 1/3 -4W/2W-0.75-1.00-36
12B- MRE 1/3 -4W/2W-0.75-1.00-60

Post Office Box 6100
Saint Joe, Indiana 46785
Telephone 260/337-1600

CUSTOMER NO/NAME
9000 BIRMINGHAM-CONS/SHIPPING

NUCOR ORDER # 857190
CUST PART # 75C300A32P/NND
CUSTOMER P.O. # 6044932

TEST REPORT SERIAL# FB420998
TEST REPORT ISSUE DATE 12/11/13
DATE SHIPPED 1/23/14
NAME OF LAB SAMPLER: RYAN UNGER, LAB TECHNICIAN

**********CERTIFIED MATERIAL TEST REPORT**********

NUCOR PART NO	QUANTITY	LOT NO.	DESCRIPTION
160600	3600	335852A	3/4-10 X 3 A325 HVY HX

MANUFACTURE DATE 11/22/13 STRUC SCREW PLAIN

--CHEMISTRY MATERIAL GRADE -1039ML1

MATERIAL NUMBER	HEAT NUMBER	**CHEMISTRY COMPOSITION (WT% HEAT ANALYSIS) BY MATERIAL SUPPLIER C	MN	P	S	SI	NUCOR STEEL - NEBRASKA
RM028677	NF13204672	.41	.89	.009	.009	.24	

--MECHANICAL PROPERTIES IN ACCORDANCE WITH ASTM A325-10

SURFACE HARDNESS (R30N)	CORE HARDNESS (RC)	PROOF LOAD 28400 LBS	TENSILE STRENGTH 10 DEG-WEDGE (LBS)	STRESS (PSI)
N/A	31.2	PASS	49580	148443
N/A	31.0	PASS	49790	149072
N/A	29.9	PASS	50190	150269
N/A	30.0			
N/A	30.9			
AVERAGE VALUES FROM TESTS		PRODUCTION LOT SIZE 38100 PCS		
	30.6		49853	149261

--VISUAL INSPECTION IN ACCORDANCE WITH ASTM A325-10 5 PCS. SAMPLED LOT PASSED
HEAT TREATMENT - AUSTENITIZED, OIL QUENCHED & TEMPERED (MIN 800 DEG F)

--DIMENSIONS PER ASME B18.2.6-2010

CHARACTERISTIC	#SAMPLES TESTED	MINIMUM	MAXIMUM
Width Across Corners	8	1.3980	1.4070
Grip Length	8	1.4900	1.5500
Head Height	8	0.4740	0.4780
Threads	8	PASS	PASS

ALL TESTS ARE IN ACCORDANCE WITH THE LATEST REVISIONS OF THE METHODS PRESCRIBED IN THE APPLICABLE SAE AND ASTM SPECIFICATIONS. THE SAMPLES TESTED CONFORM TO THE SPECIFICATIONS AS DESCRIBED/LISTED ABOVE AND WERE MANUFACTURED FREE OF MERCURY CONTAMINATION. NO HEATS TO WHICH BISMUTH, SELENIUM, TELLURIUM, OR LEAD WAS INTENTIONALLY ADDED HAVE BEEN USED TO PRODUCE THE BOLTS.
THE STEEL WAS MELTED AND MANUFACTURED IN THE U.S.A. AND THE PRODUCT WAS MANUFACTURED AND TESTED IN THE U.S.A. PRODUCT COMPLIES WITH DFARS 252.225-7014. WE CERTIFY THAT THIS DATA IS A TRUE REPRESENTATION OF INFORMATION PROVIDED BY THE MATERIAL SUPPLIER AND OUR TESTING LABORATORY. THIS CERTIFIED MATERIAL TEST REPORT RELATES ONLY TO THE ITEMS LISTED ON THIS DOCUMENT AND MAY NOT BE REPRODUCED EXCEPT IN FULL.

A2LA ACCREDITED

MECHANICAL FASTENER
CERTIFICATE NO. A2LA 0139.01
EXPIRATION DATE 12/31/13

NUCOR FASTENER
A DIVISION OF NUCOR CORPORATION

John W. Ferguson

JOHN W. FERGUSON
QUALITY ASSURANCE SUPERVISOR

NUCOR
FASTENER DIVISION

LOT NO. 320001A
6B-4W/2W-0.875-1.00-36
6B-4W/2W-0.875-1.00-60

Post Office Box 6100
Saint Joe, Indiana 46785
Telephone 260/337-1600

CUSTOMER NO/NAME
9000 BIRMINGHAM-CONS/SHIPPING

NUCOR ORDER # 848284
CUST PART # 87C325A32P/NND

TEST REPORT SERIAL# FB402003
TEST REPORT ISSUE DATE 2/07/13
DATE SHIPPED 11/13/13
CUSTOMER P.O. # 6039103
NAME OF LAB SAMPLER: LISA EDGAR, LAB TECHNICIAN

A325

**********CERTIFIED MATERIAL TEST REPORT**********

NUCOR PART NO	QUANTITY	LOT NO.	DESCRIPTION
161450	2475	320001A	7/8-9 X 3 1/4 A325 HVY HX

MANUFACTURE DATE 1/29/13 STRUC SCREW PLAIN

--CHEMISTRY MATERIAL GRADE -1037ML

MATERIAL NUMBER	HEAT NUMBER	**CHEMISTRY COMPOSITION (WT% HEAT ANALYSIS) BY MATERIAL SUPPLIER C	MN	P	S	SI	CR	
RM027879	NF12103881	.37	.77	.007	.021	.24	.35	NUCOR STEEL - NEBRASKA
	MIN	.30	.60			.15		
	MAX	.52		.040	.050	.30		

--MECHANICAL PROPERTIES IN ACCORDANCE WITH ASTM A325-10

SURFACE HARDNESS (R30N)	CORE HARDNESS (RC)	PROOF LOAD 39300 LBS	TENSILE STRENGTH 10 DEG-WEDGE (LBS)	STRESS (PSI)
N/A	31.0	PASS	69770	151017
N/A	29.5	PASS	70150	151840
N/A	29.9	PASS	68180	147576
N/A	29.7			
AVERAGE VALUES FROM TESTS		PRODUCTION LOT SIZE	12500 PCS	
	30.0		69367	150144

--VISUAL INSPECTION IN ACCORDANCE WITH ASTM A325-10 4 PCS. SAMPLED LOT PASSED
HEAT TREATMENT - AUSTENITIZED, OIL QUENCHED & TEMPERED (MIN 800 DEG F)

--DIMENSIONS PER ASME B18.2.6-2006

CHARACTERISTIC	#SAMPLES TESTED	MINIMUM	MAXIMUM
Width Across Corners	8	1.6220	1.6280
Grip Length	8	1.6700	1.6900
Head Height	8	0.5470	0.5600
Threads	8	PASS	PASS

ALL TESTS ARE IN ACCORDANCE WITH THE LATEST REVISIONS OF THE METHODS PRESCRIBED IN THE APPLICABLE SAE AND ASTM SPECIFICATIONS. THE SAMPLES TESTED CONFORM TO THE SPECIFICATIONS AS DESCRIBED/LISTED ABOVE AND WERE MANUFACTURED FREE OF MERCURY CONTAMINATION. NO HEATS TO WHICH BISMUTH, SELENIUM, TELLURIUM, OR LEAD WAS INTENTIONALLY ADDED HAVE BEEN USED TO PRODUCE THE BOLTS.
THE STEEL WAS MELTED AND MANUFACTURED IN THE U.S.A. AND THE PRODUCT WAS MANUFACTURED AND TESTED IN THE U.S.A. PRODUCT COMPLIES WITH DFARS 252.225-7014. WE CERTIFY THAT THIS DATA IS A TRUE REPRESENTATION OF INFORMATION PROVIDED BY THE MATERIAL SUPPLIER AND OUR TESTING LABORATORY. THIS CERTIFIED MATERIAL TEST REPORT RELATES ONLY TO THE ITEMS LISTED ON THIS DOCUMENT AND MAY NOT BE REPRODUCED EXCEPT IN FULL.

A2LA ACCREDITED

MECHANICAL FASTENER
CERTIFICATE NO. A2LA 0139.01
EXPIRATION DATE 12/31/13

NUCOR FASTENER
A DIVISION OF NUCOR CORPORATION

John W. Ferguson

JOHN W. FERGUSON
QUALITY ASSURANCE SUPERVISOR

12B- MRE 1/3 -4W/2W-1.00-0.75-36
12B- MRE 1/3 -4W/2W-1.00-0.75-60

FONTANA FASTENERS

TEST REPORT

Operations Center
3281 West County Road 0 NS
Frankfort, IN 46041-6966
T. 765.654.0477
F. 765.654.0857

Ship Date	
Certification	374619*3*4
Report Date	10-01-13

Cust PO	6032446
Lot No	718615
Quantity	2025
Mfg Date	09-04-13

Birmingham Fastener, Inc.
Hanceville Dist. Center
1100 Main Street S.E.
Hanceville, AL 35077

PART INFORMATION

Part Number	100C300A32P/NND
Description	1-8 X 3 A325-1 HEAVY HEX STRUCTURAL DOUBLE MADE IN USA
Finish	PLAIN
Head Marking	A325 LE USA

RAW MATERIAL ANALYSIS

Steel Heat No	Steel Supplier	Steel Grade	Code	Element	Rqd Min Pct	Rqd Max Pct	Percent
CR10266090	Charter Steel	30MnCrB1	C	Carbon	0.30	0.33	0.32
			Mn	Manganese	0.85	1.00	0.92
			P	Phosphorus	0.000	0.020	0.010
			S	Sulfur	0.000	0.015	0.007
			Si	Silicon	0.150	0.250	0.220
			Ni	Nickel	0.00	0.10	0.04
			Cr	Chromium	0.15	0.25	0.16
			Mo	Molybdenum	0.07	0.12	0.08
			Cu	Copper	0.00	0.15	0.08
			Al	Aluminum	0.020	0.050	0.025
			B	Boron	0.0010	0.0030	0.0030
			Ti	Titanium	0.010	0.050	0.018

Certification test results include those reported by the following laboratories:
Charter Steel, A2LA, 01-31-13
LEP Special Fasteners, Inc, ISO17025-A2LA Cert#0122.02, 05-31-12

MECHANICAL PROPERTIES

Wedge Angle	10
Proof Load	51500/85000 (lbs/Psi)

Test Performed	Required	High	Low	Average	Samples
Tensile, PSI	120000 / 160000	152000	150000	151500	4
Proof Load Elongation	0.0000 / 0.0005	0.0004	0	0.0003	4
Superficial R30N	45 / 54	50	48	49	4
Core Hardness, HRC	25 / 34	30	29	30	4

NUCOR
FASTENER DIVISION

LOT NO.
296893A

6B-4W/2W-1.125-0.75-36
6B-4W/2W-1.125-0.75-60

Post Office Box 6100
Saint Joe, Indiana 46785
Telephone 260/337-1600

CUSTOMER NO/NAME
9000 BIRMINGHAM-CONS/SHIPPING

NUCOR ORDER # 800846
CUST PART #

TEST REPORT SERIAL# FB374074
TEST REPORT ISSUE DATE 10/24/11
DATE SHIPPED 10/04/12
NAME OF LAB SAMPLER: JEFFREY HOERING, LAB TECHNICIAN
CUSTOMER P.O. # 6005629

A325 HVY

**********CERTIFIED MATERIAL TEST REPORT**********

NUCOR PART NO	QUANTITY	LOT NO.	DESCRIPTION
163200	680	296893A	1 1/8-7 X 3 A325 HVY HX STRUC SCREW PLAIN

MANUFACTURE DATE 10/19/11

--CHEMISTRY MATERIAL GRADE -1039ML

MATERIAL NUMBER	HEAT NUMBER	**CHEMISTRY COMPOSITION (WT% HEAT ANALYSIS) BY MATERIAL SUPPLIER C	MN	P	S	SI	CR
RM026821	NF11103101	.38	.79	.011	.020	.24	.43
	MIN	.30	.60			.10	
	MAX	.52		.040	.050	.30	

NUCOR STEEL - NEBRASKA

--MECHANICAL PROPERTIES IN ACCORDANCE WITH ASTM A325-10

SURFACE HARDNESS (R30N)	CORE HARDNESS (RC)	PROOF LOAD N/A (LBS)	TENSILE STRENGTH DEG-WEDGE STRESS (PSI)
N/A	28.9	N/A	N/A N/A
N/A	27.0	N/A	N/A N/A
N/A	27.6	N/A	N/A N/A
N/A	26.4	N/A	N/A N/A
AVERAGE VALUES FROM TESTS		PRODUCTION LOT SIZE	3275 PCS
	27.5		TOO SHORT TO TEST

--VISUAL INSPECTION IN ACCORDANCE WITH ASTM A325-10 4 PCS. SAMPLED LOT PASSED
HEAT TREATMENT - AUSTENITIZED, OIL QUENCHED & TEMPERED (MIN 800 DEG F)

--DIMENSIONS PER ASME B18.2.6-2006

CHARACTERISTIC	#SAMPLES TESTED	MINIMUM	MAXIMUM
Width Across Corners	4	2.0550	2.0630
Grip Length	4	0.8840	0.9550
Head Height	4	0.6830	0.7090
Threads	4	PASS	PASS

ALL TESTS ARE IN ACCORDANCE WITH THE LATEST REVISIONS OF THE METHODS PRESCRIBED IN THE APPLICABLE SAE AND ASTM SPECIFICATIONS. THE SAMPLES TESTED CONFORM TO THE SPECIFICATIONS AS DESCRIBED/LISTED ABOVE AND WERE MANUFACTURED FREE OF MERCURY CONTAMINATION. NO HEATS TO WHICH BISMUTH, SELENIUM, TELLURIUM, OR LEAD WAS INTENTIONALLY ADDED HAVE BEEN USED TO PRODUCE THE BOLTS.
THE STEEL WAS MELTED AND MANUFACTURED IN THE U.S.A. AND THE PRODUCT WAS MANUFACTURED AND TESTED IN THE U.S.A.
PRODUCT COMPLIES WITH DFARS 252.225-7014. WE CERTIFY THAT THIS DATA IS A TRUE REPRESENTATION OF INFORMATION PROVIDED BY THE MATERIAL SUPPLIER AND OUR TESTING LABORATORY. THIS CERTIFIED MATERIAL TEST REPORT RELATES ONLY TO THE ITEMS LISTED ON THIS DOCUMENT AND MAY NOT BE REPRODUCED EXCEPT IN FULL.

ACCREDITED

MECHANICAL FASTENER
CERTIFICATE NO. A2LA 0139.01
EXPIRATION DATE 12/31/11

NUCOR FASTENER
A DIVISION OF NUCOR CORPORATION

BOB HAYWOOD
QUALITY ASSURANCE SUPERVISOR

Appendix C Test Summaries

TEST SUMMARY

TEST NAME: TEST 1: 6B-4W/2W-0.875-1.00-36 (THICK END PLATE BEHAVIOR)
TEST DATE: 5-Dec-14

CONNECTION DESCRIPTION

TYPE	Flush - Unstiffened End-Plate, 4 Bolts Wide	
NUMBER OF TENSION BOLTS	6 (all inside)	
NUMBER OF COMPRESSION BOLTS	6	

BEAM DATA

SECTION TYPE	Built-Up	
DEPTH, h	36	in.
FLANGE WIDTH, b_f	12	in.
FLANGE THICKNESS, t_f	0.75	in.
NOMINAL WEB THICKNESS, t_w	0.25	in.
MOMENT OF INERTIA, I	6445	in^4.
NOMINAL YIELD STRESS, F_y	55	ksi

END PLATE DATA

END PLATE THICKNESS, t_p	1	in.
END PLATE WIDTH, b_p	14	in.
END PLATE LENGTH, L_p	36	in.
END PLATE EXTENSION OUTSIDE FLANGE, p_{ext}	0	in.
OUTER PITCH, BOLT TO FLANGE, p_{fo}	N.A.	in.
INNER PITCH, BOLT TO FLANGE, p_{fi}	2.25	in.
INSIDE PITCH, BOLT TO BOLT, p_b	3.5	in.
INSIDE BOLT GAGE, g	4.5	in.
OUTSIDE BOLT GAGE, g_o	3	in.
MEASURED YIELD STRESS, F_{yp}	59.3	ksi

BOLT DATA

NOMINAL BOLT DIAMETER, d_b	0.875	in.
NOMNAL BOLT LENGTH, L_b	3.25	in.
BOLT TYPE	ASTM A325	
AVERAGE BOLT PRETENSION, T_b	Turn of the Nut Method (34 kips)	
NOMINAL BOLT TENSILE STRESS(AISC J3.6), F_t:	90	ksi
NOMINAL BOLT TENSILE STRENGTH, P_t	54.13	kips

EXPERIMENTAL RESULTS

MAXIMUM APPLIED MOMENT, M_u	1030	k-ft
YIELD MOMENT (based on plate separation), M_y	770	k-ft
FAILURE MODE	Bolt Rupture with negligible end-plate yielding	

PREDICTED STRENGTHS

END PLATE STRENGTH, M_{pl}	1440	k-ft
BOLT TENSION RUPTURE (with prying), M_q	N.A.	k-ft
BOLT TENSION RUPTURE (without prying), M_{np}	851	k-ft
CONTROLLING STRENGTH, M_n	851	k-ft
BOLT TENSION RUPTURE (without prying), M_{np}^{exp}	1090	k-ft

TEST SUMMARY

TEST NAME: TEST 2: 6B-4W/2W-1.125-0.75-36 (THIN END PLATE BEHAVIOR)
TEST DATE: 19-Dec-14

CONNECTION DESCRIPTION

TYPE	Flush - Unstiffened End-Plate, 4 Bolts Wide	
NUMBER OF TENSION BOLTS	6 (all inside)	
NUMBER OF COMPRESSION BOLTS	6	

BEAM DATA

SECTION TYPE	Built-Up	
DEPTH, h	36	in.
FLANGE WIDTH, b_f	11 15/16	in.
FLANGE THICKNESS, t_f	0.755	in.
NOMINAL WEB THICKNESS, t_w	0.25	in.
MOMENT OF INERTIA, I	6447.9	in^4.
NOMINAL YIELD STRESS, F_y	55	ksi

END PLATE DATA

END PLATE THICKNESS, t_p	0.753	in.
END PLATE WIDTH, b_p	14	in.
END PLATE LENGTH, L_p	36	in.
END PLATE EXTENSION OUTSIDE FLANGE, p_{ext}	0	in.
OUTER PITCH, BOLT TO FLANGE, p_{fo}	N.A.	in.
INNER PITCH, BOLT TO FLANGE, p_{fi}	2.25	in.
INSIDE PITCH, BOLT TO BOLT, p_b	3.5	in.
INSIDE BOLT GAGE, g	4.5	in.
OUTSIDE BOLT GAGE, g_o	3	in.
MEASURED YIELD STRESS, F_{yp}	54.6	ksi

BOLT DATA

NOMINAL BOLT DIAMETER, d_b		1.125	in.
NOMNAL BOLT LENGTH, L_b		3	in.
BOLT TYPE		ASTM A325	
AVERAGE BOLT PRETENSION, T_b	(almost 1/2 turn)	58	kips
NOMINAL BOLT TENSILE STRESS(AISC J3.6), F_t:		90	ksi
NOMINAL BOLT TENSILE STRENGTH, P_t		89.47	kips

EXPERIMENTAL RESULTS

MAXIMUM APPLIED MOMENT, M_u	1110	k-ft
YIELD MOMENT (based on plate separation), M_y	730	k-ft
FAILURE MODE	End Plate Yielding followed by Bolt Rupture	

PREDICTED STRENGTHS

END PLATE STRENGTH, M_{pl}	748	k-ft
BOLT TENSION RUPTURE (with prying), M_q	957	k-ft
BOLT TENSION RUPTURE (without prying), M_{np}	1410	k-ft
CONTROLLING STRENGTH, M_n	748	k-ft
BOLT TENSION RUPTURE (with prying), M_q^{exp}	1100	k-ft

TEST SUMMARY

TEST NAME: TEST 3: 12BE-MRE 1/3-4W/2W-1.00-0.75-36 (THIN END PLATE BEHAVIOR)
TEST DATE: 28-Jan-15

CONNECTION DESCRIPTION

TYPE	Multiple Row Extended Unstiffened End-Plate, 4 Bolts Wide
NUMBER OF TENSION BOLTS	12 (4 outside in one row, 8 inside in 3 rows)
NUMBER OF COMPRESSION BOLTS	12 (4 outside in one row, 8 inside in 3 rows)

BEAM DATA

SECTION TYPE	Built-Up	
DEPTH, h	36	in.
FLANGE WIDTH, b_f	12	in.
FLANGE THICKNESS, t_f	0.75	in.
NOMINAL WEB THICKNESS, t_w	0.25	in.
MOMENT OF INERTIA, I	6447.9	in^4.
NOMINAL YIELD STRESS, F_y	55	ksi

END PLATE DATA

END PLATE THICKNESS, t_p	0.753	in.
END PLATE WIDTH, b_p	14	in.
END PLATE LENGTH, L_p	36	in.
END PLATE EXTENSION OUTSIDE FLANGE, p_{ext}	4	in.
OUTER PITCH, BOLT TO FLANGE, p_{fo}	2.25	in.
INNER PITCH, BOLT TO FLANGE, p_{fi}	2.25	in.
INSIDE PITCH, BOLT TO BOLT, p_b	3.5	in.
INSIDE BOLT GAGE, g	4.5	in.
OUTSIDE BOLT GAGE, g_o	3	in.
MEASURED YIELD STRESS, F_{yp}	54.6	ksi

BOLT DATA

NOMINAL BOLT DIAMETER, d_b		1	in.
NOMNAL BOLT LENGTH, L_b		2.75	in.
BOLT TYPE		ASTM A325	
AVERAGE BOLT PRETENSION, T_b	(aprox 150 degree)	53	kips
NOMINAL BOLT TENSILE STRESS(AISC J3.6), F_t:		90	ksi
NOMINAL BOLT TENSILE STRENGTH, P_t		70.67	kips

EXPERIMENTAL RESULTS

MAXIMUM APPLIED MOMENT, M_u	1640	k-ft
YIELD MOMENT (based on plate separation), M_y	1230	k-ft
FAILURE MODE	End Plate Yielding	

(Bolt Rupture couldn't be observed due to insufficient capacity of the section)

PREDICTED STRENGTHS

END PLATE STRENGTH, M_{pl}	1130	k-ft
BOLT TENSION RUPTURE (with prying), M_q	1420	k-ft
BOLT TENSION RUPTURE (without prying), M_{np}	2310	k-ft
CONTROLLING STRENGTH, M_n	1130	k-ft
BOLT TENSION RUPTURE (with prying), M_q^{exp}	1870	k-ft

TEST SUMMARY

TEST NAME: TEST 4: 12B-MRE 1/3-4W/2W-0.75-1.00-36 (THICK END PLATE BEHAVIOR)
TEST DATE: 3-Feb-15

CONNECTION DESCRIPTION

TYPE	Multiple Row Extended Unstiffened End-Plate, 4 Bolts Wide
NUMBER OF TENSION BOLTS	12 (4 outside in one row, 8 inside in 3 rows)
NUMBER OF COMPRESSION BOLTS	12 (4 outside in one row, 8 inside in 3 rows)

BEAM DATA

SECTION TYPE		Built-Up	
DEPTH, h		36	in.
FLANGE WIDTH, b_f		12	in.
FLANGE THICKNESS, t_f		0.75	in.
NOMINAL WEB THICKNESS, t_w		0.25	in.
MOMENT OF INERTIA, I		6447.9	in^4.
NOMINAL YIELD STRESS, F_y		55	ksi

END PLATE DATA

END PLATE THICKNESS, t_p		1	in.
END PLATE WIDTH, b_p		14	in.
END PLATE LENGTH, L_p		36	in.
END PLATE EXTENSION OUTSIDE FLANGE, p_{ext}		4	in.
OUTER PITCH, BOLT TO FLANGE, p_{fo}		2.25	in.
INNER PITCH, BOLT TO FLANGE, p_{fi}		2.25	in.
INSIDE PITCH, BOLT TO BOLT, p_b		3.5	in.
INSIDE BOLT GAGE, g		4.5	in.
OUTSIDE BOLT GAGE, g_o		3	in.
MEASURED YIELD STRESS, F_{yp}		59.3	ksi

BOLT DATA

NOMINAL BOLT DIAMETER, d_b		0.75	in.
NOMNAL BOLT LENGTH, L_b		3	in.
BOLT TYPE		ASTM A325	
AVERAGE BOLT PRETENSION, T_b	(aprox 150 degree)	28.7	kips
NOMINAL BOLT TENSILE STRESS(AISC J3.6), F_t:		90	ksi
NOMINAL BOLT TENSILE STRENGTH, P_t		39.73	kips

EXPERIMENTAL RESULTS

MAXIMUM APPLIED MOMENT, M_u	1490	k-ft
YIELD MOMENT (based on plate separation), M_y	960	k-ft
FAILURE MODE	Bolt Rupture	

PREDICTED STRENGTHS

END PLATE STRENGTH, M_{pl}	2190	k-ft
BOLT TENSION RUPTURE (with prying), M_q	N.A.	k-ft
BOLT TENSION RUPTURE (without prying), M_{np}	1300	k-ft
CONTROLLING STRENGTH, M_n	1300	k-ft
BOLT TENSION RUPTURE (without prying), M_{np}^{exp}	1630	k-ft

TEST SUMMARY

TEST NAME: TEST 5: 6B/4W-0.875-1.00-60 (THICK END PLATE BEHAVIOR)
TEST DATE: 27-Feb-15

CONNECTION DESCRIPTION

TYPE	Flush - Unstiffened End-Plate, 4 Bolts Wide	
NUMBER OF TENSION BOLTS	6 (all inside)	
NUMBER OF COMPRESSION BOLTS	6	

BEAM DATA

SECTION TYPE	Built-Up	
DEPTH, h	60	in.
FLANGE WIDTH, b_f	12	in.
FLANGE THICKNESS, t_f	0.75	in.
NOMINAL WEB THICKNESS, t_w	0.375	in.
MOMENT OF INERTIA, I	22054.7	in^4.
NOMINAL YIELD STRESS, F_y	55	ksi

END PLATE DATA

END PLATE THICKNESS, t_p	1	in.
END PLATE WIDTH, b_p	14	in.
END PLATE LENGTH, L_p	60	in.
END PLATE EXTENSION OUTSIDE FLANGE, p_{ext}	N.A.	in.
OUTER PITCH, BOLT TO FLANGE, p_{fo}	N.A.	in.
INNER PITCH, BOLT TO FLANGE, p_{fi}	2.25	in.
INSIDE PITCH, BOLT TO BOLT, p_b	3.5	in.
INSIDE BOLT GAGE, g	4.5	in.
OUTSIDE BOLT GAGE, g_o	3	in.
MEASURED YIELD STRESS, F_{yp}	59.3	ksi

BOLT DATA

NOMINAL BOLT DIAMETER, d_b		0.875	in.
NOMNAL BOLT LENGTH, L_b		3	in.
BOLT TYPE	ASTM A325		
AVERAGE BOLT PRETENSION, T_b	(aprox 165 degree)	40.0	kips
NOMINAL BOLT TENSILE STRESS(AISC J3.6), F_t:		90	ksi
NOMINAL BOLT TENSILE STRENGTH, P_t		54.13	kips

EXPERIMENTAL RESULTS

MAXIMUM APPLIED MOMENT, M_u	1730	k-ft
YIELD MOMENT (based on plate separation), M_y	1390	k-ft
FAILURE MODE	Bolt Rupture without any end-plate yielding	

PREDICTED STRENGTHS

END PLATE STRENGTH, M_{pl}	2530	k-ft
BOLT TENSION RUPTURE (with prying), M_q	N.A.	k-ft
BOLT TENSION RUPTURE (without prying), M_{np}	1500	k-ft
CONTROLLING STRENGTH, M_n	1500	k-ft
BOLT TENSION RUPTURE (without prying), M_{np}^{exp}	1920	k-ft

TEST SUMMARY

TEST NAME: TEST 6: 6B-4W/2W-1.125-0.75-60 (THIN END PLATE BEHAVIOR)
TEST DATE: 5-Mar-15

CONNECTION DESCRIPTION

TYPE	Flush - Unstiffened End-Plate, 4 Bolts Wide	
NUMBER OF TENSION BOLTS	6 (all inside)	
NUMBER OF COMPRESSION BOLTS	6	

BEAM DATA

SECTION TYPE	Built-Up	
DEPTH, h	60	in.
FLANGE WIDTH, b_f	12	in.
FLANGE THICKNESS, t_f	0.75	in.
NOMINAL WEB THICKNESS, t_w	0.375	in.
MOMENT OF INERTIA, I	22054.7	in^4.
NOMINAL YIELD STRESS, F_y	55	ksi

END PLATE DATA

END PLATE THICKNESS, t_p	0.75	in.
END PLATE WIDTH, b_p	14	in.
END PLATE LENGTH, L_p	60	in.
END PLATE EXTENSION OUTSIDE FLANGE, p_{ext}	N.A.	in.
OUTER PITCH, BOLT TO FLANGE, p_{fo}	N.A.	in.
INNER PITCH, BOLT TO FLANGE, p_{fi}	2.25	in.
INSIDE PITCH, BOLT TO BOLT, p_b	3.5	in.
INSIDE BOLT GAGE, g	4.5	in.
OUTSIDE BOLT GAGE, g_o	3	in.
MEASURED YIELD STRESS, F_{yp}	54.6	ksi

BOLT DATA

NOMINAL BOLT DIAMETER, d_b		1.125	in.
NOMNAL BOLT LENGTH, L_b		3	in.
BOLT TYPE		ASTM A325	
AVERAGE BOLT PRETENSION, T_b	(aprox 165 degree)	59.0	kips
NOMINAL BOLT TENSILE STRESS(AISC J3.6), F_t:		90	ksi
NOMINAL BOLT TENSILE STRENGTH, P_t		89.47	kips

EXPERIMENTAL RESULTS

MAXIMUM APPLIED MOMENT, M_u	1980	k-ft
YIELD MOMENT (based on plate separation), M_y	1400	k-ft
FAILURE MODE	End-Plate Yielding followed by Bolt Rupture	

PREDICTED STRENGTHS

END PLATE STRENGTH, M_{pl}	1310	k-ft
BOLT TENSION RUPTURE (with prying), M_q	1680	k-ft
BOLT TENSION RUPTURE (without prying), M_{np}	2480	k-ft
CONTROLLING STRENGTH, M_n	1310	k-ft
BOLT TENSION RUPTURE (with prying), M_q^{exp}	1930	k-ft

TEST SUMMARY

TEST NAME: TEST 7: 12B-MRE 1/3-4W/2W-1.00-0.75-60 (THIN END PLATE BEHAVIOR)
TEST DATE: 20-Mar-15

CONNECTION DESCRIPTION

TYPE	Extended - Unstiffened End-Plate, 4 Bolts Wide	
NUMBER OF TENSION BOLTS	8 inside + 4 outside	
NUMBER OF COMPRESSION BOLTS	12	

BEAM DATA

SECTION TYPE	Built-Up	
DEPTH, h	60	in.
FLANGE WIDTH, b_f	12	in.
FLANGE THICKNESS, t_f	0.75	in.
NOMINAL WEB THICKNESS, t_w	0.375	in.
MOMENT OF INERTIA, I	22054.7	in^4.
NOMINAL YIELD STRESS, F_y	55	ksi

END PLATE DATA

END PLATE THICKNESS, t_p	0.75	in.
END PLATE WIDTH, b_p	14	in.
END PLATE LENGTH, L_p	60	in.
END PLATE EXTENSION OUTSIDE FLANGE, p_{ext}	4	in.
OUTER PITCH, BOLT TO FLANGE, p_{fo}	2.25	in.
INNER PITCH, BOLT TO FLANGE, p_{fi}	2.25	in.
INSIDE PITCH, BOLT TO BOLT, p_b	3.5	in.
INSIDE BOLT GAGE, g	4.5	in.
OUTSIDE BOLT GAGE, g_o	3	in.
MEASURED YIELD STRESS, F_{yp}	54.5	ksi

BOLT DATA

NOMINAL BOLT DIAMETER, d_b		1	in.
NOMNAL BOLT LENGTH, L_b		2.75	in.
BOLT TYPE		ASTM A325	
AVERAGE BOLT PRETENSION, T_b	(aprox 120 degree)	52.0	kips
NOMINAL BOLT TENSILE STRESS(AISC J3.6), F_t:		90	ksi
NOMINAL BOLT TENSILE STRENGTH, P_t		70.69	kips

EXPERIMENTAL RESULTS

MAXIMUM APPLIED MOMENT, M_u	2760	k-ft
YIELD MOMENT (based on plate separation), M_y	2230	k-ft
FAILURE MODE	No Bolt Rupture but end-plate yielding seen	

PREDICTED STRENGTHS

END PLATE STRENGTH, M_{pl}	1980	k-ft
BOLT TENSION RUPTURE (with prying), M_q	2450	k-ft
BOLT TENSION RUPTURE (without prying), M_{np}	4000	k-ft
CONTROLLING STRENGTH, M_n	1980	k-ft
BOLT TENSION RUPTURE (with prying), M_q^{exp}	3220	k-ft

TEST SUMMARY

TEST NAME: TEST 8: 12B-MRE 1/3-4W/2W-0.75-1.00-60 (THICK END PLATE BEHAVIOR)
TEST DATE: 3-Apr-15

CONNECTION DESCRIPTION

TYPE	Extended - Unstiffened End-Plate, 4 Bolts Wide	
NUMBER OF TENSION BOLTS	8 inside + 4 outside	
NUMBER OF COMPRESSION BOLTS	12	

BEAM DATA

SECTION TYPE	Built-Up	
DEPTH, h	60	in.
FLANGE WIDTH, b_f	12	in.
FLANGE THICKNESS, t_f	0.75	in.
NOMINAL WEB THICKNESS, t_w	0.375	in.
MOMENT OF INERTIA, I	22054.7	in^4.
NOMINAL YIELD STRESS, F_y	55	ksi

END PLATE DATA

END PLATE THICKNESS, t_p	1	in.
END PLATE WIDTH, b_p	14	in.
END PLATE LENGTH, L_p	60	in.
END PLATE EXTENSION OUTSIDE FLANGE, p_{ext}	4	in.
OUTER PITCH, BOLT TO FLANGE, p_{fo}	2.25	in.
INNER PITCH, BOLT TO FLANGE, p_{fi}	2.25	in.
INSIDE PITCH, BOLT TO BOLT, p_b	3.5	in.
INSIDE BOLT GAGE, g	4.5	in.
OUTSIDE BOLT GAGE, g_o	3	in.
MEASURED YIELD STRESS, F_{yp}	59.3	ksi

BOLT DATA

NOMINAL BOLT DIAMETER, d_b		0.75	in.
NOMNAL BOLT LENGTH, L_b		3	in.
BOLT TYPE	ASTM A325		
AVERAGE BOLT PRETENSION, T_b	(aprox 150 degree)	32.0	kips
NOMINAL BOLT TENSILE STRESS(AISC J3.6), F_t:		90	ksi
NOMINAL BOLT TENSILE STRENGTH, P_t		39.76	kips

EXPERIMENTAL RESULTS

MAXIMUM APPLIED MOMENT, M_u	2490	k-ft
YIELD MOMENT (based on plate separation), M_y	2100	k-ft
FAILURE MODE	Bolt Rupture with no end-plate yielding	

PREDICTED STRENGTHS

END PLATE STRENGTH, M_{pl}	3830	k-ft
BOLT TENSION RUPTURE (with prying), M_q	N.A.	k-ft
BOLT TENSION RUPTURE (without prying), M_{np}	2250	k-ft
CONTROLLING STRENGTH, M_n	2250	k-ft
BOLT TENSION RUPTURE (without prying), M_{np}^{exp}	2820	k-ft

TEST SUMMARY

TEST NAME: TEST 9: 8ES-1.00-1.00-56 (THICK END PLATE BEHAVIOR)
TEST DATE: 10-Apr-15

CONNECTION DESCRIPTION

TYPE	Extended - Stiffened End-Plate	
NUMBER OF TENSION BOLTS	4 inside + 4 outside	
NUMBER OF COMPRESSION BOLTS	12	

BEAM DATA

SECTION TYPE	Built-Up	
DEPTH, h	56	in.
FLANGE WIDTH, b_f	10	in.
FLANGE THICKNESS, t_f	1	in.
NOMINAL WEB THICKNESS, t_w	0.5	in.
MOMENT OF INERTIA, I	21688	in^4.
NOMINAL YIELD STRESS, F_y	55	ksi

END PLATE DATA

END PLATE THICKNESS, t_p	1	in.
END PLATE WIDTH, b_p	10	in.
END PLATE LENGTH, L_p	71	in.
END PLATE EXTENSION OUTSIDE FLANGE, p_{ext}	7.5	in.
OUTER PITCH, BOLT TO FLANGE, p_{fo}	2.25	in.
INNER PITCH, BOLT TO FLANGE, p_{fi}	2.25	in.
INSIDE PITCH, BOLT TO BOLT, p_b	3.5	in.
INSIDE BOLT GAGE, g	5	in.
OUTSIDE BOLT GAGE, g_o	N.A	in.
MEASURED YIELD STRESS, F_{yp}	58.2	ksi

BOLT DATA

NOMINAL BOLT DIAMETER, d_b		1	in.
NOMNAL BOLT LENGTH, L_b		3.5	in.
BOLT TYPE	ASTM A325		
AVERAGE BOLT PRETENSION, T_b	(aprox 120 degree)	53.0	kips
NOMINAL BOLT TENSILE STRESS(AISC J3.6), F_t:		90	ksi
NOMINAL BOLT TENSILE STRENGTH, P_t		70.69	kips

EXPERIMENTAL RESULTS

MAXIMUM APPLIED MOMENT, M_u	3050	k-ft
YIELD MOMENT (based on plate separation), M_y	2520	k-ft
FAILURE MODE	Bolt Rupture with minimal end-plate yielding	

PREDICTED STRENGTHS

END PLATE STRENGTH, M_{pl}	4160	k-ft
BOLT TENSION RUPTURE (with prying), M_q	N.A.	k-ft
BOLT TENSION RUPTURE (without prying), M_{np}	2630	k-ft
CONTROLLING STRENGTH, M_n	2630	k-ft
BOLT TENSION RUPTURE (without prying), M_{np}^{exp}	3420	k-ft

TEST SUMMARY

TEST NAME: TEST 10: 8ES-1.25-0.75-56 (THICK END PLATE BEHAVIOR)
TEST DATE: 17-Apr-15

CONNECTION DESCRIPTION

TYPE	Extended - Stiffened End-Plate	
NUMBER OF TENSION BOLTS	4 inside + 4 outside	
NUMBER OF COMPRESSION BOLTS	12	

BEAM DATA

SECTION TYPE	Built-Up	
DEPTH, h	56	in.
FLANGE WIDTH, b_f	10	in.
FLANGE THICKNESS, t_f	1	in.
NOMINAL WEB THICKNESS, t_w	0.5	in.
MOMENT OF INERTIA, I	21688	in^4
NOMINAL YIELD STRESS, F_y	55	ksi

END PLATE DATA

END PLATE THICKNESS, t_p	1	in.
END PLATE WIDTH, b_p	10	in.
END PLATE LENGTH, L_p	71	in.
END PLATE EXTENSION OUTSIDE FLANGE, p_{ext}	7.5	in.
OUTER PITCH, BOLT TO FLANGE, p_{fo}	2.25	in.
INNER PITCH, BOLT TO FLANGE, p_{fi}	2.25	in.
INSIDE PITCH, BOLT TO BOLT, p_b	3.5	in.
INSIDE BOLT GAGE, g	5	in.
OUTSIDE BOLT GAGE, g_o	N.A	in.
MEASURED YIELD STRESS, F_{yp}	57.2	ksi

BOLT DATA

NOMINAL BOLT DIAMETER, d_b		1.25	in.
NOMNAL BOLT LENGTH, L_b		3.5	in.
BOLT TYPE	ASTM A325		
AVERAGE BOLT PRETENSION, T_b	(aprox 120 degree)	72.0	kips
NOMINAL BOLT TENSILE STRESS(AISC J3.6), F_t:		90	ksi
NOMINAL BOLT TENSILE STRENGTH, P_t		110.45	kips

EXPERIMENTAL RESULTS

MAXIMUM APPLIED MOMENT, M_u	2920	k-ft
YIELD MOMENT (based on plate separation), M_y	2400	k-ft
FAILURE MODE	No Bolt Rupture, but end-plate yielding seen	

PREDICTED STRENGTHS

END PLATE STRENGTH, M_{pl}	2300	k-ft
BOLT TENSION RUPTURE (with prying), M_q	2650	k-ft
BOLT TENSION RUPTURE (without prying), M_{np}	4110	k-ft
CONTROLLING STRENGTH, M_n	2300	k-ft
BOLT TENSION RUPTURE (with prying), M_q^{exp}	2960	k-ft

Appendix D Fabrication Drawings

NOTE: SPECIMENS WILL BE REUSED FOR A SECOND TEST BY ROTATING BEAM 180 DEGREES, FLIPPING OVER, AND CONNECTING THE UNTESTED END-PLATES

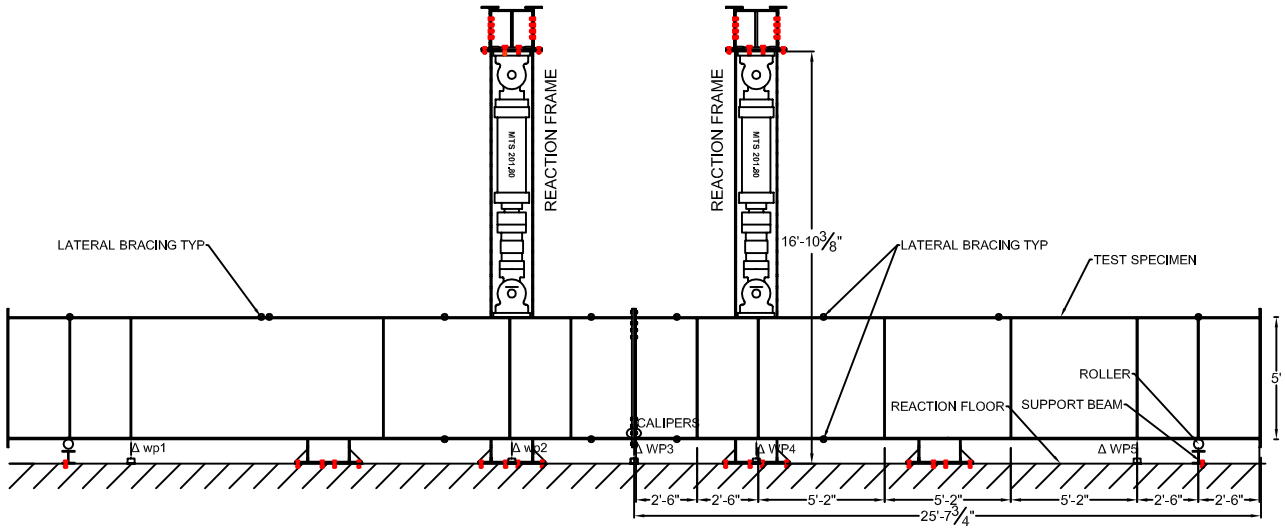

DEEP BEAM TEST SET-UP

NOTE: SPECIMENS WILL BE REUSED FOR A SECOND TEST BY ROTATING BEAM 180 DEGREES, FLIPPING OVER, AND CONNECTING THE UNTESTED END-PLATES

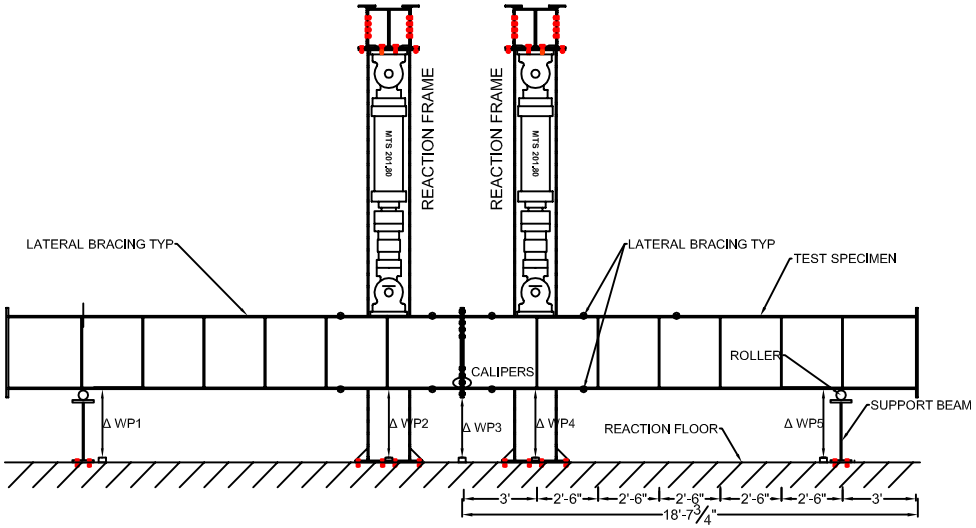

SHALLOW BEAM TEST SET-UP

VIRGINIA TECH	TITLE: TEST SET-UP ELEVATION	
PROJECT: MBMA END-PLATE MOMENT CONNECTIONS	05/09/14	SHEET 01

GIRDER SPECIMEN 01

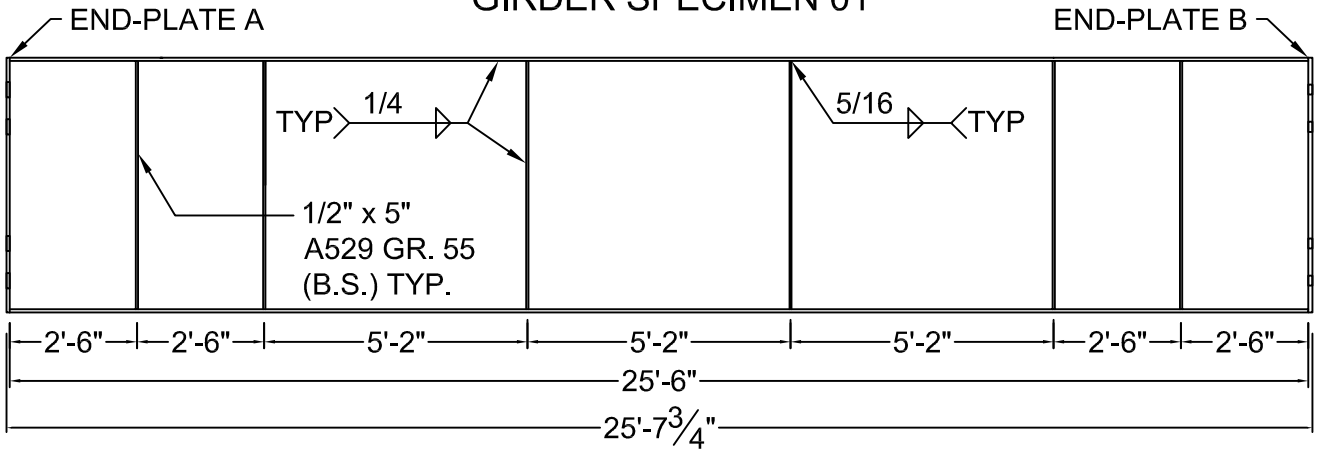

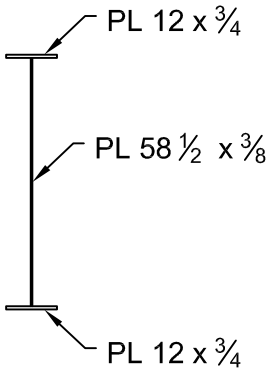

END PLATE A
THIN PLATE BEHAVIOR

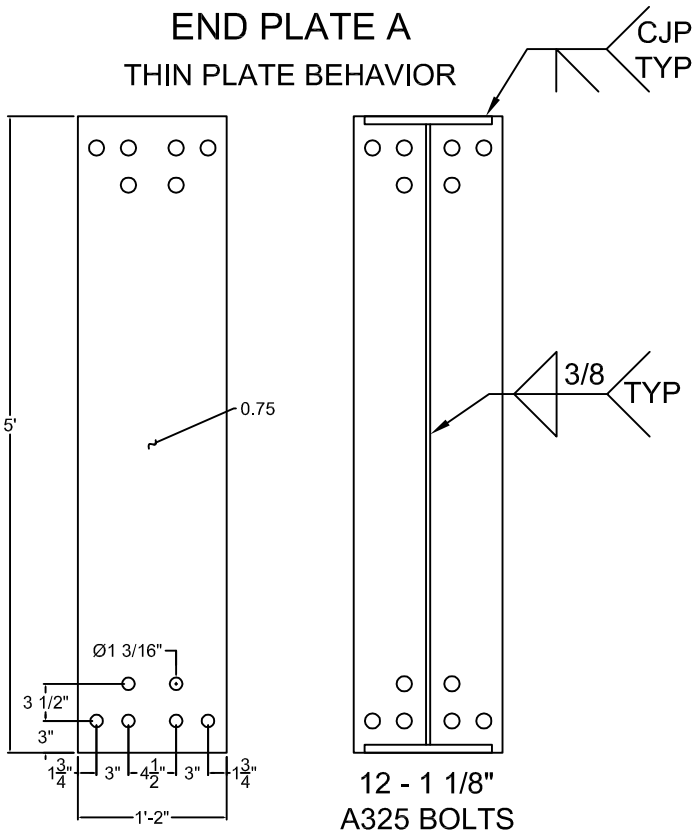

6B-4W/2W-1.125-0.75-60

END PLATE B
THICK PLATE BEHAVIOR

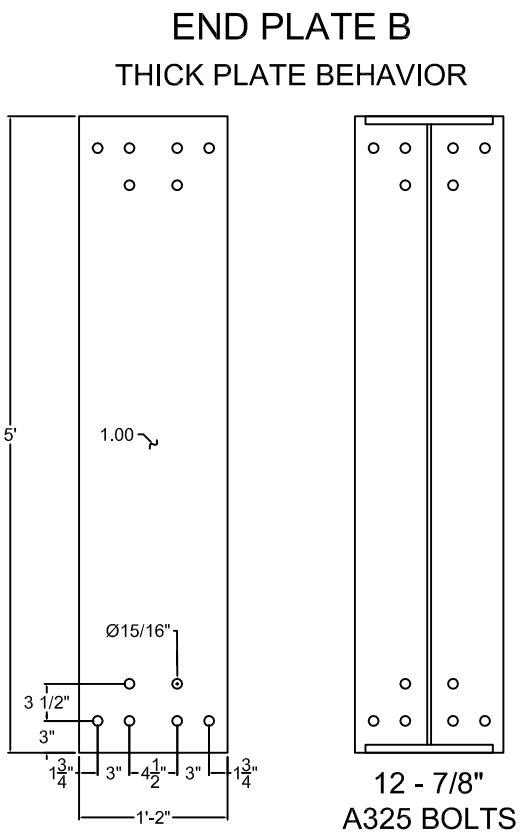

6B-4W/2W-0.875-1.00-60

QUANTITY: 2 EACH AND INCLUDE 18in x 14in COUPON FROM SAME HEAT OF MATERIAL AS END-PLATE. MATCH MARK COUPON AND END-PLATE FOR VERIFICATION

$F_{y\ end\text{-}plate}$ = 50 ksi ASSUMED

NO BLAST, NO PAINT

E70 ELECTRODES FOR ALL WELDS

VIRGINIA TECH	TITLE: SPECIMEN 01		
PROJECT: MBMA END-PLATE MOMENT CONNECTIONS		05/09/14	SHEET 02

GIRDER SPECIMEN 02

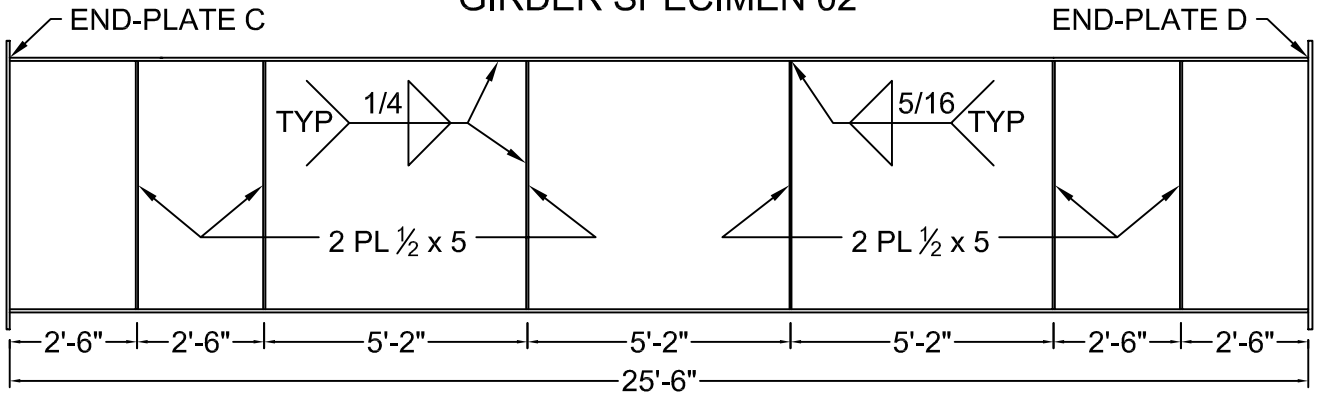

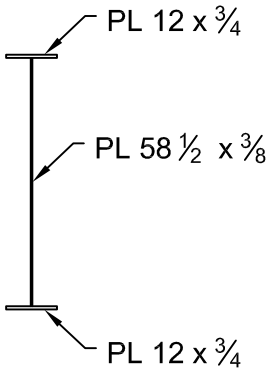

END PLATE C

THIN PLATE BEHAVIOR

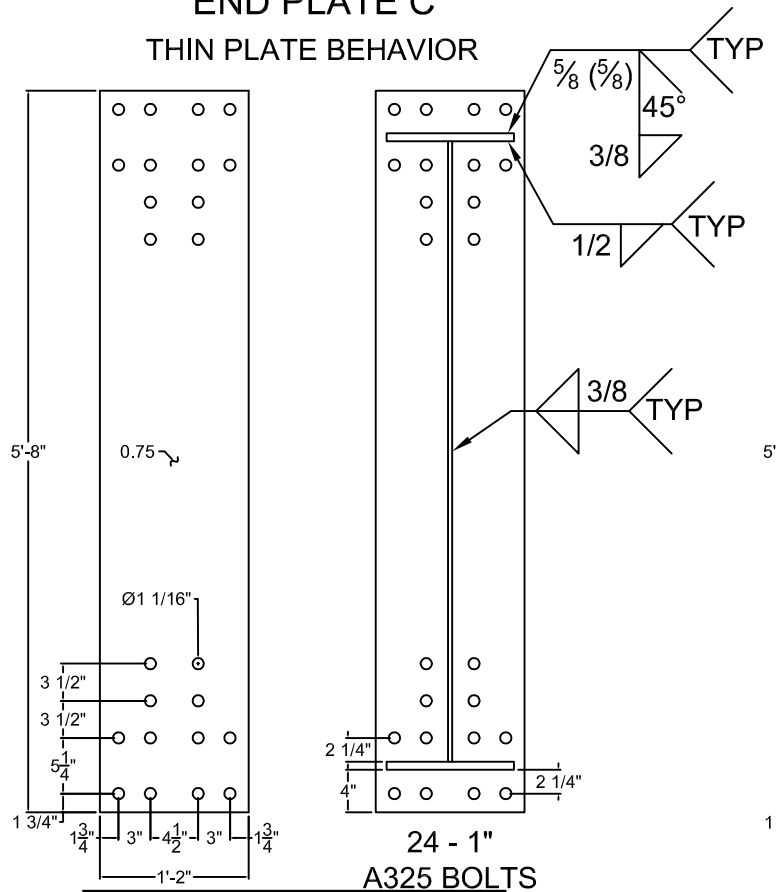

24 - 1"
A325 BOLTS

12B- MRE 1/3 -4W/2W-1.00-0.75-60

END PLATE D

THICK PLATE BEHAVIOR

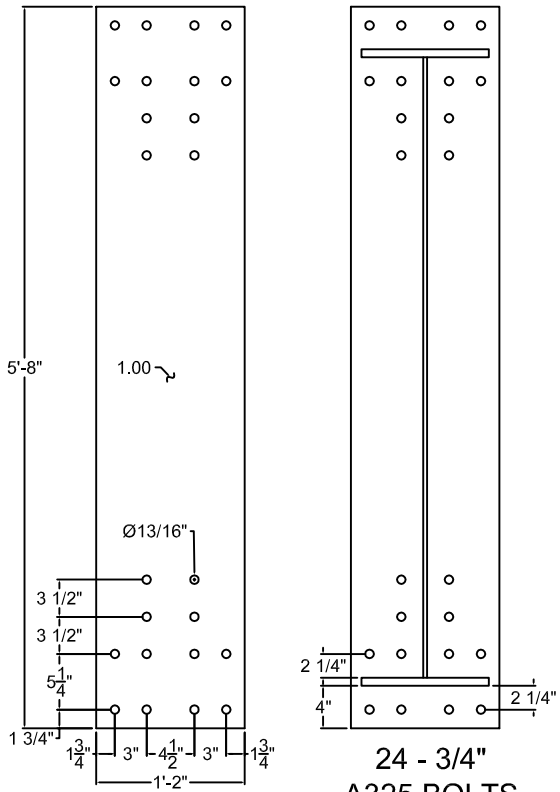

24 - 3/4"
A325 BOLTS

12B- MRE 1/3 -4W/2W-0.75-1.00-60

QUANTITY: 2 EACH AND INCLUDE 18in x 14in COUPON FROM SAME HEAT OF MATERIAL AS END-PLATE. MATCH MARK COUPON AND END-PLATE FOR VERIFICATION

$F_{y\ end\text{-}plate}$ = 50 ksi ASSUMED

NO BLAST, NO PAINT

E70 ELECTRODES FOR ALL WELDS

VIRGINIA TECH	TITLE: SPECIMEN 02	
PROJECT: MBMA END-PLATE MOMENT CONNECTIONS	05/09/14	SHEET 03

GIRDER SPECIMEN 03

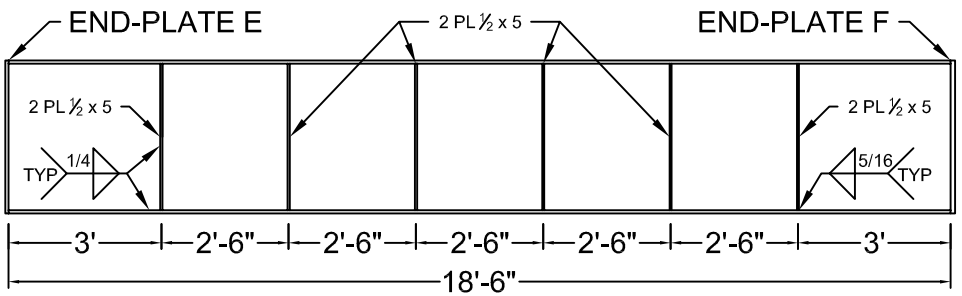

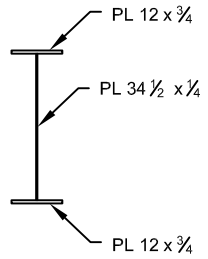

END PLATE E

THIN PLATE BEHAVIOR

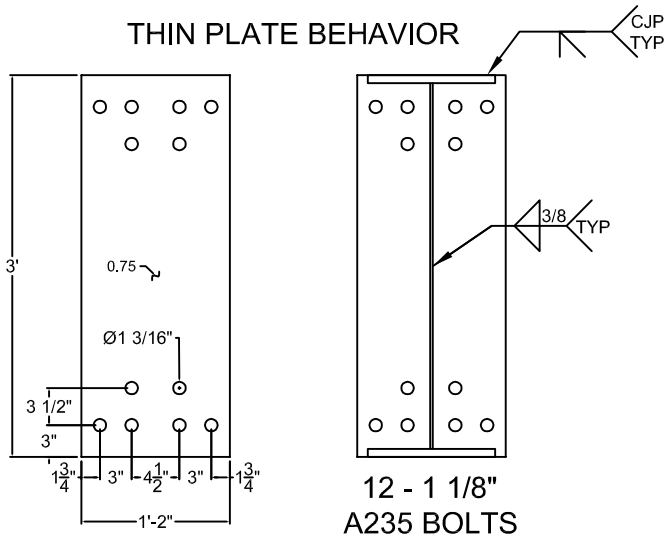

12 - 1 1/8"
A235 BOLTS

6B-4W/2W-1.125-0.75-36

END PLATE F

THICK PLATE BEHAVIOR

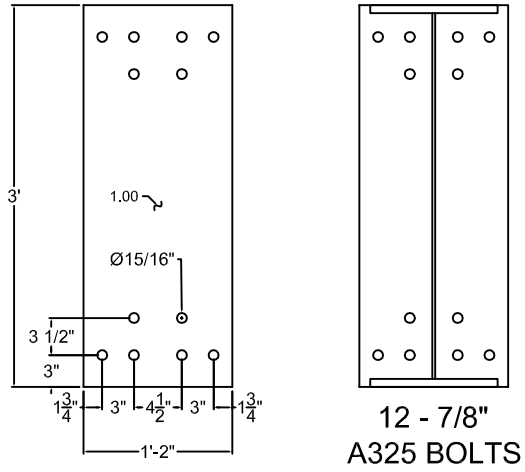

12 - 7/8"
A325 BOLTS

6B-4W/2W-0.875-1.00-36

QUANTITY: 2 EACH AND INCLUDE 18in x 14in COUPON FROM SAME HEAT OF MATERIAL AS END-PLATE. MATCH MARK COUPON AND END-PLATE FOR VERIFICATION

$F_{y\ end\text{-}plate}$ = 50 ksi ASSUMED

NO BLAST, NO PAINT

E70 ELECTRODES FOR ALL WELDS

VIRGINIA TECH	TITLE: SPECIMEN 03	
PROJECT: MBMA END-PLATE MOMENT CONNECTIONS	05/09/14	SHEET 04

GIRDER SPECIMEN 04

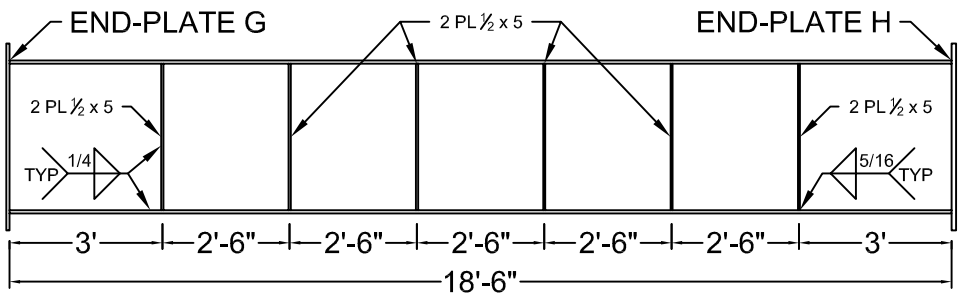

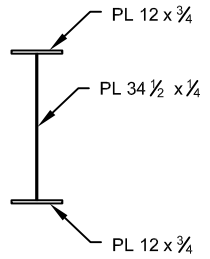

END PLATE G

THIN PLATE BEHAVIOR

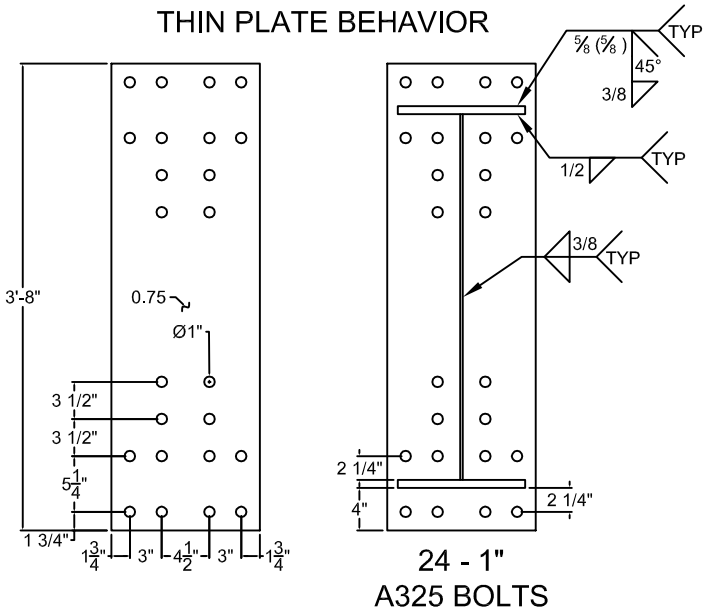

24 - 1"
A325 BOLTS

12B- MRE 1/3 -4W/2W-1.00-0.75-36

END PLATE H

THICK PLATE BEHAVIOR

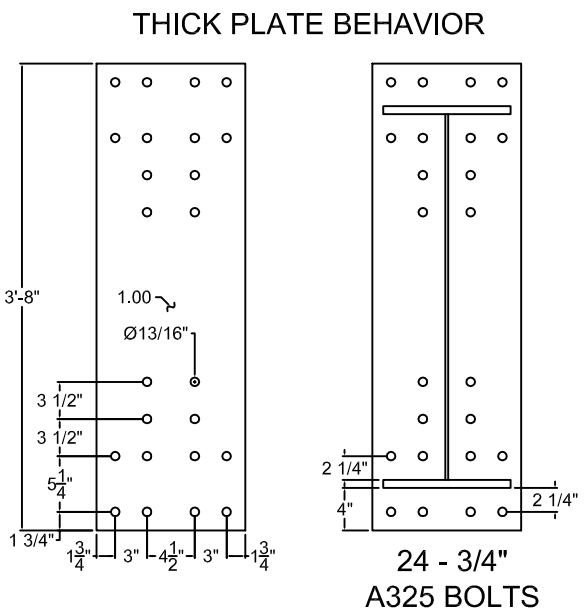

24 - 3/4"
A325 BOLTS

12B- MRE 1/3 -4W/2W-0.75-1.00-36

QUANTITY: 2 EACH AND INCLUDE 18in x 14in COUPON FROM SAME HEAT OF MATERIAL AS END-PLATE. MATCH MARK COUPON AND END-PLATE FOR VERIFICATION

$F_{y\ end\text{-}plate}$ = 50 ksi ASSUMED

NO BLAST, NO PAINT

E70 ELECTRODES FOR ALL WELDS

VIRGINIA TECH	TITLE: SPECIMEN 04		
PROJECT: MBMA END-PLATE MOMENT CONNECTIONS		05/09/14	SHEET 05

GIRDER SPECIMEN 05

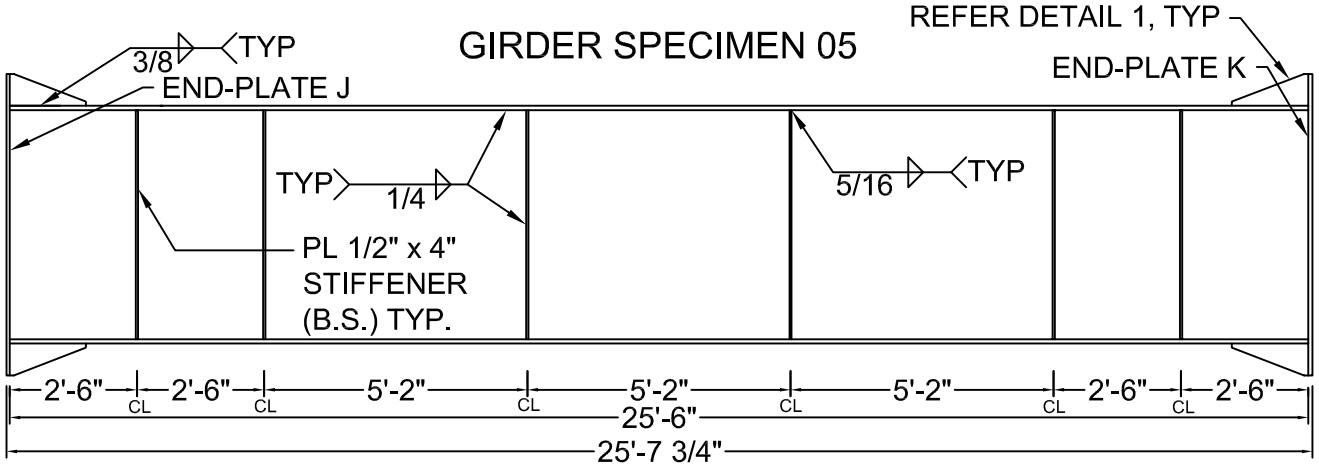

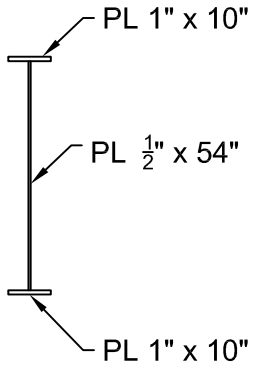

END PLATE J
(THIN PLATE BEHAVIOR)

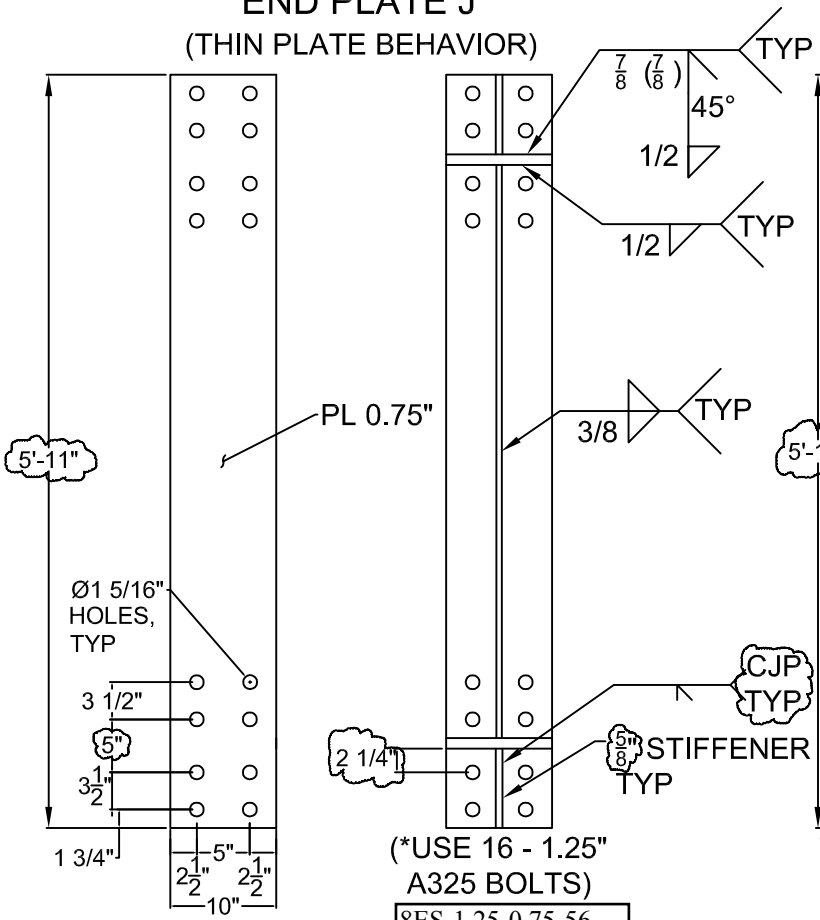

(*USE 16 - 1.25"
A325 BOLTS)

8ES-1.25-0.75-56

END PLATE K
(THICK PLATE BEHAVIOR)

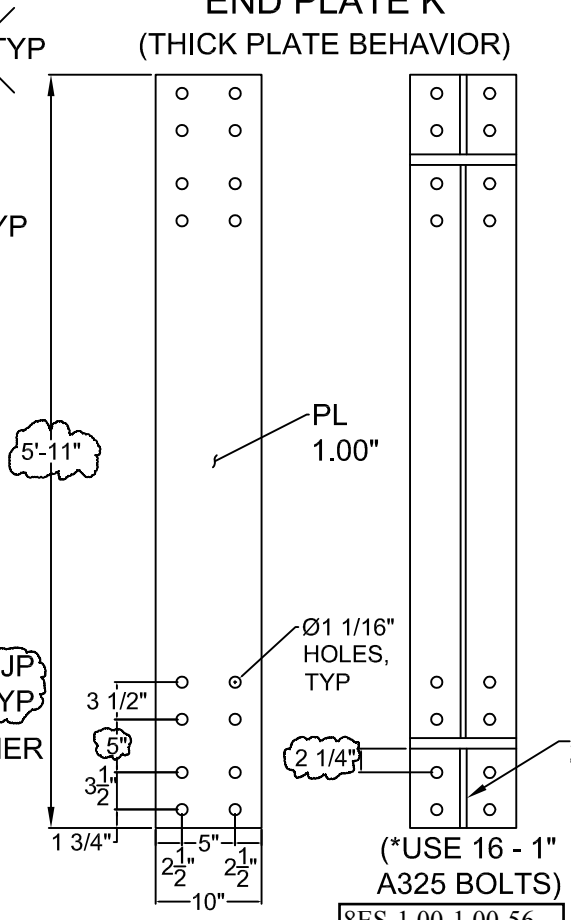

(*USE 16 - 1"
A325 BOLTS)

8ES-1.00-1.00-56

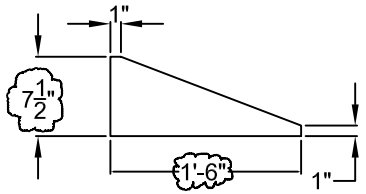

DETAIL 1

QUANTITY: 2 SPECIMENS EACH AND ALSO SHIP LOOSE ONE ADDITIONAL END PLATE OF EACH TYPE (J AND K) FROM THE SAME HEAT OF MATERIAL AS USED FOR THE SPECIMEN.

$F_{y\ end\text{-}plate}$ = 55 ksi ASSUMED

NO BLAST, NO PAINT

E70 ELECTRODES FOR ALL WELDS

NOTE: HOLE LOCATION ON OPPOSITE END OF PLATE ARE SYMMETRICAL

VIRGINIA TECH	TITLE: SPECIMEN 05	DRAWN BY: NJ, REV 1
PROJECT: MBMA END-PLATE MOMENT CONNECTIONS	11/19/14	SHEET 14

Appendix E Specimen Design Calculations

VIRGINIA TECH	PLATE GIRDER - DEEP	DATE	MADE	SHEET NO. 36
		04/16/14	PRB	of

Material Properties

E	Elastic Modulus	29000	ksi	Fy	Yield Strength	55	ksi
L_B	Unbraced Length	0	in				

Plate Girder Dimensions

	Width		Height		Area		Distance From Centroid of Shape to Top of Plate Girder		Distance From Centroid of Shape to Centroid of Plate Girder	
Top Flange	12	in	0.75	in	9	in^2	0.375	in	17.625	in
Web	0.25	in	34.5	in	8.625	in^2	18	in	0	in
Bottom Flange	12	in	0.75	in	9	in^2	35.625	in	17.625	in

Plate Girder Properties

Centroid	18.0	in	Measured from top of plate girder.
Moment of Inertia	6447.9	in^4	
Elastic Neutral Axis	18.0	in	Measured from top of plate girder.
Plastic Neutral Axis	18.0	in	Measured from top of plate girder. Assume is in web.
h_c	34.5	in	S_{xc} 358.21 in^3
h_p	34.5	in	

Slenderness

K_c	0.3500			
F_L	38.5	ksi	Verify that conditions are valid for $F_L=0.7*F_y$	
	λ	λ_p	λ_r	
Flange	8	8.726	15.425	COMPACT
Web*	138	86.339	130.886	SLENDER

*Based upon doubly symmetric cross section

Determine RPG

a_w	0.96	h_c/t_w	138
5.7*(E/Fy)^1/2	130.89	RPG	0.995

Limit State Analysis

F_{CR} Compression Flange Strength 55.00 ksi

Yield

F_{CR} 55.00 ksi

Flange Local Buckling

F_{CR} 55.00 ksi

VIRGINIA TECH	PLATE GIRDER - DEEP	DATE	MADE	SHEET NO. 36
		04/16/14	PRB	of

Lateral Torsional Buckling

F_{CR} 55.00

I_{CY}	108.01	in^4	A	10.44	in^2
r_t	3.22		C_b	1	
L_P	81.25	in	L_R	277.36	in

NO LTB

Bend-Buckling of the Web

F_{CR} 55.00 (IF Applicable) F_{CR} 49.88 ksi

$5.7*SQRT(E/F_{CR})$ 138.00 = h/tw 138.00

NOT APPLICABLE

Design Moment

Mn	19611.5	k·in	ϕMn	17650.4	k·in
Mn	1634.3	k·ft	ϕMn	1470.9	k·ft

DESIGN M_u[1]	4600	k·in	**A992**	**F_{py}**	61.1	ksi				
1) DESIGN M_U IS SET AT APPROXIMATELY 75% OF ϕM_N OF THE PLATE GIRDER SECTION. THIS ENSURES THE CONNECTION WILL FAIL PRIOR TO THE GIRDER. ACHIEVING DESIGN M_U IS NOT REQUIRED FOR CONNECTION DESIGN. DESIGN M_U IS ONLY A REFERENCE POINT TO SELECT PLATE THICKNESS AND BOLT DIAMETER.										
b_p	13.85	in	**p_{ext}**	3.25	in	**$p_{f,o}$**	1.46	in	**$p_{f,i}$**	1.26	in
t_f	0.78	in	**t_w**	0.375	in	**g**	3.50	in	**g_o**	3.49	in

h	61.5	in	**h_0**	62.96	in	**h_1**	59.46	in	**s**	3.4812	in
			d_0	62.57	in	**d_1**	59.08	in	$s = \frac{1}{2}\sqrt{b_p g}$		
END-PLATE TYPE			EXTENDED			γ	1				

ϕ	0.75	**ϕ_b**	0.9
Y		901	in

$$Y = \frac{b_p}{2}\left[h_0\left(\frac{1}{p_{f,o}}\right) + h_1\left(\frac{1}{p_{f,i}} + \frac{1}{s}\right) - \frac{1}{2}\right] + \frac{2}{g}\left[h_1(p_{f,i} + s)\right]$$

THICK PLATE PROCEDURE				
PROCEDURE				NOTES
A325	**F_t**	90	ksi	
$d_{b,reqd}$		0.37	in	*SINCE M_U IS ONLY A REFERENCE POINT, IT IS NOT NECESSARY TO USE A BOLT SIZE GREATER THAN $D_{B,REQD}$.*
$d_{b,reqd} = \sqrt{\frac{2M_u}{\pi F_t(2d_0 + 2d_1)}}$				
d_b		0.75	in	
P_t		40	kips	
$P_t = \pi d_b^2 F_t / 4$				
M_{np}		19350	k·in	
$M_{np} = 2P_t(2d_0 + 2d_1)$				
$t_{p,reqd}$		0.62	in	*TO INCITE THICK PLATE BEHAVIOR,SELECT A PLATE THICKNESS GREATER THAN $T_{P,REQD}$.*
$t_{p,reqd} = \sqrt{\frac{\gamma M_{np}}{0.9 F_{py} Y}}$				
$t_{p,act}$		0.753	in	

THICK PLATE PROCEDURE (cont.)			
PROCEDURE (cont.)			**NOTES (cont.)**
OTHER LIMIT STATES			
M_{pl}	31230	k·in	*MUST CONSIDER ALL LIMIT STATES TO DETERMINE CONTROLLING FAILURE MODE*
$M_{pl} = F_{py} t_p^2 Y$			
SUMMARY			
M_{np}	19350	k·in	*MUST REMOVE ϕ AND ϕb FACTORS IN ORDER TO DETERMINE CONTROLLING FAILURE MODE FOR **EXPERIMENTAL** TESTS*
$M_{np} = 2P_t(2d_0 + 2d_1)$			
M_{pl}	31230	k·in	
$M_{pl} = F_{py} t_p^2 Y$			
RATIOS			*A Mpl/Mnp RATIO BETWEEN 1.10 AND 1.40 IS DESIREABLE SO AS TO ACHIEVE PROPER PROGRESSION THROUGH LIMIT STATES DURING **EXPERIMENTAL** TESTS*
M_{pl}/M_{np}	1.61		

M_u			4600	k·in	**A992**	**F_{py}**		53.8		ksi

1) DESIGN M_U IS SET AT APPROXIMATELY 75% OF ϕM_N OF THE PLATE GIRDER SECTION. THIS ENSURES THE CONNECTION WILL FAIL PRIOR TO THE GIRDER. ACHIEVING DESIGN M_U IS NOT REQUIRED FOR CONNECTION DESIGN. DESIGN M_U IS ONLY A REFERENCE POINT TO SELECT PLATE THICKNESS AND BOLT DIAMETER.

b_p	13.96	in	**p_{ext}**	3.12	in	**$p_{f,o}$**	1.38	in	**$p_{f,i}$**	1.35	in
t_f	0.78	in	**t_w**	0.375	in	**g**	3.48	in	**g_o**	3.49	in

h	61.5	in	**h_0**	62.88	in	**h_1**	59.37	in	**s**	3.485	in
			d_0	62.49	in	**d_1**	58.99	in	$s = \frac{1}{2}\sqrt{b_p g}$		
END-PLATE TYPE			EXTENDED			γ	1				

ϕ	0.75	**ϕ_b**	0.9
Y		905	in

$$Y = \frac{b_p}{2}\left[h_0\left(\frac{1}{p_{f,o}}\right) + h_1\left(\frac{1}{p_{f,i}} + \frac{1}{s}\right) - \frac{1}{2}\right] + \frac{2}{g}\left[h_1(p_{f,i} + s)\right]$$

THIN PLATE PROCEDURE

PROCEDURE				NOTES
PLATE				
$t_{p,reqd}$		0.307	in	*PLATE THICKNESS SELECTION MADE BY ROUNDING DOWN FROM $T_{P,REQD}$ TO INDUCE THIN PLATE BEHAVIOR. SINCE M_U IS ONLY A REFERENCE POINT, IT IS NOT NECESSARY TO USE A PLATE THICKNESS GREATER THAN $T_{P,REQD}$.*
$t_{p,reqd} = \sqrt{\frac{\gamma M_u}{F_{py} Y}}$				
t_p		0.504	in	
BOLTS				
A325	**F_t**	90	ksi	
d_b (trial)		1.000	in	
BOLT DISTRIBUTION FACTORS				
α_0	1	**α_1**	0.5	
β_1	1	**β_2**	0.75	
γ_1	-	**γ_2**	-	
δ_1	-	**δ_3**	-	
P_t		71	kips	
$P_t = \pi d_b^2 F_t / 4$				

THIN PLATE PROCEDURE (cont.)

PROCEDURE (cont.)

T_b	51	kips
AISC MANUAL TABLE J3.1		
T_b (snug)	11.2	kips

PRYING FORCES

INNER COLUMNS (1)			*OUTER COLUMNS (2)*		
$w_{0,1}$	3.49	in	$w_{0,2}$	3.50	in
$w_{0,1}'$	2.42	in	$w_{0,2}'$	2.43	in
$w_{1,1}$	3.49	in	$w_{1,2}$	3.50	in
$w_{1,1}'$	2.42	in	$w_{1,2}'$	2.43	in

a_o	0.386	in
a_i	0.386	in

INNER COLUMNS (1)			*OUTER COLUMNS (2)*		
$F_{0,1}'$	18.53	kips	$F_{0,2}'$	18.58	kips
$F_{1,1}'$	18.95	kips	$F_{1,2}'$	18.99	kips

$$F_{o,n}^{'} = \frac{t_p^2 F_{py}\left(0.85 w_n + 0.80 w_n^{'}\right) + \frac{\pi d_b^3 F_t}{8}}{4 p_{f,o}}$$

$$F_{i,n}^{'} = \frac{t_p^2 F_{py}\left(0.85 w_n + 0.80 w_n^{'}\right) + \frac{\pi d_b^3 F_t}{8}}{4 p_{f,i}}$$

INNER COLUMNS (1)			*OUTER COLUMNS (2)*		
$Q_{max,0,1}$	18.69	kips	$Q_{max,0,2}$	18.78	kips
$Q_{max,1,1}$	18.56	kips	$Q_{max,1,2}$	18.64	kips

$$Q_{\max,o,n} = \frac{w_n^{'} t_p^2}{4 a_o} \sqrt{F_{py}^2 - 3\left(\frac{F_o^{'}}{w_n^{'} t_p}\right)^2}$$

$$Q_{\max,i,n} = \frac{w_n^{'} t_p^2}{4 a_i} \sqrt{F_{py}^2 - 3\left(\frac{F_i^{'}}{w_n^{'} t_p}\right)^2}$$

BOLT ROW PRYING COMBINATIONS

COMBINATION	B. ROW	PRY.[1]	M_q
1	0	YES	20500
	1	YES	
2	0	YES	12060
	1	NO[2]	

NOTES (cont.)

FOR A325 SNUG-TIGHTENED BOLTS

d_b (in)	≤ 5/8	3/4	7/8	≥ 1
% of T_b min	75	50	38	25

EXCEL USER NOTE: VERIFY ϕMq EQUATIONS REFERENCE PROPER Tb (MINIMUM PRETENSION OR SNUG-TIGHT)

THIN PLATE PROCEDURE (cont.)

PROCEDURE (cont.)	NOTES (cont.)

BOLT ROW PRYING COMBINATIONS (cont.)

COMBINATION	B. ROW	PRY.[1]	M_q
3	0	YES	12850
	1	NO	
4	0	NO	4410
	1	NO	

EXCEL USER NOTE: VERIFY ϕMq EQUATIONS REFERENCE PROPER Tb (MINIMUM PRETENSION OR SNUG-TIGHT)

M_q	20500	k·in

$$M_q = max(\, prying\,,\, pretension\,)$$

AS PER DG16, MAXIMUM Mq VALUE CONTROLS

1) YES: BOLT ROW UNDERGOES PRYING
NO: PRETENSION FORCE ONLY

BOLT ROW PRYING COMBINATION ASSUMPTIONS ARE BASED UPON PRIOR EXPERIMENTAL TESTING

OTHER LIMIT STATES

BOLT RUPTURE w/o PRYING ACTION (M_{np})

M_{np}	34350	k·in

$$M_{np} = 2P_t(2d_0 + 2d_1)$$

END-PLATE YIELDING (M_{pl})

M_{pl}	12370	k·in

$$M_{pl} = F_{py} t_p^2 Y$$

CONSIDER ALL LIMIT STATES TO DETERMINE CONTROLLING FAILURE MODE

SUMMARY

M_{np}	34350	k·in

$$M_{np} = 2P_t(2d_0 + 2d_1)$$

M_q	20500	k·in

$$M_q = max(\, prying\,,\, pretension\,)$$

M_{pl}	12370	k·in

$$M_{pl} = F_{py} t_p^2 Y$$

RATIOS

M_{np}/M_q	1.68
M_q/M_{pl}	1.66

*A M_q/M_{pl} RATIO BETWEEN 1.10 AND 1.40 IS DESIREABLE SO AS TO INDUCE PROPER PROGRESSION THROUGH LIMIT STATES DURING **EXPERIMENTAL** TESTS*

DESIGN M_u[1]			k·in	**A992**	**F_{py}**	40.8	ksi			

1) DESIGN M_U IS SET AT APPROXIMATELY 75% OF ϕM_N OF THE PLATE GIRDER SECTION. THIS ENSURES THE CONNECTION WILL FAIL PRIOR TO THE GIRDER. ACHIEVING DESIGN M_U IS NOT REQUIRED FOR CONNECTION DESIGN. DESIGN M_U IS ONLY A REFERENCE POINT TO SELECT PLATE THICKNESS AND BOLT DIAMETER.

b_p	15.06	in	**p_{ext}**	3.56	in	**$p_{f,o}$**	1.78	in	**$p_{f,i}$**	1.7835	in
t_f	0.90	in	**t_w**	0.6875	in	**g**	4.99	in	**g_o**	3.40	in

h	35.875	in	**h_0**	37.66	in	**h_1**	33.19	in	**s**	4.3349	in
			d_0	37.21	in	**d_1**	32.75	in	$s = \frac{1}{2}\sqrt{b_p g}$		
END-PLATE TYPE			EXTENDED			γ	1			

ϕ	0.75	**ϕ_b**	0.9
Y		435	in

$$Y = \frac{b_p}{2}\left[h_0\left(\frac{1}{p_{f,o}}\right) + h_1\left(\frac{1}{p_{f,i}} + \frac{1}{s}\right) - \frac{1}{2}\right] + \frac{2}{g}\left[h_1(p_{f,i} + s)\right]$$

THICK PLATE PROCEDURE				
PROCEDURE				NOTES
A325	**F_t**	90	ksi	
$d_{b,reqd}$		0.00	in	*SINCE M_U IS ONLY A REFERENCE POINT, IT IS NOT NECESSARY TO USE A BOLT SIZE GREATER THAN $D_{B,REQD}$.*
$d_{b,reqd} = \sqrt{\frac{2M_u}{\pi F_t(2d_0 + 2d_1)}}$				
d_b		1.25	in	
P_t		110	kips	
$P_t = \pi d_b^2 F_t / 4$				
M_{np}		30910	k·in	
$M_{np} = 2P_t(2d_0 + 2d_1)$				
$t_{p,reqd}$		1.39	in	*TO INCITE THICK PLATE BEHAVIOR,SELECT A PLATE THICKNESS GREATER THAN $T_{P,REQD}$.*
$t_{p,reqd} = \sqrt{\frac{\gamma M_{np}}{0.9 F_{py} Y}}$				
$t_{p,act}$		1.404	in	

THICK PLATE PROCEDURE (cont.)			
PROCEDURE (cont.)			**NOTES (cont.)**
OTHER LIMIT STATES			
M_{pl}	34950	k·in	*MUST CONSIDER ALL LIMIT STATES TO DETERMINE CONTROLLING FAILURE MODE*
$M_{pl} = F_{py} t_p^2 Y$			
SUMMARY			
M_{np}	30910	k·in	*MUST REMOVE ϕ AND ϕb FACTORS IN ORDER TO DETERMINE CONTROLLING FAILURE MODE FOR **EXPERIMENTAL** TESTS*
$M_{np} = 2P_t(2d_0 + 2d_1)$			
M_{pl}	34950	k·in	
$M_{pl} = F_{py} t_p^2 Y$			
RATIOS			*A Mpl/Mnp RATIO BETWEEN 1.10 AND 1.40 IS DESIREABLE SO AS TO ACHIEVE PROPER PROGRESSION THROUGH LIMIT STATES DURING **EXPERIMENTAL** TESTS*
M_{pl}/M_{np}	1.13		

M_u			k·in	**A992**	**F_{py}**	40.4	ksi			

1) DESIGN M_U IS SET AT APPROXIMATELY 75% OF ϕM_N OF THE PLATE GIRDER SECTION. THIS ENSURES THE CONNECTION WILL FAIL PRIOR TO THE GIRDER. ACHIEVING DESIGN M_U IS NOT REQUIRED FOR CONNECTION DESIGN. DESIGN M_U IS ONLY A REFERENCE POINT TO SELECT PLATE THICKNESS AND BOLT DIAMETER.

b_p	15.00	in	**p_{ext}**	3.69	in	**$p_{f,o}$**	1.78	in	**$p_{f,i}$**	1.7755	in
t_f	0.66	in	**t_w**	0.5	in	**g**	4.99	in	**g_o**	3.38	in

h	29.688	in	**h_0**	31.46	in	**h_1**	27.25	in	**s**	4.3241	in
			d_0	31.13	in	**d_1**	26.92	in	$s = \frac{1}{2}\sqrt{b_p g}$		
END-PLATE TYPE			EXTENDED			γ	1				

ϕ	0.75	**ϕ_b**	0.9
Y		358	in

$$Y = \frac{b_p}{2}\left[h_0\left(\frac{1}{p_{f,o}}\right) + h_1\left(\frac{1}{p_{f,i}} + \frac{1}{s}\right) - \frac{1}{2}\right] + \frac{2}{g}\left[h_1(p_{f,i} + s)\right]$$

THIN PLATE PROCEDURE

PROCEDURE			NOTES
PLATE			
$t_{p,reqd}$	0.000	in	*PLATE THICKNESS SELECTION MADE BY ROUNDING DOWN FROM $T_{P,REQD}$ TO INDUCE THIN PLATE BEHAVIOR. SINCE M_U IS ONLY A REFERENCE POINT, IT IS NOT NECESSARY TO USE A PLATE THICKNESS GREATER THAN $T_{P,REQD}$.*
$t_{p,reqd} = \sqrt{\frac{\gamma M_u}{F_{py} Y}}$			
t_p	1.025	in	
BOLTS			
A325	**F_t** 90	ksi	
d_b (trial)	1.250	in	

BOLT DISTRIBUTION FACTORS

α_0	1	**α_1**	0.5
β_1	1	**β_2**	0.75
γ_1	-	**γ_2**	-
δ_1	-	**δ_3**	-

P_t	110	kips

$$P_t = \pi d_b^2 F_t / 4$$

THIN PLATE PROCEDURE (cont.)

PROCEDURE (cont.)

T_b	71	kips
AISC MANUAL TABLE J3.1		
T_b (snug)	17.8	kips

PRYING FORCES

INNER COLUMNS (1)			*OUTER COLUMNS (2)*		
$w_{0,1}$	4.19	in	$w_{0,2}$	3.32	in
$w_{0,1}'$	2.87	in	$w_{0,2}'$	2.00	in
$w_{1,1}$	4.19	in	$w_{1,2}$	3.32	in
$w_{1,1}'$	2.87	in	$w_{1,2}'$	2.00	in

a_o	1.910	in
a_i	1.945	in

INNER COLUMNS (1)			*OUTER COLUMNS (2)*		
$F_{0,1}'$	44.71	kips	$F_{0,2}'$	36.13	kips
$F_{1,1}'$	44.71	kips	$F_{1,2}'$	36.13	kips

$$F_{o,n}^{'} = \frac{t_p^2 F_{py}\left(0.85 w_n + 0.80 w_n^{'}\right) + \frac{\pi d_b^3 F_t}{8}}{4 p_{f,o}}$$

$$F_{i,n}^{'} = \frac{t_p^2 F_{py}\left(0.85 w_n + 0.80 w_n^{'}\right) + \frac{\pi d_b^3 F_t}{8}}{4 p_{f,i}}$$

INNER COLUMNS (1)			*OUTER COLUMNS (2)*		
$Q_{max,0,1}$	12.12	kips	$Q_{max,0,2}$	7.30	kips
$Q_{max,1,1}$	11.89	kips	$Q_{max,1,2}$	7.17	kips

$$Q_{\max,o,n} = \frac{w_n^{'} t_p^2}{4 a_o}\sqrt{F_{py}^2 - 3\left(\frac{F_o^{'}}{w_n^{'} t_p}\right)^2}$$

$$Q_{\max,i,n} = \frac{w_n^{'} t_p^2}{4 a_i}\sqrt{F_{py}^2 - 3\left(\frac{F_i^{'}}{w_n^{'} t_p}\right)^2}$$

BOLT ROW PRYING COMBINATIONS

COMBINATION	B. ROW	PRY.[1]	M_q
1	0	YES	18810
	1	YES	
2	0	YES	11010
	1	NO[2]	

NOTES (cont.)

FOR A325 SNUG-TIGHTENED BOLTS

d_b (in)	≤ 5/8	3/4	7/8	≥ 1
% of T_b min	75	50	38	25

EXCEL USER NOTE: VERIFY ϕMq EQUATIONS REFERENCE PROPER Tb (MINIMUM PRETENSION OR SNUG-TIGHT)

THIN PLATE PROCEDURE (cont.)

PROCEDURE (cont.)	NOTES (cont.)

BOLT ROW PRYING COMBINATIONS (cont.)

COMBINATION	B. ROW	PRY.[1]	M_q
3	0	YES	11140
	1	NO	
4	0	NO	3330
	1	NO	

EXCEL USER NOTE: VERIFY ϕMq EQUATIONS REFERENCE PROPER Tb (MINIMUM PRETENSION OR SNUG-TIGHT)

M_q	18810	k·in

$$M_q = max(\, prying\,,\, pretension\,)$$

AS PER DG16, MAXIMUM Mq VALUE CONTROLS

1) YES: BOLT ROW UNDERGOES PRYING
NO: PRETENSION FORCE ONLY

BOLT ROW PRYING COMBINATION ASSUMPTIONS ARE BASED UPON PRIOR EXPERIMENTAL TESTING

OTHER LIMIT STATES

BOLT RUPTURE w/o PRYING ACTION (M_{np})

M_{np}	25650	k·in

$$M_{np} = 2P_t(2d_0 + 2d_1)$$

END-PLATE YIELDING (M_{pl})

M_{pl}	15210	k·in

$$M_{pl} = F_{py} t_p^2 Y$$

CONSIDER ALL LIMIT STATES TO DETERMINE CONTROLLING FAILURE MODE

SUMMARY

M_{np}	25650	k·in

$$M_{np} = 2P_t(2d_0 + 2d_1)$$

M_q	18810	k·in

$$M_q = max(\, prying\,,\, pretension\,)$$

M_{pl}	15210	k·in

$$M_{pl} = F_{py} t_p^2 Y$$

RATIOS

M_{np}/M_q	1.36
M_q/M_{pl}	1.24

*A M_q/M_{pl} RATIO BETWEEN 1.10 AND 1.40 IS DESIREABLE SO AS TO INDUCE PROPER PROGRESSION THROUGH LIMIT STATES DURING **EXPERIMENTAL** TESTS*

DESIGN M_u[1]	26000	k·in	**A992**	**F_{py}**	59.3	ksi					
1) DESIGN M_U IS SET AT APPROXIMATELY 75% OF ϕM_N OF THE PLATE GIRDER SECTION. THIS ENSURES THE CONNECTION WILL FAIL PRIOR TO THE GIRDER. ACHIEVING DESIGN M_U IS NOT REQUIRED FOR CONNECTION DESIGN. DESIGN M_U IS ONLY A REFERENCE POINT TO SELECT PLATE THICKNESS AND BOLT DIAMETER.											
t_f	0.75	in	**t_w**	0.375	in	**b_p**	14	in			
p_f	2.25	in	**p_b**	3.5	in	**g**	4.5	in	**g_o**	3	in

h	60	in	**h_1**	57.00	in	**h_2**	53.50	in	**s**	3.97	in
			d_1	56.63	in	**d_2**	53.13	in	$s = \frac{1}{2}\sqrt{b_p g}$		
END-PLATE TYPE			FLUSH			**γ_r**	1.25				

ϕ	0.75	**ϕ_b**	0.9
Y		513	in

$$Y = \frac{b_p}{2}\left[h_1\left(\frac{1}{p_f}\right) + h_2\left(\frac{1}{s}\right)\right] + \frac{2}{g}\left[h_1(p_f + 0.75p_b) + h_2(s + 0.25p_b)\right] + \frac{g}{2}$$

THICK PLATE PROCEDURE				
PROCEDURE				**NOTES**
A325	**F_t**	90	ksi	
$d_{b,reqd}$		1.05	in	*SINCE M_U IS ONLY A REFERENCE POINT, IT IS NOT NECESSARY TO USE A BOLT SIZE GREATER THAN $D_{B,REQD}$.*
$d_{b,reqd} = \sqrt{\frac{2M_u}{\pi F_t(2d_1 + d_2)}}$				
d_b		0.875	in	
P_t		54	kips	
$P_t = \pi d_b^2 F_t / 4$				
M_{np}		18010	k·in	
$M_{np} = 2P_t(2d_1 + d_2)$				
$t_{p,reqd}$		0.91	in	*IN ORDER TO INDUCE THICK PLATE BEHAVIOR, SELECT A PLATE THICKNESS GREATER THAN $T_{P,REQD}$.*
$t_{p,reqd} = \sqrt{\frac{\gamma M_{np}}{0.9F_{py}Y}}$				
$t_{p,act}$		1.000	in	

THICK PLATE PROCEDURE (cont.)			
PROCEDURE (cont.)			**NOTES (cont.)**
OTHER LIMIT STATES			
$\mathbf{M_{pl}}$	30400	k·in	*CONSIDER ALL LIMIT STATES TO DETERMINE CONTROLLING FAILURE MODE*
$M_{pl} = F_{py} t_p^2 Y$			
SUMMARY			
$\mathbf{M_{np}}$	18010	k·in	*REMOVE ϕ AND ϕb FACTORS IN ORDER TO DETERMINE CONTROLLING FAILURE MODE FOR **EXPERIMENTAL** TESTS*
$M_{np} = 2P_t(2d_1 + d_2)$			
$\mathbf{M_{pl}}$	30400	k·in	
$M_{pl} = F_{py} t_p^2 Y$			
RATIOS			*A Mpl/Mnp RATIO BETWEEN 1.10 AND 1.40 IS DESIREABLE SO AS TO INDUCE PROPER PROGRESSION THROUGH LIMIT STATES DURING **EXPERIMENTAL** TESTS*
$\mathbf{M_{pl}/M_{np}}$	1.69		

NOTE:

DESIGN M_u[1]		26000	k·in	**A992**	**F_{py}**		54.6	ksi			
1) DESIGN M_U IS SET AT APPROXIMATELY 75% OF ϕM_N OF THE PLATE GIRDER SECTION. THIS ENSURES THE CONNECTION WILL FAIL PRIOR TO THE GIRDER. ACHIEVING DESIGN M_U IS NOT REQUIRED FOR CONNECTION DESIGN. DESIGN M_U IS ONLY A REFERENCE POINT TO SELECT PLATE THICKNESS AND BOLT DIAMETER.											
t_f	0.75	in	**t_w**	0.375	in	**b_p**	14	in			
p_f	2.25	in	**p_b**	3.5	in	**g**	4.5	in	**g_o**	3	in

h	60	in	**h_1**	57.00	in	**h_2**	53.50	in	**s**	3.97	in
			d_1	56.63	in	**d_2**	53.13	in	$s = \frac{1}{2}\sqrt{b_p g}$		
END-PLATE TYPE			FLUSH			**γ_r**	1.25				

ϕ	0.75	**ϕ_b**	0.9
Y		513	in

$$Y = \frac{b_p}{2}\left[h_1\left(\frac{1}{p_f}\right) + h_2\left(\frac{1}{s}\right)\right] + \frac{2}{g}\left[h_1(p_f + 0.75p_b) + h_2(s + 0.25p_b)\right] + \frac{g}{2}$$

THIN PLATE PROCEDURE

PROCEDURE			NOTES
PLATE			
$t_{p,reqd}$	1.078	in	*PLATE THICKNESS SELECTION MADE BY ROUNDING DOWN FROM $T_{P,REQD}$ TO INDUCE THIN PLATE BEHAVIOR. SINCE M_U IS ONLY A REFERENCE POINT, IT IS NOT NECESSARY TO USE A PLATE THICKNESS GREATER THAN $T_{P,REQD}$.*
$t_{p,reqd} = \sqrt{\frac{\gamma M_u}{F_{py} Y}}$			
t_p	0.750	in	
BOLTS			
A325 **F_t**	90	ksi	
d_b (trial)	1.125	in	
P_t	89	kips	
$P_t = \pi d_b^2 F_t / 4$			
T_b	56	kips	*FOR A325 SNUG-TIGHTENED BOLTS*
AISC MANUAL TABLE J3.1			*d_b (in)* ≤ 5/8 | 3/4 | 7/8 | ≥ 1
T_b (snug)	14	kips	*% of T_b min* 75 | 50 | 38 | 25

THIN PLATE PROCEDURE (cont.)

PROCEDURE (cont.)

BOLT DISTRIBUTION FACTORS

β_1	1	β_2	0.75
γ_1	0.75	γ_2	-

PRYING ACTION

INNER COLUMNS (1)			*OUTER COLUMNS (2)*		
$w_{1,1}$	3.75	in	$w_{1,2}$	3.25	in
$w_{1,1}'$	2.56	in	$w_{1,2}'$	2.06	in
$w_{2,1}$	3.75	in			
$w_{2,1}'$	2.56	in			
a	1.006	in			

INNER COLUMNS (1)			*OUTER COLUMNS (2)*		
$F_{1,1}'$	23.46	kips	$F_{1,2}'$	23.46	kips
$F_{2,1}'$	23.46	kips			

$$F_{i,n}^{'} = \frac{t_p^2 F_{py}\left(0.85 w_n + 0.80 w_n^{'}\right) + \frac{\pi d_b^3 F_t}{8}}{4 p_{f,i}}$$

INNER COLUMNS (1)			*OUTER COLUMNS (2)*		
$Q_{max,1,1}$	18.03	kips	$Q_{max,1,2}$	13.80	kips
$Q_{max,2,1}$	18.03	kips			

$$Q_{\max,i,n} = \frac{w_n^{'} t_p^2}{4a}\sqrt{F_{py}^2 - 3\left(\frac{F_t^{'}}{w_n^{'} t_p}\right)^2}$$

BOLT ROW PRYING COMBINATIONS

COMBINATION	B. ROW	PRY.[1]	M_q
1	1	YES	20210
	2	YES	
2	1	YES	18980
	2	NO[2]	
3	1	NO	16790
	2	YES	
4	1	NO	15560
	2	NO	

M_q	20210	k·in

$$M_q = max(\, prying\,,\, pretension\,)$$

1) YES: BOLT ROW UNDERGOES PRYING
NO: BOLT ROW DOES NOT UNDERGO PRYING
2) BOLT SUBJECTED TO PRETENSION FORCE ONLY

NOTES (cont.)

EXCEL USER NOTE: VERIFY ϕMq EQUATIONS REFERENCE PROPER Tb (MINIMUM PRETENSION OR SNUG-TIGHT)

AS PER DG16, MAXIMUM ϕM_q VALUE CONTROLS

BOLT ROW PRYING COMBINATION ASSUMPTIONS ARE BASED UPON PRIOR EXPERIMENTAL TESTING

THIN PLATE PROCEDURE (cont.)

PROCEDURE (cont.)			NOTES (cont.)
OTHER LIMIT STATES			*CONSIDER ALL LIMIT STATES TO DETERMINE CONTROLLING FAILURE MODE*
BOLT RUPTURE w/o PRYING ACTION (M_{np})			
M_{np}	29770	k·in	
$M_{np} = 2P_t(2d_1 + d_2)$			
END-PLATE YIELDING (M_{pl})			
M_{pl}	15740	k·in	
$M_{pl} = F_{py} t_p^2 Y$			
SUMMARY			*REMOVE ϕ AND ϕ_b FACTORS IN ORDER TO DETERMINE CONTROLLING FAILURE MODE FOR **EXPERIMENTAL** TESTS*
M_{np}	29770	k·in	
$M_{np} = 2P_t(2d_1 + d_2)$			
M_q	20210	k·in	
$M_q = max(\ prying\ ,\ pretension\ )$			
M_{pl}	15740	k·in	
$M_{pl} = F_{py} t_p^2 Y$			
RATIOS			*A Mq/Mpl RATIO BETWEEN 1.10 AND 1.40 IS DESIREABLE SO AS TO INDUCE PROPER PROGRESSION THROUGH LIMIT STATES DURING **EXPERIMENTAL** TESTS*
M_{np}/M_q	1.47		
M_q/M_{pl}	1.28		

DESIGN M_u[1]		13000	k·in	**A992**	**F_{py}**		59.3	ksi			

1) DESIGN M_U IS SET AT APPROXIMATELY 75% OF ϕM_N OF THE PLATE GIRDER SECTION. THIS ENSURES THE CONNECTION WILL FAIL PRIOR TO THE GIRDER. ACHIEVING DESIGN M_U IS NOT REQUIRED FOR CONNECTION DESIGN. DESIGN M_U IS ONLY A REFERENCE POINT TO SELECT PLATE THICKNESS AND BOLT DIAMETER.

t_f	0.75	in	**t_w**	0.375	in	**b_p**	14	in			
p_f	2.25	in	**p_b**	3.5	in	**g**	4.5	in	**g_o**	3	in

h	36	in	**h_1**	33.00	in	**h_2**	29.50	in	**s**	3.97	in
			d_1	32.63	in	**d_2**	29.13	in	$s = \frac{1}{2}\sqrt{b_p g}$		
END-PLATE TYPE			FLUSH			**γ_r**	1.25				

ϕ	0.75	**ϕ_b**	0.9
Y		292	in

$$Y = \frac{b_p}{2}\left[h_1\left(\frac{1}{p_f}\right) + h_2\left(\frac{1}{s}\right)\right] + \frac{2}{g}\left[h_1(p_f + 0.75p_b) + h_2(s + 0.25p_b)\right] + \frac{g}{2}$$

THICK PLATE PROCEDURE				
PROCEDURE				**NOTES**
A325	**F_t**	90	ksi	
$d_{b,reqd}$		0.99	in	*SINCE M_U IS ONLY A REFERENCE POINT, IT IS NOT NECESSARY TO USE A BOLT SIZE GREATER THAN $D_{B,REQD}$.*
$d_{b,reqd} = \sqrt{\frac{2M_u}{\pi F_t(2d_1 + d_2)}}$				
d_b		0.875	in	
P_t		54	kips	
$P_t = \pi d_b^2 F_t / 4$				
M_{np}		10210	k·in	
$M_{np} = 2P_t(2d_1 + d_2)$				
$t_{p,reqd}$		0.91	in	*TO INCITE THICK PLATE BEHAVIOR,SELECT A PLATE THICKNESS GREATER THAN $T_{P,REQD}$.*
$t_{p,reqd} = \sqrt{\frac{\gamma M_{np}}{0.9 F_{py} Y}}$				
$t_{p,act}$		1.000	in	

THICK PLATE PROCEDURE (cont.)			
PROCEDURE (cont.)			**NOTES (cont.)**
OTHER LIMIT STATES			
$\mathbf{M_{pl}}$	17310	k·in	*MUST CONSIDER ALL LIMIT STATES TO DETERMINE CONTROLLING FAILURE MODE*
$M_{pl} = F_{py} t_p^2 Y$			
SUMMARY			*MUST REMOVE ϕ AND ϕb FACTORS IN ORDER TO DETERMINE CONTROLLING FAILURE MODE FOR **EXPERIMENTAL** TESTS*
$\mathbf{M_{np}}$	10210	k·in	
$M_{np} = 2P_t(2d_1 + d_2)$			
$\mathbf{M_{pl}}$	17310	k·in	
$M_{pl} = F_{py} t_p^2 Y$			
RATIOS			*A Mpl/Mnp RATIO BETWEEN 1.10 AND 1.40 IS DESIREABLE SO AS TO ACHIEVE PROPER PROGRESSION THROUGH LIMIT STATES DURING **EXPERIMENTAL** TESTS*
$\mathbf{M_{pl}/M_{np}}$	1.70		

DESIGN M_u[1]	13000	k·in	A992	F_{py}	54.6	ksi

1) DESIGN M_U IS SET AT APPROXIMATELY 75% OF ϕM_N OF THE PLATE GIRDER SECTION. THIS ENSURES THE CONNECTION WILL FAIL PRIOR TO THE GIRDER. ACHIEVING DESIGN M_U IS NOT REQUIRED FOR CONNECTION DESIGN. DESIGN M_U IS ONLY A REFERENCE POINT TO SELECT PLATE THICKNESS AND BOLT DIAMETER.

t_f	0.75	in	t_w	0.375	in	b_p	14	in			
p_f	2.25	in	p_b	3.5	in	g	4.5	in	g_o	3	in

h	36	in	h_1	33.00	in	h_2	29.50	in	s	3.97	in
			d_1	32.63	in	d_2	29.13	in	$s = \frac{1}{2}\sqrt{b_p g}$		
END-PLATE TYPE			FLUSH			γ_r	1.25				

ϕ	0.75	ϕ_b	0.9
Y	292	in	

$$Y = \frac{b_p}{2}\left[h_1\left(\frac{1}{p_f}\right) + h_2\left(\frac{1}{s}\right)\right] + \frac{2}{g}\left[h_1(p_f + 0.75p_b) + h_2(s + 0.25p_b)\right] + \frac{g}{2}$$

THIN PLATE PROCEDURE

PROCEDURE			NOTES
PLATE			
$t_{p,reqd}$	1.01	in	*PLATE THICKNESS SELECTION MADE BY ROUNDING DOWN FROM $T_{P,REQD}$ TO INCITE THIN PLATE BEHAVIOR. SINCE M_U IS ONLY A REFERENCE POINT, IT IS NOT NECESSARY TO USE A PLATE THICKNESS GREATER THAN $T_{P,REQD}$.*
$t_{p,reqd} = \sqrt{\frac{\gamma M_u}{F_{py} Y}}$			
t_p	0.750	in	
BOLTS			
A325 F_t	90	ksi	
d_b (trial)	1.125	in	
P_t	89	kips	
$P_t = \pi d_b^2 F_t / 4$			
T_b	56	kips	*FOR A325 SNUG-TIGHTENED BOLTS*
AISC MANUAL TABLE J3.1			
T_b (snug)	14	kips	

d_b (in)	≤ 5/8	3/4	7/8	≥ 1
% of T_b min	75	50	38	25

THIN PLATE PROCEDURE (cont.)

PROCEDURE (cont.)

BOLT DISTRIBUTION FACTORS

β_1	1	β_2	0.75
γ_1	0.75	γ_2	-

PRYING ACTION

INNER COLUMNS (1)			*OUTER COLUMNS (2)*		
$w_{1,1}$	3.75	in	$w_{1,2}$	3.25	in
$w_{1,1}'$	2.56	in	$w_{1,2}'$	2.06	in
$w_{2,1}$	3.75	in			
$w_{2,1}'$	2.56	in			

a	1.006	in

INNER COLUMNS (1)			*OUTER COLUMNS (2)*		
$F_{1,1}'$	23.46	kips	$F_{1,2}'$	23.46	kips
$F_{2,1}'$	23.46	kips			

$$F_{i,n}^{'} = \frac{t_p^2 F_{py}\left(0.85 w_n + 0.80 w_n^{'}\right) + \frac{\pi d_b^3 F_t}{8}}{4 p_{f,i}}$$

INNER COLUMNS (1)			*OUTER COLUMNS (2)*		
$Q_{max,1,1}$	18.03	kips	$Q_{max,1,2}$	13.80	kips
$Q_{max,2,1}$	18.03	kips			

$$Q_{\max,i,n} = \frac{w_n^{'} t_p^2}{4a}\sqrt{F_{py}^2 - 3\left(\frac{F_t^{'}}{w_n^{'} t_p}\right)^2}$$

BOLT ROW PRYING COMBINATIONS

COMBINATION	B. ROW	PRY.[1]	M_q
1	1	YES	11480
	2	YES	
2	1	YES	10810
	2	NO[2]	
3	1	NO	9520
	2	YES	
4	1	NO	8840
	2	NO	

M_q	11480	k·in

$$M_q = max(\, prying\,,\, pretension\,)$$

1) YES: BOLT ROW UNDERGOES PRYING
NO: BOLT ROW DOES NOT UNDERGO PRYING
2) BOLT SUBJECTED TO PRETENSION FORCE ONLY

NOTES (cont.)

EXCEL USER NOTE: VERIFY ϕMq EQUATIONS REFERENCE PROPER Tb (MINIMUM PRETENSION OR SNUG-TIGHT)

AS PER DG16, MAXIMUM ϕM_q VALUE CONTROLS

BOLT ROW PRYING COMBINATION ASSUMPTIONS ARE BASED UPON PRIOR EXPERIMENTAL TESTING

THIN PLATE PROCEDURE (cont.)			
PROCEDURE (cont.)			**NOTES (cont.)**
OTHER LIMIT STATES			*CONSIDER ALL LIMIT STATES TO DETERMINE CONTROLLING FAILURE MODE*
BOLT RUPTURE w/o PRYING ACTION (M_{np})			
M_{np}	16890	k·in	
$M_{np} = 2P_t(2d_1 + d_2)$			
END-PLATE YIELDING (M_{pl})			
M_{pl}	8970	k·in	
$M_{pl} = F_{py} t_p^2 Y$			
SUMMARY			*REMOVE ϕ AND ϕ_b FACTORS IN ORDER TO DETERMINE CONTROLLING FAILURE MODE FOR **EXPERIMENTAL** TESTS*
M_{np}	16890	k·in	
$M_{np} = 2P_t(2d_1 + d_2)$			
M_q	11480	k·in	
$M_q = max(prying, pretension)$			
M_{pl}	8970	k·in	
$M_{pl} = F_{py} t_p^2 Y$			
RATIOS			*A Mq/Mpl RATIO BETWEEN 1.10 AND 1.40 IS DESIREABLE SO AS TO INDUCE PROPER PROGRESSION THROUGH LIMIT STATES DURING **EXPERIMENTAL** TESTS*
M_{np}/M_q	1.47		
M_q/M_{pl}	1.28		

DESIGN M_u[1]	26000	k·in	A992	F_{py}	59.3	ksi

1) DESIGN M_U IS SET AT APPROXIMATELY 75% OF ϕM_N OF THE PLATE GIRDER SECTION. THIS ENSURES THE CONNECTION WILL FAIL PRIOR TO THE GIRDER. ACHIEVING DESIGN M_U IS NOT REQUIRED FOR CONNECTION DESIGN. DESIGN M_U IS ONLY A REFERENCE POINT TO SELECT PLATE THICKNESS AND BOLT DIAMETER.

p_{ext}	4	in	$p_{f,o}$	2.25	in	$p_{f,i}$	2.25	in	p_b	3.5	in
t_f	0.75	in	t_w	0.375	in	g	4.5	in	g_o	3	in
			b_p	14	in	h				60	in

h_0	62.25	in	h_1	57.00	in	h_2	53.50	in	h_3	50.00	in
d_0	61.88	in	d_1	56.63	in	d_2	53.13	in	d_3	49.63	in

END-PLATE TYPE	EXTENDED	γ	1	s	3.97	in
Y	775	in		$s = \frac{1}{2}\sqrt{b_p g}$		
$Y = \frac{b_p}{2}\left[h_0\left(\frac{1}{p_{f,o}}\right)+h_1\left(\frac{1}{p_{f,i}}\right)+h_3\left(\frac{1}{s}\right)-\frac{1}{2}\right]+\frac{2}{g}\left[h_1(p_{f,i}+1.5p_b)+h_3(s+0.5p_b)\right]+\frac{g}{2}$				ϕ	0.75	
				ϕ_b	0.9	

THICK PLATE PROCEDURE				
PROCEDURE				NOTES
A325	F_t	90	ksi	
$d_{b,reqd}$		0.74	in	*SINCE M_U IS ONLY A REFERENCE POINT, IT IS NOT NECESSARY TO USE A BOLT SIZE GREATER THAN $D_{B,REQD}$.*
$d_{b,reqd} = \sqrt{\frac{2M_u}{\pi F_t(2d_0+2d_1+d_2+d_3)}}$				
d_b		0.750	in	
P_t		40	kips	
$P_t = \pi d_b^2 F_t / 4$				
M_{np}		27020	k·in	
$M_{np} = 2P_t(2d_0+2d_1+d_2+d_3)$				
$t_{p,reqd}$		0.81	in	*TO INDUCE THICK PLATE BEHAVIOR, SELECT A PLATE THICKNESS GREATER THAN $T_{P,REQD}$.*
$t_{p,reqd} = \sqrt{\frac{\gamma M_{np}}{0.9 F_{py} Y}}$				
t_p		1.00	in	

THICK PLATE PROCEDURE (cont.)			
PROCEDURE (cont.)			**NOTES (cont.)**
OTHER LIMIT STATES			
$\mathbf{M_{pl}}$	45960	k·in	*CONSIDER ALL LIMIT STATES TO DETERMINE CONTROLLING FAILURE MODE*
$M_{pl} = F_{py} t_p^2 Y$			
SUMMARY			
$\mathbf{M_{np}}$	27020	k·in	*REMOVE ϕ AND ϕb FACTORS IN ORDER TO DETERMINE CONTROLLING FAILURE MODE FOR **EXPERIMENTAL** TESTS*
$M_{np} = 2P_t(2d_0 + 2d_1 + d_2 + d_3)$			
$\mathbf{M_{pl}}$	45960	k·in	
$M_{pl} = F_{py} t_p^2 Y$			
RATIOS			*A Mpl/Mnp RATIO BETWEEN 1.10 AND 1.40 IS DESIREABLE SO AS TO INDUCE PROPER PROGRESSION THROUGH LIMIT STATES DURING **EXPERIMENTAL** TESTS*
$\mathbf{M_{pl}/M_{np}}$	1.70		

DESIGN M_u[1]	26000	k·in	A992	F_{py}	54.6	ksi

1) DESIGN M_U IS SET AT APPROXIMATELY 75% OF ϕM_N OF THE PLATE GIRDER SECTION. THIS ENSURES THE CONNECTION WILL FAIL PRIOR TO THE GIRDER. ACHIEVING DESIGN M_U IS NOT REQUIRED FOR CONNECTION DESIGN. DESIGN M_U IS ONLY A REFERENCE POINT TO SELECT PLATE THICKNESS AND BOLT DIAMETER.

p_{ext}	4	in	$p_{f,o}$	2.25	in	$p_{f,i}$	2.25	in	p_b	3.5	in
g	4.5	in	g_o	3	in	t_f	0.75	in	t_w	0.375	in
b_p				14	in	h				60	in

h_0	62.25	in	h_1	57.00	in	h_2	53.50	in	h_3	50.00	in
d_0	61.88	in	d_1	56.63	in	d_2	53.13	in	d_3	49.63	in

END-PLATE TYPE	EXTENDED	γ	1	s	3.97	in

Y = 775 in

$$Y = \frac{b_p}{2}\left[h_0\left(\frac{1}{p_{f,o}}\right)+h_1\left(\frac{1}{p_{f,i}}\right)+h_3\left(\frac{1}{s}\right)-\frac{1}{2}\right]+\frac{2}{g}\left[h_1(p_{f,i}+1.5p_b)+h_3(s+0.5p_b)\right]+\frac{g}{2}$$

$$s = \frac{1}{2}\sqrt{b_p g}$$

ϕ
0.75

ϕ_b
0.9

THIN PLATE PROCEDURE

PROCEDURE				NOTES
PLATE				
$t_{p,reqd}$	0.784	in		*PLATE THICKNESS SELECTION MADE BY ROUNDING DOWN FROM $T_{P,REQD}$ TO INDUCE THIN PLATE BEHAVIOR. SINCE M_U IS ONLY A REFERENCE POINT, IT IS NOT NECESSARY TO USE A PLATE THICKNESS GREATER THAN $T_{P,REQD}$.*
$t_{p,reqd} = \sqrt{\frac{\gamma M_u}{F_{py} Y}}$				
t_p	0.750	in		
BOLTS				
A325	F_t	90	ksi	
d_b (trial)	1.000	in		
BOLT DISTRIBUTION FACTORS				
α_0	1	α_1	0.5	
β_1	1	β_2	0.75	
γ_1	0.75	γ_2	-	
δ_1	0.50	δ_3	-	
P_t	71	kips		
$P_t = \pi d_b^2 F_t / 4$				

THIN PLATE PROCEDURE (cont.)

PROCEDURE (cont.)

T_b	51	kips
AISC MANUAL TABLE J3.1		
T_b (snug)	13	kips

PRYING FORCES

INNER COLUMNS (1)			*OUTER COLUMNS (2)*		
$w_{0,1}$	3.75	in	$w_{0,2}$	3.25	in
$w_{0,1}'$	2.69	in	$w_{0,2}'$	2.19	in
$w_{1,1}$	3.75	in	$w_{1,2}$	3.25	in
$w_{1,1}'$	2.69	in	$w_{1,2}'$	2.19	in
$w_{2,1}$	3.75	in			
$w_{2,1}'$	2.69	in			
$w_{3,1}$	3.75	in			
$w_{3,1}'$	2.69	in			

a_o	1.47	in
a_i	1.47	in

INNER COLUMNS (1)			*OUTER COLUMNS (2)*		
$F_{0,1}'$	22.141	kips	$F_{0,2}'$	19.326	kips
$F_{1,1}'$	22.141	kips	$F_{1,2}'$	19.326	kips
$F_{2,1}'$	22.141	kips			
$F_{3,1}'$	22.141	kips			

$$F_{o,n}' = \frac{t_p^2 F_{py}\left(0.85 w_n + 0.80 w_n'\right) + \frac{\pi d_b^3 F_t}{8}}{4 p_{f,o}}$$

$$F_{i,n}' = \frac{t_p^2 F_{py}\left(0.85 w_n + 0.80 w_n'\right) + \frac{\pi d_b^3 F_t}{8}}{4 p_{f,i}}$$

INNER COLUMNS (1)			*OUTER COLUMNS (2)*		
$Q_{max,0,1}$	13.172	kips	$Q_{max,0,2}$	10.61	kips
$Q_{max,1,1}$	13.172	kips	$Q_{max,1,2}$	10.61	kips
$Q_{max,2,1}$	13.172	kips			
$Q_{max,3,2}$	13.172	kips			

$$Q_{\max,o,n} = \frac{w_n' t_p^2}{4 a_o}\sqrt{F_{py}^2 - 3\left(\frac{F_o'}{w_n' t_p}\right)^2}$$

$$Q_{\max,i,n} = \frac{w_n' t_p^2}{4 a_i}\sqrt{F_{py}^2 - 3\left(\frac{F_i'}{w_n' t_p}\right)^2}$$

NOTES (cont.)

FOR A325 SNUG-TIGHTENED BOLTS

d_b (in)	≤ 5/8	3/4	7/8	≥ 1
% of T_b min	75	50	38	25

THIN PLATE PROCEDURE (cont.)

PROCEDURE (cont.)	NOTES (cont.)

BOLT ROW PRYING COMBINATIONS

COMBINATION	B. ROW	PRY.[1]	M_q
1	0	YES	29370
	1	YES	
	2	NO[2]	
	3	YES	
2	0	NO	28000
	1	YES	
	2	NO	
	3	YES	
3	0	YES	27540
	1	NO	
	2	NO	
	3	NO	
4	0	NO	26170
	1	NO	
	2	NO	
	3	NO	

EXCEL USER NOTE: VERIFY ϕMq EQUATIONS REFERENCE PROPER Tb (MINIMUM PRETENSION OR SNUG-TIGHT)

M_q 29370 k·in

$$M_q = max(\, prying\,,\, pretension\,)$$

AS PER DG16, MAXIMUM ϕMq VALUE CONTROLS

1) YES: BOLT ROW UNDERGOES PRYING
NO: BOLT ROW DOES NOT UNDERGO PRYING
2) BOLT SUBJECTED TO PRETENSION FORCE ONLY

BOLT ROW PRYING COMBINATION ASSUMPTIONS ARE BASED UPON PRIOR EXPERIMENTAL TESTING

OTHER LIMIT STATES

BOLT RUPTURE w/o PRYING ACTION (M_{np})

M_{np} 48030 k·in

$$M_{np} = 2P_t\left(2d_0 + 2d_1 + d_2 + d_3\right)$$

END-PLATE YIELDING (M_{pl})

M_{pl} 23800 k·in

$$M_{pl} = F_{py} t_p^2 Y$$

CONSIDER ALL LIMIT STATES TO DETERMINE CONTROLLING FAILURE MODE

SUMMARY

M_{np} 48030 k·in

$$M_{np} = 2P_t\left(2d_0 + 2d_1 + d_2 + d_3\right)$$

REMOVE ϕ AND ϕb FACTORS IN ORDER TO DETERMINE CONTROLLING FAILURE MODE FOR **EXPERIMENTAL** TESTS

THIN PLATE PROCEDURE (cont.)			
PROCEDURE (cont.)			**NOTES (cont.)**
SUMMARY (cont.)			REMOVE ϕ AND ϕb FACTORS IN ORDER TO DETERMINE CONTROLLING FAILURE MODE FOR **EXPERIMENTAL** TESTS
$\mathbf{M_q}$	29370	k·in	
$M_q = max(\, prying\, ,\, pretension\,)$			
$\mathbf{M_{pl}}$	23800	k·in	
$M_{pl} = F_{py} t_p^2 Y$			
RATIOS			*A M_q/M_{pl} RATIO BETWEEN 1.10 AND 1.40 IS DESIREABLE SO AS TO INDUCE PROPER PROGRESSION THROUGH LIMIT STATES DURING **EXPERIMENTAL** TESTS*
$\mathbf{M_{np}/M_q}$	1.64		
$\mathbf{M_q/M_{pl}}$	1.23		

DESIGN M_u[1]	13000	k·in	A992	F_{py}	59.3	ksi

1) DESIGN M_U IS SET AT APPROXIMATELY 75% OF ϕM_N OF THE PLATE GIRDER SECTION. THIS ENSURES THE CONNECTION WILL FAIL PRIOR TO THE GIRDER. ACHIEVING DESIGN M_U IS NOT REQUIRED FOR CONNECTION DESIGN. DESIGN M_U IS ONLY A REFERENCE POINT TO SELECT PLATE THICKNESS AND BOLT DIAMETER.

p_{ext}	4	in	$p_{f,o}$	2.25	in	$p_{f,i}$	2.25	in	p_b	3.5	in
t_f	0.75	in	t_w	0.375	in	g	4.5	in	g_o	3	in
			b_p	14	in	h				36	in

h_0	38.25	in	h_1	33.00	in	h_2	29.50	in	h_3	26.00	in
d_0	37.88	in	d_1	32.63	in	d_2	29.13	in	d_3	25.63	in

END-PLATE TYPE	EXTENDED	γ	1	s	3.97	in
Y	442	in		$s = \frac{1}{2}\sqrt{b_p g}$		
$Y = \frac{b_p}{2}\left[h_0\left(\frac{1}{p_{f,o}}\right)+h_1\left(\frac{1}{p_{f,i}}\right)+h_3\left(\frac{1}{s}\right)-\frac{1}{2}\right]+\frac{2}{g}\left[h_1(p_{f,i}+1.5p_b)+h_3(s+0.5p_b)\right]+\frac{g}{2}$				ϕ	0.75	
				ϕ_b	0.9	

THICK PLATE PROCEDURE				
PROCEDURE				NOTES
A325	F_t	90	ksi	
$d_{b,reqd}$		0.69	in	*SINCE M_U IS ONLY A REFERENCE POINT, IT IS NOT NECESSARY TO USE A BOLT SIZE GREATER THAN $D_{B,REQD}$.*
$d_{b,reqd} = \sqrt{\frac{2M_u}{\pi F_t(2d_0+2d_1+d_2+d_3)}}$				
d_b		0.750	in	
P_t		40	kips	
$P_t = \pi d_b^2 F_t / 4$				
M_{np}		15570	k·in	
$M_{np} = 2P_t(2d_0+2d_1+d_2+d_3)$				
$t_{p,reqd}$		0.81	in	*TO INDUCE THICK PLATE BEHAVIOR, SELECT A PLATE THICKNESS GREATER THAN $T_{P,REQD}$.*
$t_{p,reqd} = \sqrt{\frac{\gamma M_{np}}{0.9F_{py}Y}}$				
t_p		1.00	in	

THICK PLATE PROCEDURE (cont.)			
PROCEDURE (cont.)			**NOTES (cont.)**
OTHER LIMIT STATES			
M_{pl}	26230	k·in	*CONSIDER ALL LIMIT STATES TO DETERMINE CONTROLLING FAILURE MODE*
$M_{pl} = F_{py} t_p^2 Y$			
SUMMARY			
M_{np}	15570	k·in	*REMOVE ϕ AND ϕb FACTORS IN ORDER TO DETERMINE CONTROLLING FAILURE MODE FOR **EXPERIMENTAL** TESTS*
$M_{np} = 2P_t(2d_0 + 2d_1 + d_2 + d_3)$			
M_{pl}	26230	k·in	
$M_{pl} = F_{py} t_p^2 Y$			
RATIOS			*A Mpl/Mnp RATIO BETWEEN 1.10 AND 1.40 IS DESIREABLE SO AS TO INDUCE PROPER PROGRESSION THROUGH LIMIT STATES DURING **EXPERIMENTAL** TESTS*
M_{pl}/M_{np}	1.68		

VIRGINIA TECH	12 BOLT - EXT - MRE 1/3 4W/2W - SHALLOW - THIN	DATE 05/09/14	MADE PRB	SHEET NO. 33 of 36

DESIGN M_u [1]	13000	k·in	A992	F_{py}	54.6	ksi

1) DESIGN M_U IS SET AT APPROXIMATELY 75% OF ϕM_N OF THE PLATE GIRDER SECTION. THIS ENSURES THE CONNECTION WILL FAIL PRIOR TO THE GIRDER. ACHIEVING DESIGN M_U IS NOT REQUIRED FOR CONNECTION DESIGN. DESIGN M_U IS ONLY A REFERENCE POINT TO SELECT PLATE THICKNESS AND BOLT DIAMETER.

p_{ext}	4	in	$p_{f,o}$	2.25	in	$p_{f,i}$	2.25	in	p_b	3.5	in
t_f	0.75	in	t_w	0.375	in	g	4.5	in	g_o	3	in
			b_p	14	in				h	36	in

h_0	38.25	in	h_1	33.00	in	h_2	29.50	in	h_3	26.00	in
d_0	37.88	in	d_1	32.63	in	d_2	29.13	in	d_3	25.63	in

END-PLATE TYPE	EXTENDED	γ	1	s	3.97	in
Y	442	in		$s = \frac{1}{2}\sqrt{b_p g}$		
$Y = \frac{b_p}{2}\left[h_0\left(\frac{1}{p_{f,o}}\right)+h_1\left(\frac{1}{p_{f,i}}\right)+h_3\left(\frac{1}{s}\right)-\frac{1}{2}\right]+\frac{2}{g}\left[h_1(p_{f,i}+1.5p_b)+h_3(s+0.5p_b)\right]+\frac{g}{2}$				ϕ	0.75	
				ϕ_b	0.9	

THIN PLATE PROCEDURE

PROCEDURE				NOTES
PLATE				
$t_{p,reqd}$	0.734	in		*PLATE THICKNESS SELECTION MADE BY ROUNDING DOWN FROM $T_{P,REQD}$ TO INDUCE THIN PLATE BEHAVIOR. SINCE M_U IS ONLY A REFERENCE POINT, IT IS NOT NECESSARY TO USE A PLATE THICKNESS GREATER THAN $T_{P,REQD}$.*
$t_{p,reqd} = \sqrt{\frac{\gamma M_u}{F_{py} Y}}$				
t_p	0.750	in		
BOLTS				
A325	F_t	90	ksi	
d_b (trial)	1.000	in		
BOLT DISTRIBUTION FACTORS				
α_0	1	α_1	0.5	
β_1	1	β_2	0.75	
γ_1	0.75	γ_2	-	
δ_1	0.50	δ_3	-	
P_t	71	kips		
$P_t = \pi d_b^2 F_t / 4$				

THIN PLATE PROCEDURE (cont.)

PROCEDURE (cont.)

T_b	51	kips
AISC MANUAL TABLE J3.1		
T_b (snug)	13	kips

PRYING FORCES

INNER COLUMNS (1)			*OUTER COLUMNS (2)*		
$w_{0,1}$	3.75	in	$w_{0,2}$	3.25	in
$w_{0,1}'$	2.69	in	$w_{0,2}'$	2.19	in
$w_{1,1}$	3.75	in	$w_{1,2}$	3.25	in
$w_{1,1}'$	2.69	in	$w_{1,2}'$	2.19	in
$w_{2,1}$	3.75	in			
$w_{2,1}'$	2.69	in			
$w_{3,1}$	3.75	in			
$w_{3,1}'$	2.69	in			

a_o	1.47	in
a_i	1.47	in

INNER COLUMNS (1)			*OUTER COLUMNS (2)*		
$F_{0,1}'$	22.141	kips	$F_{0,2}'$	19.326	kips
$F_{1,1}'$	22.141	kips	$F_{1,2}'$	19.326	kips
$F_{2,1}'$	22.141	kips			
$F_{3,1}'$	22.141	kips			

$$F_{o,n}^{'} = \frac{t_p^2 F_{py}\left(0.85 w_n + 0.80 w_n^{'}\right) + \frac{\pi d_b^3 F_t}{8}}{4 p_{f,o}}$$

$$F_{i,n}^{'} = \frac{t_p^2 F_{py}\left(0.85 w_n + 0.80 w_n^{'}\right) + \frac{\pi d_b^3 F_t}{8}}{4 p_{f,i}}$$

INNER COLUMNS (1)			*OUTER COLUMNS (2)*		
$Q_{max,0,1}$	13.172	kips	$Q_{max,0,2}$	10.61	kips
$Q_{max,1,1}$	13.172	kips	$Q_{max,1,2}$	10.61	kips
$Q_{max,2,1}$	13.172	kips			
$Q_{max,3,2}$	13.172	kips			

$$Q_{\max,o,n} = \frac{w_n^{'} t_p^2}{4 a_o} \sqrt{F_{py}^2 - 3\left(\frac{F_o^{'}}{w_n^{'} t_p}\right)^2}$$

$$Q_{\max,i,n} = \frac{w_n^{'} t_p^2}{4 a_i} \sqrt{F_{py}^2 - 3\left(\frac{F_i^{'}}{w_n^{'} t_p}\right)^2}$$

NOTES (cont.)

FOR A325 SNUG-TIGHTENED BOLTS

d_b (in)	≤ 5/8	3/4	7/8	≥ 1
% of T_b min	75	50	38	25

THIN PLATE PROCEDURE (cont.)

PROCEDURE (cont.)

BOLT ROW PRYING COMBINATIONS

COMBINATION	B. ROW	PRY.[1]	M_q
1	0	YES	17030
	1	YES	
	2	NO[2]	
	3	YES	
2	0	NO	16190
	1	YES	
	2	NO	
	3	YES	
3	0	YES	15990
	1	NO	
	2	NO	
	3	NO	
4	0	NO	15150
	1	NO	
	2	NO	
	3	NO	

M_q 17030 k·in

$$M_q = max(\, prying\,,\, pretension\,)$$

1) YES: BOLT ROW UNDERGOES PRYING
NO: BOLT ROW DOES NOT UNDERGO PRYING
2) BOLT SUBJECTED TO PRETENSION FORCE ONLY

OTHER LIMIT STATES

BOLT RUPTURE w/o PRYING ACTION (M_{np})

M_{np} 27670 k·in

$$M_{np} = 2P_t\left(2d_0 + 2d_1 + d_2 + d_3\right)$$

END-PLATE YIELDING (M_{pl})

M_{pl} 13590 k·in

$$M_{pl} = F_{py} t_p^2 Y$$

SUMMARY

M_{np} 27670 k·in

$$M_{np} = 2P_t\left(2d_0 + 2d_1 + d_2 + d_3\right)$$

NOTES (cont.)

EXCEL USER NOTE: VERIFY ϕMq EQUATIONS REFERENCE PROPER Tb (MINIMUM PRETENSION OR SNUG-TIGHT)

AS PER DG16, MAXIMUM ϕMq VALUE CONTROLS

BOLT ROW PRYING COMBINATION ASSUMPTIONS ARE BASED UPON PRIOR EXPERIMENTAL TESTING

CONSIDER ALL LIMIT STATES TO DETERMINE CONTROLLING FAILURE MODE

REMOVE ϕ AND ϕb FACTORS IN ORDER TO DETERMINE CONTROLLING FAILURE MODE FOR **EXPERIMENTAL** TESTS

THIN PLATE PROCEDURE (cont.)			
PROCEDURE (cont.)			**NOTES (cont.)**
SUMMARY (cont.)			REMOVE ϕ AND ϕb FACTORS IN ORDER TO DETERMINE CONTROLLING FAILURE MODE FOR **EXPERIMENTAL** TESTS
M_q	17030	k·in	
$M_q = max(\ prying\ ,\ pretension\ )$			
M_{pl}	13590	k·in	
$M_{pl} = F_{py} t_p^2 Y$			
RATIOS			*A M_q/M_{pl} RATIO BETWEEN 1.10 AND 1.40 IS DESIREABLE SO AS TO INDUCE PROPER PROGRESSION THROUGH LIMIT STATES DURING **EXPERIMENTAL** TESTS*
M_{np}/M_q	1.62		
M_q/M_{pl}	1.25		

VIRGINIA TECH	PLATE GIRDER - DEEP	DATE 04/16/14	MADE PRB	SHEET NO. 36 of

Material Properties

E	Elastic Modulus	29000	ksi	Fy	Yield Strength	55	ksi
L_B	Unbraced Length	0	in				

Plate Girder Dimensions

	Width		Height		Area		Distance From Centroid of Shape to Top of Plate Girder		Distance From Centroid of Shape to Centroid of Plate Girder	
Top Flange	12	in	0.75	in	9	in^2	0.375	in	29.625	in
Web	0.375	in	58.5	in	21.938	in^2	30	in	0	in
Bottom Flange	12	in	0.75	in	9	in^2	59.625	in	29.625	in

Plate Girder Properties

Centroid	30.0	in	Measured from top of plate girder.	
Moment of Inertia	22054.7	in^4		59.25
Elastic Neutral Axis	30.0	in	Measured from top of plate girder.	
Plastic Neutral Axis	30.0	in	Measured from top of plate girder. Assume is in web.	
h_c	58.5	in	S_{xc}	735.16 in^3
h_p	58.5	in		

Slenderness

K_c	0.3500			
F_L	38.5	ksi	Verify that conditions are valid for $F_L=0.7*F_y$	

	λ	λ_p	λ_r	
Flange	8	8.726	15.425	COMPACT
Web*	156	86.339	130.886	SLENDER

*Based upon doubly symmetric cross section

Determine RPG

a_w	2.44	h_c/t_w	156
5.7*(E/Fy)^1/2	130.89	RPG	0.968

Limit State Analysis

F_{CR} Compression Flange Strength 55.00 ksi

Yield

F_{CR} 55.00 ksi

Flange Local Buckling

F_{CR} 55.00 ksi

VIRGINIA TECH	PLATE GIRDER - DEEP	DATE 04/16/14	MADE PRB	SHEET NO. 36 of

Lateral Torsional Buckling

F_{CR} 55.00

I_{CY}	108.04	in^4	A	12.66	in^2
r_t	2.92		C_b	1	
L_P	73.80	in	L_R	251.92	in

NO LTB

Bend-Buckling of the Web

F_{CR} 55.00 (IF Applicable) F_{CR} 39.04 ksi

$5.7*SQRT(E/F_{CR})$ 156.00 = h/tw 156.00

NOT APPLICABLE

Design Moment

Mn	39151.9	k·in	ϕMn	35236.7	k·in
Mn	3262.7	k·ft	ϕMn	2936.4	k·ft

Eight Bolt - Extended, Stiffened End Plate Configuration

Specimen: **8ES-0.875-0.75-24 (EP-1) - Thin**
Reference: **Ghassemieh et al. 1983**

Rafter Input Information (W24x100):

b_f	12.00	in
t_f	0.75	in
t_w	0.4375	in
depth, d	24	in
E	29000	ksi
L_B	0	in
F_y	36	ksi
F_u	58	ksi

End Plate Input Information:

b_p	12.00	in	
g	5.50	in	
p_{ext}	5.75	in	guess
$p_{f,o}$	1.38	in	
$p_{f,i}$	1.375	in	
p_b	3	in	guess

ϕ	0.75	
ϕ_b	0.9	
t_p	0.75	in
F_{py}	38.7	ksi
F_{pu}	58	ksi

Bolts	A325	
F_t	90	ksi
d_b	0.875	in
T_b	39 kips	

Summary:

M_{np}	10230	k·in	853	k·ft
$M_{q\ -\ DG16}$	7780	k·in	648	k·ft
$M_{q\ -\ proposed}$	6941	k·in	578	k·ft
$M_{pl\ -\ old}$	9460	k·in	788	k·ft
$M_{pl\ -\ new}$	9460	k·in	788	k·ft

Rafter Section Limit States

M_n	8546	k·in	712	k·ft
φM_n	7691	k·in	641	k·ft
M_p	9526	k·in	794	k·ft
M_{pe}	12437	k·in	1036	k·ft

$M_{np}/M_{q\ -\ DG16}$	1.31
$M_{q\ -\ DG16}/M_{pl\ -\ old}$	0.82

Calculations:

s	4.062	in
	$p_{ext} \le s$	NO
	$p_{ext} > s$	YES
	CASE II	
EXTENDED		
γ	1	

$$s = \frac{1}{2}\sqrt{b_p g}$$

h_0	28.38	in
h_1	25.38	in
h_2	22.625	in
h_3	19.625	in
d_0	28.00	in
d_1	25.00	in
d_2	22.25	in
d_3	19.25	in
t_p	1	in

Check End Plate Yielding (Based on Sumner 2003)

Case I:

$$Y = \frac{b_p}{2}\left[h_0\left(\frac{1}{2p_{ext}}\right)+h_1\left(\frac{1}{p_{f,o}}\right)+h_2\left(\frac{1}{p_{f,i}}\right)+h_3\left(\frac{1}{s}\right)\right]+\frac{2}{g}\left[h_0\left(p_{ext}+\frac{p_b}{4}\right)+h_1\left(p_{f,o}+\frac{3p_b}{4}\right)+h_2\left(p_{f,i}+\frac{p_b}{4}\right)+h_3\left(s+\frac{3p_b}{4}\right)+p_b^2\right]+g$$

Y_1 425.06

Case II:

$$Y = \frac{b_p}{2}\left[h_0\left(\frac{1}{s}\right)+h_1\left(\frac{1}{p_{f,o}}\right)+h_2\left(\frac{1}{p_{f,i}}\right)+h_3\left(\frac{1}{s}\right)\right]+\frac{2}{g}\left[h_0\left(s+\frac{p_b}{4}\right)+h_1\left(p_{f,o}+\frac{3p_b}{4}\right)+h_2\left(p_{f,i}+\frac{p_b}{4}\right)+h_3\left(s+\frac{3p_b}{4}\right)+p_b^2\right]+g$$

Y_2 434.76

Controlling Case:

Y 434.76

M_{pl} 9460 k·in $M_{pl} = F_{py} t_p^2 Y$

Check Plate Yielding with New Yield Line Solution

$$Y = \frac{b_p}{2}\left[\frac{h_0}{s}+\frac{h_1}{p_{f,o}}+\frac{h_2}{p_{f,i}}+\frac{h_3}{s}\right]+\frac{2}{g}\left[h_0\left(s+\frac{3p_b}{4}\right)+h_1\left(p_{f,o}+\frac{p_b}{4}\right)+h_2\left(p_{f,i}+\frac{3p_b}{4}\right)+h_3(s+\frac{p_b}{4})\right]+g$$

Y_1 425.06

Y_2 434.76

Y 434.76

M_{pl} 9460 k-in

Check Bolt Rupture Without Prying Action

M_{np} 10230 k·in $M_{np} = 2P_t(d_1 + d_2 + d_3 + d_4)$

Check Bolt Rupture with Prying Action

P_t	54	kips

$$P_t = \pi d_b^2 F_t / 4$$

BOLT DISTRIBUTION FACTORS		
α_1	1.00	
β_1	1.00	
γ_1	1.00	
δ_1	1.00	
PRYING FORCES		
$w_{\alpha,1}$	6.00	in
$w_{\alpha,1}'$	5.06	in
$w_{\beta,1}$	6.00	in
$w_{\beta,1}'$	5.06	in
$w_{\gamma,1}$	6.00	in
$w_{\gamma,1}'$	5.06	in
$w_{\delta,1}$	6.00	in
$w_{\delta,1}'$	5.06	in
$a_{\alpha,o}$	1.375	in
a_o	2.234	in
a_i	2.234	in
$F_{\alpha,1}'$	40.52	kips
$F_{\beta,1}'$	40.52	kips
$F_{\gamma,1}'$	40.52	kips
$F_{\delta,1}'$	40.52	kips
$Q_{max,\alpha,1}$	17.60	kips
$Q_{max,\beta,1}$	10.84	kips
$Q_{max,\gamma,1}$	10.84	kips
$Q_{max,\delta,1}$	10.84	kips

There were some references that reduced the amount of force in some bolt lines farther from the flange. We set this to 1.00 here.
For instance, Ghassemieh (1983) divides total flange force by 6.8 to say the bolts are 85% effective.

Follows the procedures in the design guide 16

$$F_{o,n}' = \frac{t_p^2 F_{py}\left(0.85 w_n + 0.80 w_n'\right) + \frac{\pi d_b^3 F_t}{8}}{4 p_{f,o}}$$

$$F_{i,n}' = \frac{t_p^2 F_{py}\left(0.85 w_n + 0.80 w_n'\right) + \frac{\pi d_b^3 F_t}{8}}{4 p_{f,i}}$$

$$Q_{\max,o,n} = \frac{w_n' t_p^2}{4 a_o}\sqrt{F_{py}^2 - 3\left(\frac{F_o'}{w_n' t_p}\right)^2}$$

$$Q_{\max,i,n} = \frac{w_n' t_p^2}{4 a_i}\sqrt{F_{py}^2 - 3\left(\frac{F_i'}{w_n' t_p}\right)^2}$$

BOLT ROW PRYING COMBINATIONS			
COMBINATION	**B. ROW**	**PRY.[1]**	**M_q**
Not Normally checked	1	YES	7800
	2	YES	
	3	YES	
	4	YES	
1	1	NO	7780
	2	YES	
	3	YES	
	4	NO	
2	1	NO	7590
	2	YES	
	3	NO	
	4	NO	
3	1	NO	7560
	2	NO	
	3	YES	
	4	NO	
4	1	NO	7370
	2	NO	
	3	NO	
	4	NO	
M_q	7780		k·in

Ignore this answer because the prying forces aren't correct for rows 1 and 4

AS PER DG16, MAXIMUM Mq VALUE CONTROLS

$$M_q = max(\,prying\,,\,pretension\,)$$

Proposed Procedure for Bolt Prying Action Based on AISC 360-10

	Rows 1 and 4			Row 2			Row 3		
	$a=(b_p-g)/2$	3.25	in	$a=p_b/2$	1.50	in	$a=p_b/2$	1.50	in
	$a'=a+d_b/2$	3.69	in	$a'=a+d_b/2$	1.94	in	$a'=a+d_b/2$	1.94	in
	$b=(g+t_w)/2$	2.97	in	$b=p_{fo}$	1.38	in	$b=p_{fi}$	1.38	in
	$b'=b-d_b/2$	2.53	in	$b'=b-d_b/2$	0.94	in	$b'=b-d_b/2$	0.94	in
	$p=\min(b, p_b)$	2.97	in	$p=b_p-t_w/2$	5.78	in	$p=b_p-t_w/2$	5.78	in
	$d_{hole}=d_b+1/16$	0.94	in						
	$T=\phi F_t A_b$	40.6	kips						
	$\phi M_p=\frac{\phi t_p^2 p F_{pu}}{4}$	21.8	k-in		42.4	k-in		42.4	k-in
	$\delta=1-\frac{d_{hole}}{p}$	0.68			0.84			0.84	
	$\alpha=\frac{1}{\delta}\left(\frac{Tb'}{\phi M_p}-1\right)$	5.43			-0.12			-0.12	
		two plastic hinges			thick plate			thick plate	
For one plastic hinge:									
	$q=T\left(\frac{\delta\alpha}{1+\delta\alpha}\right)\left(\frac{b'}{a'}\right)$	22.0	kips		-2.3	kips		-2.3	kips
	$T_{allow}=T-q$	18.6	kips		42.9	kips		42.9	kips
For two plastic hinges:									
	$T_{allow}=\frac{1}{b'}\phi M_p \delta p(1+\delta)$	29.5	kips		403.0	kips		403.0	kips
	T_{allow} based on α	29.5	kips		42.9	kips		42.9	kips

Moment Capacity

$M_q=\sum(2T_{allow}d_n)$ 6941.4 kip-in

Plate Girder Dimensions

	Width		Height		Area		Distance From Centroid of Shape to Top of Plate Girder		Distance From Centroid of Shape to Centroid of Plate Girder	
Top Flange	12.00	in	0.75	in	9	in^2	0.375	in	11.625	in
Web	0.4375	in	22.5	in	9.8438	in^2	12	in	0	in
Bottom Flange	12.00	in	0.75	in	9	in^2	23.625	in	11.625	in

Plate Girder Properties

Centroid	12.0	in	Measured from top of plate girder.		
Moment of Inertia	2848.7	in^4			59.25
Elastic Neutral Axis	12.0	in	Measured from top of plate girder.		
Plastic Neutral Axis	12.0	in	Measured from top of plate girder. Assume is in web.		

h_c	22.5	in	S_{xc}	237	in^3
h_p	22.5	in	Z_x	265	in^3

Slenderness

K_c	0.5578			
F_L	25.2	ksi	Verify that conditions are valid for $F_L=0.7*F_y$	

	λ	λ_p	λ_r	
Flange	8	10.785	24.069	COMPACT
Web*	51.42857143	106.717	161.779	COMPACT

*Based upon doubly symmetric cross section

Determine RPG

a_w	1.09	h_c/t_w	51.42857143
5.7*(E/Fy)^1/2	161.78	RPG	1.000

Limit State Analysis

F_{CR} Compression Flange Strength 36.00 ksi

Yield

F_{CR} 36.00 ksi

Flange Local Buckling

F_{CR} 36.00 ksi

Lateral Torsional Buckling

F_{CR} 36.00

I_{CY}	108.03	in^4	A	10.64	in^2
r_t	3.19		C_b	1	
L_P	99.48	in	L_R	339.57	in

NO LTB

Bend-Buckling of the Web

F_{CR} 36.00 (IF Applicable) F_{CR} 359.18 ksi

5.7*SQRT(E/F_{CR}) 52.00 > h/tw 51.43

NOT APPLICABLE

Design Moment

M_n	8546	k·in
φM_n	7691	k·in
M_p	9526	k·in
M_{pe}	12437	k·in

Eight Bolt - Extended, Stiffened End Plate Configuration

Specimen: **8ES-1.25-1.25-36 - Thick**

Reference: **Sumner 2003 and Sumner and Murray 2000**

Rafter Input Information (W24x100):

b_f	12.25	in
t_f	0.93	in
t_w	0.6875	in
depth, d	35.813	in
E	29000	ksi
L_B	0	in
F_y	54.5	ksi
F_u	70.4	ksi

End Plate Input Information:

b_p	13.00	in	
g	5.98	in	
p_{ext}	7.31	in	guess
$p_{f,o}$	1.90	in	
$p_{f,i}$	1.90	in	
p_b	3.761	in	guess

ϕ	0.75	
ϕ_b	0.9	
t_p	1.265	in
F_{py}	40.5	ksi
F_{pu}	67.1	ksi

Bolts	A325	
F_t	90	ksi
d_b	1.250	in
T_b	71 kips	

Summary:

M_{np}	31230	k·in	2603	k·ft
$M_{q\ -\ DG16}$	23100	k·in	1925	k·ft
$M_{q\ -\ proposed}$	28175	k·in	2348	k·ft
$M_{pl\ -\ old}$	38920	k·in	3243	k·ft
$M_{pl\ -\ new}$	38920	k·in	3243	k·ft

Rafter Section Limit States

M_n	27947	k·in	2329	k·ft
φM_n	25152	k·in	2096	k·ft
M_p	32478	k·in	2707	k·ft
M_{pe}	37216	k·in	3101	k·ft

$M_{np}/M_{q\ -\ DG16}$	1.35
$M_{q\ -\ DG16}/M_{pl\ -\ old}$	0.59

Calculations:

s	4.4085	in
	$p_{ext} \le s$	NO
	$p_{ext} > s$	YES
	CASE II	
EXTENDED		
γ	1	

$$s = \frac{1}{2}\sqrt{b_p g}$$

h_0	41.47	in
h_1	37.71	in
h_2	33.916	in
h_3	30.155	in
d_0	41.01	in
d_1	37.24	in
d_2	33.451	in
d_3	29.69	in
t_p	1	in

Check End Plate Yielding (Based on Sumner 2003)

Case I:

$$Y = \frac{b_p}{2}\left[h_0\left(\frac{1}{2p_{ext}}\right)+h_1\left(\frac{1}{p_{f,o}}\right)+h_2\left(\frac{1}{p_{f,i}}\right)+h_3\left(\frac{1}{s}\right)\right]+\frac{2}{g}\left[h_0\left(p_{ext}+\frac{p_b}{4}\right)+h_1\left(p_{f,o}+\frac{3p_b}{4}\right)+h_2\left(p_{f,i}+\frac{p_b}{4}\right)+h_3\left(s+\frac{3p_b}{4}\right)+p_b^2\right]+g$$

Y_1 598.06

Case II:

$$Y = \frac{b_p}{2}\left[h_0\left(\frac{1}{s}\right)+h_1\left(\frac{1}{p_{f,o}}\right)+h_2\left(\frac{1}{p_{f,i}}\right)+h_3\left(\frac{1}{s}\right)\right]+\frac{2}{g}\left[h_0\left(s+\frac{p_b}{4}\right)+h_1\left(p_{f,o}+\frac{3p_b}{4}\right)+h_2\left(p_{f,i}+\frac{p_b}{4}\right)+h_3\left(s+\frac{3p_b}{4}\right)+p_b^2\right]+g$$

Y_2 600.52

Controlling Case:

Y 600.52

M_{pl} 38920 k·in $M_{pl} = F_{py} t_p^2 Y$

Check Plate Yielding with New Yield Line Solution

$$Y = \frac{b_p}{2}\left[\frac{h_0}{s}+\frac{h_1}{p_{f,o}}+\frac{h_2}{p_{f,i}}+\frac{h_3}{s}\right]+\frac{2}{g}\left[h_0\left(s+\frac{3p_b}{4}\right)+h_1\left(p_{f,o}+\frac{p_b}{4}\right)+h_2\left(p_{f,i}+\frac{3p_b}{4}\right)+h_3(s+\frac{p_b}{4})\right]+g$$

Y_1 598.06

Y_2 600.52

Y 600.52

M_{pl} 38920 k-in

Check Bolt Rupture Without Prying Action

M_{np} 31230 k·in $M_{np} = 2P_t(d_1 + d_2 + d_3 + d_4)$

Check Bolt Rupture with Prying Action

P_t	110	kips

$$P_t = \pi d_b^2 F_t / 4$$

BOLT DISTRIBUTION FACTORS		
α_1	1.00	
β_1	1.00	
γ_1	1.00	
δ_1	1.00	
PRYING FORCES		
$w_{\alpha,1}$	6.50	in
$w_{\alpha,1}'$	5.19	in
$w_{\beta,1}$	6.50	in
$w_{\beta,1}'$	5.19	in
$w_{\gamma,1}$	6.50	in
$w_{\gamma,1}'$	5.19	in
$w_{\delta,1}$	6.50	in
$w_{\delta,1}'$	5.19	in
$a_{\alpha,o}$	1.652	in
a_o	3.731	in
a_i	3.731	in
$F_{\alpha,1}'$	91.73	kips
$F_{\beta,1}'$	91.73	kips
$F_{\gamma,1}'$	91.73	kips
$F_{\delta,1}'$	91.73	kips
$Q_{max,\alpha,1}$	40.78	kips
$Q_{max,\beta,1}$	18.06	kips
$Q_{max,\gamma,1}$	18.06	kips
$Q_{max,\delta,1}$	18.06	kips

There were some references that reduced the amount of force in some bolt lines farther from the flange. We set this to 1.00 here.
For instance, Ghassemieh (1983) divides total flange force by 6.8 to say the bolts are 85% effective.

Follows the procedures in the design guide 16

$$F_{o,n}' = \frac{t_p^2 F_{py}\left(0.85 w_n + 0.80 w_n'\right) + \frac{\pi d_b^3 F_t}{8}}{4 p_{f,o}}$$

$$F_{i,n}' = \frac{t_p^2 F_{py}\left(0.85 w_n + 0.80 w_n'\right) + \frac{\pi d_b^3 F_t}{8}}{4 p_{f,i}}$$

$$Q_{\max,o,n} = \frac{w_n' t_p^2}{4 a_o}\sqrt{F_{py}^2 - 3\left(\frac{F_o'}{w_n' t_p}\right)^2}$$

$$Q_{\max,i,n} = \frac{w_n' t_p^2}{4 a_i}\sqrt{F_{py}^2 - 3\left(\frac{F_i'}{w_n' t_p}\right)^2}$$

BOLT ROW PRYING COMBINATIONS			
COMBINATION	**B. ROW**	**PRY.[1]**	**M_q**
Not Normally checked	1	YES	24260
	2	YES	
	3	YES	
	4	YES	
1	1	NO	23100
	2	YES	
	3	YES	
	4	NO	
2	1	NO	21670
	2	YES	
	3	NO	
	4	NO	
3	1	NO	21510
	2	NO	
	3	YES	
	4	NO	
4	1	NO	20080
	2	NO	
	3	NO	
	4	NO	
M_q	23100		k·in

Ignore this answer because the prying forces aren't correct for rows 1 and 4

AS PER DG16, MAXIMUM Mq VALUE CONTROLS

$$M_q = max(\,prying\,,\,pretension\,)$$

Proposed Procedure for Bolt Prying Action Based on AISC 360-10

	Rows 1 and 4		Row 2		Row 3	
$a = (b_p - g)/2$	3.51 in	$a = p_b/2$	1.88 in	$a = p_b/2$	1.88 in	
$a' = a + d_b/2$	4.14 in	$a' = a + d_b/2$	2.51 in	$a' = a + d_b/2$	2.51 in	
$b = (g + t_w)/2$	3.33 in	$b = p_{fo}$	1.90 in	$b = p_{fi}$	1.90 in	
$b' = b - d_b/2$	2.71 in	$b' = b - d_b/2$	1.27 in	$b' = b - d_b/2$	1.27 in	
$p = \min(b, p_b)$	3.33 in	$p = b_p - t_w/2$	6.16 in	$p = b_p - t_w/2$	6.16 in	
$d_{hole} = d_b + 1/16$	1.31 in					
$T = \phi F_t A_b$	82.8 kips					
$\phi M_p = \frac{\phi t_p^2 p F_{pu}}{4}$	80.5 k-in		148.7 k-in		148.7 k-in	
$\delta = 1 - \frac{d_{hole}}{p}$	0.61		0.79		0.79	
$\alpha = \frac{1}{\delta}\left(\frac{Tb'}{\phi M_p} - 1\right)$	2.95		-0.37		-0.37	
	two plastic hinges		thick plate		thick plate	
For one plastic hinge:						
$q = T\left(\frac{\delta\alpha}{1+\delta\alpha}\right)\left(\frac{b'}{a'}\right)$	34.8 kips		-17.3 kips		-17.3 kips	
$T_{allow} = T - q$	48.0 kips		100.1 kips		100.1 kips	
For two plastic hinges:						
$T_{allow} = \frac{1}{b'}\phi M_p \delta p(1+\delta)$	96.5 kips		1012.0 kips		1012.0 kips	
$T_{allow}\ based\ on\ \alpha$	96.5 kips		100.1 kips		100.1 kips	

Moment Capacity

$M_q = \sum(2T_{allow} d_n)$ 28175 kip-in

Plate Girder Dimensions

	Width		Height		Area		Distance From Centroid of Shape to Top of Plate Girder		Distance From Centroid of Shape to Centroid of Plate Girder	
Top Flange	12.25	in	0.93	in	11.405	in^2	0.4655	in	17.441	in
Web	0.6875	in	33.951	in	23.341	in^2	17.9065	in	3.5527E-15	in
Bottom Flange	12.25	in	0.93	in	11.405	in^2	35.3475	in	17.441	in

Plate Girder Properties

Centroid	17.9	in	Measured from top of plate girder.	
Moment of Inertia	9182.1	in^4		59.25
Elastic Neutral Axis	17.9	in	Measured from top of plate girder.	
Plastic Neutral Axis	17.9	in	Measured from top of plate girder. Assume is in web.	

h_c	34.0	in	S_{xc}	513	in^3
h_p	34.0	in	Z_x	596	in^3

Slenderness

K_c	0.5692		
F_L	38.15	ksi	Verify that conditions are valid for $F_L=0.7*F_y$

	λ	λ_p	λ_r	
Flange	6.578947368	8.766	19.761	COMPACT
Web*	49.38327273	86.734	131.485	COMPACT

*Based upon doubly symmetric cross section

Determine RPG

a_w	2.05	h_c/t_w	49.38327273
5.7*(E/Fy)^1/2	131.48	RPG	1.000

Limit State Analysis

F_{CR} Compression Flange Strength 54.50 ksi

Yield

F_{CR} 54.50 ksi

Flange Local Buckling

F_{CR} 54.50 ksi

Lateral Torsional Buckling

F_{CR} 54.50

I_{CY}	142.77	in^4	A	15.29	in^2
r_t	3.06		C_b	1	
L_P	77.52	in	L_R	264.64	in

NO LTB

Bend-Buckling of the Web

F_{CR} 54.50 (IF Applicable) F_{CR} 389.55 ksi

5.7*SQRT(E/F_{CR}) 50.00 > h/tw 49.38

NOT APPLICABLE

Design Moment

M_n	27947	k·in
φM_n	25152	k·in
M_p	32478	k·in
M_{pe}	37216	k·in

Eight Bolt - Extended, Stiffened End Plate Configuration

Specimen: **8ES-0.875-1-24 (EP-2) - Thick**

Reference: **Ghassemieh et al. 1983**

Rafter Input Information (W24x100):

b_f	12.00	in
t_f	0.75	in
t_w	0.4375	in
depth, d	24	in
E	29000	ksi
L_B	0	in
F_y	36	ksi
F_u	58	ksi

End Plate Input Information:

b_p	12.00	in	
g	5.50	in	
p_{ext}	5.75	in	guess
$p_{f,o}$	1.38	in	
$p_{f,i}$	1.375	in	
p_b	3	in	guess

ϕ	0.75	
ϕ_b	0.9	
t_p	1	in
F_{py}	40.3	ksi
F_{pu}	58	ksi

Bolts	A325	
F_t	90	ksi
d_b	0.875	in
T_b	39 kips	

Summary:

M_{np}	10230	k·in	853	k·ft
$M_{q\ -\ DG16}$	8090	k·in	674	k·ft
$M_{q\ -\ proposed}$	10776	k·in	898	k·ft
$M_{pl\ -\ old}$	17520	k·in	1460	k·ft
$M_{pl\ -\ new}$	17520	k·in	1460	k·ft

Rafter Section Limit States

M_n	8546	k·in	712	k·ft
φM_n	7691	k·in	641	k·ft
M_p	9526	k·in	794	k·ft
M_{pe}	12437	k·in	1036	k·ft

$M_{np}/M_{q\ -\ DG16}$	1.26
$M_{q\ -\ DG16}/M_{pl\ -\ old}$	0.46

Calculations:

s	4.062	in
	$p_{ext} \le s$	NO
	$p_{ext} > s$	YES
	CASE II	
EXTENDED		
γ	1	

$$s = \frac{1}{2}\sqrt{b_p g}$$

h_0	28.38	in
h_1	25.38	in
h_2	22.625	in
h_3	19.625	in
d_0	28.00	in
d_1	25.00	in
d_2	22.25	in
d_3	19.25	in
t_p	1	in

Check End Plate Yielding (Based on Sumner 2003)

Case I:

$$Y = \frac{b_p}{2}\left[h_0\left(\frac{1}{2p_{ext}}\right)+h_1\left(\frac{1}{p_{f,o}}\right)+h_2\left(\frac{1}{p_{f,i}}\right)+h_3\left(\frac{1}{s}\right)\right]+\frac{2}{g}\left[h_0\left(p_{ext}+\frac{p_b}{4}\right)+h_1\left(p_{f,o}+\frac{3p_b}{4}\right)+h_2\left(p_{f,i}+\frac{p_b}{4}\right)+h_3\left(s+\frac{3p_b}{4}\right)+p_b^2\right]+g$$

Y_1 425.06

Case II:

$$Y = \frac{b_p}{2}\left[h_0\left(\frac{1}{s}\right)+h_1\left(\frac{1}{p_{f,o}}\right)+h_2\left(\frac{1}{p_{f,i}}\right)+h_3\left(\frac{1}{s}\right)\right]+\frac{2}{g}\left[h_0\left(s+\frac{p_b}{4}\right)+h_1\left(p_{f,o}+\frac{3p_b}{4}\right)+h_2\left(p_{f,i}+\frac{p_b}{4}\right)+h_3\left(s+\frac{3p_b}{4}\right)+p_b^2\right]+g$$

Y_2 434.76

Controlling Case:

Y 434.76

M_{pl} 17520 k·in $M_{pl} = F_{py} t_p^2 Y$

Check Plate Yielding with New Yield Line Solution

$$Y = \frac{b_p}{2}\left[\frac{h_0}{s}+\frac{h_1}{p_{f,o}}+\frac{h_2}{p_{f,i}}+\frac{h_3}{s}\right]+\frac{2}{g}\left[h_0\left(s+\frac{3p_b}{4}\right)+h_1\left(p_{f,o}+\frac{p_b}{4}\right)+h_2\left(p_{f,i}+\frac{3p_b}{4}\right)+h_3(s+\frac{p_b}{4})\right]+g$$

Y_1 425.06

Y_2 434.76

Y 434.76

M_{pl} 17520 k-in

Check Bolt Rupture Without Prying Action

M_{np} 10230 k·in $M_{np} = 2P_t(d_1 + d_2 + d_3 + d_4)$

Check Bolt Rupture with Prying Action

P_t	54	kips

$$P_t = \pi d_b^2 F_t / 4$$

BOLT DISTRIBUTION FACTORS		
α_1	1.00	
β_1	1.00	
γ_1	1.00	
δ_1	1.00	
PRYING FORCES		
$w_{\alpha,1}$	6.00	in
$w_{\alpha,1}'$	5.06	in
$w_{\beta,1}$	6.00	in
$w_{\beta,1}'$	5.06	in
$w_{\gamma,1}$	6.00	in
$w_{\gamma,1}'$	5.06	in
$w_{\delta,1}$	6.00	in
$w_{\delta,1}'$	5.06	in
$a_{\alpha,o}$	1.375	in
a_o	5.411	in
a_i	5.411	in
$F_{\alpha,1}'$	71.35	kips
$F_{\beta,1}'$	71.35	kips
$F_{\gamma,1}'$	71.35	kips
$F_{\delta,1}'$	71.35	kips
$Q_{max,\alpha,1}$	29.51	kips
$Q_{max,\beta,1}$	7.50	kips
$Q_{max,\gamma,1}$	7.50	kips
$Q_{max,\delta,1}$	7.50	kips

There were some references that reduced the amount of force in some bolt lines farther from the flange. We set this to 1.00 here.
For instance, Ghassemieh (1983) divides total flange force by 6.8 to say the bolts are 85% effective.

Follows the procedures in the design guide 16

$$F_{o,n}' = \frac{t_p^2 F_{py}\left(0.85 w_n + 0.80 w_n'\right) + \frac{\pi d_b^3 F_t}{8}}{4 p_{f,o}}$$

$$F_{i,n}' = \frac{t_p^2 F_{py}\left(0.85 w_n + 0.80 w_n'\right) + \frac{\pi d_b^3 F_t}{8}}{4 p_{f,i}}$$

$$Q_{\max,o,n} = \frac{w_n' t_p^2}{4 a_o}\sqrt{F_{py}^2 - 3\left(\frac{F_o'}{w_n' t_p}\right)^2}$$

$$Q_{\max,i,n} = \frac{w_n' t_p^2}{4 a_i}\sqrt{F_{py}^2 - 3\left(\frac{F_i'}{w_n' t_p}\right)^2}$$

BOLT ROW PRYING COMBINATIONS			
COMBINATION	**B. ROW**	**PRY.[1]**	**M_q**
Not Normally checked	1	YES	7580
	2	YES	
	3	YES	
	4	YES	
1	1	NO	8090
	2	YES	
	3	YES	
	4	NO	
2	1	NO	7750
	2	YES	
	3	NO	
	4	NO	
3	1	NO	7710
	2	NO	
	3	YES	
	4	NO	
4	1	NO	7370
	2	NO	
	3	NO	
	4	NO	
M_q	8090		k·in

Ignore this answer because the prying forces aren't correct for rows 1 and 4

AS PER DG16, MAXIMUM Mq VALUE CONTROLS

$$M_q = max(\,prying\,,\,pretension\,)$$

Proposed Procedure for Bolt Prying Action Based on AISC 360-10

	Rows 1 and 4			Row 2			Row 3		
	$a = (b_p - g)/2$	3.25	in	$a = p_b/2$	1.50	in	$a = p_b/2$	1.50	in
	$a' = a + d_b/2$	3.69	in	$a' = a + d_b/2$	1.94	in	$a' = a + d_b/2$	1.94	in
	$b = (g + t_w)/2$	2.97	in	$b = p_{fo}$	1.38	in	$b = p_{fi}$	1.38	in
	$b' = b - d_b/2$	2.53	in	$b' = b - d_b/2$	0.94	in	$b' = b - d_b/2$	0.94	in
	$p = \min(b, p_b)$	2.97	in	$p = b_p - t_w/2$	5.78	in	$p = b_p - t_w/2$	5.78	in
	$d_{hole} = d_b + 1/16$	0.94	in						
	$T = \phi F_t A_b$	40.6	kips						
$\phi M_p = \frac{\phi t_p^2 p F_{pu}}{4}$		38.7	k-in		75.4	k-in		75.4	k-in
$\delta = 1 - \frac{d_{hole}}{p}$		0.68			0.84			0.84	
$\alpha = \frac{1}{\delta}\left(\frac{Tb'}{\phi M_p} - 1\right)$		2.41			-0.59			-0.59	
		two plastic hinges			thick plate			thick plate	
For one plastic hinge:									
$q = T\left(\frac{\delta\alpha}{1+\delta\alpha}\right)\left(\frac{b'}{a'}\right)$		17.4	kips		-19.3	kips		-19.3	kips
$T_{allow} = T - q$		23.2	kips		59.9	kips		59.9	kips
For two plastic hinges:									
$T_{allow} = \frac{1}{b'}\phi M_p \delta p(1+\delta)$		52.4	kips		716.4	kips		716.4	kips
T_{allow} *based on* α		52.4	kips		59.9	kips		59.9	kips

Moment Capacity

$M_q = \sum(2T_{allow} d_n)$ 10776 kip-in

Plate Girder Dimensions

	Width		Height		Area		Distance From Centroid of Shape to Top of Plate Girder		Distance From Centroid of Shape to Centroid of Plate Girder	
Top Flange	12.00	in	0.75	in	9	in^2	0.375	in	11.625	in
Web	0.4375	in	22.5	in	9.8438	in^2	12	in	0	in
Bottom Flange	12.00	in	0.75	in	9	in^2	23.625	in	11.625	in

Plate Girder Properties

Centroid	12.0	in	Measured from top of plate girder.	
Moment of Inertia	2848.7	in^4		59.25
Elastic Neutral Axis	12.0	in	Measured from top of plate girder.	
Plastic Neutral Axis	12.0	in	Measured from top of plate girder. Assume is in web.	

h_c	22.5	in	S_{xc}	237	in^3
h_p	22.5	in	Z_x	265	in^3

Slenderness

K_c	0.5578			
F_L	25.2	ksi	Verify that conditions are valid for $F_L=0.7*F_y$	

	λ	λ_p	λ_r	
Flange	8	10.785	24.069	COMPACT
Web*	51.42857143	106.717	161.779	COMPACT

*Based upon doubly symmetric cross section

Determine RPG

a_w	1.09	h_c/t_w	51.42857143
5.7*(E/Fy)^1/2	161.78	RPG	1.000

Limit State Analysis

F_{CR} Compression Flange Strength 36.00 ksi

Yield

F_{CR} 36.00 ksi

Flange Local Buckling

F_{CR} 36.00 ksi

Lateral Torsional Buckling

F_{CR} 36.00

I_{CY}	108.03	in^4	A	10.64	in^2
r_t	3.19		C_b	1	
L_P	99.48	in	L_R	339.57	in

NO LTB

Bend-Buckling of the Web

F_{CR} 36.00 (IF Applicable) F_{CR} 359.18 ksi

5.7*SQRT(E/F_{CR}) 52.00 > h/tw 51.43

NOT APPLICABLE

Design Moment

M_n	8546	k·in
φM_n	7691	k·in
M_p	9526	k·in
M_{pe}	12437	k·in

Eight Bolt - Extended, Stiffened End Plate Configuration

Specimen: **Thin End Plate Specimen - 8ES-1.25-0.75-56**

Reference: **VT**

Rafter Input Information:

b_f	10.00	in
t_f	1.00	in
t_w	0.5	in
depth, d	56	in
E	29000	ksi
L_B	0	in
F_y	55	ksi
F_u	70	ksi

End Plate Input Information:

b_p	10.00	in
g	5.00	in
p_{ext}	7.50	in
$p_{f,o}$	2.25	in
$p_{f,i}$	1.75	in
p_b	3.5	in

ϕ	0.75	
ϕ_b	0.9	
t_p	0.75	in
F_{py}	57.2	ksi
F_{pu}	80.7	ksi

Bolts	**A325**	
F_t	90	ksi
d_b	1.250	in
T_b	71 kips	

Summary:

M_{np}	49260	k·in	4105	k·ft
$M_{q\ -\ DG16}$	31800	k·in	2650	k·ft
$M_{q\ -\ proposed}$	54842	k·in	4570	k·ft
$M_{pl\ -\ old}$	27610	k·in	2301	k·ft
$M_{pl\ -\ new}$	27610	k·in	2301	k·ft

Rafter Section Limit States

M_n	42601	k·in	3550	k·ft
φM_n	38341	k·in	3195	k·ft
M_p	50298	k·in	4191	k·ft
M_{pe}	57156	k·in	4763	k·ft

$M_{np}/M_{q\ -\ DG16}$	1.55
$M_{q\ -\ DG16}/M_{pl\ -\ old}$	1.15

Calculations:

s	3.5355	in
	$p_{ext} \le s$	NO
	$p_{ext} > s$	YES
	CASE II	
EXTENDED		
γ	1	

$$s = \frac{1}{2}\sqrt{b_p g}$$

h_0	61.75	in
h_1	58.25	in
h_2	54.25	in
h_3	50.75	in
d_0	61.25	in
d_1	57.75	in
d_2	53.75	in
d_3	50.25	in
t_p	1	in

Check End Plate Yielding (Based on Sumner 2003)

Case I:

$$Y = \frac{b_p}{2}\left[h_0\left(\frac{1}{2p_{ext}}\right)+h_1\left(\frac{1}{p_{f,o}}\right)+h_2\left(\frac{1}{p_{f,i}}\right)+h_3\left(\frac{1}{s}\right)\right]+\frac{2}{g}\left[h_0\left(p_{ext}+\frac{p_b}{4}\right)+h_1\left(p_{f,o}+\frac{3p_b}{4}\right)+h_2\left(p_{f,i}+\frac{p_b}{4}\right)+h_3\left(s+\frac{3p_b}{4}\right)+p_b^2\right]+g$$

Y_1 889.17

Case II:

$$Y = \frac{b_p}{2}\left[h_0\left(\frac{1}{s}\right)+h_1\left(\frac{1}{p_{f,o}}\right)+h_2\left(\frac{1}{p_{f,i}}\right)+h_3\left(\frac{1}{s}\right)\right]+\frac{2}{g}\left[h_0\left(s+\frac{p_b}{4}\right)+h_1\left(p_{f,o}+\frac{3p_b}{4}\right)+h_2\left(p_{f,i}+\frac{p_b}{4}\right)+h_3\left(s+\frac{3p_b}{4}\right)+p_b^2\right]+g$$

Y_2 857.99

Controlling Case:

Y 857.99

M_{pl} 27610 k·in $M_{pl} = F_{py} t_p^2 Y$

Check Plate Yielding with New Yield Line Solution

$$Y = \frac{b_p}{2}\left[\frac{h_0}{s}+\frac{h_1}{p_{f,o}}+\frac{h_2}{p_{f,i}}+\frac{h_3}{s}\right]+\frac{2}{g}\left[h_0\left(s+\frac{3p_b}{4}\right)+h_1\left(p_{f,o}+\frac{p_b}{4}\right)+h_2\left(p_{f,i}+\frac{3p_b}{4}\right)+h_3(s+\frac{p_b}{4})\right]+g$$

Y_1 889.17

Y_2 857.99

Y 857.99

M_{pl} 27610 k-in

Check Bolt Rupture Without Prying Action

M_{np} 49260 k·in $M_{np} = 2P_t(d_1 + d_2 + d_3 + d_4)$

Check Bolt Rupture with Prying Action

P_t	110	kips

$$P_t = \pi d_b^2 F_t / 4$$

BOLT DISTRIBUTION FACTORS		
α_1	1.00	
β_1	1.00	
γ_1	1.00	
δ_1	1.00	
PRYING FORCES		
$w_{\alpha,1}$	5.00	in
$w_{\alpha,1}'$	3.69	in
$w_{\beta,1}$	5.00	in
$w_{\beta,1}'$	3.69	in
$w_{\gamma,1}$	5.00	in
$w_{\gamma,1}'$	3.69	in
$w_{\delta,1}$	5.00	in
$w_{\delta,1}'$	3.69	in
$a_{\alpha,o}$	0.710	in
a_o	0.710	in
a_i	0.710	in
$F_{\alpha,1}'$	33.41	kips
$F_{\beta,1}'$	33.41	kips
$F_{\gamma,1}'$	33.41	kips
$F_{\delta,1}'$	33.41	kips
$Q_{max,\alpha,1}$	38.86	kips
$Q_{max,\beta,1}$	38.86	kips
$Q_{max,\gamma,1}$	38.86	kips
$Q_{max,\delta,1}$	38.86	kips

There were some references that reduced the amount of force in some bolt lines farther from the flange. We set this to 1.00 here.
For instance, Ghassemieh (1983) divides total flange force by 6.8 to say the bolts are 85% effective.

Follows the procedures in the design guide 16

$$F_{o,n}' = \frac{t_p^2 F_{py}\left(0.85 w_n + 0.80 w_n'\right) + \frac{\pi d_b^3 F_t}{8}}{4 p_{f,o}}$$

$$F_{i,n}' = \frac{t_p^2 F_{py}\left(0.85 w_n + 0.80 w_n'\right) + \frac{\pi d_b^3 F_t}{8}}{4 p_{f,i}}$$

$$Q_{\max,o,n} = \frac{w_n' t_p^2}{4 a_o}\sqrt{F_{py}^2 - 3\left(\frac{F_o'}{w_n' t_p}\right)^2}$$

$$Q_{\max,i,n} = \frac{w_n' t_p^2}{4 a_i}\sqrt{F_{py}^2 - 3\left(\frac{F_i'}{w_n' t_p}\right)^2}$$

BOLT ROW PRYING COMBINATIONS			
COMBINATION	**B. ROW**	**PRY.[1]**	**M_q**
Not Normally checked	1	YES	31930
	2	YES	
	3	YES	
	4	YES	
1	1	NO	31800
	2	YES	
	3	YES	
	4	NO	
2	1	NO	31730
	2	YES	
	3	NO	
	4	NO	
3	1	NO	31730
	2	NO	
	3	YES	
	4	NO	
4	1	NO	31670
	2	NO	
	3	NO	
	4	NO	
M_q	31800		k·in

Ignore this answer because the prying forces aren't correct for rows 1 and 4

AS PER DG16, MAXIMUM Mq VALUE CONTROLS

$$M_q = max(\,prying\,,\,pretension\,)$$

Proposed Procedure for Bolt Prying Action Based on AISC 360-10

	Rows 1 and 4			Row 2			Row 3		
	$a = (b_p - g)/2$	2.50	in	$a = p_b/2$	1.75	in	$a = p_b/2$	1.75	in
	$a' = a + d_b/2$	3.13	in	$a' = a + d_b/2$	2.38	in	$a' = a + d_b/2$	2.38	in
	$b = (g + t_w)/2$	2.75	in	$b = p_{fo}$	2.25	in	$b = p_{fi}$	1.75	in
	$b' = b - d_b/2$	2.13	in	$b' = b - d_b/2$	1.63	in	$b' = b - d_b/2$	1.13	in
	$p = \min(b, p_b)$	2.75	in	$p = b_p - t_w/2$	4.75	in	$p = b_p - t_w/2$	4.75	in
	$d_{hole} = d_b + 1/16$	1.31	in						
	$T = \phi F_t A_b$	82.8	kips						
	$\phi M_p = \frac{\phi t_p^2 p F_{pu}}{4}$	28.1	k-in		48.5	k-in		48.5	k-in
	$\delta = 1 - \frac{d_{hole}}{p}$	0.52			0.72			0.72	
	$\alpha = \frac{1}{\delta}\left(\frac{Tb'}{\phi M_p} - 1\right)$	10.08			2.45			1.27	
		two plastic hinges			two plastic hinges			two plastic hinges	
For one plastic hinge:									
	$q = T\left(\frac{\delta\alpha}{1+\delta\alpha}\right)\left(\frac{b'}{a'}\right)$	47.3	kips		36.2	kips		18.8	kips
	$T_{allow} = T - q$	35.5	kips		46.6	kips		64.0	kips
For two plastic hinges:									
	$T_{allow} = \frac{1}{b'}\phi M_p \delta p(1+\delta)$	28.9	kips		176.9	kips		255.5	kips
	T_{allow} *based on* α	28.9	kips		176.9	kips		255.5	kips

Moment Capacity

$M_q = \sum(2T_{allow} d_n)$ 54842 kip-in

Plate Girder Dimensions

	Width		Height		Area		Distance From Centroid of Shape to Top of Plate Girder		Distance From Centroid of Shape to Centroid of Plate Girder	
Top Flange	10.00	in	1.00	in	10	in^2	0.5	in	27.5	in
Web	0.5	in	54	in	27	in^2	28	in	0	in
Bottom Flange	10.00	in	1.00	in	10	in^2	55.5	in	27.5	in

Plate Girder Properties

Centroid	28.0	in	Measured from top of plate girder.	
Moment of Inertia	21687.7	in^4		59.25
Elastic Neutral Axis	28.0	in	Measured from top of plate girder.	
Plastic Neutral Axis	28.0	in	Measured from top of plate girder. Assume is in web.	

h_c	54.0	in	S_{xc}	775	in^3
h_p	54.0	in	Z_x	915	in^3

Slenderness

K_c	0.3849		
F_L	38.5	ksi	Verify that conditions are valid for $F_L=0.7*F_y$

	λ	λ_p	λ_r	
Flange	5	8.726	16.176	COMPACT
Web*	108	86.339	130.886	NONCOMPACT

*Based upon doubly symmetric cross section

Determine RPG

a_w	2.70	h_c/t_w	108
5.7*(E/Fy)^1/2	130.89	RPG	1.000

Limit State Analysis

F_{CR} Compression Flange Strength 55.00 ksi

Yield

F_{CR} 55.00 ksi

Flange Local Buckling

F_{CR} 55.00 ksi

Lateral Torsional Buckling

F_{CR} 55.00

I_{CY}	83.43	in^4	A	14.50	in^2
r_t	2.40		C_b	1	
L_P	60.59	in	L_R	206.82	in

NO LTB

Bend-Buckling of the Web

F_{CR} 55.00 (IF Applicable) F_{CR} 81.45 ksi

5.7*SQRT(E/F_{CR}) 108.00 = h/tw 108.00

NOT APPLICABLE

Design Moment

M_n	42601	k·in
φM_n	38341	k·in
M_p	50298	k·in
M_{pe}	57156	k·in

Eight Bolt - Extended, Stiffened End Plate Configuration

Specimen: **Thick End Plate Specimen - 8ES-1.00-1.00-56**

Reference: **VT**

Rafter Input Information:

b_f	10.00	in
t_f	1.00	in
t_w	0.5	in
depth, d	56	in
E	29000	ksi
L_B	0	in
F_y	55	ksi
F_u	70	ksi

End Plate Input Information:

b_p	10.00	in
g	5.00	in
p_{ext}	7.50	in
$p_{f,o}$	2.25	in
$p_{f,i}$	1.75	in
p_b	3.5	in

ϕ	0.75	
ϕ_b	0.9	
t_p	1	in
F_{py}	58.2	ksi
F_{pu}	84.5	ksi

Bolts	A325	
F_t	90	ksi
d_b	1.000	in
T_b	51 kips	

Summary:

M_{np}	31530	k·in	2628	k·ft	2627.5
$M_{q\ -\ DG16}$	23870	k·in	1989	k·ft	2639.2
$M_{q\ -\ proposed}$	27197	k·in	2266	k·ft	1933.7
$M_{pl\ -\ old}$	49940	k·in	4162	k·ft	4161.7
$M_{pl\ -\ new}$	49940	k·in	4162	k·ft	4161.7

Rafter Section Limit States

M_n	42601	k·in	3550	k·ft
φM_n	38341	k·in	3195	k·ft
M_p	50298	k·in	4191	k·ft
M_{pe}	57156	k·in	4763	k·ft

$M_{np}/M_{q\ -\ DG16}$	1.32
$M_{q\ -\ DG16}/M_{pl\ -\ old}$	0.48

Calculations:

s	3.5355	in
	$p_{ext} \le s$	NO
	$p_{ext} > s$	YES
	CASE II	
EXTENDED		
γ	1	

$$s = \frac{1}{2}\sqrt{b_p g}$$

h_0	61.75	in
h_1	58.25	in
h_2	54.25	in
h_3	50.75	in
d_0	61.25	in
d_1	57.75	in
d_2	53.75	in
d_3	50.25	in
t_p	1	in

Check End Plate Yielding (Based on Sumner 2003)

Case I:

$$Y = \frac{b_p}{2}\left[h_0\left(\frac{1}{2p_{ext}}\right) + h_1\left(\frac{1}{p_{f,o}}\right) + h_2\left(\frac{1}{p_{f,i}}\right) + h_3\left(\frac{1}{s}\right)\right] + \frac{2}{g}\left[h_0\left(p_{ext} + \frac{p_b}{4}\right) + h_1\left(p_{f,o} + \frac{3p_b}{4}\right) + h_2\left(p_{f,i} + \frac{p_b}{4}\right) + h_3\left(s + \frac{3p_b}{4}\right) + p_b^2\right] + g$$

Y_1 889.17

Case II:

$$Y = \frac{b_p}{2}\left[h_0\left(\frac{1}{s}\right) + h_1\left(\frac{1}{p_{f,o}}\right) + h_2\left(\frac{1}{p_{f,i}}\right) + h_3\left(\frac{1}{s}\right)\right] + \frac{2}{g}\left[h_0\left(s + \frac{p_b}{4}\right) + h_1\left(p_{f,o} + \frac{3p_b}{4}\right) + h_2\left(p_{f,i} + \frac{p_b}{4}\right) + h_3\left(s + \frac{3p_b}{4}\right) + p_b^2\right] + g$$

Y_2 857.99

Controlling Case:

Y 857.99

M_{pl} 49940 k·in $M_{pl} = F_{py} t_p^2 Y$

Check Plate Yielding with New Yield Line Solution

$$Y = \frac{b_p}{2}\left[\frac{h_0}{s} + \frac{h_1}{p_{f,o}} + \frac{h_2}{p_{f,i}} + \frac{h_3}{s}\right] + \frac{2}{g}\left[h_0\left(s + \frac{3p_b}{4}\right) + h_1\left(p_{f,o} + \frac{p_b}{4}\right) + h_2\left(p_{f,i} + \frac{3p_b}{4}\right) + h_3(s + \frac{p_b}{4})\right] + g$$

Y_1 889.17

Y_2 857.99

Y 857.99

M_{pl} 49940 k-in

Check Bolt Rupture Without Prying Action

M_{np} 31530 k·in $M_{np} = 2P_t(d_1 + d_2 + d_3 + d_4)$

Check Bolt Rupture with Prying Action

P_t	71	kips

$$P_t = \pi d_b^2 F_t / 4$$

BOLT DISTRIBUTION FACTORS		
α_1	1.00	
β_1	1.00	
γ_1	1.00	
δ_1	1.00	
PRYING FORCES		
$w_{\alpha,1}$	5.00	in
$w_{\alpha,1}'$	3.94	in
$w_{\beta,1}$	5.00	in
$w_{\beta,1}'$	3.94	in
$w_{\gamma,1}$	5.00	in
$w_{\gamma,1}'$	3.94	in
$w_{\delta,1}$	5.00	in
$w_{\delta,1}'$	3.94	in
$a_{\alpha,o}$	1.750	in
a_o	3.597	in
a_i	3.597	in
$F_{\alpha,1}'$	51.78	kips
$F_{\beta,1}'$	51.78	kips
$F_{\gamma,1}'$	51.78	kips
$F_{\delta,1}'$	51.78	kips
$Q_{max,\alpha,1}$	30.13	kips
$Q_{max,\beta,1}$	14.66	kips
$Q_{max,\gamma,1}$	14.66	kips
$Q_{max,\delta,1}$	14.66	kips

There were some references that reduced the amount of force in some bolt lines farther from the flange. We set this to 1.00 here.
For instance, Ghassemieh (1983) divides total flange force by 6.8 to say the bolts are 85% effective.

Follows the procedures in the design guide 16

$$F_{o,n}' = \frac{t_p^2 F_{py}\left(0.85 w_n + 0.80 w_n'\right) + \frac{\pi d_b^3 F_t}{8}}{4 p_{f,o}}$$

$$F_{i,n}' = \frac{t_p^2 F_{py}\left(0.85 w_n + 0.80 w_n'\right) + \frac{\pi d_b^3 F_t}{8}}{4 p_{f,i}}$$

$$Q_{\max,o,n} = \frac{w_n' t_p^2}{4 a_o}\sqrt{F_{py}^2 - 3\left(\frac{F_o'}{w_n' t_p}\right)^2}$$

$$Q_{\max,i,n} = \frac{w_n' t_p^2}{4 a_i}\sqrt{F_{py}^2 - 3\left(\frac{F_i'}{w_n' t_p}\right)^2}$$

BOLT ROW PRYING COMBINATIONS			
COMBINATION	**B. ROW**	**PRY.[1]**	**M_q**
Not Normally checked	1	YES	23090
	2	YES	
	3	YES	
	4	YES	
1	1	NO	23870
	2	YES	
	3	YES	
	4	NO	
2	1	NO	23330
	2	YES	
	3	NO	
	4	NO	
3	1	NO	23290
	2	NO	
	3	YES	
	4	NO	
4	1	NO	22750
	2	NO	
	3	NO	
	4	NO	
M_q	23870		k·in

Ignore this answer because the prying forces aren't correct for rows 1 and 4

AS PER DG16, MAXIMUM Mq VALUE CONTROLS

$$M_q = max(\,prying\,,\,pretension\,)$$

Proposed Procedure for Bolt Prying Action Based on AISC 360-10

	Rows 1 and 4		Row 2		Row 3	
	$a = (b_p - g)/2$	2.50 in	$a = p_b/2$	1.75 in	$a = p_b/2$	1.75 in
	$a' = a + d_b/2$	3.00 in	$a' = a + d_b/2$	2.25 in	$a' = a + d_b/2$	2.25 in
	$b = (g + t_w)/2$	2.75 in	$b = p_{fo}$	2.25 in	$b = p_{fi}$	1.75 in
	$b' = b - d_b/2$	2.25 in	$b' = b - d_b/2$	1.75 in	$b' = b - d_b/2$	1.25 in
	$p = \min(b, p_b)$	2.75 in	$p = b_p - t_w/2$	4.75 in	$p = b_p - t_w/2$	4.75 in
	$d_{hole} = d_b + 1/16$	1.06 in				
	$T = \phi F_t A_b$	53.0 kips				
$\phi M_p = \frac{\phi t_p^2 p F_{pu}}{4}$		52.3 k-in		90.3 k-in		90.3 k-in
$\delta = 1 - \frac{d_{hole}}{p}$		0.61		0.78		0.78
$\alpha = \frac{1}{\delta}\left(\frac{Tb'}{\phi M_p} - 1\right)$		2.09		0.04		-0.34
		two plastic hinges		one plastic hinge		thick plate

For one plastic hinge:

$q = T\left(\frac{\delta\alpha}{1+\delta\alpha}\right)\left(\frac{b'}{a'}\right)$	22.3	kips	1.1	kips	-10.7	kips
$T_{allow} = T - q$	30.7	kips	51.9	kips	63.7	kips

For two plastic hinges:

$T_{allow} = \frac{1}{b'}\phi M_p \delta p(1+\delta)$	63.3	kips	338.0	kips	473.2	kips
T_{allow} *based on* α	63.3	kips	51.9	kips	63.7	kips

Moment Capacity

$M_q = \sum(2T_{allow} d_n)$ 27197 kip-in

Plate Girder Dimensions

	Width		Height		Area		Distance From Centroid of Shape to Top of Plate Girder		Distance From Centroid of Shape to Centroid of Plate Girder	
Top Flange	10.00	in	1.00	in	10	in^2	0.5	in	27.5	in
Web	0.5	in	54	in	27	in^2	28	in	0	in
Bottom Flange	10.00	in	1.00	in	10	in^2	55.5	in	27.5	in

Plate Girder Properties

Centroid	28.0	in	Measured from top of plate girder.	
Moment of Inertia	21687.7	in^4		59.25
Elastic Neutral Axis	28.0	in	Measured from top of plate girder.	
Plastic Neutral Axis	28.0	in	Measured from top of plate girder. Assume is in web.	

h_c	54.0	in	S_{xc}	775	in^3
h_p	54.0	in	Z_x	915	in^3

Slenderness

K_c	0.3849		
F_L	38.5	ksi	Verify that conditions are valid for $F_L=0.7*F_y$

	λ	λ_p	λ_r	
Flange	5	8.726	16.176	COMPACT
Web*	108	86.339	130.886	NONCOMPACT

*Based upon doubly symmetric cross section

Determine RPG

a_w	2.70	h_c/t_w	108
5.7*(E/Fy)^1/2	130.89	RPG	1.000

Limit State Analysis

F_{CR} Compression Flange Strength 55.00 ksi

Yield

F_{CR} 55.00 ksi

Flange Local Buckling

F_{CR} 55.00 ksi

Lateral Torsional Buckling

F_{CR} 55.00

I_{CY}	83.43	in^4	A	14.50	in^2
r_t	2.40		C_b	1	
L_P	60.59	in	L_R	206.82	in

NO LTB

Bend-Buckling of the Web

F_{CR} 55.00 (IF Applicable) F_{CR} 81.45 ksi

5.7*SQRT(E/F_{CR}) 108.00 = h/tw 108.00

NOT APPLICABLE

Design Moment

M_n	42601	k·in
φM_n	38341	k·in
M_p	50298	k·in
M_{pe}	57156	k·in

Eight Bolt - Extended, Stiffened End Plate Configuration

Specimen: **8ES-1.25-1-30 - Thin**

Reference: **Sumner 2003 and Sumner and Murray 2000**

Rafter Input Information (W24x100):

b_f	10.56	in
t_f	0.64	in
t_w	0.5	in
depth, d	30	in
E	29000	ksi
L_B	0	in
F_y	54.9	ksi
F_u	70.8	ksi

End Plate Input Information:

b_p	11.50	in	
g	5.51	in	
p_{ext}	7.38	in	guess
$p_{f,o}$	1.77	in	
$p_{f,i}$	1.77	in	
p_b	3.77	in	guess

ϕ	0.75	
ϕ_b	0.9	
t_p	1.01	in
F_{py}	37.8	ksi
F_{pu}	60.8	ksi

Bolts	A325	
F_t	90	ksi
d_b	1.250	in
T_b	71 kips	

Summary:

M_{np}	26220	k·in	2185	k·ft
$M_{q\ -\ DG16}$	19290	k·in	1608	k·ft
$M_{q\ -\ proposed}$	14666	k·in	1222	k·ft
$M_{pl\ -\ old}$	19170	k·in	1598	k·ft
$M_{pl\ -\ new}$	19170	k·in	1598	k·ft

Rafter Section Limit States

M_n	14263	k·in	1189	k·ft
φM_n	12837	k·in	1070	k·ft
M_p	16541	k·in	1378	k·ft
M_{pe}	18937	k·in	1578	k·ft

$M_{np}/M_{q\ -\ DG16}$	1.36
$M_{q\ -\ DG16}/M_{pl\ -\ old}$	1.01

Calculations:

s	3.9794	in
	$p_{ext} \le s$	NO
	$p_{ext} > s$	YES
	CASE II	
EXTENDED		
γ	1	

$$s = \frac{1}{2}\sqrt{b_p g}$$

h_0	35.54	in
h_1	31.77	in
h_2	28.23	in
h_3	24.46	in
d_0	35.22	in
d_1	31.45	in
d_2	27.911	in
d_3	24.141	in
t_p	1	in

Check End Plate Yielding (Based on Sumner 2003)

Case I:

$$Y = \frac{b_p}{2}\left[h_0\left(\frac{1}{2p_{ext}}\right)+h_1\left(\frac{1}{p_{f,o}}\right)+h_2\left(\frac{1}{p_{f,i}}\right)+h_3\left(\frac{1}{s}\right)\right]+\frac{2}{g}\left[h_0\left(p_{ext}+\frac{p_b}{4}\right)+h_1\left(p_{f,o}+\frac{3p_b}{4}\right)+h_2\left(p_{f,i}+\frac{p_b}{4}\right)+h_3\left(s+\frac{3p_b}{4}\right)+p_b^2\right]+g$$

Y_1 503.42

Case II:

$$Y = \frac{b_p}{2}\left[h_0\left(\frac{1}{s}\right)+h_1\left(\frac{1}{p_{f,o}}\right)+h_2\left(\frac{1}{p_{f,i}}\right)+h_3\left(\frac{1}{s}\right)\right]+\frac{2}{g}\left[h_0\left(s+\frac{p_b}{4}\right)+h_1\left(p_{f,o}+\frac{3p_b}{4}\right)+h_2\left(p_{f,i}+\frac{p_b}{4}\right)+h_3\left(s+\frac{3p_b}{4}\right)+p_b^2\right]+g$$

Y_2 497.09

Controlling Case:

Y 497.09

M_{pl} 19170 k·in $M_{pl} = F_{py} t_p^2 Y$

Check Plate Yielding with New Yield Line Solution

$$Y = \frac{b_p}{2}\left[\frac{h_0}{s}+\frac{h_1}{p_{f,o}}+\frac{h_2}{p_{f,i}}+\frac{h_3}{s}\right]+\frac{2}{g}\left[h_0\left(s+\frac{3p_b}{4}\right)+h_1\left(p_{f,o}+\frac{p_b}{4}\right)+h_2\left(p_{f,i}+\frac{3p_b}{4}\right)+h_3(s+\frac{p_b}{4})\right]+g$$

Y_1 503.42

Y_2 497.09

Y 497.09

M_{pl} 19170 k-in

Check Bolt Rupture Without Prying Action

M_{np} 26220 k·in $M_{np} = 2P_t(d_1 + d_2 + d_3 + d_4)$

Check Bolt Rupture with Prying Action

P_t	110	kips

$P_t = \pi d_b^2 F_t / 4$

BOLT DISTRIBUTION FACTORS		
α_1	1.00	
β_1	1.00	
γ_1	1.00	
δ_1	1.00	
PRYING FORCES		
$w_{\alpha,1}$	5.75	in
$w_{\alpha,1}'$	4.44	in
$w_{\beta,1}$	5.75	in
$w_{\beta,1}'$	4.44	in
$w_{\gamma,1}$	5.75	in
$w_{\gamma,1}'$	4.44	in
$w_{\delta,1}$	5.75	in
$w_{\delta,1}'$	4.44	in
$a_{\alpha,o}$	1.835	in
a_o	1.857	in
a_i	1.857	in
$F_{\alpha,1}'$	55.70	kips
$F_{\beta,1}'$	55.70	kips
$F_{\gamma,1}'$	55.70	kips
$F_{\delta,1}'$	55.70	kips
$Q_{max,\alpha,1}$	19.16	kips
$Q_{max,\beta,1}$	18.93	kips
$Q_{max,\gamma,1}$	18.93	kips
$Q_{max,\delta,1}$	18.93	kips

There were some references that reduced the amount of force in some bolt lines farther from the flange. We set this to 1.00 here.
For instance, Ghassemieh (1983) divides total flange force by 6.8 to say the bolts are 85% effective.

Follows the procedures in the design guide 16

$$F_{o,n}' = \frac{t_p^2 F_{py}\left(0.85 w_n + 0.80 w_n'\right) + \frac{\pi d_b^3 F_t}{8}}{4 p_{f,o}}$$

$$F_{i,n}' = \frac{t_p^2 F_{py}\left(0.85 w_n + 0.80 w_n'\right) + \frac{\pi d_b^3 F_t}{8}}{4 p_{f,i}}$$

$$Q_{\max,o,n} = \frac{w_n' t_p^2}{4 a_o}\sqrt{F_{py}^2 - 3\left(\frac{F_o'}{w_n' t_p}\right)^2}$$

$$Q_{\max,i,n} = \frac{w_n' t_p^2}{4 a_i}\sqrt{F_{py}^2 - 3\left(\frac{F_i'}{w_n' t_p}\right)^2}$$

BOLT ROW PRYING COMBINATIONS			
COMBINATION	**B. ROW**	**PRY.[1]**	**M_q**
Not Normally checked	1	YES	21710
	2	YES	
	3	YES	
	4	YES	
1	1	NO	19290
	2	YES	
	3	YES	
	4	NO	
2	1	NO	18150
	2	YES	
	3	NO	
	4	NO	
3	1	NO	18000
	2	NO	
	3	YES	
	4	NO	
4	1	NO	16860
	2	NO	
	3	NO	
	4	NO	
M_q	19290		k·in

Ignore this answer because the prying forces aren't correct for rows 1 and 4

AS PER DG16, MAXIMUM Mq VALUE CONTROLS

$$M_q = max(\,prying\,,\,pretension\,)$$

Proposed Procedure for Bolt Prying Action Based on AISC 360-10

	Rows 1 and 4		Row 2		Row 3	
$a = (b_p - g)/2$	3.00 in		$a = p_b/2$	1.89 in	$a = p_b/2$	1.89 in
$a' = a + d_b/2$	3.62 in		$a' = a + d_b/2$	2.51 in	$a' = a + d_b/2$	2.51 in
$b = (g + t_w)/2$	3.00 in		$b = p_{fo}$	1.77 in	$b = p_{fi}$	1.77 in
$b' = b - d_b/2$	2.38 in		$b' = b - d_b/2$	1.15 in	$b' = b - d_b/2$	1.15 in
$p = \min(b, p_b)$	3.00 in		$p = b_p - t_w/2$	5.50 in	$p = b_p - t_w/2$	5.50 in
$d_{hole} = d_b + 1/16$	1.31 in					
$T = \phi F_t A_b$	82.8 kips					
$\phi M_p = \frac{\phi t_p^2 p F_{pu}}{4}$	41.9 k-in		76.8 k-in		76.8 k-in	
$\delta = 1 - \frac{d_{hole}}{p}$	0.56		0.76		0.76	
$\alpha = \frac{1}{\delta}\left(\frac{Tb'}{\phi M_p} - 1\right)$	6.57		0.31		0.31	
	two plastic hinges		one plastic hinge		one plastic hinge	

For one plastic hinge:

$q = T\left(\frac{\delta\alpha}{1+\delta\alpha}\right)\left(\frac{b'}{a'}\right)$	42.8	kips	7.2	kips	7.2	kips
$T_{allow} = T - q$	40.0	kips	75.6	kips	75.6	kips

For two plastic hinges:

$T_{allow} = \frac{1}{b'}\phi M_p \delta p(1+\delta)$	46.6	kips	494.4	kips	494.4	kips
T_{allow} *based on* α	46.6	kips	75.6	kips	75.6	kips

Moment Capacity

$M_q = \sum(2T_{allow} d_n)$	14666	kip-in

Plate Girder Dimensions

	Width		Height		Area		Distance From Centroid of Shape to Top of Plate Girder		Distance From Centroid of Shape to Centroid of Plate Girder	
Top Flange	10.56	in	0.64	in	6.7498	in^2	0.3195	in	14.6805	in
Web	0.5	in	28.722	in	14.361	in^2	15	in	1.776E-15	in
Bottom Flange	10.56	in	0.64	in	6.7498	in^2	29.6805	in	14.6805	in

Plate Girder Properties

Centroid	15.0	in	Measured from top of plate girder.			
Moment of Inertia	3897.1	in^4				59.25
Elastic Neutral Axis	15.0	in	Measured from top of plate girder.			
Plastic Neutral Axis	15.0	in	Measured from top of plate girder. Assume is in web.			
h_c	28.7	in		S_{xc}	260	in^3
h_p	28.7	in		Z_x	301	in^3

Slenderness

K_c	0.5278			
F_L	38.43	ksi	Verify that conditions are valid for $F_L=0.7*F_y$	

	λ	λ_p	λ_r	
Flange	8.265258216	8.734	18.959	COMPACT
Web*	57.444	86.417	131.005	COMPACT

*Based upon doubly symmetric cross section

Determine RPG

a_w	2.13	h_c/t_w	57.444
5.7*(E/Fy)^1/2	131.00	RPG	1.000

Limit State Analysis

F_{CR} Compression Flange Strength 54.90 ksi

Yield

F_{CR} 54.90 ksi

Flange Local Buckling

F_{CR} 54.90 ksi

Lateral Torsional Buckling

F_{CR} 54.90

I_{CY}	62.81	in^4	A	9.14	in^2
r_t	2.62		C_b	1	
L_P	66.26	in	L_R	226.19	in

NO LTB

Bend-Buckling of the Web

F_{CR} 54.90 (IF Applicable) F_{CR} 287.90 ksi

$5.7*SQRT(E/F_{CR})$	58.00	>	h/tw	57.44

NOT APPLICABLE

Design Moment

M_n	14263	k·in
φM_n	12837	k·in
M_p	16541	k·in
M_{pe}	18937	k·in

Appendix F Lateral Bracing Design Calculations

NODAL BRACE FOR LTB(Appendix 6, AISC Manual)

DEEP BEAM - 60 in.		
M_r	35237	k-in
C_d	1	
h_o	59.25	in
ϕ	0.75	
L_b	74.52	in
β_{br}	106.40	kip/in
P_{rb}	11.89	kips
θ	45	degree
$\frac{EA}{L}\cos^2\theta$	106.40	kip/in
A/L	0.0073	in^2/in
L	60	in
A	0.44	in^2
AF_y	11.89	kips
F_y	36	ksi
A	0.33	in^2
A_{req}	0.44	in^2
dia.	0.75	in

SHALLOW BEAM - 36 in.		
M_r	17650	k-in
C_d	1	
h_o	35.25	in
ϕ	0.75	
L_b	84.63	in
β_{br}	78.89	kip/in
P_{rb}	10.014	kips
θ	45	degree
$\frac{EA}{L}\cos^2\theta$	78.89	kip/in
A/L	0.0054	in^2/in
L	60	in
A	0.33	in^2
AF_y	10.01	kips
F_y	36	ksi
A	0.28	in^2
A_{req}	0.33	in^2
dia.	0.64	in

DEEP BEAM - 56 in.		
M_r	38341	k-in
C_d	1	
h_o	55	in
ϕ	0.75	
L_b	60.59	in
β_{br}	153.40	kip/in
P_{rb}	13.94	kips
θ	45	degree
$\frac{EA}{L}\cos^2\theta$	153.40	kip/in
A/L	0.0106	in^2/in
L	60	in
A	0.63	in^2
AF_y	13.94	kips
F_y	36	ksi
A	0.39	in^2
A_{req}	0.63	in^2
dia.	0.90	in

Appendix G Unreported Data from String Potentiometers

6B-4W/2W-1.125-0.75-36

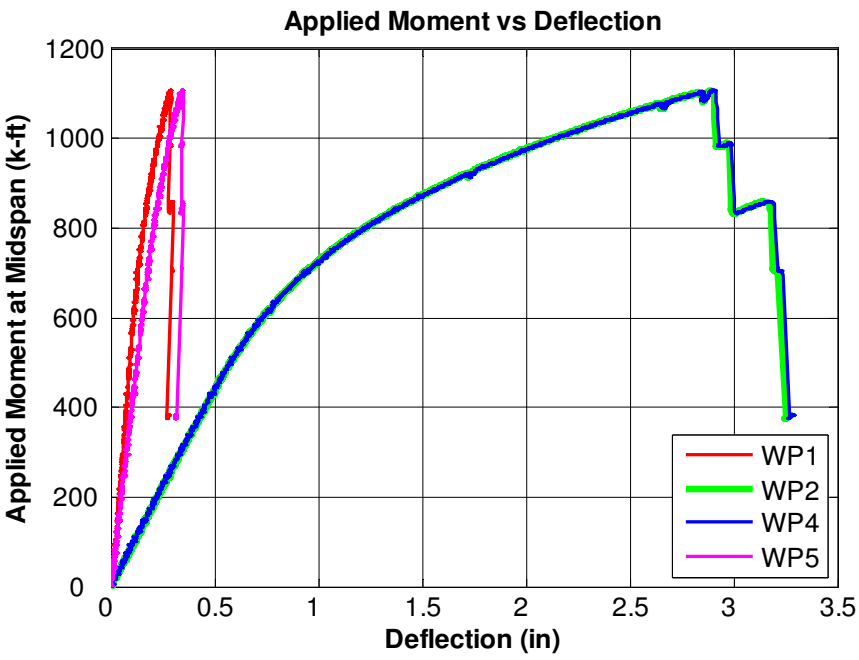

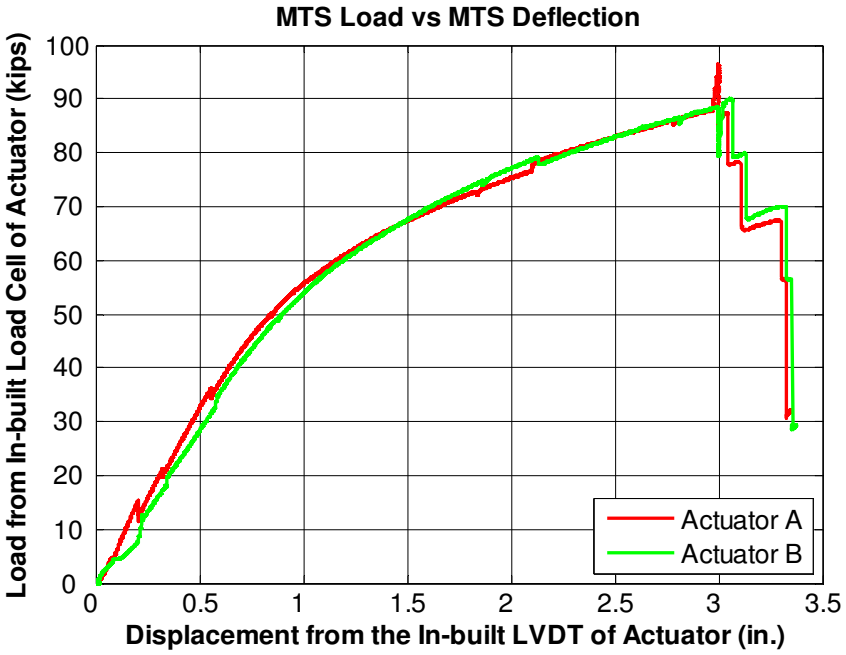

6B-4W/2W-0.875-1.00-36

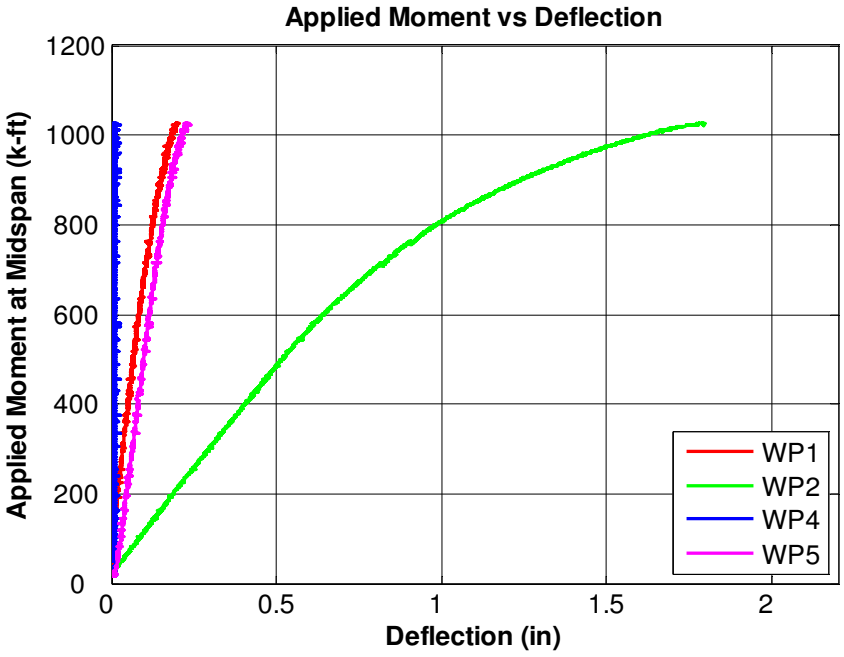

Note: WP4 didn't work

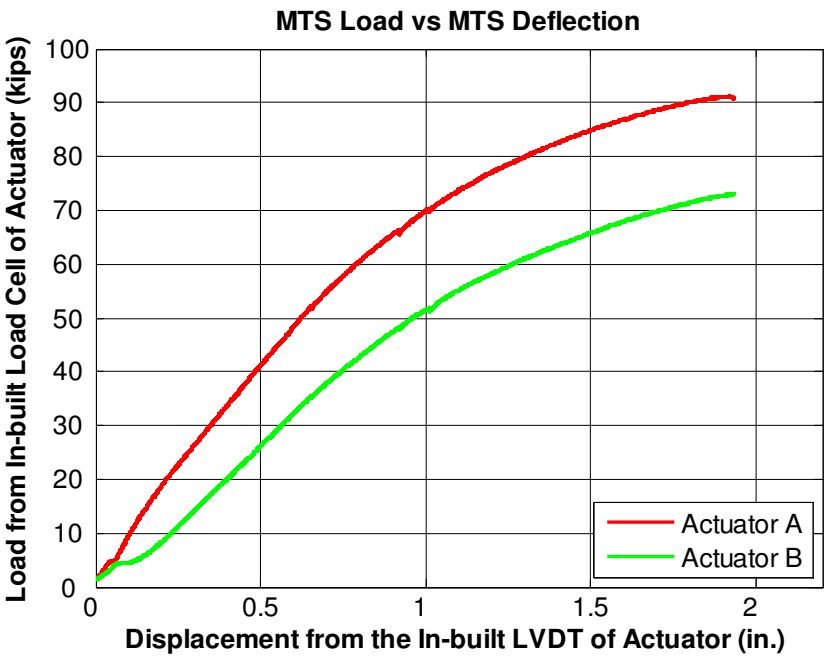

6B-4W/2W-1.125-0.75-60

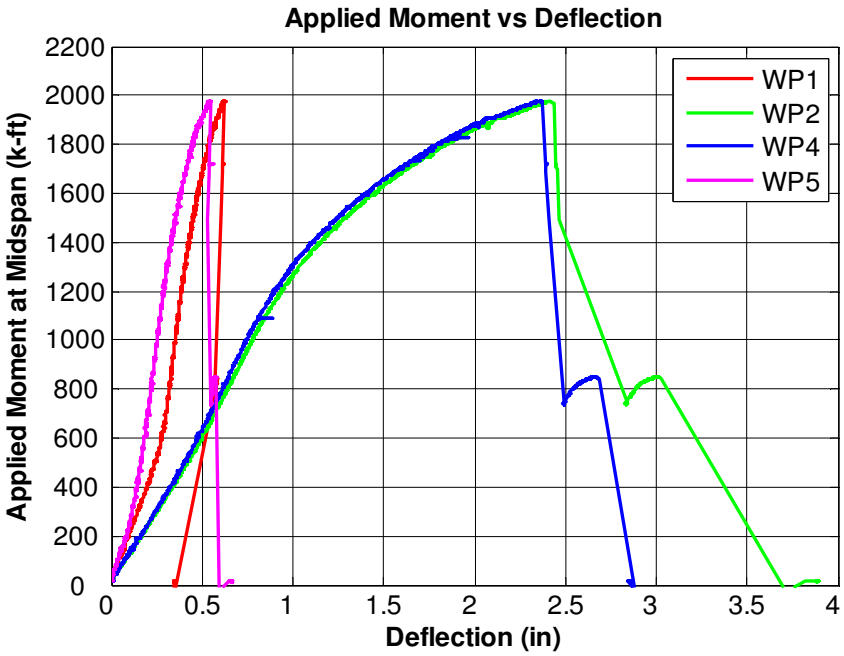

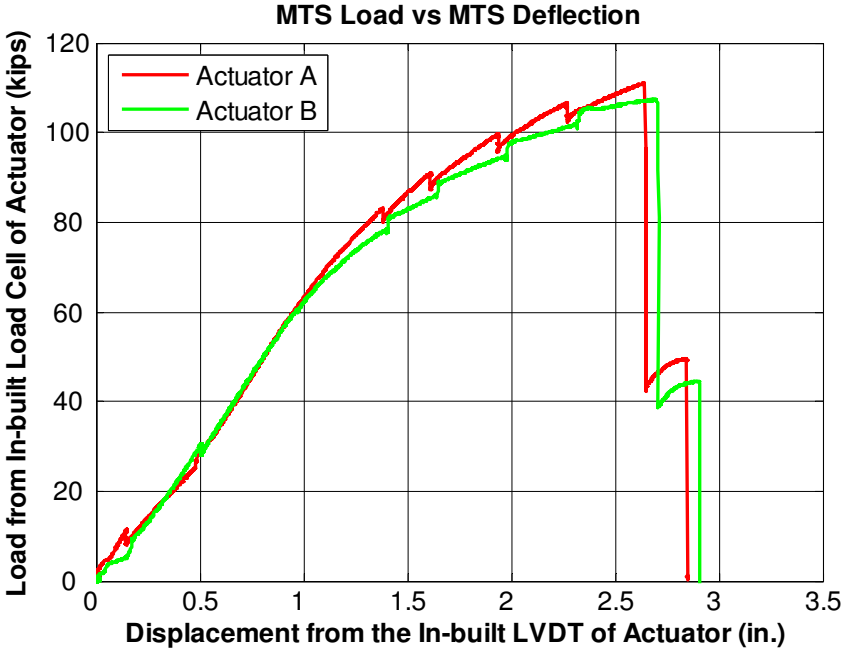

6B-4W/2W-0.875-1.00-60

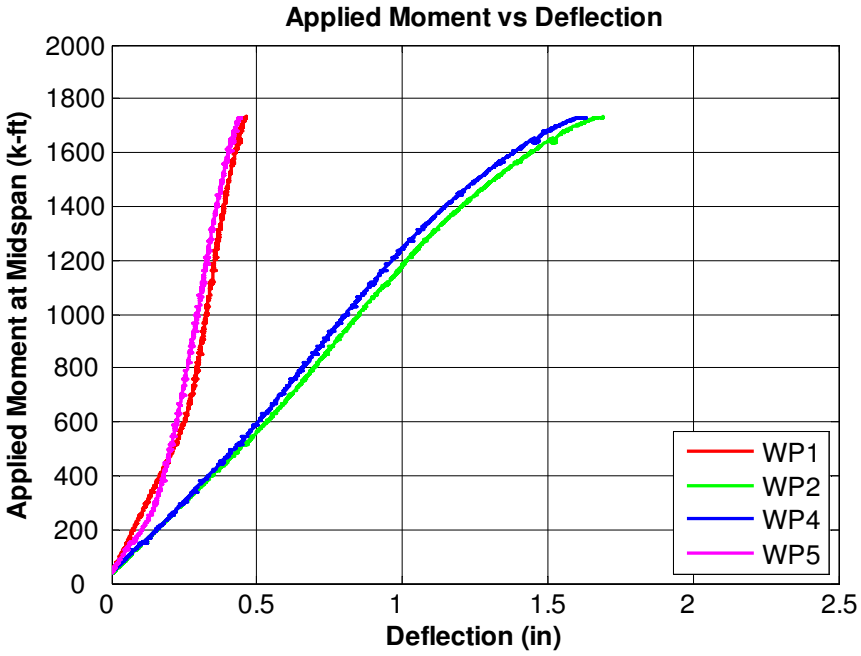

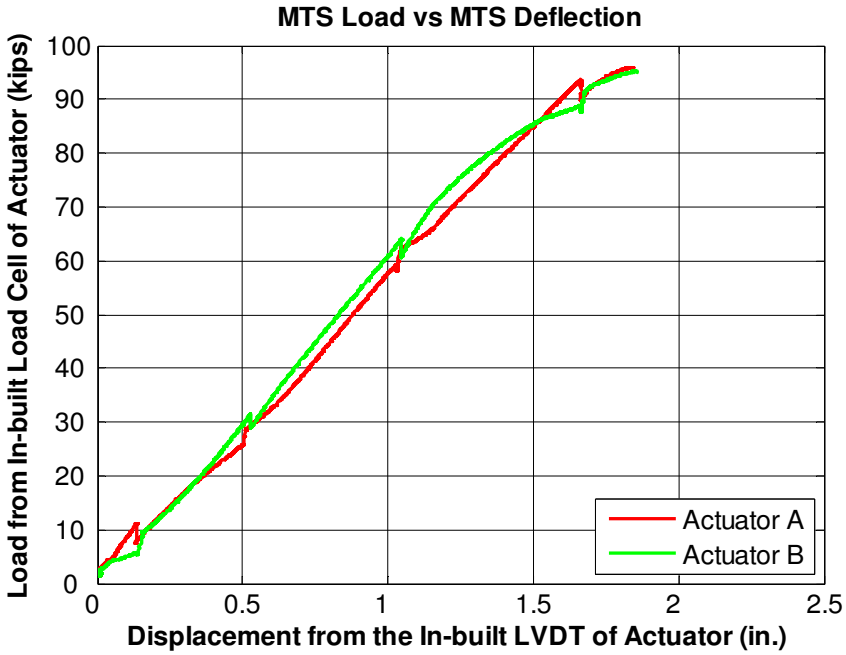

12B-MRE 1/3-4W/2W-1.00-0.75-36

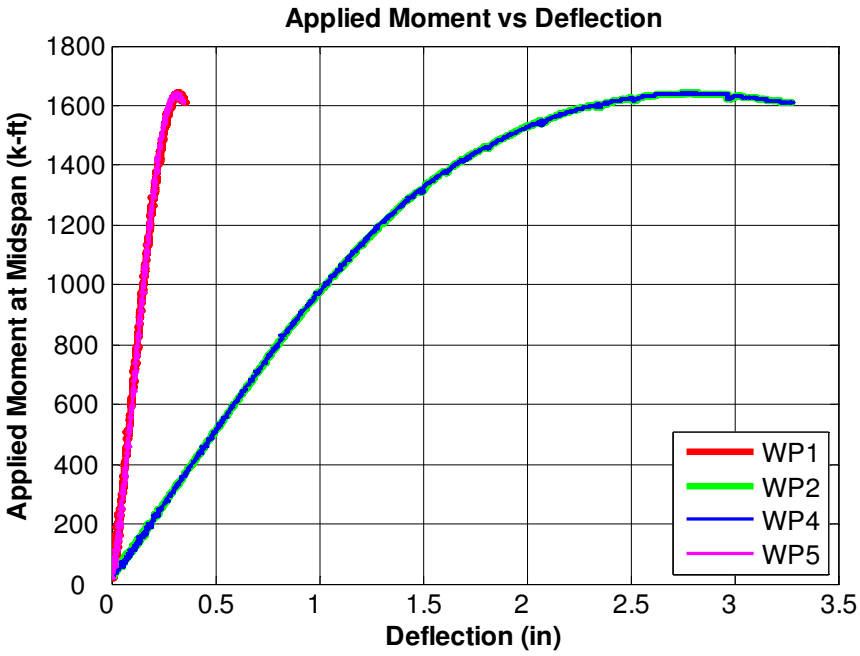

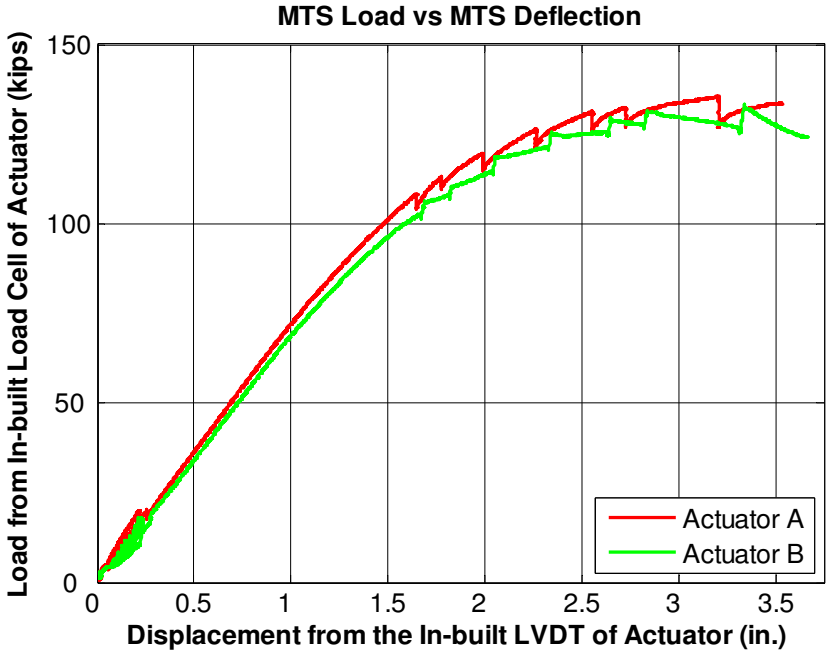

12B-MRE 1/3-4W/2W-0.75-1.00-36

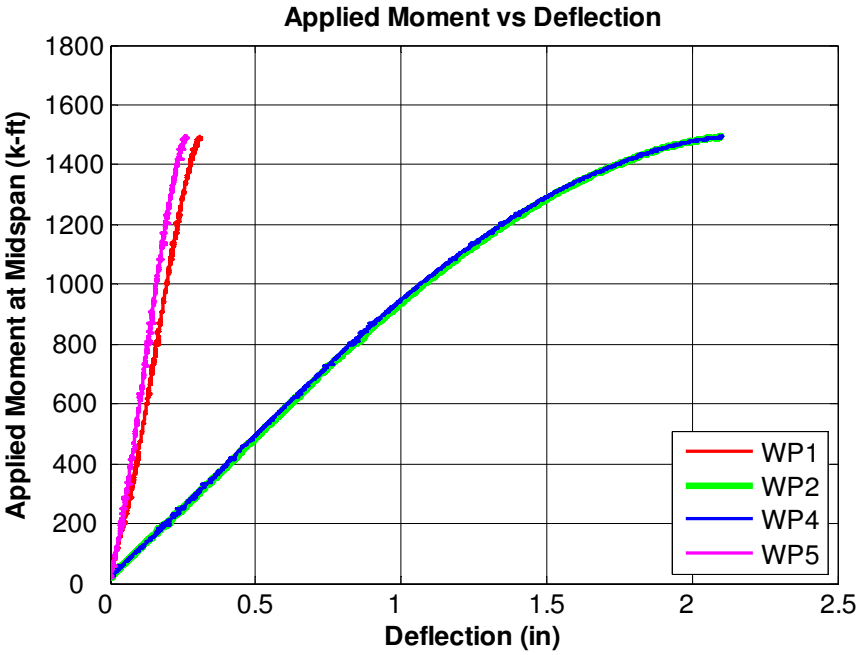

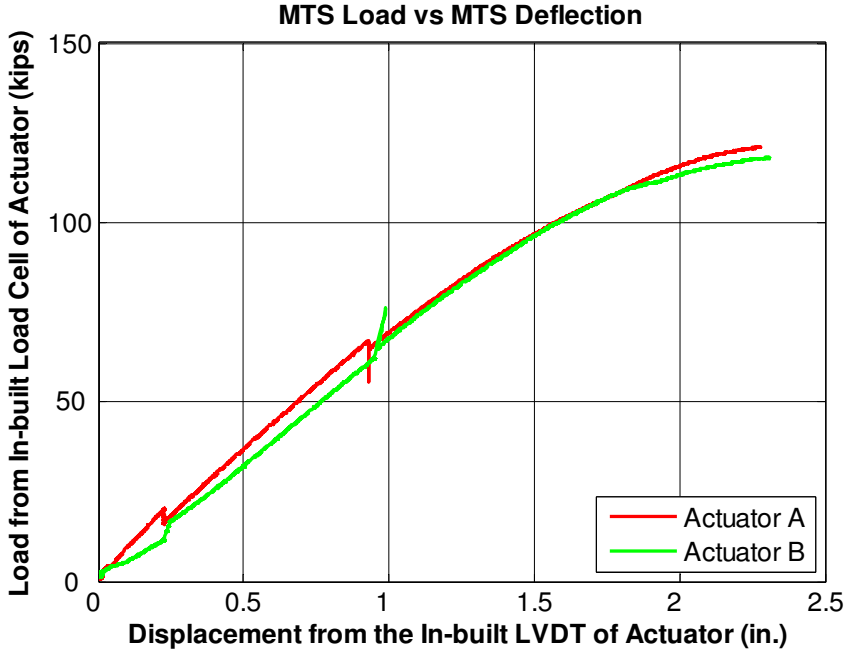

12B-MRE 1/3-4W/2W-1.00-0.75-60

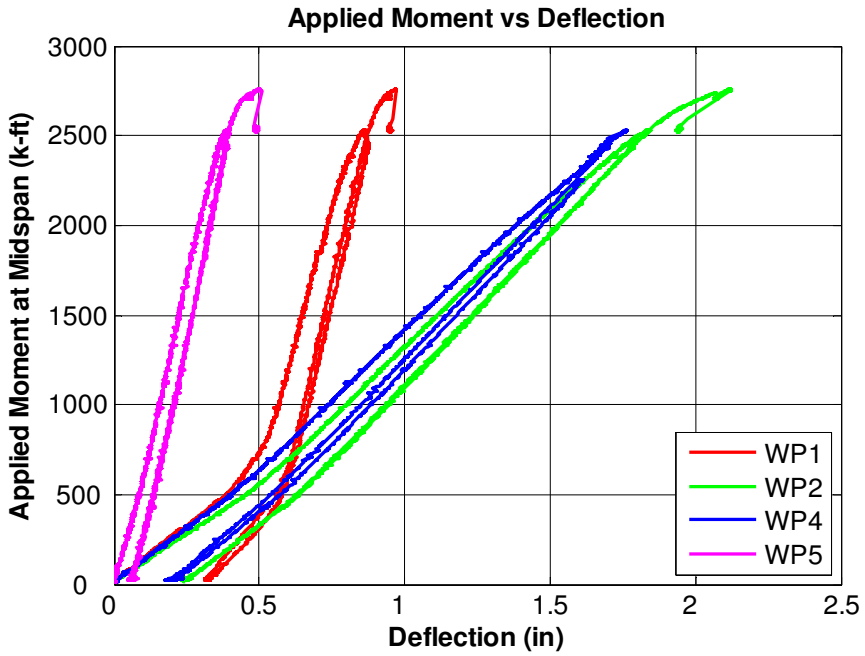

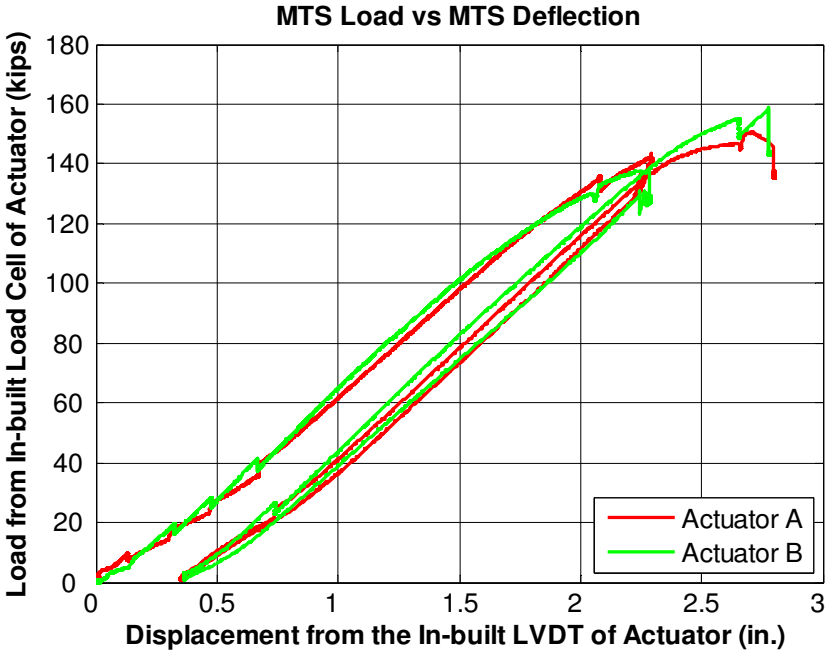

12B-MRE 1/3-4W/2W-0.75-1.00-60

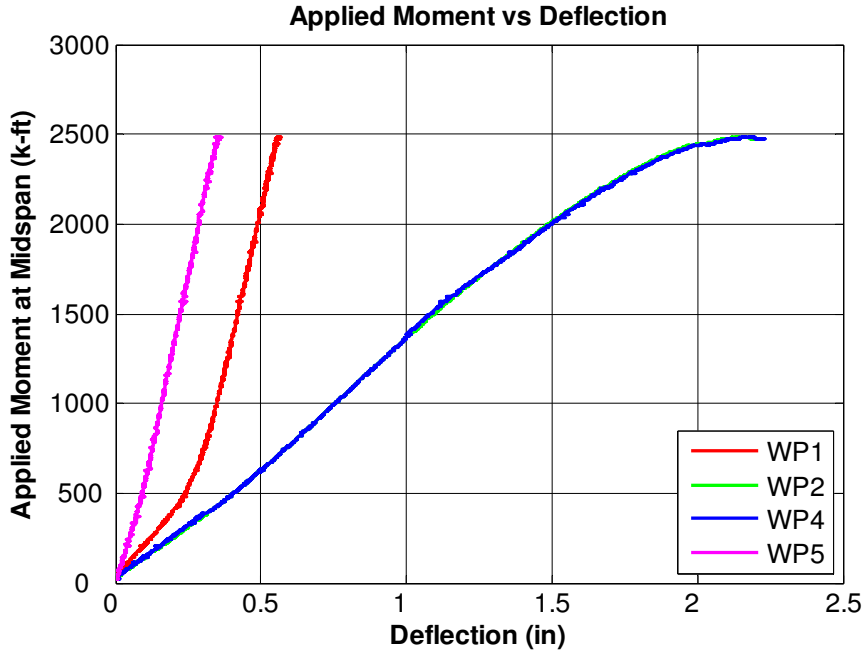

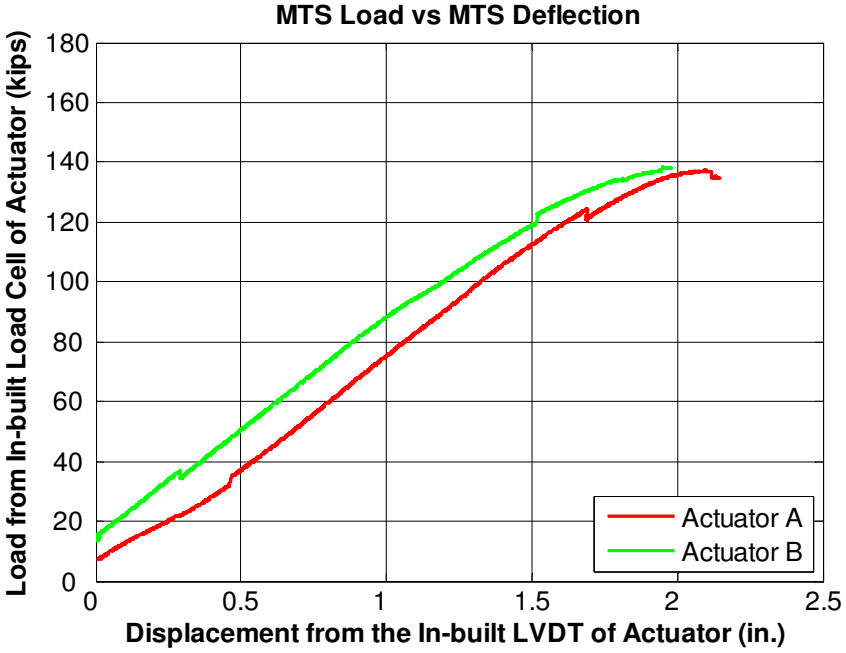

8ES-1.25-0.75-56

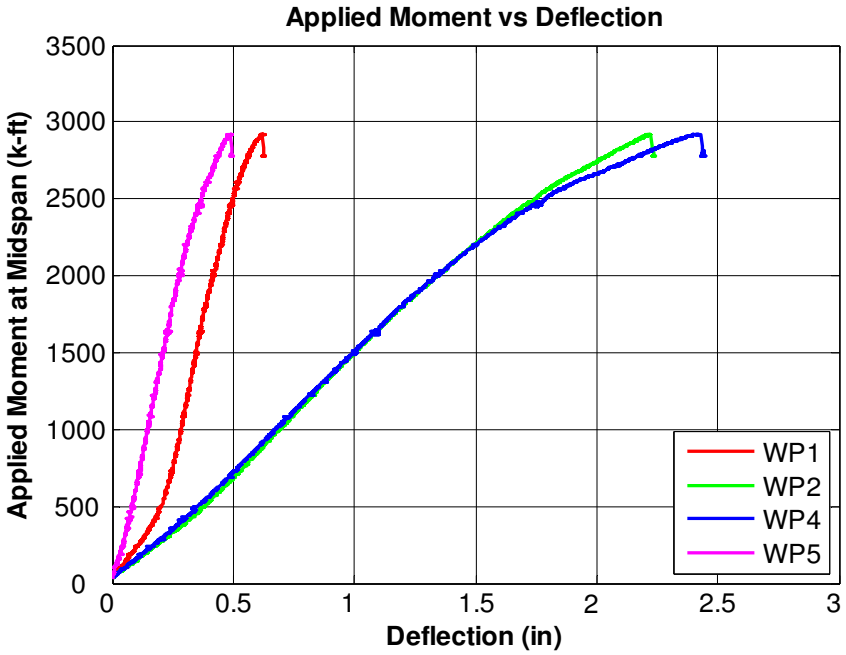

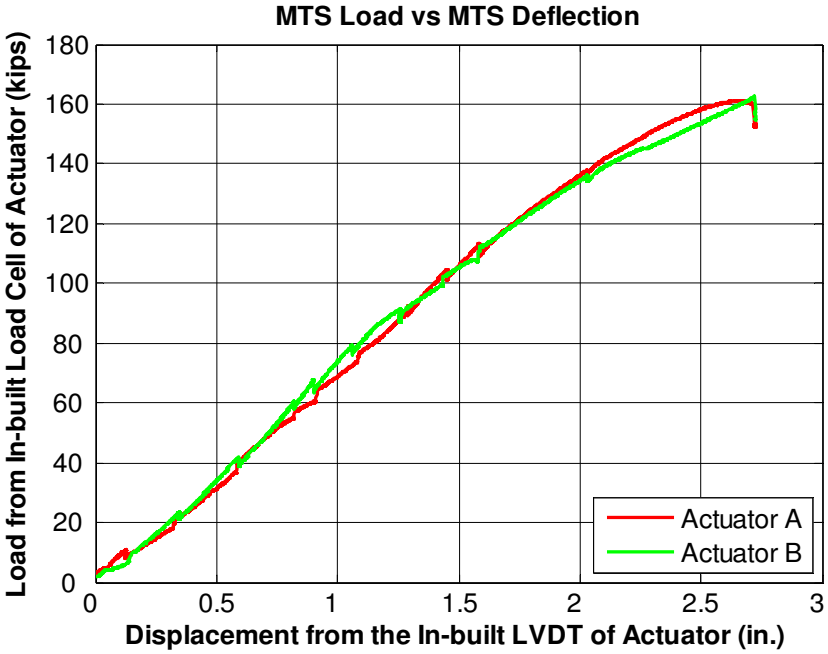

8ES-1.00-1.00-56

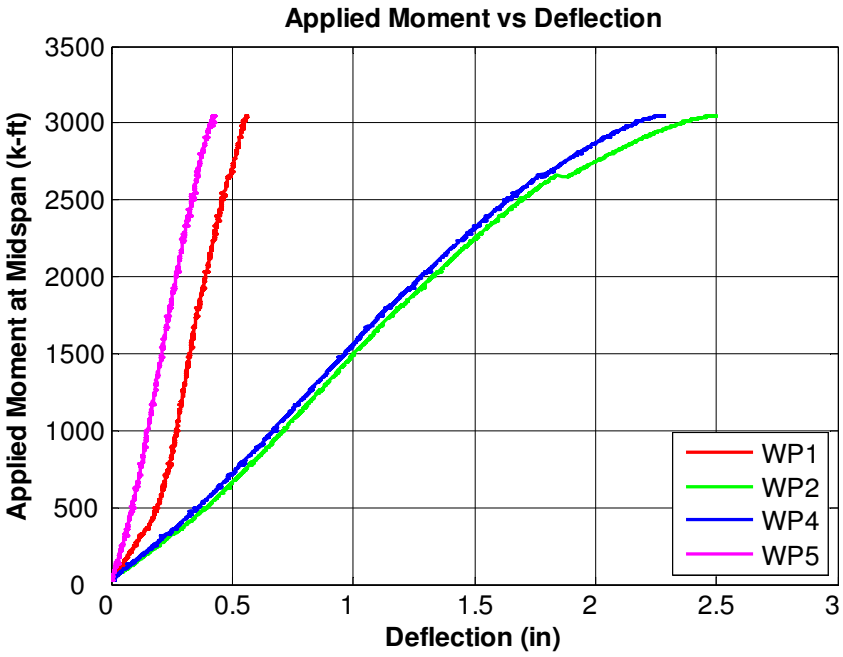

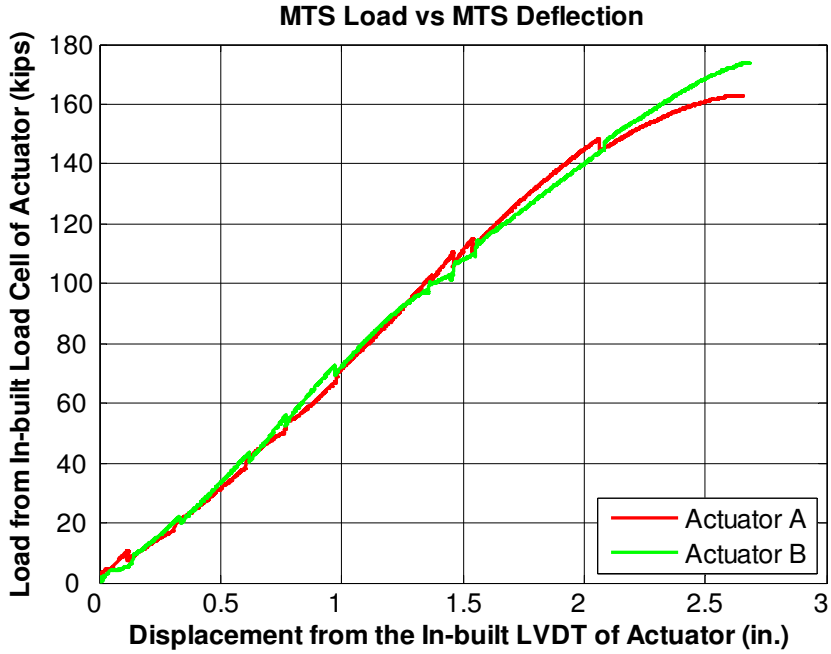

Appendix H Citations of Copyrighted Works

1. [Murray, T. M., & Shoemaker, W. L. (2002). Flush and Extended Multiple-Row Moment End-Plate Connections. *AISC*.] fair use

Figure 2-1 Flush End-Plate Connections Fair use determination attached
Figure 2-2 Extended End-Plate Connections Fair use determination attached

2. [Sumner, E. A., & Murray, T. M. (2001). *Experimental Investigation of Four Bolt Wide Extended End-Plate Moment Connections.* Blacksburg, VA: Department of Civil Engineering, Virginia Polytechnic Institute and State University.] permission attached

Figure 4-11 8E-4W-1-1/2-62 Specimen Dimensions
Figure 4-12 End Plate Layout for Specimen 8E-4W-1-1/2-62
Figure 4-13 Load-deformation behavior for Specimen 8E-4W-1-1/2-62
Figure 4-14 End-Plate Separation for Specimen 8E-4W-1-1/2-62
Figure 4-15 Bolt forces for Specimen 8E-4W-1-1/2-62
Figure 4-16 8E-4W-3/4-3/4-62 Specimen Dimensions
Figure 4-17 End Plate Layout for Specimen 8E-4W-3/4-3/4-62
Figure 4-18 Load-deformation behavior for Specimen 8E-4W-3/4-3/4-62
Figure 4-19 End-Plate Separation for Specimen 8E-4W-3/4-3/4-62
Figure 4-20 Bolt forces for Specimen 8E-4W-3/4-3/4-62

3. [Sumner, E. A., Mays, T. W., & Murray, T. M. (2000). *Cyclic Testing of Bolted Moment End-Plate Connections.* Blacksburg, VA: Virginia Polytechnic Institute and State University.] permission attached

Figure 4-1 8E-4W-1.25-1-30 Specimen Dimensions
Figure 4-2 End Plate Layout for Specimen 8E-4W-1.25-1-30
Figure 4-3 Load-deformation behavior for Specimen 8E-4W-1.25-1-30

Figure 4-4 End-plate separation for Specimen 8E-4W-1.25-1-30

Figure 4-5 Bolt 2 strains for Specimen 8E-4W-1.25-1-30

Figure 4-6 8E-4W-1.25-1.375-36 Specimen Dimensions

Figure 4-7 End Plate Layout for Specimen 8E-4W-1.25-1.375-36

Figure 4-8 Load-deformation behavior for Specimen 8E-4W-1.25-1.375-36

Figure 4-9 End-plate separation for Specimen 8E-4W-1.25-1.375-36

Figure 4-10 Bolt 2 strains for Specimen 8E-4W-1.25-1.375-36

Figure 4-21 8ES-1.25-1-30 Specimen Dimensions

Figure 4-22 End-Plate Layout for Specimen 8ES-1.25-1-30

Figure 4-23 Load-deformation behavior for Specimen 8ES-1.25-1-30

Figure 4-24 End-plate separation for Specimen 8ES-1.25-1-30

Figure 4-25 Bolt 11 strains for Specimen 8ES-1.25-1-30

Figure 4-31 8ES-1.25-1.25-36 Specimen Dimensions

Figure 4-32 End-plate Layout for Specimen 8ES-1.25-1.25-36

Figure 4-33 Load-deformation behavior for Specimen 8ES-1.25-1.25-36

Figure 4-34 End-plate separation for Specimen 8ES-1.25-1.25-36

Figure 4-35 Bolt 3 strains for Specimen 8ES-1.25-1.25-36

4. [Ghassemieh, M., Kukreti, A., and Murray, T.M. (1983) *Inelastic Finite Element Analysis of Stiffened End-Plate Moment Connections*, Report No. FSEL/AISC 83-02, School of Civil Engineering and Environmental Science, University of Oklahoma, Norman, OK.] permission attached

Figure 4-26 8ES-0.875-0.75-24 Specimen Dimensions

Figure 4-27 End-Plate Layout for Specimen 8ES-0.875-0.75-24 [redrawn]

Figure 4-28 Moment-Deflection behavior for Specimen 8ES-0.875-0.75-24

Figure 4-29 End-plate separation for Specimen 8ES-0.875-0.75-24

Figure 4-30 Bolt forces for 8ES-0.875-0.75-24

Figure 4-36 8ES-0.875-1-24 Specimen Dimensions

Figure 4-37 End-Plate Layout for Specimen 8ES-0.875-1-24 [redrawn]

Figure 4-38 Load-deformation behavior for Specimen 8ES-0.875-1-24
Figure 4-39 End-plate separation for Specimen 8ES-0.875-1-24
Figure 4-40 Bolt forces for Specimen 8ES-0.875-1-24